National Library
of Canada

Bibliothèque nationale
du Canada

Acquisitions and
Bibliographic Services Branch

Direction des acquisitions et
des services bibliographiques

395 Wellington Street
Ottawa, Ontario
K1A 0N4

395, rue Wellington
Ottawa (Ontario)
K1A 0N4

Your file *Votre référence*

Our file *Notre référence*

NOTICE

The quality of this microform is heavily dependent upon the quality of the original thesis submitted for microfilming. Every effort has been made to ensure the highest quality of reproduction possible.

If pages are missing, contact the university which granted the degree.

Some pages may have indistinct print especially if the original pages were typed with a poor typewriter ribbon or if the university sent us an inferior photocopy.

Reproduction in full or in part of this microform is governed by the Canadian Copyright Act, R.S.C. 1970, c. C-30, and subsequent amendments.

AVIS

La qualité de cette microforme dépend grandement de la qualité de la thèse soumise au microfilmage. Nous avons tout fait pour assurer une qualité supérieure de reproduction.

S'il manque des pages, veuillez communiquer avec l'université qui a conféré le grade.

La qualité d'impression de certaines pages peut laisser à désirer, surtout si les pages originales ont été dactylographiées à l'aide d'un ruban usé ou si l'université nous a fait parvenir une photocopie de qualité inférieure.

La reproduction, même partielle, de cette microforme est soumise à la Loi canadienne sur le droit d'auteur, SRC 1970, c. C-30, et ses amendements subséquents.

Canada

UNIVERSITY OF ALBERTA

AN ISOTOPIC, GEOCHEMICAL AND PETROGRAPHIC INVESTIGATION OF THE GENESIS OF EARLY PROTEROZOIC MAFIC INTRUSIONS AND ASSOCIATED VOLCANISM NEAR SUDBURY, ONTARIO

BY

STEPHEN ANTHONY PREVEC ©

A thesis submitted to the Faculty of Graduate Studies and Research in partial fulfillment of the requirements for the degree of Doctor of Philosophy.

DEPARTMENT OF GEOLOGY

Edmonton, Alberta
Spring 1993

National Library
of Canada

Acquisitions and
Bibliographic Services Branch

395 Wellington Street
Ottawa, Ontario
K1A 0N4

Bibliothèque nationale
du Canada

Direction des acquisitions et
des services bibliographiques

395, rue Wellington
Ottawa (Ontario)
K1A 0N4

Your file Votre référence

Our file Notre référence

The author has granted an irrevocable non-exclusive licence allowing the National Library of Canada to reproduce, loan, distribute or sell copies of his/her thesis by any means and in any form or format, making this thesis available to interested persons.

L'auteur a accordé une licence irrévocable et non exclusive permettant à la Bibliothèque nationale du Canada de reproduire, prêter, distribuer ou vendre des copies de sa thèse de quelque manière et sous quelque forme que ce soit pour mettre des exemplaires de cette thèse à la disposition des personnes intéressées.

The author retains ownership of the copyright in his/her thesis. Neither the thesis nor substantial extracts from it may be printed or otherwise reproduced without his/her permission.

L'auteur conserve la propriété du droit d'auteur qui protège sa thèse. Ni la thèse ni des extraits substantiels de celle-ci ne doivent être imprimés ou autrement reproduits sans son autorisation.

ISBN 0-315-82037-3

Canada

UNIVERSITY OF ALBERTA

RELEASE FORM

NAME OF AUTHOR: Stephen Anthony Prevec

TITLE OF THESIS: An isotopic, geochemical and petrographic investigation of the genesis of Early Proterozoic mafic intrusions and associated volcanism near Sudbury, Ontario

DEGREE: Doctor of Philosophy

YEAR THIS DEGREE GRANTED: 1993

Permission is hereby granted to the University of Alberta Library to reproduce single copies of this thesis and to lend or sell such copies for private, scholarly or scientific research purposes only.

The author reserves all other publication and other rights in association with the copyright in the thesis, and except as hereintofore provided neither the thesis nor any substantial portion thereof may be printed or otherwise reproduced in any material form whatever without the author's prior written permission.

944 LaSalle Park Road
Burlington, Ontario
Canada L7T 1M9

Date: March 16/93

UNIVERSITY OF ALBERTA

FACULTY OF GRADUATE STUDIES AND RESEARCH

The undersigned certify that they have read, and recommend to the Faculty of Graduate Studies and Research for acceptance, a thesis entitled An isotopic, geochemical and petrographic investigation of the genesis of Early Proterozoic mafic intrusions and associated volcanism near Sudbury, Ontario submitted by Stephen Anthony Prevec in partial fulfillment of the requirements for the degree of Doctor of Philosophy.

H. Baadsgaard
Dr. H. Baadsgaard (Supervisor)

Philippe Erdmer
Dr. P. Erdmer (Chairman)

R A Burwash
Dr. R.A. Burwash

Dr. T. Chacko

GL Cumming
Dr. G. Cumming (Physics)

RS James
Dr. R.S. James (External)

Date: March 31, 1993

TABLE OF CONTENTS

Page No.	Chapter	Title
1	1	**INTRODUCTION**
2	1.1	PREVIOUS WORK: REGIONAL GEOLOGY
3	1.1.1	The Southern Province
5	2	**LATE ARCHEAN TO EARLY PROTEROZOIC GEOLOGY OF THE STUDY AREA**
5	2.0	INTRODUCTION
5	2.1	ALGOMAN GRANITES
9	2.2	EARLY PROTEROZOIC MAFIC ROCKS
9	2.2.1	Gabbro-Anorthosite Intrusives
10	2.2.1.1	The East Bull Lake Intrusion
15	2.2.1.2	The Shakespeare Dunlop Intrusion
16	2.2.1.3	May Township Intrusion
18	2.2.1.4	Drury Township Intrusion
22	2.2.1.5	Falconbridge Township Intrusion
23	2.2.1.6	Wanapitei Intrusion
23	2.2.1.7	St. Charles Anorthosite Sill
24	2.2.1.8	Mercer Anorthosite
24	2.2.2	Basal Huronian Volcanics
31	2.3	REGIONAL TECTONIC EVOLUTION
33	2.4	LOGISTICS
35	3	**PETROGRAPHY**
35	3.0	INTRODUCTION
35	3.1	SUPERIOR PROVINCE GRANITOIDS
35	3.1.1	Algoman Granitoids
36	3.1.2	Levack Gneiss Complex
38	3.2	PROTEROZOIC GABBRO-ANORTHOSITES
38	3.2.1	East Bull Lake Intrusion
40	3.2.2	Shakespeare-Dunlop Intrusion

Page No.	Chapter	Title
45	3.2.3	Tennyson Township Intrusion
45	3.2.4	May Township Intrusion
46	3.2.5	Drury Township Intrusion
47	3.2.6	Falconbridge Township Intrusion
48	3.2.7	Wanapitei Intrusion
49	3.2.8	St. Charles Anorthosite
50	3.2.9	Mercer Township Intrusion
50	3.3	HURONIAN MAFIC VOLCANICS
53	3.4	DISCUSSION AND SUMMARY
53	3.4.1	Superior Province Granitoids
54	3.4.2	Proterozoic Mafic Rocks
56	3.4.3	Conclusions
58	4	**GEOCHRONOLOGY**
58	4.0	INTRODUCTION
58	4.1	GABBRO-ANORTHOSITES
58	4.1.1	Mercer Anorthosite
61	4.1.1.1	U-Pb results
61	4.1.1.2	Interpretation
61	4.1.2	St. Charles Anorthosite
61	4.1.2.1	U-Pb results
62	4.1.2.2	Interpretation
62	4.1.3	Wanapitei Intrusion
62	4.1.3.1	U-Pb results
63	4.1.3.2	Interpretation
63	4.1.4	Falconbridge Twp. Intrusion
63	4.1.4.1	U-Pb results
67	4.1.4.2	Interpretation
67	4.1.5	Drury Twp. Intrusion
68	4.1.5.1	U-Pb results
68	4.1.5.2	Interpretation

Page No.	Chapter	Title
68	4.2	GRANITOIDS
68	4.2.1	Algoman Granitoid
71	4.2.1.1	U-Pb results
71	4.2.2	Abitibi Granitoid
71	4.2.2.1	U-Pb results
71	4.2.3	Interpretation
72	4.3	DISCUSSION
72	4.3.1	Anorthosites
73	4.3.2	Wanapitei Intrusion
74	4.3.3	Metagabbroic Intrusives
75	4.3.4	Abitibi Subprovince Granitoids
75	4.4	SUMMARY
77	5	**GEOCHEMISTRY**
77	5.0	INTRODUCTION
77	5.1	CLASSIFICATION
78	5.2	MAJOR ELEMENT GEOCHEMISTRY
83	5.2.1	Normative Classification
86	5.2.2	Variation Diagrams
90	5.3	TRACE ELEMENT GEOCHEMISTRY
90	5.3.1	Large Ion Lithophile Elements
94	5.3.2	Compatible Elements
94	5.3.3	Incompatible Elements
95	5.4	"SPIDERGRAMS" AND REE
95	5.4.1	Spidergrams
97	5.4.2	REE Profiles
98	5.5	DISCUSSION AND SUMMARY
98	5.5.1	Effects of Fract. Crystallization
102	5.5.2	Comparison with Observed Data
103	5.5.3	Effects of "Contamination"

Page No.	Chapter	Title
112	6	**ISOTOPE GEOCHEMISTRY**
112	6.0	INTRODUCTION
112	6.1	Sm-Nd Isotope Geochemistry
113	6.1.1	Results
113	6.1.1.1	Isochron Diagram
113	6.1.1.2	ϵ_{Nd} diagrams
114	6.1.2	Discussion
123	6.2	Pb-Pb ISOTOPE GEOCHEMISTRY
124	6.2.1	Results
125	6.2.2	Discussion
126	6.3	Rb-Sr ISOTOPE GEOCHEMISTRY
127	6.3.1	Results
127	6.3.2	Discussion
128	6.4	DISCUSSION
130	7	**SUMMARY AND CONCLUSIONS**
130	7.0	INTRODUCTION
130	7.1	LATE-PROTEROZOIC ANORTHOSITES
132	7.2	MID-PROTEROZOIC MAFIC INTRUSION
133	7.3	EARLY-PROTEROZOIC MAFIC INTRUSIONS
133	7.3.1	Gabbro-Anorthosite Sills
133	7.3.1.1	Drury and Falconbridge Twp.
135	7.3.1.2	May and Tennyson Twp.
135	7.3.2	Gabbro-Anorthosite Plutons
136	7.4	CONSTRAINTS ON CRUST-MANTLE MIXING
137	7.4.1	Constraints on Ancient Crustal Contributions
140	7.4.2	Constraints on Mantle-Derived End Member
142	7.5	EVOLUTIONARY SUMMARY AND TECTONIC IMPLICATIONS

Page No.	Chapter	Title
146		REFERENCES
	APPENDIX 1	Research Methods
	APPENDIX 2	Geochemical Data
	APPENDIX 3	Spidergrams and REE profiles
	APPENDIX 4	Isotopic Data

LIST OF TABLES

Page No.	Table No.	Title
59	4.1	U-Pb isotopic data: "conventional"
60	4.2	U-Pb isotopic data: SHRIMP
96	5.1	Summary of spidergram features

LIST OF FIGURES

Page No.	Figure No.	Contents
6	2.1	Field area map
13	2.2	EBL map, sample locations
14	2.3	S-D map, " "
19	2.4	May Twp. map, " "
20	2.5	Drury Twp. map, " "
21	2.6	Falconbridge Twp. map, " "
26	2.7	Wanapitei map, sample locations
27	2.8	St. Charles map, " "
28	2.9	Mercer Twp. map, " "
29	2.10	Huronian volcanics map, " "
42	3.1	Cumulate textures from EBL
43	3.2	Cooling and/or reheating phenomena from EBL
44	3.3	a) granite xenolith b) amphibolitized S-D rock c) myrmekite in granophyric S-D sample d) metagabbroic Drury Twp. rock.
51	3.4	Figure 14 a) intercumulus textures from Falconbridge b) Coronitic olivine cumlate from Wanapitei c) Two-pyroxene texture typical of Wanapitei d) Biotitized equivalent.
52	3.5	Anorthositic textures from St. Charles and Mercer Twp.
64	4.1	Zircons from Mercer Twp., St. Charles, Wanapitei and Drury Twp.
65	4.2	Concordia diagrams: Mercer and St. Charles anorthosites
66	4.3	Concordia diagram: Wanapitei
69	4.4	Concordia diagrams: Falconbridge and Drury Twp.

Page No.	Figure No.	Contents
70	4.5	Concordia diagrams: Granitoids
79	5.1	SiO_2 *vs*. (Na_2O + K_2O)
80	5.2	A-F-M, FeO*/MgO *vs*. TiO_2
81	5.3	TiO_2-MnO-P_2O_5
82	5.4	logCr *vs*. logTi, Ti/1000 *vs*. V
87	5.5	SiO_2 *vs*. Al_2O_3, MgO, $Mg^{\#}$, (Fe_2O_3 + FeO), CaO and CaO (EBL and S-D only)
88	5.6	SiO_2 *vs*. K_2O, Na_2O, TiO_2, P_2O_5, MnO and MnO (EBL and S-D only)
91	5.7	K_2O *vs*. Rb, Ba
92	5.8	Ni *vs*. Cr, V, Co, Zn, TiO_2, FeO
93	5.9	Y *vs*. Zr, Ti/Zr
105	5.10	Spidergrams and REE: Model 1 liquids, Model 2 cumulates and liquids
106	5.11	Spidergrams and REE: Model 2A, plagioclase and cpx fractionation
107	5.12	Spidergrams and REE: comparison of modelled and observed cumulates
109	5.13	Spidergram of possible contaminants and contaminee
110	5.14	Spidergrams and REE showing bulk mixing with various local sial
116	6.1	Sm-Nd isochron plot, ϵ_{Nd}-time diagram
117	6.2	ϵ_{Nd}-time diagram and ϵ_{Nd}-$f_{Sm/Nd}$ diagram (T=2.5 Ga)
121	6.3	ϵ_{Nd}-$f_{Sm/Nd}$ diagram for Wanapitei
122	6.4	Common lead plot; Rb-Sr isochron diagram

Page No.	Figure No.	Contents
138	7.1	Spidergrams of cumulates derived from contaminated source magmas
139	7.2	ϵ_{Nd}-$f_{Sm/Nd}$ evolution diagram

LIST OF SYMBOLS

Symbols used in geochemical and isotopic plots (in Chapters 5, 6 and 7):

Cumulates		**Non-cumulates (?)**		**Grenville intrusives**	
East Bull Lake	●	May Twp.	○	Wanapitei	○
Shakespeare-Dunlop	■	Huronian volc.	□		
Drury Twp.	▲			St. Charles	△
Falconbridge Twp.	▼			Mercer Twp.	▽
Tennyson Twp.	◆				

ABSTRACT

Ten metamorphosed gabbro-anorthosites sampled between Elliot Lake and Lake Nipissing are compared with available and some new data for the basal Huronian basalts. Geochemical modelling involving fractional crystallization plus mixing with geologically reasonable volumes of trapped liquids indicates that the the cumulates at East Bull Lake, Shakespeare-Dunlop, May, Tennyson, Drury and Falconbridge Twps. can be derived from a relatively primitive Huronian basalt-type parent. The May Twp. intrusion is geochemically the closest approximation to the parent liquid represented by any of the intrusives sampled.

U-Pb zircon, Sm-Nd and Pb-Pb isotopic evidence indicate that the Falconbridge Twp. body contains a significant Archean component, some of which is probably pre-2.7 Ga. The Drury Twp. body contains zircon apparently wholly reset by *ca.* 1850 Ma shock metamorphism related to the formation of the adjacent Sudbury Nickel Irruptive. Geochemical and Sm-Nd isotopic evidence indicates that substantial contamination of the East Bull Lake and Shakespeare-Dunlop intrusions has occurred, mainly by juvenile (*ca.* 2.7 Ga) crust. However, Sm-Nd data for the latter body, suggest a contribution from significantly older, perhaps 3.5 Ga sialic material. This is supported by a similar result from a mafic granulite from lower crust exposed in the Levack Gneiss Complex.

The Wanapitei intrusion is dated at *ca.* 1747 Ma, suggesting an association with Killarnean orogenic material to the west, rather than with Early Proterozoic material to the north and east. Trace element and Sm-Nd isotopic data are consistent with contamination of this intrusion by late Archean crust. A Grenvillian lower intercept and extensive recrystallization suggests that double-coronas of hypersthene and pargasite between cumulate olivine and plagioclase were generated during Grenville-aged heating.

Two anorthosites in the Burwash area near St. Charles and

in Mercer Twp. are dated at *ca*. 1220 Ma. However, a combination of slight discordancy (1%), analytical imprecision, and potential Grenville-aged influence allows sufficient flexibility in both ages to permit potential correlation with *ca*. 1240 Ma intrusions to the north, rather than invoking a very localized anorogenic mafic event. The geochemistry of both units is dominated by the effects of plagioclase fractionation.

ACKNOWLEDGEMENTS

Acknowledgements are due firstly to Dr. Halfdan Baadsgaard, for his scientific, technical and financial support and his enthusiasm in general. Dr. Patricia Cavell and John Duke are also gratefully acknowledged for invaluable assistance in the lab, on the mass spectrometer, and for general support and excellent company during the course of four years in Edmonton.

Drs. Michael Hamilton, James Mortensen, Richard Stern and Ron Burwash are acknowledged, for uncomplainingly sacrificing their time to provide the author with valuable geological and technical input, references, programs and sounding boards, especially during the final year. The geochronological aspects of this project could not have been accomplished without the efforts of Drs. Baadsgaard and Mortensen, who exceeded their obligations. Dr. Lewis Ashwal is acknowledged for his interest and early input which initiated this research.

Brian Turner is acknowledged for technical support at various levels, in addition to extremely good company, Guinness, and extensive vehicular support of the author for a year. Additional technical support has been provided by Alex Stelmach, Wayne Day, and Ron Stewart.

The field aspects of this project have been aided immensely by contributions from Dr. Ken Card, Wilf Meyer in Sudbury, and field assistance from Kelly Arnold and Robert Hardy. Dr. D.C. Kamineni of Atomic Energy of Canada Limited is acknowledged for providing unpublished information and drill core. Funding for the field work was provided by Energy, Mines and Resources.

Lastly, but certainly not least, I would like to acknowledge all those, in addition to those listed above, who gave friendship and support during my time in Edmonton and in Ottawa during the tenure of this doctorate, especially Bonnie Halvorson. Bud, John and Walt are acknowledged for Wednesday afternoon R&D in Sherwood Park. I would like finally to acknowledge my parents, for their support and encouragement.

CHAPTER ONE: INTRODUCTION

The intent of this study is to investigate the genesis of mafic magmatism at or around the end of the Archean and the beginning of the Proterozoic in its "type" location (Stockwell *et al.*, 1970) in the Sudbury area. Mafic magmatism at *ca.* 2500 to 2450 Ma represents the only major crust-forming event in the area between the end of the formation of the Superior Province (by *ca.* 2670 Ma) and 1900 to 1850 Ma Penokean (?)-Sudbury-related activity. It represents an apparently non-orogenic, extensional, rift-related mantle-derived magmatic event in this 900 Ma long period of cratonic relative stability, otherwise interrupted only by dyke swarm emplacement. The extent, the exact nature, and the genesis of this magmatism are unclear.

The Sudbury area is one of the most intensively studied regions in Canada in terms of geology. This provides an excellent database for detailed work on adjacent rocks from the Southern and Superior Provinces. Eight gabbro-anorthosite bodies have been selected to the west and south of the Sudbury Nickel Irruptive structure, the largest of which are the East Bull Lake (EBL) and the Shakespeare-Dunlop (S-D) intrusions. The EBL intrusion lies entirely within the Superior Province, whereas four of the other bodies straddle the contact between the Superior and Southern Provinces. Three bodies lie to the south within the Grenville Province, and a similar gabbro-anorthosite body to the southeast in the Grenville Province, the River Valley Complex, has been investigated isotopically by Ashwal and Wooden (1989). Mafic volcanics from the base of the Elliot Lake Group of the Huronian Supergroup may be cogenetic, if not comagmatic with the intrusive bodies (*e.g.* Card et al, 1977).

This study requires geochronological, geochemical and geological characterization of numerous potentially inter-related mafic intrusions and of the basal Huronian basalts.

The mafic intrusions may be characterized by their trace element and radiometric-isotopic signatures. Major element geochemistry and petrology are utilized to formulate broad evolutionary constraints. Temporal control for extrusion ages is provided by precise U-Pb dating using trace minerals, specifically zircon. This is limited by the availability of suitable phases for precise U-Pb dating, generally scarce in mafic rocks, and particularly in the basal Huronian volcanics (Corfu, pers. comm., 1988). Whole-rock Sm-Nd, Pb-Pb and Rb-Sr can potentially generate precise emplacement ages also. Given the ages of the units involved, Sm-Nd and Pb-Pb isotope systems are used to investigate the origins thereof, in terms of possible mantle sources, the degree of homogeneity of these sources in the late Archean, and the degree of contamination from various crustal sources. By using multiple isotope systems as well as trace element geochemistry, particularly the "rare earth elements" (REE), the characteristics and therefore the relative contributions of involved reservoirs can be constrained, where these can be distinguished from the effects of secondary processes.

This study clarifies the relationships between the individual gabbro-anorthosite plutons, and the genetic relationship between the EBL and S-D intrusions and the mafic volcanics from the base of the Huronian, speculated on by previous workers (*e.g.* Card, 1988; Krogh *et al.*, 1984). This has implications regarding the nature of the southern boundary of the Superior Province in the early Proterozoic.

1.1 PREVIOUS WORK: REGIONAL GEOLOGY

Precambrian rocks in Ontario have been classified into three geological provinces, based on K-Ar geochronology (Stockwell, 1969). Due to ambiguities invited by geochronological definitions, lithotectonically defined criteria are now favoured, distinguishing, in order of decreasing average age, the Superior, Southern and Grenville Provinces. The interprovincial boundaries trend roughly southwest to northeast. The Superior Province has been divided into a series of sub-parallel subprovinces dominantly consisting of tonalitic gneisses hosting granite-greenstone belts. These show a general trend of decreasing age from the northwest towards the southeast; from > 3000 Ma in the Sachigo Subprovince (Corfu and Wood, 1986) to > 2990 Ma in the Uchi Subprovince (Corfu and Wallace, 1986) to > 2800 Ma in the English River Subprovince and > 2700 Ma in the Wabigoon Subprovince (Beakhouse, 1985), and finally to the Wawa and Abitibi Subprovinces at 2690 to 2720 Ma old (*e.g.* Corfu and Stott, 1986). Between the Superior and Grenville Provinces (1000 Ma; *e.g.* Easton, 1986) lies the Southern Province.

1.1.1 The Southern Province

The Southern Province consists of Early Proterozoic or younger mafic intrusive rocks, mafic and felsic volcanics, and metasedimentary rocks lying unconformably on Superior Province granitoids (Stockwell *et al.*, 1970). Stockwell *et al.* divide the Southern Province into three subprovinces; the Penokean Fold Belt, the Port Arthur Homocline and the Lake Superior Basin. The Early Proterozoic sediments of the latter two subprovinces consist of basal conglomerate (the Kakabeka and Sibly Formations respectively, where the former includes granite pebbles up to two inches in diameter). The conglomerates are overlain by dominantly argillitic and carbonate-cemented clastic and biogenic sediments.

The Penokean Fold Belt is dominated by sediments of the Huronian Supergroup, which can be subdivided into four groups; the Elliot Lake, Hough Lake, Quirke Lake and Cobalt Groups. The latter three groups represent cyclic glacially-controlled sequences (Stockwell *et al.*, 1970). The basal Elliot Lake Group consists of the Matinenda Formation, which is composed of quartzite and uraniferous conglomerate, overlain by the McKim Formation, consisting of interbedded argillite, quartzite and greywacke. At or near the base of the Matinenda Formation lie a series of bimodal (mafic and felsic) volcanics. In the area between Sudbury, Elliot Lake and the north shore of Lake Huron, the mafic volcanics are known variously as the Thessalon, Pater, Salmay Lake, Stobie and Elsie Mountain Formations, from west to east. A number of mafic intrusive rocks occurring at or near the Superior-Southern Province boundary to the west and southwest of Sudbury have been tentatively correlated with the basal volcanics (Card *et al.*, 1977).

The Huronian sediments are cut by a prolific mafic dyke swarm known as the Nipissing Diabase. In the Sudbury area the Southern Province is intruded by the Sudbury Irruptive which postdates deposition of the Huronian rocks and emplacement of the Nipissing Diabase intrusion.

CHAPTER TWO: LATE ARCHEAN TO EARLY PROTEROZOIC GEOLOGY OF THE STUDY AREA

2.0 INTRODUCTION

The study area, shown in Figure 2.1, extends from east of Elliot Lake to west of Lake Nipissing, straddling the boundaries of three geological provinces; the Superior, the Southern and the Grenville.

2.1 ALGOMAN GRANITES

The oldest intrusive rocks in the study area are the late Archean granitic batholiths referred to *en masse* as Algoman granites (Moore and Armstrong, 1945). These intrude older, heterogeneous high-grade granitic to tonalitic gneissic rocks (Card, 1978) known as the Levack Gneiss Complex, exposed adjacent to the Sudbury Structure. These represent the oldest crust underlying the study area rocks, and therefore an important potential crustal contaminant of the mafic igneous rocks along with the Algoman granites, unless isotopically distinct lower crustal rocks are identified (*i.e.* Kapuskasing uplift?).

The Algoman granites consist of the Dinny Lake Granite (McCrank *et al.*, 1981), associated with the East Bull Lake gabbro-anorthosite pluton, the Birch Lake Batholith in the Agnew Lake area (Card and Palonen, 1976), and the Cartier Batholith to the west of the Sudbury Structure (Card and Innes, 1981). These granites are interpreted as syn- or post-Kenoran (characterized by zircon ages of *circa* 2900 to 2700 Ma (see references in Previous Work, Regional Geology section) and *circa* 2500 Ma K-Ar ages; Stockwell *et al.*, 1970) due to the lack of severe deformation or metamorphism (Card, 1978). These rocks are medium- to coarse-grained and leucocratic, varying in colour from grey to pink to brick-red (*e.g.* Moore

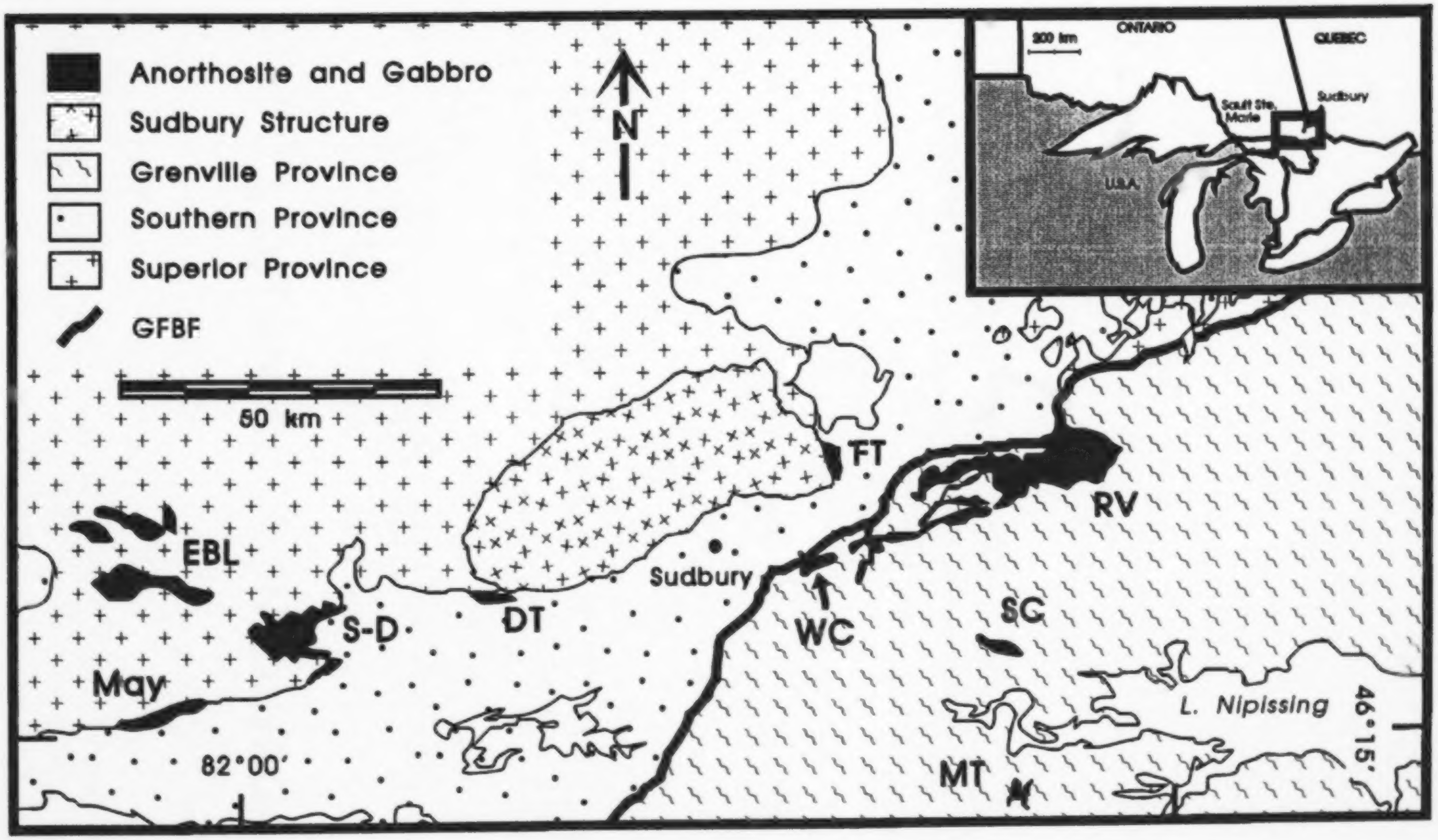
Anorthosite and Gabbro
Sudbury Structure
Grenville Province
Southern Province
Superior Province
GFBF
50 km
N
200 km
ONTARIO
QUEBEC
Sault Ste. Marie
Sudbury
U.S.A.
EBL
S-D
May
DT
82°00′
Sudbury
FT
WC
RV
SC
MT
L. Nipissing
46°15′

Figure 2.1. Location of study area, showing the distribution of Early Proterozoic gabbro-anorthositic rocks. EBL=East Bull Lake; S-D=Shakespeare-Dunlop; DT=Drury Twp.; FT=Falconbridge Twp.; WC= Wanapitei *Complex*; RV=River Valley; SC=St. Charles; MT=Mercer Twp.; *GFBF=Grenville Front Boundary Fault*

and Armstrong, 1945; Robertson, 1976). The texture varies generally north to south from massive and equigranular (the Cartier Batholith; Card and Innes, 1981) to foliated (the Dinny Lake Granite; McCrank *et al.*, 1983) to the partly gneissose and migmatised Birch Lake Batholith (Card, 1978). Much of the granite reflects regional greenschist-facies metamorphism (Card, 1965). Porphyritic quartz monzonite and granodiorite are common. More rarely, late porphyritic granite, aplite and quartz monzonitic pegmatite are present (Card, 1978), and locally, rapakivi and graphic textures are developed (Card and Innes, 1981). The batholiths may be granodiorite, sodic granite (Robertson, 1976), or more commonly quartz monzonite (Card, 1978).

The field relationships between the Algoman granites and the adjacent Huronian metasediments, mafic volcanics and mafic intrusions are complex. *Lit-par-lit* injection of granites into metavolcanic amphibolites is observed in Drury Township (Card, 1965). The granitic rocks contain xenoliths of biotite, chlorite, and hornblende-bearing mafic rocks (probably of mafic volcanic origin), quartzose paragneiss, and granitoid gneiss (Robertson, 1976; Card, 1978). No primary textures or structures are present in the mafic inclusions (Robertson, 1976), which are assimilated to varying degrees (Card and Innes, 1981). Early workers interpreted the Algoman granites as post-Huronian, mainly on the basis of these mafic inclusions, and as a result of a correlation with Killarnean granites (Collins, 1936). These were later shown to postdate dykes which cut the Algoman rocks (Moore and Armstrong, 1945). The mafic xenoliths, originally interpreted as metavolcanic in origin (Card, 1965), were subsequently identified as mafic intrusions, postdating the granite (Card, 1978). The contact between the granite and the metasediments and metavolcanics, where not fault-bounded or sheared, supports an older age for the granite, based on the absence of granite apophyses or contact metamorphic effects in the sediments, or a chilled margin in the granite (Card, 1965; Card, 1978). The contact is gently undulating and very regular where visible, with the sediments unconformably overlying the granite (Card, 1965). Also, green, sericitised feldspars in the granite below the contact may represent pre-Huronian weathering (Card, 1965).

All of the Algoman batholiths are mineralogically similar, consisting of approximately equal proportions of quartz, plagioclase (albite to oligoclase), and perthitic microcline, where porphyritic phases are dominated by coarse phenocrysts of the latter mineral. Hornblende or biotite are the dominant accessory minerals, but also present are chlorite, muscovite, epidote, sphene, zircon, apatite, monazite, iron-titanium oxides, sulphides, and very rarely, augite (Moore and Armstrong, 1945; Card, 1978; Card and Palonen, 1978; Card and Innes, 1981). Foliation is present locally, expressed by alignment of femic minerals and elongation and alignment of quartz grains (Card, 1978; McCrank *et al.*, 1983). Plagioclase- and femic mineral- (particularly hornblende) enriched diorite gneiss in the Birch Lake Batholith is thought to represent partially assimilated mafic intrusive or volcanic rock (Card and Palonen, 1978).

The lower age constraint for the pre-Huronian basement is a U-Pb zircon age of 2668 +2.3/-2.2 Ma from the Kasubeck Creek granodiorite (Krogh and Turek, 1982), a plutonic high-level intrusive from the Wawa Subprovince. There is no precise isotopic data for the Algoman granites. The most recent geochronological data is that of Van Schmus (1965), who presents Rb-Sr mineral-whole rock ages of 1925 ± 35 Ma and 1715 ± 30 Ma from a feldspar and a biotite from Algoman basement. Earlier K-Ar ages on biotite and muscovite range from around 1500 Ma to about 2650 Ma (Lowdon, 1960; 1961; 1962; 1963), and Rb-Sr ages of 2035 ± 200 Ma and 2400 ± 120 Ma were obtained by Fairbairn *et al.* (1960). A possible minimum age for the Algoman granites is provided by a U-Pb zircon age of *circa* 2450 Ma (Heaman, 1989) and an Rb-Sr whole-rock plus mineral age of 2690 ± 93 Ma (Gates and Hurley, 1973) for the Matachewan dykes, which have been tentatively correlated with an essentially undeformed porphyritic diabase dyke swarm which cuts the granites (Moore and Armstrong, 1945).

2.2 EARLY PROTEROZOIC MAFIC ROCKS

Along with various shallow level mafic dyke swarms, the Algoman granites have been intruded and overlain by gabbro-anorthosite plutons and extensive sheets of mafic volcanics, respectively. These are classified locally as basal or sub-basal Huronian (*e.g.* Card, 1978; Card, 1988).

2.2.1 Gabbro Anorthosite Intrusions

Three sill-like layered gabbro-anorthosite bodies have been intruded along the contact between the Superior Province Algoman granites and the Huronian volcanics and sediments. The largest of these is the Shakespeare-Dunlop intrusion, which includes a smaller offshoot to the south known as the Beaver Pond Gabbro (McCrank *et al.*, 1981). Two narrow, elongate smaller gabbro-anorthosite bodies located in May and Drury Townships lie to the south and east, respectively, of the Shakespeare-Dunlop intrusion. A large funnel-shaped lopolithic body, the East-Bull Lake pluton, intrudes the Algoman granites and is entirely within the Superior Province. A narrow, east-west trending body is located in Tennyson Twp., midway between the East Bull Lake and May Twp. intrusions. Presumably genetically related dykes of similar composition to these larger bodies are associated with the gabbro-anorthosite plutons.

2.2.1.1 The East Bull Lake Pluton

Of all of the rocks in this study area, the East Bull Lake (EBL) intrusion has been by far the most intensively studied, courtesy of the Canadian Nuclear Waste Management Program of Atomic Energy of Canada Limited (A.E.C.L.), as well as a M.Sc. thesis from Laurentian University (Born, 1979). As a result of work over the past ten years, particularly that of D.C. Kamineni, thorough data is available concerning the effects of both low- and high-temperature alteration. Consequently, the intrusion is also well mapped. Recent remapping of the EBL intrusion has been undertaken emphasizing PGE mineralization (Peck *et al.*, 1991).

Originally mapped as "Haileyburian" in age, and thought to predate the Algoman granites (Moore and Armstrong, 1945), the EBL intrusion consists of one large gabbro-anorthosite pluton trending roughly east-west and three smaller, possibly unrelated metagabbro bodies two or three kilometres to the north, all hosted by Algoman granite. The local geology and sample locations for this study are shown in Figure 2.2. The main pluton is elliptically shaped, about 13 km long and 4 km wide, with an underlying area of about 43 km^2 (Peck *et al.*, 1991). The presence of gently inwards dipping (5-30°, averaging 20°) cumulate layers is consistent with preservation of a basin-type structure (Born and James, 1978). These authors interpret the lack of chilled margins and of intrusive relationships between the EBL and older units as indicating post-crystallisational tectonic emplacement of the gabbro-anorthosite.

Although the smaller outlying bodies, referred to as gabbro dykes by McCrank *et al.* (1983), are strongly metamorphosed and mapped as metagabbro (unpublished A.E.C.L. data), the main pluton contains fresh gabbro-anorthosite, particularly towards the central plateau. Born and James (1978) have distinguished nine different zones, based on compositional and textural criteria, and more intensive work by Kamineni *et al.* (1984) has distinguished twelve zones in the central plateau alone. Remnant primary mineralogy includes olivine, showing evidence of disequilibrium with adjacent orthopyroxenes (James *et al.*, 1983), preserved near the centre of the pluton (near the west side of East Bull Lake). Olivine, calcic plagioclase and augitic clinopyroxene are commonly cumulate textured (James *et al.*, 1983). Primary textures include subophitic plagioclase, nodular anorthositic gabbro, and dendritic gabbro (McCrank *et al.*, 1983), as well as primary layering including cross-bedding (Born and James, 1978). Locally, granophyric K-feldspar-bearing phases are present, displaying graphic quartz-feldspar intergrowths (McCrank *et al.*, 1983).

In general, the olivine has been replaced by tremolite, pyroxene (augite or diopside) by actinolite and/or blue-green hornblende, and the plagioclase (labradorite to andesine) by chlorite and epidote minerals (*i.e.* saussuritised, as well as kaolinitised) (Moore and Armstrong, 1945; James *et al.*, 1983). Primary apatite, orthopyroxene (occasionally enstatite), and ilmenite (altered to leucoxene) also occur. An extensive study of the petrographic effects of various secondary alterations undertaken by A.E.C.L. and the G.S.C. is presented in a series of papers (Kamineni *et al.*, 1984;1985;1987; Kerrich *et al.*, 1987) plus a study of the fluids involved (McNutt *et al.*, 1987). In summary, three forms of secondary minerals were identified, consisting of rims on primary crystals, replacement of primary minerals by hydrous phases, and microfracture fillings. These minerals were interpreted in terms of traditional metamorphic facies presenting a sequence progressing from epidote-amphibolite/greenschist to low-temperature (< 100°) water-rock interaction. These "facies" were found to correlate with orogenic events, anorogenic magmatic heating, or subsedimentary burial, rather than representing a continuous sequence generated by slow cooling.

The pluton itself and the local area has been strongly affected by younger (mid-Proterozoic) faulting, particularly by the Folson Lake fault zone, which traverses the pluton from northwest to southeast. The extent of the faulting has been examined through preliminary magnetotelluric geophysical work (Kurtz and Niblett, 1984).

Major element geochemistry on 32 relatively fresh, mostly cumulate samples indicates a dominantly calc-alkaline to weakly tholeiitic affinity (Born, 1979). Born suggests that the observed EBL intrusion represents a more fractionated product of a sub-alkaline, possibly high-alumina tholeiitic basaltic magma, and is therefore not itself representative of the original parent magma. He suggests relatively low-pressure fractionation (*i.e.* at shallow crustal levels) crystallising cumulate olivine and plagioclase, followed by intercumulate clino- and orthopyroxene, dominated by the latter variety. Major element data are available for a number of secondary minerals, particularly amphiboles (Kamineni, 1986) and extensive major and trace element data (excluding the REE) are available for 26 whole-rock samples in various states of replacement (none of them "fresh") from Kerrich *et al.* (1987).

The EBL intrusion has been precisely dated by U-Pb isotopes on one zircon and two baddeleyite fractions at 2480 +10/-5 Ma (Krogh *et al.*, 1984). Precise Rb, Sr, ^{87}Rb/^{86}Sr, and ^{87}Sr/^{86}Sr data is available for some low-temperature minerals and altered whole-rocks (McNutt *et al.*, 1987). The Rb-Sr isotopic data is geochronologically meaningless, roughly constrained by reference isochrons of 2500 and 500 Ma with I_{Sr} varying from around 0.703 to 0.710 respectively. Unpublished Sm-Nd isotopic data from two whole-rock-clinopyroxene-plagioclase isochrons gives one age of 2472 ± 76 Ma and one much less precise but similar age, with I_{Nd} values around

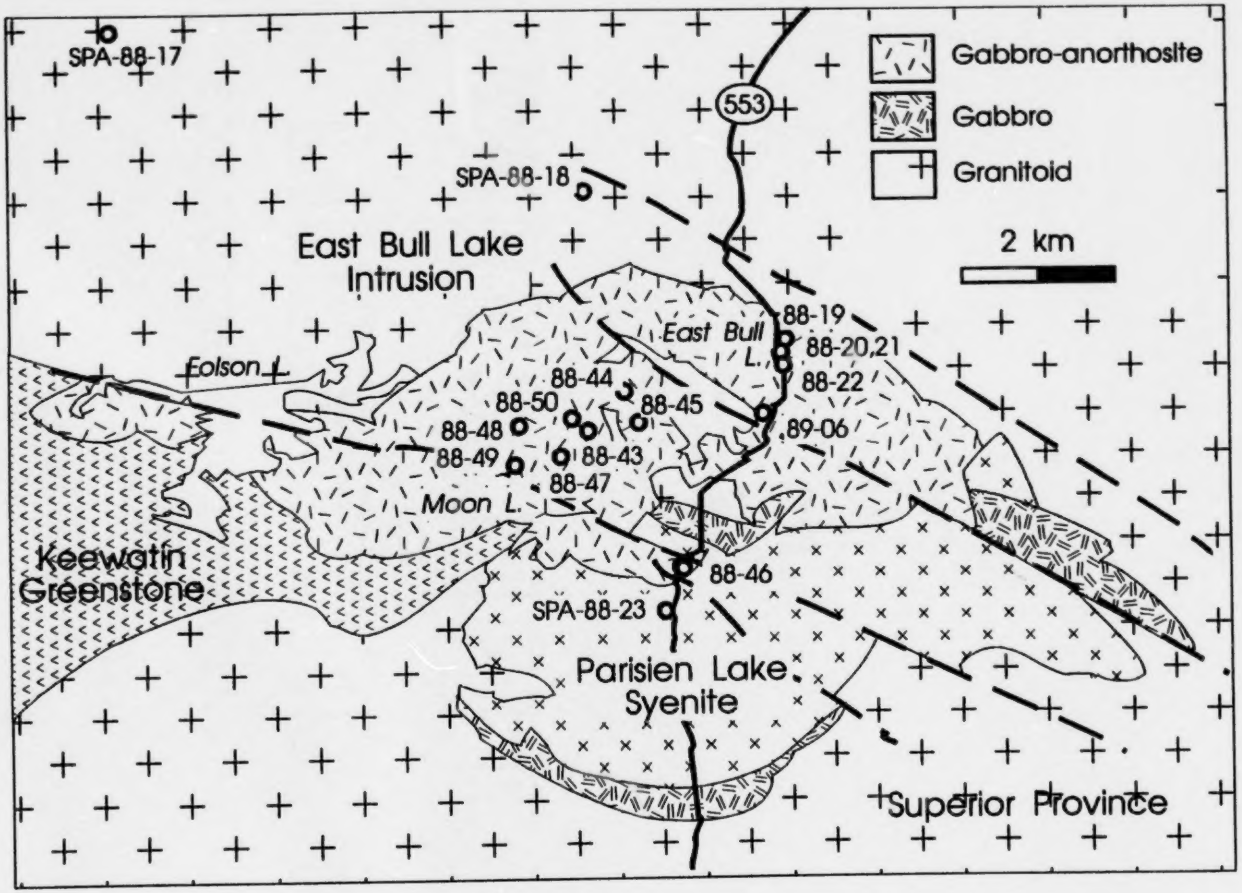
Gabbro-anorthosite
Gabbro
Granitoid
2 km
553
SPA-88-17
SPA-88-18
East Bull Lake
Intrusion
Folson L.
East Bull
L.
88-19
88-20,21
88-22
89-06
88-44
88-45
88-50
88-48
88-49
88-43
88-47
Moon L.
Keewatin
Greenstone
88-46
SPA-88-23
Parisien Lake
Syenite
Superior Province

Figure 2.2. The East Bull Lake intrusion, showing sample locations.

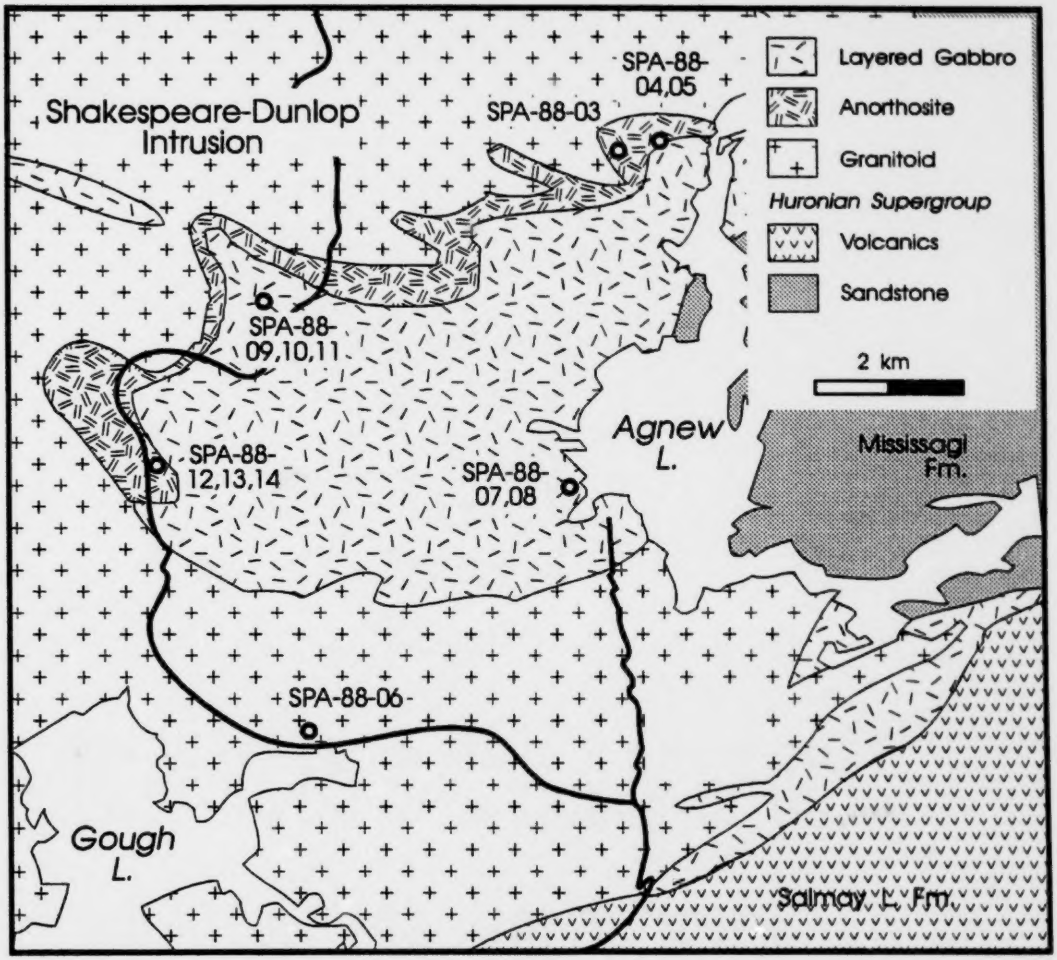
Shakespeare-Dunlop Intrusion
SPA-88-04,05
SPA-88-03
SPA-88-09,10,11
SPA-88-12,13,14
SPA-88-07,08
SPA-88-06
Agnew L.
Gough L.
Mississagi Fm.
Salmay L. Fm.
Layered Gabbro
Anorthosite
Granitoid
Huronian Supergroup
Volcanics
Sandstone
2 km

Figure 2.3. The Shakespeare-Dunlop intrusion, showing sample locations.

0.5093 (D.C. Kamineni, pers. comm., 1987). This suggests that the REE isotopes have been relatively unaffected by secondary processes at the mineral scale, at least in the fresher rocks.

2.2.1.2 The Shakespeare-Dunlop Intrusion

In contrast to the East Bull Lake intrusion, surprisingly little data is available for the Shakespeare-Dunlop (S-D) intrusion. This layered gabbro-anorthosite body coincides with the Superior Province - Southern Province boundary adjacent to the north and west sides of Agnew Lake, at the western boundary of Shakespeare and Dunlop townships., shown in Figure 2.3. It is the largest mafic intrusion in the area, occupying an area of 12 km^2 (James and Harris, 1977). A smaller body to the southeast known as the Beaver Pond Gabbro (McCrank *et al.*, 1981) is not discussed independently of the S-D intrusion and probably represents a fault-removed slice thereof.

The intrusive contact with the Algoman granite (the Birch Lake Batholith, in this area) is characterised by a chilled margin in the gabbroic rock, gabbroic dykes extending out into the granite, and partially remobilised or remelted xenoliths of granite within the marginal zones (Card and Palonen, 1976; Card, 1978). The contact between the S-D intrusion and the mafic volcanics to the south varies locally from tectonic or unconformable to a gradation between coarse-grained gabbroic-anorthosite or medium-grained basalt and fine-grained pillow basalt interbedded with sediments (Card and Palonen, 1976).

The attitude of primary magmatic layering in the western and northern parts of the pluton suggests that the S-D intrusion is a thick sill-like or funnel-shaped lopolithic body (Card and Palonen, 1976). The thickness of the layering varies from 5 cm up to 90 m (Card, 1978) where not destroyed by the recrystallisation and deformation more prevalent in the southern and eastern areas. Magmatic flow alignment of plagioclase laths is present locally, and magmatic differentiation has produced cumulate variation in mineralogy and texture. James and Harris (1977) recognised three main subdivisions. From the margin inwards, the gross structure consists of an outer (and basal) "anorthosite zone" consisting of variably textured anorthosite to gabbro, a second, "outer layered zone" dominated by layered pyroxenitic gabbro, and a third "inner layered zone" dominated by layered coarse-grained gabbro. Eight distinct compositional and/or textural zones were identified within the three main subdivisions. The basal anorthositic rocks were emplaced as a partially crystalline mush, and upper porphyritic and dendritic phases are interpreted as representing crystallisation of trapped intercumulus liquids (James and Harris, 1977).

The original mineralogy of the pluton is very poorly preserved; plagioclase (originally labradorite?) has been extensively saussuritised, and augitic clinopyroxene has been almost completely replaced by actinolite and blue-green hornblende (Card and Palonen, 1976). Quartz, biotite, chlorite, epidote and iron-titanium oxides are also present in minor amounts. Sub-alkaline tholeiitic to calc-alkaline affinity is indicated, based on six analyses (Card, 1978).

An upper, coarse-grained granophyric phase of the Shakespeare-Dunlop intrusion has been precisely dated at 2491 ± 5 Ma by U-Pb on three zircon fractions (Krogh *et al.*, 1984). The $^{207}Pb/^{206}Pb$ ages of the three fractions range from 2224 to 2465 Ma. No other isotopic data is available for this intrusion.

2.2.1.3 May Township Gabbro-Anorthosite

This elongate intrusion lies in Victoria, Salter and May Townships, north of (but not cut by) the Murray Fault. It has been referred to as the "Salmay Township" intrusion (Ashwal and Wooden, 1989), but this name has not been used here both because of its inaccuracy and to avoid confusion with the associated Salmay Lake Volcanics (Robertson, 1976). Most of the available information on this body originates from Cape (1973), who studied its eastern extension, summarised in Robertson (1976).

The May Township gabbro-anorthosite intrusion (MT), shown in Figure 2.4, is exposed discontinuously along the contact with unspecified Algoman granite and the basal Huronian volcanics (the Salmay Lake Volcanics) and sediments for a length of near 20 km. The width varies from nearly a kilometre in places to less than 100 m in May Township and pinches out entirely to the west in two or three places beneath basal Huronian sediments (Robertson, 1976). Although the granite-gabbro contact is not exposed, a chilled margin is present in the gabbro-anorthosite, or coarser-grained gabbro suggesting magma movement along the contact during crystallisation (Cape, 1973).

Cape identifies three main subdivisions in the gabbro-anorthosite; an upper, extremely coarse-grained anorthositic to melanocratic (metamorphosed) gabbro, a middle coarser-grained, mottled gabbro to anorthositic gabbro, and a lower, medium to fine-grained mafic gabbro. Very limited rhythmic layering is evident, relative to the Shakespeare-Dunlop intrusion, although this may reflect lack of preservation due to recrystallisation and deformation (Cape, 1973). Mineralogies and textures similar to those observed in the S-D intrusion are described by Cape, including the basal granulated anorthosite, cumulate plagioclase, heavily saussuritised plagioclase (originally labradorite or bytownite), and (in this case) complete replacement of pyroxene by amphiboles. Cape suggests a crystallisation sequence of apatite-magnetite-ilmenite-plagioclase-pyroxene-quartz and alkali-feldspar.

The upper zone of this body consists of heterogeneous-textured, coarse-grained anorthositic gabbro veined by epidote. The irregularity of the variations in mineralogy and grain size, as well as the absence of an upper fine-grained (chilled) margin suggests that the original upper members of the intrusion have been eroded away (Cape, 1973). If a thickness to width ratio typical of lopolithic intrusions is assumed (0.1 to 0.05; Carmichael *et al.*, 1974, p. 462) then loss of approximately 150 to 300 metres is suggested (based on Cape's assumption of length not more than 6 miles). This does not take into account material lost due to tectonic displacement (faulting).

Major element and limited trace element data (not including Rb, Sr, Pb, or REE) are available for the intrusion, indicating a subalkaline tholeiitic to calc-alkaline affinity (Robertson, 1976), comparable to the S-D intrusion. No isotopic work has been done on the May Township gabbro-anorthosite prior to this study.

2.2.1.4 Drury Township Gabbro-Anorthosite

The smallest of the mafic intrusions included in this study is located in eastern-central Drury Township, shown in Figure 2.5. The actual extent of the intrusion is difficult to determine, as it was originally mapped as a hornblende-syenite phase of the basal Huronian volcanics (Card, 1965), which begin in western Drury Township and continue eastwards around the Sudbury Structure. The "hornblende-syenite" crops out in an area of about five by two kilometres in eastern Drury Township (Card, 1965), and was not identified by the same author in the adjacent township (Denison) to the east (Card, 1968). This unit, later identified as an intrusive (Card, 1978), intrudes the Algoman Birch Lake Batholith to the north, and is bounded to the south by Nipissing Diabase and basal Huronian volcanics (Card, 1965; Card, 1978).

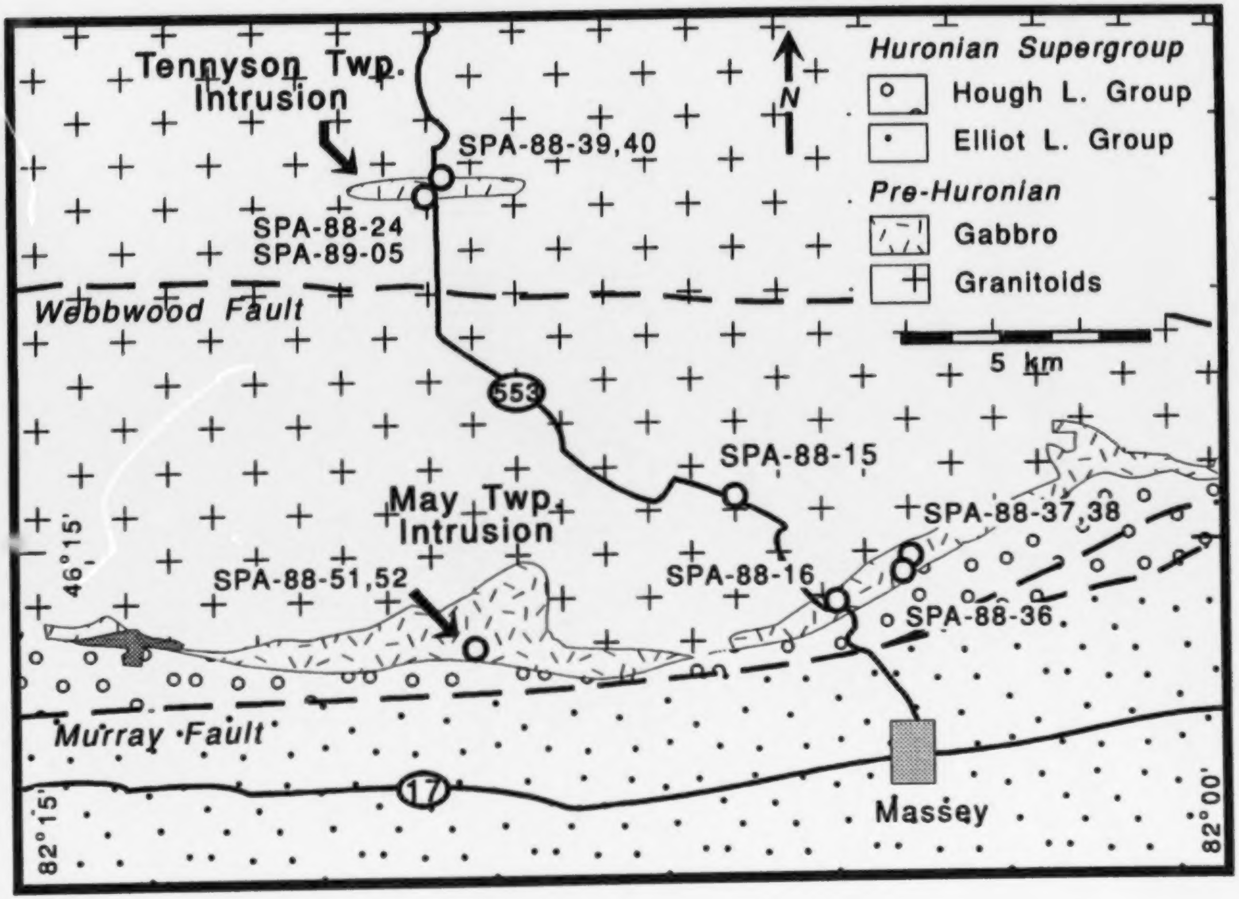
Tennyson Twp.
Intrusion
SPA-88-39,40
SPA-88-24
SPA-89-05
N
Huronian Supergroup
Hough L. Group
Elliot L. Group
Pre-Huronian
Gabbro
Granitoids
5 km
Webbwood Fault
553
SPA-88-15
May Twp.
Intrusion
SPA-88-37,38
SPA-88-16
SPA-88-51,52
SPA-88-36
46°15'
Murray Fault
17
Massey
82°15'
82°00'

Figure 2.4. The May Township intrusion, showing sample locations.

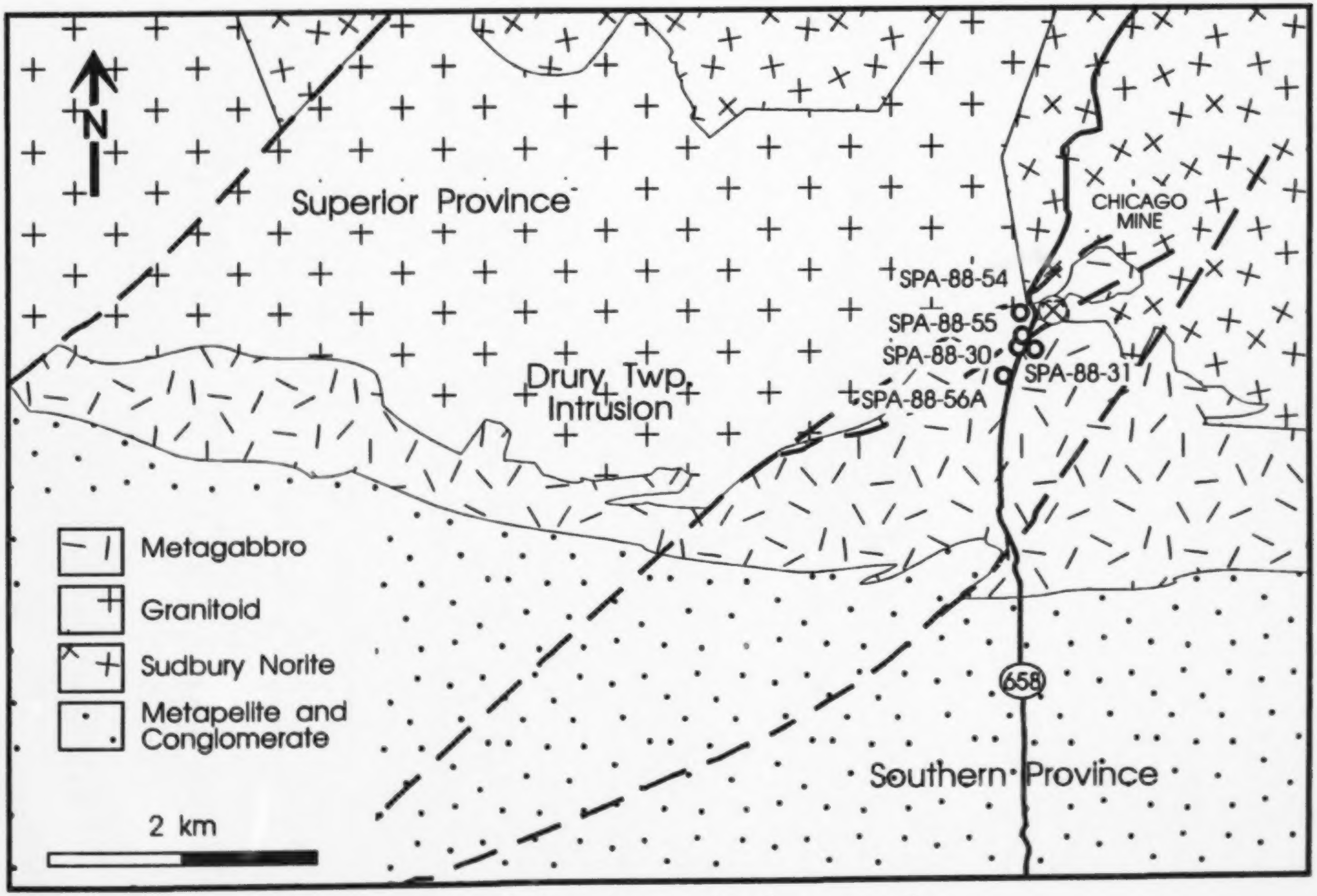
N
Superior Province
Drury Twp. Intrusion
CHICAGO MINE
SPA-88-54
SPA-88-55
SPA-88-30
SPA-88-31
SPA-88-56A
658
Southern Province
Metagabbro
Granitoid
Sudbury Norite
Metapelite and Conglomerate
2 km

Figure 2.5. *The Drury Township intrusion, showing sample locations.*

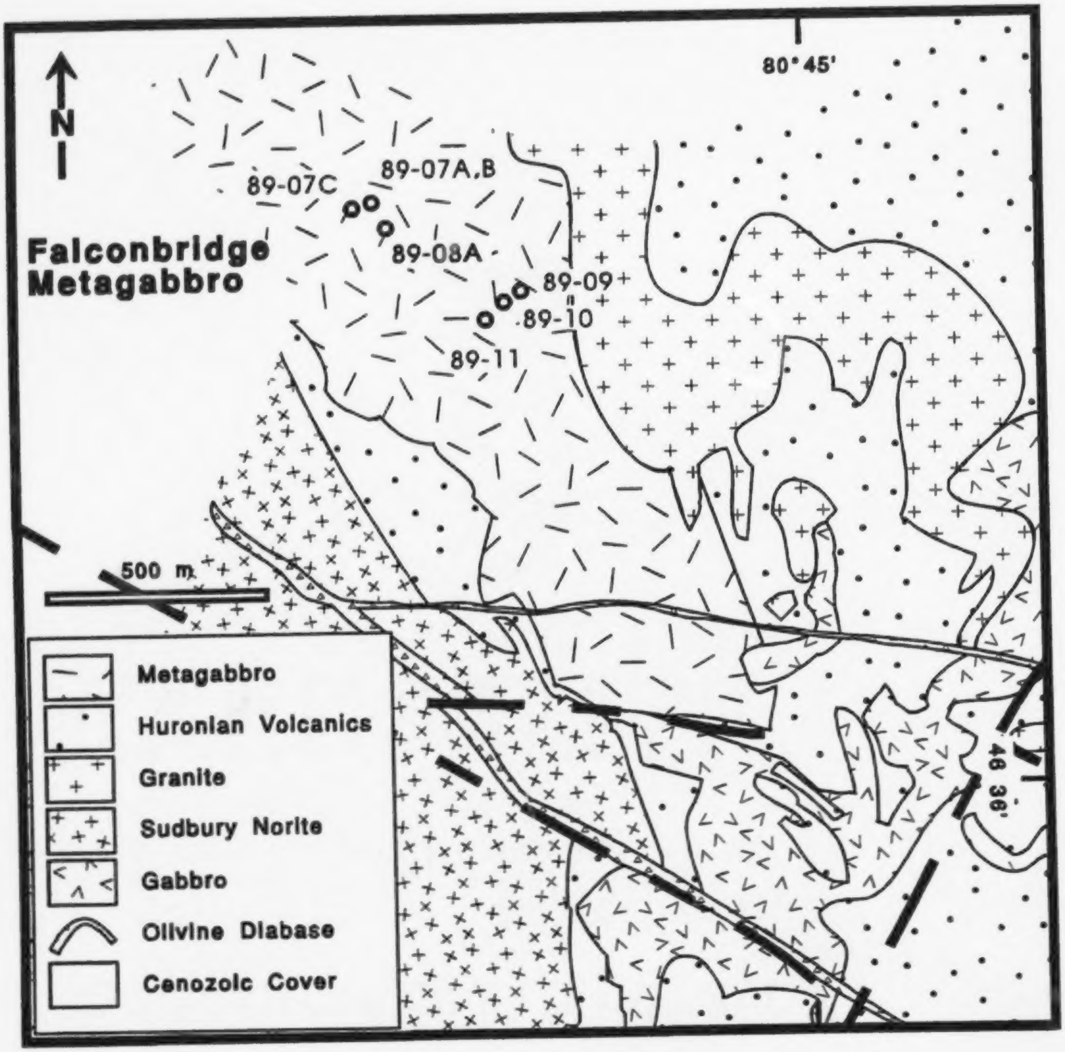
N
80°45'
Falconbridge Metagabbro
89-07C
89-07A,B
89-08A
89-09
89-10
89-11
500 m
46°36'
Metagabbro
Huronian Volcanics
Granite
Sudbury Norite
Gabbro
Olivine Diabase
Cenozoic Cover

Figure 2.6. The Falconbridge Township intrusion, showing sample locations.

The Drury Twp. metagabbro is a leucocratic, massive to osed of saussuritised plagioclase and chloritised hornblende. It is heterogeneous in terms of grain size and composition. Pegmatitic (with phenocrystic hornblendes up to 30 cm long) and anorthositic varieties are present, locally. The metagabbro is associated with medium to coarse-grained massive to gneissic amphibolite (Card, 1965), which is likely also part of the intrusion (Card, 1978). The mineralogy is again dominated by amphibole (hornblende and tremolite), plagioclase, epidote and chlorite, plus lesser quantities of alkali-feldspar, biotite, garnet, quartz, carbonate, white mica, ilmenite, sphene, and magnetite (Card, 1965). This body is much more strongly metamorphosed than the previous gabbro-anorthosites, as shown by the absence of any primary structure and the alteration mineralogy, including three minerals not mentioned from the other bodies (garnet, carbonate, and white mica).

Prior geochemistry on this intrusion consists of major element plus limited trace element analyses from one sample, from which the (high) alumina content was used to infer a gabbro-anorthositic affinity (Card, 1965). No isotope geochemistry has been undertaken on the Drury Township gabbro-anorthosite intrusion prior to this study.

2.2.1.5 Falconbridge Twp. Intrusion

In addition to the four gabbro-anorthosite intrusions discussed above, there exist other smaller or less obviously related bodies. These include a small hornblende-feldspar body in Falconbridge Township which is about two kilometres long and half a kilometre wide, elongated in a north-south direction, shown in Figure 2.6. This appears to be even more poorly preserved than the Drury Township intrusion, although of similar composition (Thomson, 1957). No prior geochemistry is available for this body, and only superficial petrology.

2.2.1.6 Wanapitei Intrusion

The Wanapitei intrusive complex (Figure 2.7) is a small elliptical body lying immediately south of the Grenville Front Boundary Fault east of Sudbury. It was mapped by Lumbers (1975) and in more detail by Rousell and Trevisiol (1988). The latter authors divide it into two main zones; a gabbroic zone and a strongly deformed hornblende plagioclase gneissic zone. There is not sufficient published chemistry to compare with the gabbro-anorthosite intrusions west of Sudbury, although the degree of preservation (given the proximity to the Irruptive) and the absence of an anorthositic component suggest different geneses. Lumbers (1975) indicates that the gabbro is cut by an anorthosite on its southeastern margin, but this unit is mapped by Rousell and Trevisiol (1988) as hornblende plagioclase gneiss.

2.2.1.7 St. Charles Anorthosite Sill

A small sill-like layered anorthositic body south of the Grenville Front in Casimir Township near St. Charles, Ontario (shown in Figure 2.8), may also represent early Proterozoic mafic magmatism based on its mineralogical similarity and proximity to the early Proterozoic River Valley Complex to the northeast (Ashwal and Wooden, 1989). This is in spite of the fact that the previously suggested association is with *circa* 1500 to 1200 Ma old igneous activity (Lumbers, 1975) such as the Whitestone Anorthosite to the south near Parry Sound, Ontario, dated at 1350 ± 50 Ma (van Breemen *et al.*, 1986). Extensive petrographic work has been done by Rousell (1978, 1981), as well as major element whole-rock geochemistry on nine samples of gabbro and gabbroic anorthosite (Rousell, 1978) and trace element geochemistry (Simmons and Hanson, 1978).

2.2.1.8 Mercer Anorthosite

A small highly deformed anorthositic body in Mercer Township (Figure 2.9), southwest of Lake Nipissing has been mapped by Lumbers (1975) and included by Simmons and Hanson (1978) as a "Burwash area" anorthosite. They suggest an origin for the St. Charles and Mercer anorthosites similar to that of the Nain and Adirondack massif anorthosites, based on trace element (especially REE) geochemical evidence.

2.2.2 Basal Huronian Volcanics

The Elliot Lake Group is the basal unit of the Huronian supracrustal sequence and consists of both mafic and felsic volcanics as well as quartzitic, argillitic and conglomeratic members, with increasing proportions of the latter units towards the top. The basal volcanics are dominantly mafic and are bimodal, with volumetrically small quantities of intermediate compositions between basaltic and rhyolitic. In the Sudbury area the sequence upwards consists of the mafic Elsie Mountain and Stobie Formations, overlain by the felsic Copper Cliff Formation. Although the Huronian Supergroup continues extensively to the northeast of the Sudbury Structure, the basal volcanics thin out at the southeast end of the Structure. To the west and southwest, lateral equivalents of the Stobie Formation include the Salmay Lake Volcanics, in the area north of Espanola and Massey, Ontario. The volcanics thin out in this area, disappearing entirely southeast of Elliot Lake (Robertson, 1977), but thickening again at the western end near Thessalon, Ontario. The laterally equivalent volcanic sequences are described by Jolly (1987a), Robertson (1976), Card (1965, 1968, 1978) and Thomson (1957), from west to east. Sample locations for this study are indicated in Figure 2.10 (see appendix 1.4 also).

The mafic volcanics are interbedded with metasediments of the Matinenda Formation as well as with metasediments derived from the volcanics and from which the metabasalts can be difficult to distinguish in the field. Well-preserved pillows and amygdular textures can be found throughout the lateral extent of the volcanics, but are much more common at the eastern end in the Sudbury area. In general, however, the flows are massive and structureless, and have been metamorphosed to the greenschist or amphibolite facies (Card, 1978). The metabasalts are fine to medium grained, dark green rocks dominated by amphiboles (actinolite and hornblende) and plagioclase (andesine to labradorite) plus lesser amounts of quartz, biotite, chlorite, epidote, garnet, carbonate, sphene, Fe-Ti oxides and sulphides (Card, 1978). These lesser minerals plus the quartz-plagioclase-chlorite-amphibole-bearing amygdules represent secondary metamorphically induced phases. In the geochemical work by Jolly (1987a, b) the amygdules were hand picked out of the analysed samples in order to reduce the effects of secondary components on the geochemistry.

The upper volcanic sequence in the Sudbury area is the Copper Cliff Formation, which consists mainly of equal proportions of rhyolitic flows and pyroclastics. Felsic volcanics are also present at the western end of the series in the Thessalon Volcanics (Jolly, 1987a), but are absent in between.

Although some major and trace element geochemistry is available for the volcanics mapped through the various Ontario government survey projects, the most extensive geochemical study of the Huronian volcanics is that undertaken by W.T. Jolly and coworkers, mainly on the thick, relatively weakly metamorphosed pile in the Thessalon area (Sawiuk, 1978; Cumming, 1985; Jolly, 1987a, b; Jolly *et al.*, 1992). As this study is concerned with the most basal (*i.e.* therefore presumably least evolved) mafic volcanics, a more thorough

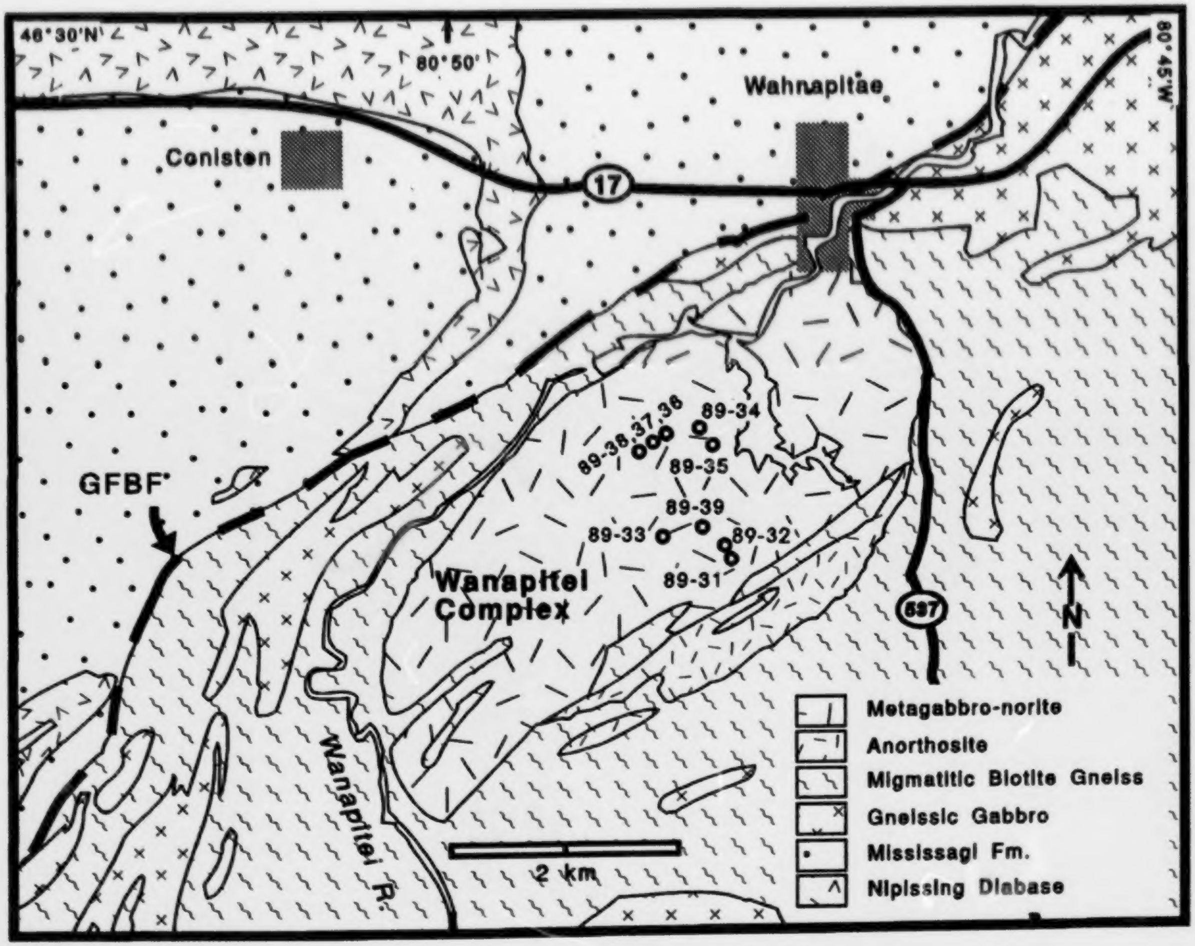
46°30'N
80°50'
80°45'W
Wahnapitae
Coniston
17
537
GFBF
Wanapitei Complex
Wanapitei R.
89-38,37,36
89-34
89-35
89-39
89-33
89-32
89-31
N
2 km
Metagabbro-norite
Anorthosite
Migmatitic Biotite Gneiss
Gneissic Gabbro
Mississagi Fm.
Nipissing Diabase

Figure 2.7. The Wanapitei intrusion, showing sample locations.

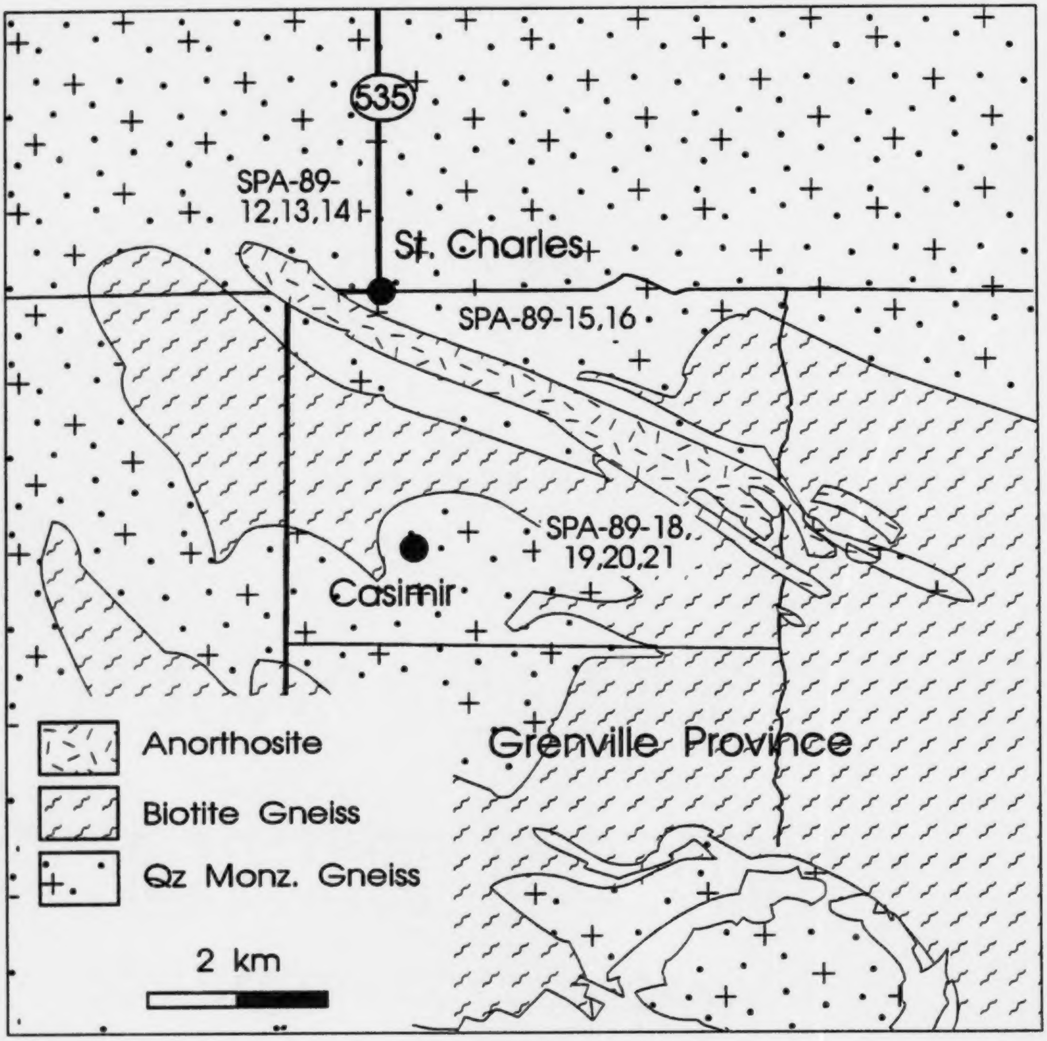
535
SPA-89-
12,13,14
St. Charles
SPA-89-15,16
SPA-89-18,
19,20,21
Casimir
Grenville Province
Anorthosite
Biotite Gneiss
Qz Monz. Gneiss
2 km

Figure 2.8. The St. Charles anorthosite, showing sample locations.

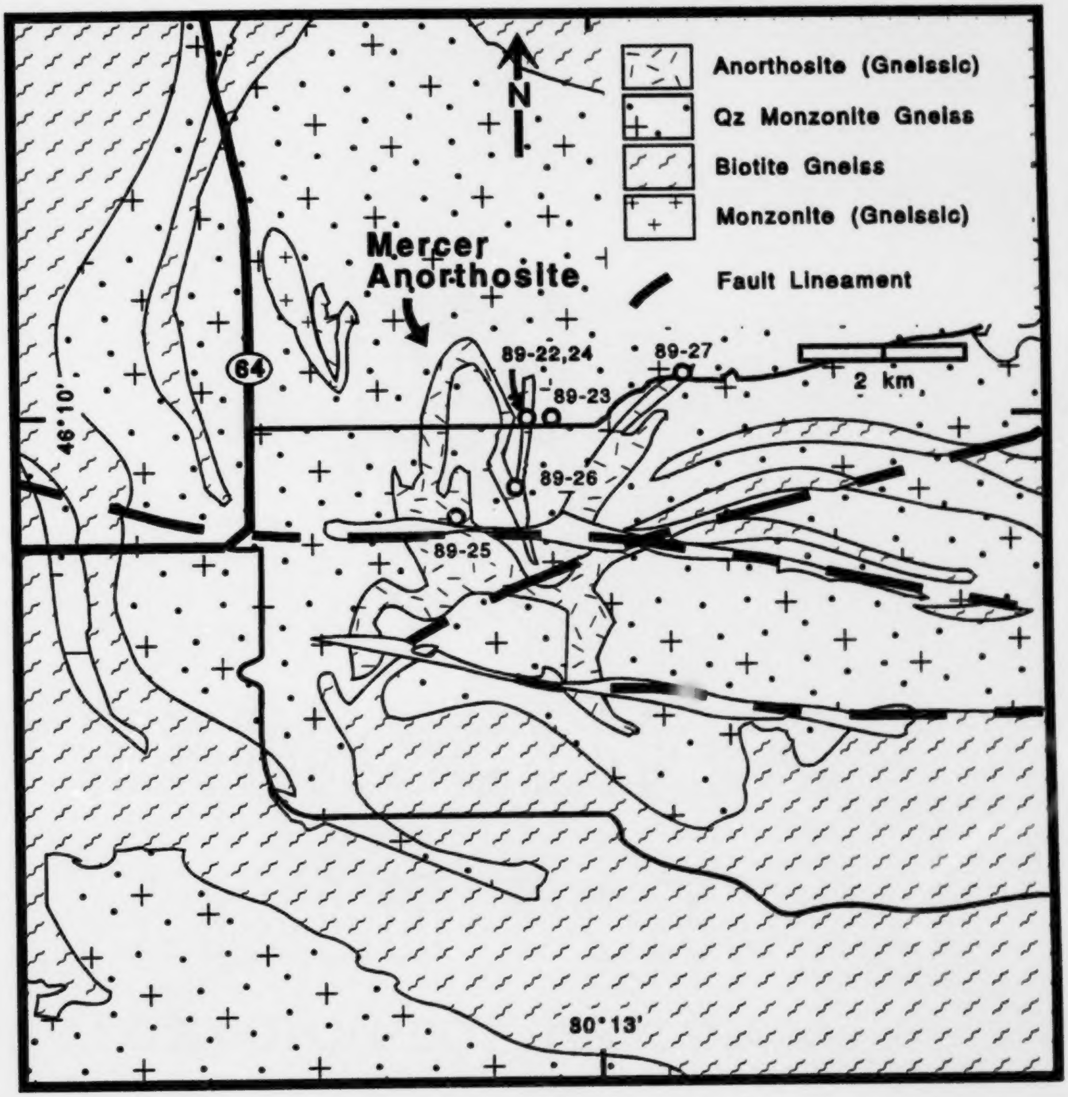
N
Anorthosite (Gneissic)
Qz Monzonite Gneiss
Biotite Gneiss
Monzonite (Gneissic)
Fault Lineament
2 km
Mercer Anorthosite
64
46°10'
89-22,24
89-23
89-27
89-26
89-25
80°13'

Figure 2.9. The Mercer Township anorthosite, showing sample locations.

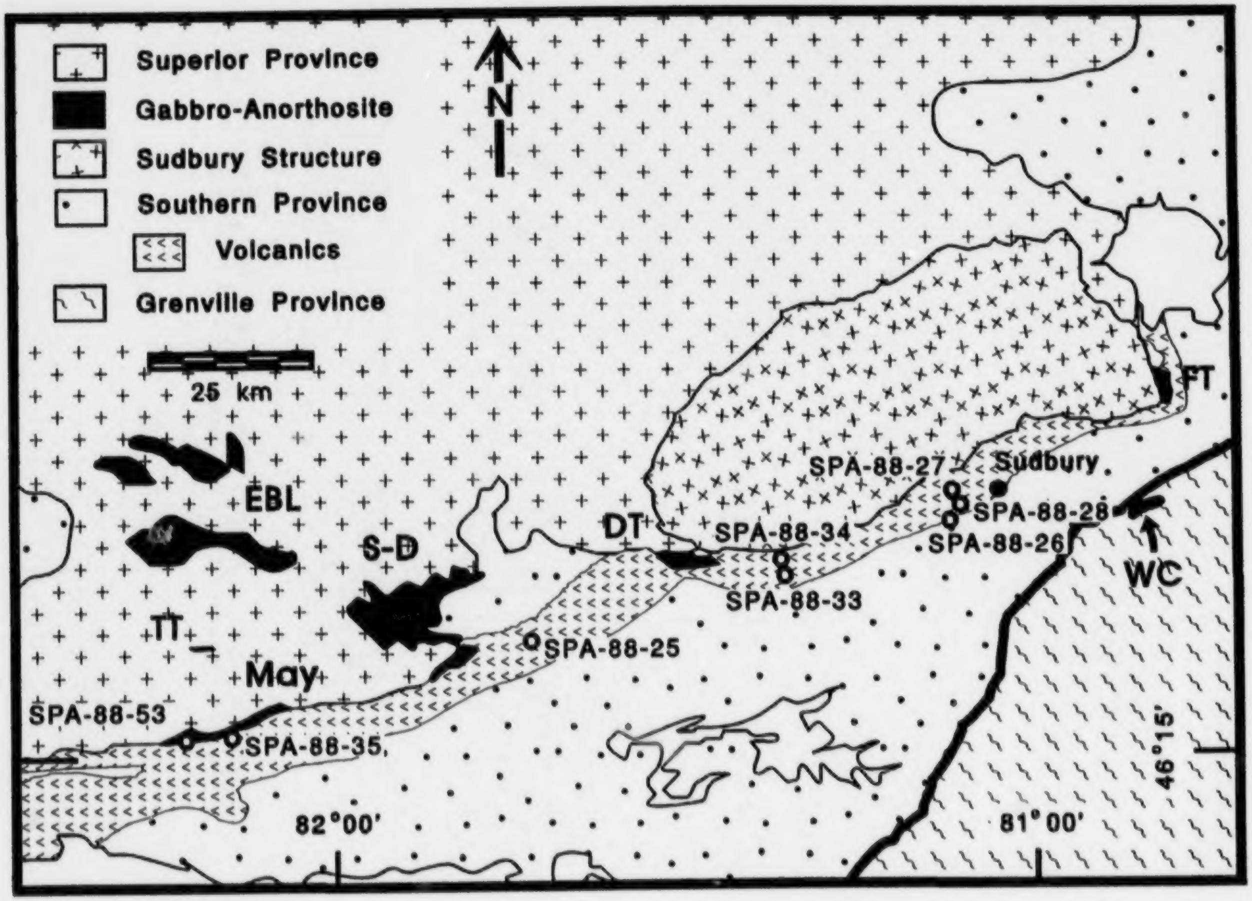
Superior Province
Gabbro-Anorthosite
Sudbury Structure
Southern Province
Volcanics
Grenville Province
N
25 km
EBL
S-D
TT
May
DT
FT
WC
Sudbury
SPA-88-53
SPA-88-35
SPA-88-25
SPA-88-34
SPA-88-33
SPA-88-27
SPA-88-28
SPA-88-26
82°00'
81°00'
46°15'

Figure 2.10. Huronian volcanics, showing sample locations.

summary of Jolly's work is warranted here. Jolly (1987a) identifies five components in the Thessalon sequence, listed with increasing height as follows;

1) Lower mafic sequence (< 500 m), consisting of early basalts and basaltic andesites, both massive and with pillows and amygdules.

2) Early felsic flows (< 200 m), consisting of massive to amygdular rhyolite, as well as porphyritic devitrified glass.

3) Massive basalts (< 100 m), dominated by plagioclase, clinopyroxene, and amygdules, and with hematised flow tops suggesting subaerial eruption.

4) A questionable member, containing both basaltic and rhyolitic volcanics, but as a fault-bounded block with very poor stratigraphic control.

5) Massive mafic basalt, with minor intermediate lavas.

The primary mineralogy of the basalts was labradorite, now albitised, and augitic clinopyroxene. The clinopyroxene is commonly preserved, but the plagioclase is only preserved in thicker flows distant from later intrusions.

The geochemistry of the Thessalon Volcanics defies a simple (*i.e.* one or two stage) evolutionary model. Whereas the LILE are potentially easily mobilised in these relatively "porous" rocks (*i.e.* amygdules, flow-top breccias, fracture zones), incompatible elements and the REE behave coherently. Jolly (1987a, b) proposes that the basalts originated from about 20 % partial melting of a peridotitic mantle with a LILE and LREE enriched source. The more intermediate composition lavas represent mixtures of the basalts and crustal material represented by the rhyolitic lavas, which in turn originated by a combination of 20 to 40 % partial melting of granitic crust and tonalitic granulite crust. The implied source mantle chemistry suggests a previous (Archean) depletion event involving extraction of tholeiitic basaltic melt as well as a mantle metasomatic enrichment in incompatible elements (Jolly, 1987b). The early, basal basalts in particular appear to have undergone significant amounts of assimilation-fractional crystallisation (AFC) with depleted lower crustal material. This contamination is not evident in later cycles (Jolly *et al.*, 1992)

Relatively little isotopic work has been undertaken on the Huronian volcanics, and available material is limited to some unpublished Rb-Sr work (Knight, 1967) which suggests variable amounts of crustal component reflected by initial $^{87}Sr/^{86}Sr$ ratios (Card, 1978), or alternatively, variable disturbance of the Rb-Sr system.

Geochronology is limited to a U-Pb mineral age on the upper member of the volcanics (the Copper Cliff rhyolite) providing a minimum extrusion age of 2450 +25/-10 Ma (Krogh *et al.*, 1984) from three crack-free and two cracked zircon populations.

2.3 REGIONAL TECTONIC EVOLUTION

The regional tectonic evolution of the Precambrian of the Great Lakes area has been extensively studied around Lake Superior, particularly with regard to the role of basement terrains and their control on subsequent geology and depositional environments (*e.g.* Sims, 1976; Cambray, 1978; Sims *et al.*, 1981). Information on the depositional environment into which the Huronian Supergroup was deposited has evolved through essentially the same criteria (Sims *et al.*, 1981). Sims (1976) suggests a sequence of early development involving the existence of a protocontinental mass with an area in excess of 100,000 square kilometres as of 3.5 Ga ago. Cyclic volcanic activity between 2.75 and 2.70 Ga ago generated the granite-greenstone terrains, composed dominantly of submarine mafic flows, greywackes, and associated granitic intrusions. These were accreted onto the edge of the pre-existing, now gneissic, material, to the south. In the Lake

Superior region the older gneiss is typefied by the Minnesota River Valley Gneisses, dated as old as 3.8 Ga (Goldich and Hedge, 1974).

Sims *et al.* (1981) suggest that the "ancient" boundary between these two (now) basement terrains (*i.e.* gneissic and the granite-greenstone) represents a major crustal feature which separates two distinct geological environments controlled by their respective basements. They also suggest that in the Lake Huron region this feature is manifested in the overlying rocks as the Murray Fault System, a major fault system running hundreds of kilometres from the Sudbury area to Lake Huron along an approximately west-southwesterly trend. Whereas the relative stability of the two basement terrains may have had dramatic effects on the subsequent styles of deposition, the mafic volcanics and gabbro-anorthosites at the base of the Huronian relate to the apparently regional existence of an extensional regime following the Algoman or Kenoran Orogeny. This environment probably also facilitated emplacement of Nipissing-aged (*ca.* 2220 Ma) dyke swarms in Minnesota and the Southern Province (Sims, 1976). Sims *et al.* (1981) attribute the relative instability of the gneiss terrane and therefore presumably also the extensional regime to "crustal foundering" of the gneissic basement. Zolnai *et al.* (1984) attribute local extension and basin subsidence to the south to the presence of a convergent margin such that the older gneisses were thrust to the northwest onto the continental margin, now underlying the Huronian Supergroup. A brief compressional episode followed, demonstrated by the presence of the *circa* 2330 Ma Creighton and Murray granites in the Sudbury area. The presence of an extensive olivine diabase dyke swarm, the Nipissing Diabase, dated at about 2220 Ma (Corfu and Andrews, 1986), suggests the existence of an extensional regime again, at least briefly, for which Zolnai *et al.* (1984) suggest a hot-spot influence.

Subsequent activity in the area includes a major deformational and metamorphic episode beginning at around 1900 Ma known as the Penokean Orogeny, culminating at about 1850 Ma. This coincides with the time of formation of the enigmatic Sudbury Structure. However, the effects of the Penokean Orogeny are most manifest to the southwest in Minnesota, Wisconsin and Michigan. The Murray Fault System was reactivated during this episode, and again during the later Grenville Orogeny (*ca*. 1150 to 950 Ma). Several episodes of mafic dyke emplacement occurred between the Penokean and Grenville Orogenies. The effects of these episodes might be expected to be relatively local and minor, although low-temperature hydrothermal mineralisation in the East Bull Lake complex has been correlated with some of these events (McNutt *et al*., 1987).

In summary, the environment of emplacement of the mafic volcanics and gabbro-anorthosite intrusions at around 2480 Ma was a rifting environment involving an extensional stress regime with associated depression of the craton or cratonic margin to the south, creating the sedimentary basin into which the Huronian sediments were deposited. The actual mechanism responsible for the extensional tectonics and basin subsidence remains problematic.

2.4 LOGISTICS

All of the units under investigation in this study are generally readily accessible by roads suitable for non-four-wheel-drive vehicles, or by short traverses on foot. The East Bull Lake and Shakepeare Dunlop intrusions are accessed by well kept A.E.C.L. and logging roads, respectively, while "highways" pass through the May, Drury and Tennyson Township gabbro-anorthosites. The Falconbridge Township, Wanapitei and St. Charles gabbro-anorthosites are also relatively easily accessible. In essentially every case, vehicle access to a given pluton is limited to a single road, and although the terrain is amenable to short sampling traverses, in most cases suitable outcrop is itself limited to roadside exposures (where "suitable" outcrop implies the availability of "fresh" material and an outcrop morphology which can be sampled without resort to blasting). Sample availability is also limited by extensive surface weathering, particularly for the gabbro-anorthosites (but is not a factor in sampling the basement granites).

Databases for the units sampled are on the order of ten samples per unit. While this (minimum) number is perhaps slightly lower than ideal, whole-rock isotopic data is not expected to be geochronologically meaningful for various reasons (see Chapter 6), so that collection of a large suite for isochron purposes was unnecessary. In the case of the larger intrusions, particularly the EBL complex, it is not the intent to sample representatively each of the various texturally and mineralogically distinct phases of the intrusion, because such an enterprise would dramatically change the scope of this study, and also because primary geochemical and/or isotopic variations may be indistinguishable from and/or masked by the pervasive multiple secondary effects.

A large geochemical database is already available for the basal Huronian volcanics in the Thessalon area (Jolly, 1987a, b).

CHAPTER THREE: PETROGRAPHY

3.0 INTRODUCTION

The purpose of this chapter is to establish the petrologic character and extent of metamorphism of the units involved in this study. This allows constraints to be placed on the potential mobility of various trace and major elements and their isotopes and the relative timing thereof. Due to the relatively narrow sampling base of this study, both in absolute terms and especially in terms of the often extensive and heterogeneous nature of the units under investigation, this chapter does not purport to a be a detailed petrographic discussion of each unit. The range of compositions sampled and the degree and extent of metamorphism for each unit are characterized.

3.1 SUPERIOR PROVINCE GRANITOIDS

3.1.1 Algoman Granitoids

The Algoman Granitoids, comprising in the study area the Dinny Lake, Birch Lake and Cartier Batholiths, are red-coloured, medium- to coarse-grained quartz-microcline-plagioclase granites (*s.s.*) (to tonalitic; D. Peck, pers. comm., 1991), with relatively minor quantities (≤ 10%) of femic minerals and accessory phases. Quartz occurs as coarse grains showing moderately undulose extinction and irregular, sub-sutured grain boundaries between adjacent quartz grains (see SPA-88-17), and also in symplectites with feldspar. The feldpars are dominantly microcline-variety alkali-feldpar, showing characteristic tartan polysynthetic twinning which is often obscured by perthitic exsolution, except at grain rims. Coarse-grained microcline may also contain inclusions of subhedral, Carlsbad-twinned plagioclase, which is in turn studded with muscovite laths. Microcline also occurs as inclusions (possibly products of exsolution) in albite-twinned plagioclase feldspar (anti-perthite in SPA-88-17). Coarse-grained microcline (in 88-17) shows complex intergrowths of fine-grained microcline, quartz, and granular-textured kaolinite-chlorite-muscovite-bearing aggregate which is probably heavily-altered or relict sodic plagioclase. Less-altered equivalents of this texture are distinctly myrmekitic in nature. Plagioclase occurs as coarse, anhedral grains which are commonly untwinned.

Accessory minerals include chlorite, biotite, muscovite and epidote, plus trace quantities of hematite, opaque oxides, zircon, apatite and titanite. Sample SPA-88-18 is relatively heavily altered and well-foliated. There is strong evidence for brittle deformation such as subgraining and crushing along grain boundaries, warping and fracturing of albite twins in plagioclase, and calcite-filled lineament-parallel fractures. Metamorphic titanite is also prominent.

3.1.2 Levack Gneiss Complex

The Levack Gneiss Complex consists of a variety of compositionally-distinct rock types which have been integrated at high metamorphic grades. The following petrographic descriptions are listed in order of increasing metamorphic grade, and do not represent equivalent rock types. The grade varies from amphibolite facies in the mafic gneiss sampled (SPA-89-04) through relict granulite facies (to incipient melting, as exemplified by felsic migmatite SPA-89-01).

The mafic gneiss consists mainly (70%) of plagioclase plus quartz (10-15%), as well as relict amphibole. The plagioclase is moderately calcic but optical determination of composition is not possible due to the extensive and ubiquitous sericitization and kaolinitization of the feldspar. Grain boundaries are sutured and somewhat indistinct in places. The amphibole is green to yellow pleochroic and commonly contains opaque exsolution lamellae which often continue across grain boundaries between adjacent acicular amphibole grains. The amphibole has been largely superceded by biotite, chlorite, and epidote plus titanite, in that order. Accessory apatite and opaques are also present. A distinct foliation and lineation are present in thin section.

Two samples of medium- to coarse-grained relatively mafic granulite were obtained (SPA-89-02 and 03). These also consist dominantly (60 to 70%) of plagioclase plus quartz (about 3:1 feldspar to quartz) plus femic minerals dominated by amphibole, biotite and relict orthopyroxene. The plagioclase is granular and the degree of preservation varies from quite clean with sharply-defined albite twin planes to completely saussuritized, often in adjacent grains. Michel-Lévy tests on the albite twins indicate a composition of calcic oligoclase. The amphibole varies in colour pleochroically from light green to pale brown, with optical properties favouring a magnesian-hornblende composition. All grains are anhedral, and only one cleavage (at most) is observed. All of the amphibole is somewhat corroded. Biotite laths are dark brown and fairly strongly pleochroic, and are not associated particularly with the amphibole. The presence of distinct opaque patterns strongly resembling schiller exsolution textures suggests that the biotites are, at least in part, pseudomorphs after pyroxene. Relicts of both clino- and orthopyroxene exist in the rock, with the latter commonly altering to biotite, although not displaying prominent oxide exsolution. Relict hypersthene occurs (5 to 10%), displaying characteristic pleochroism and cleavages, and is altered along rims and fractures to biotite and opaques, as well as chlorite. Trace amounts of augitic clinopyroxene are also present. Accessory phases include epidote, apatite and zircon.

One sample of felsic migmatite was obtained (SPA-89-01), characterized by extensive alteration of the main minerals, which include plagioclase (about 60 modal percent), quartz (30 %), and various femic minerals. The plagioclase is heavily sericitized and/or saussuritized, and although albite and pericline twinning is visible, preservation was too poor to facilitate composition determinations. Quartz occurs as equant, granular grains with linear boundaries, showing triple junctions and commonly octahedral outlines. The femic minerals are largely related to orthopyroxene breakdown, as biotite and opaques are commonly associated with relict skeletal and fragmental hypersthene. Biotite rimming skeletal opaques are also observed. White mica, clinozoisite, epidote, and chlorite exist as late alteration products of feldspars. Other accessory minerals include titanite and apatite.

3.2 PROTEROZOIC GABBRO-ANORTHOSITES

3.2.1 East Bull Lake Intrusion

The EBL pluton shows a wide range of mineralogical proportions and degrees of preservation, but can be characterized as a variably-metamorphosed, olivine-plagioclase-pyroxene cumulate. Proportions of cumulate minerals vary such that troctolitic, anorthositic, gabbroic and noritic phases exist locally. Plagioclase-pyroxene layering is shown in Figure 3.1a. Metamorphism varies from essentially pristine igneous rocks to ones so extensively converted to low-temperature hydrous minerals as to be unidentifiable as gabbro (*e.g.* SPA-88-47).

All samples show cumulate or relict cumulate textures, with the order of crystallization being plagioclase-olivine (where present)-pyroxene (monoclinic and orthorhombic). Olivine and plagioclase both display cumulate textures, and inclusions of plagioclase in olivine are common (see Fig. 3.1b and c). Plagioclase exhibits albite, pericline and carlsbad twinning, and is labradorite composition (based on twin determinations). It commonly occurs as laths (Fig. 3.1d), often showing ophitic and sub-ophitic textures with pyroxene. Both (augitic) clino- and (hypersthene) orthopyroxene occur invariably as intercumulus phases, both displaying igneous cooling textures such as exsolution lamellae of pyroxene and rutile (schiller texture) and two-pyroxene symplectite (*e.g.* SPA-89-06B, shown in Fig. 3.2a).

In samples where olivine is preserved (SPA-89-06B, SPA-88-21 and EBL-prefix samples), olivine is invariably separated from plagioclase by a thin double layer consisting of an inner rim of white mica (talc?) and an outer rim of chlorite (pennite), shown in Figure 3.2b. The two rims vary in thickness, increasing with the degree of alteration of the sample in approximately equal amounts (volumes). Opaques which originated within fractures in the olivine extend out into the talc layer, or to its outer edge, less commonly. The inner rim (in contact with olivine) consists largely, if not entirely, of talc, oriented randomly or, more commonly, radially to the relict olivine-plagioclase grain boundary. The outer rim consists of radial fibrous pennite chlorite, characterized by anomalous (blue) interference colours and bluish-green pleochroism. The outer edge of the chlorite rim which protrudes into the plagioclase contains green, very weakly pleochroic amphibole (pargasite?). The two rims are generally separated by a very thin layer of colourless, grey-green birefringent chlorite. With increasing amounts of alteration, as the olivine grain becomes replaced by iddingsite or antigorite, the inner talc rim moves inwards also, eventually replacing the olivine entirely. The original boundaries of the olivine remain as pseudomorphs of the hydrous oxides and opaques which originally occurred within fractures. The olivine becomes an interlocking, non-oriented talc-grey-green chlorite assemblage, plus relict opaque. The outer radial pennite rim thickens into the plagioclase slightly, but becomes overgrown by tangentially-oriented grey-green chlorite. The outer amphibole fringe expands into the plagioclase as well. Contacts between olivine and either clinopyroxene or orthopyroxene show either a very narrow talc band, or more commonly, no reaction at all. Similarly, there is no reaction between the pyroxenes and plagioclase.

With increasing degree of metamorphism the plagioclase does not cloud with opaques or spinel as in corona formation (*e.g.* Prevec, 1988). Eventually the plagioclase becomes replaced by fine grained, randomly-oriented epidote, and the pyroxenes are replaced by pale green tremolitic amphibole. Orthopyroxene may be serpentinized and subsequently amphibolitized along outer rims and along fractures (*e.g.* EBL-4-132), and may be pseudomorphed by an assemblage which includes a three-directional linear arrangement of opaques, associated with calcite, chlorite and biotite and rimmed by fibrous amphibole (*e.g.* SPA-88-19).

In heavily altered rocks clumps of randomly-oriented amphibole, biotite, epidote and chlorite represent relict femic phases, presumably olivine or pyroxene originally. Biotite and blue-green hornblende commonly follow tremolite. Fibrous amphibolite is shown in Fig. 3.2 c. Late zoisite occurs after epidote in altered plagioclase (SPA-88-49; Fig. 3.2d), and small amounts of quartz, present in symplectites with plagioclase (*e.g.* SPA-88-48), and alkali-feldspar (orthoclase in SPA-88-50) may occur in trace amounts. Zircon, apatite, and titanite were not observed in thin section, although trace baddeleyite was identified.

3.2.2 Shakespeare-Dunlop Intrusion

The Shakespeare-Dunlop intrusion is relatively poorly preserved, such that the primary igneous mineralogy and textures are preserved only as relicts or pseudomorphs, if at all. No olivine or olivine pseudomorphs are observed. Plagioclase may display cumulate textures, laths and subophitic textures with intercumulus augitic clinopyroxene or amphibole pseudomorphs thereof. Although the feldspar is usually recrystallized, albite twinning indicates andesine composition. Pyroxene is invariably replaced by amphibole, usually as fine-grained masses of elongate grains of pale-green tremolite (Fig. 3.3b). Coarser-grained pale brown amphibole showing simple twins may also replace pyroxene, which is subsequently replaced by finer-grained tremolite at an unrelated orientation. Relict schiller exsolution textures and two-pyroxene exsolution lamellae are commonly preserved in the early amphiboles, as are pseudomorphs of excellent intercumulus textures with plagioclase. The early amphiboles may be overgrown by pale green amphibole with grey interference colours, which occurs as aggregates of very fine-grained fibres (*e.g.* SPA-88-07). The amphiboles are very commonly rimmed and then replaced by equant to weakly prismatic blue-green hornblende.

With increasing alteration the plagioclase becomes replaced by epidote and clinozoisite until eventually the feldspar is completely replaced. Chlorite occurs as radial rims surrounding amphibole grains and along fractures through the feldspar. Quartz-plagioclase symplectites occur interstitially in SPA-88-10 and as the main tectosilicate phase in granophyric sample SPA-88-14 (corresponding with descriptions by Krogh et. al, 1984; Figure 3.3c). Relatively fine-grained brown biotite appears (*e.g.* SPA-88-11) as a later femic alteration, but predates the blue-green hornblende, which postdates most of the other alteration minerals.

Fine-grained radioactive minerals (zircon) occur, identified by pleochroic haloes in amphibole and biotite.

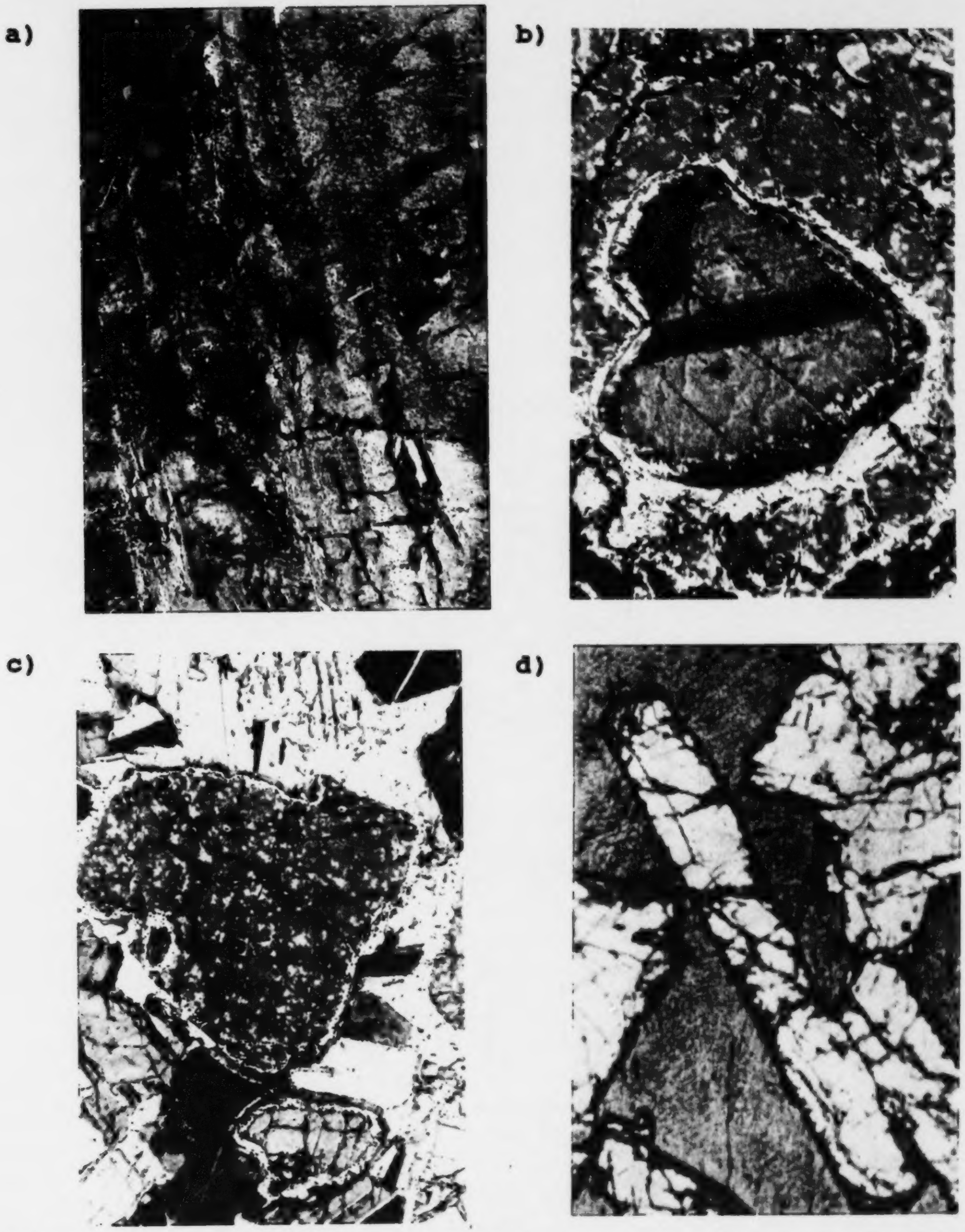

***Figure 3.1.** Evidence of cumulate textures from East Bull Lake: **a)** Plagioclase-pyroxene layering from EBL intrusion. **b)** Rimmed plagioclase (stained) in olivine, from EBL-1-182 (xpolars, 0.9 cm wide). **c)** Rimmed olivines in twinned plagioclase in SPA-89-06B (xpolars, 2.2 cm wide). **d)** Relict plag. laths in amphibolitized intercumulus clinopyroxene from SPA-88-43 (ppl, 2.2 cm wide).*

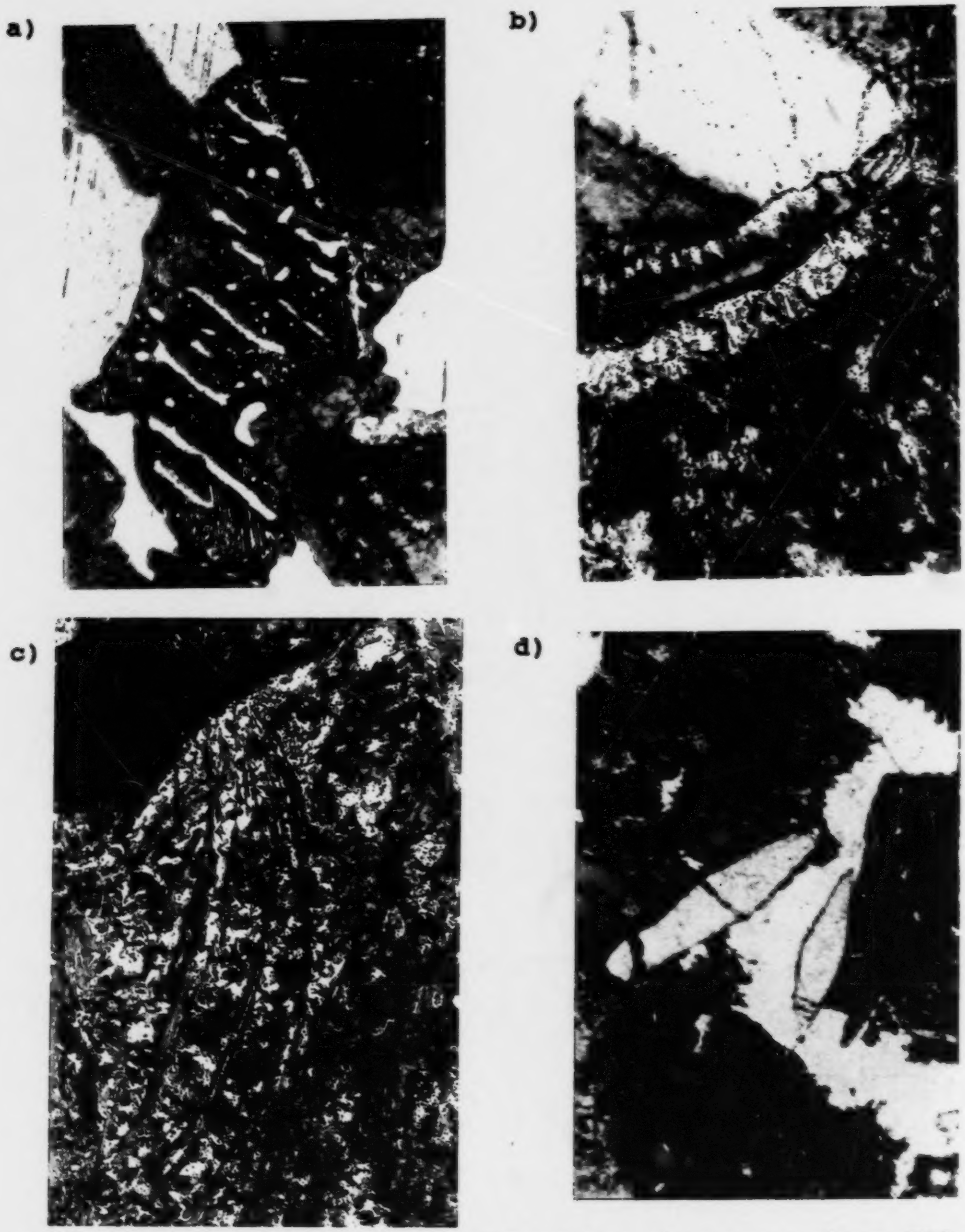

*Figure 3.2. Cooling and/or reheating phenomena from EBL: **a)** Two-pyroxene symplectites in EBL-1-183 (xpolars, 0.9 cm wide). **b)** Plagioclase (left side) separated from olivine by double rim of chlorite (left) and talc (right), from SPA-89-06B (xpolars,0.3 cm wide). **c)** Fibrous amphibole from near EBL-4 drill site **d)** Late clinozoisite in altered sample SPA-88-49 (xpolar,0.9 cm wide).*

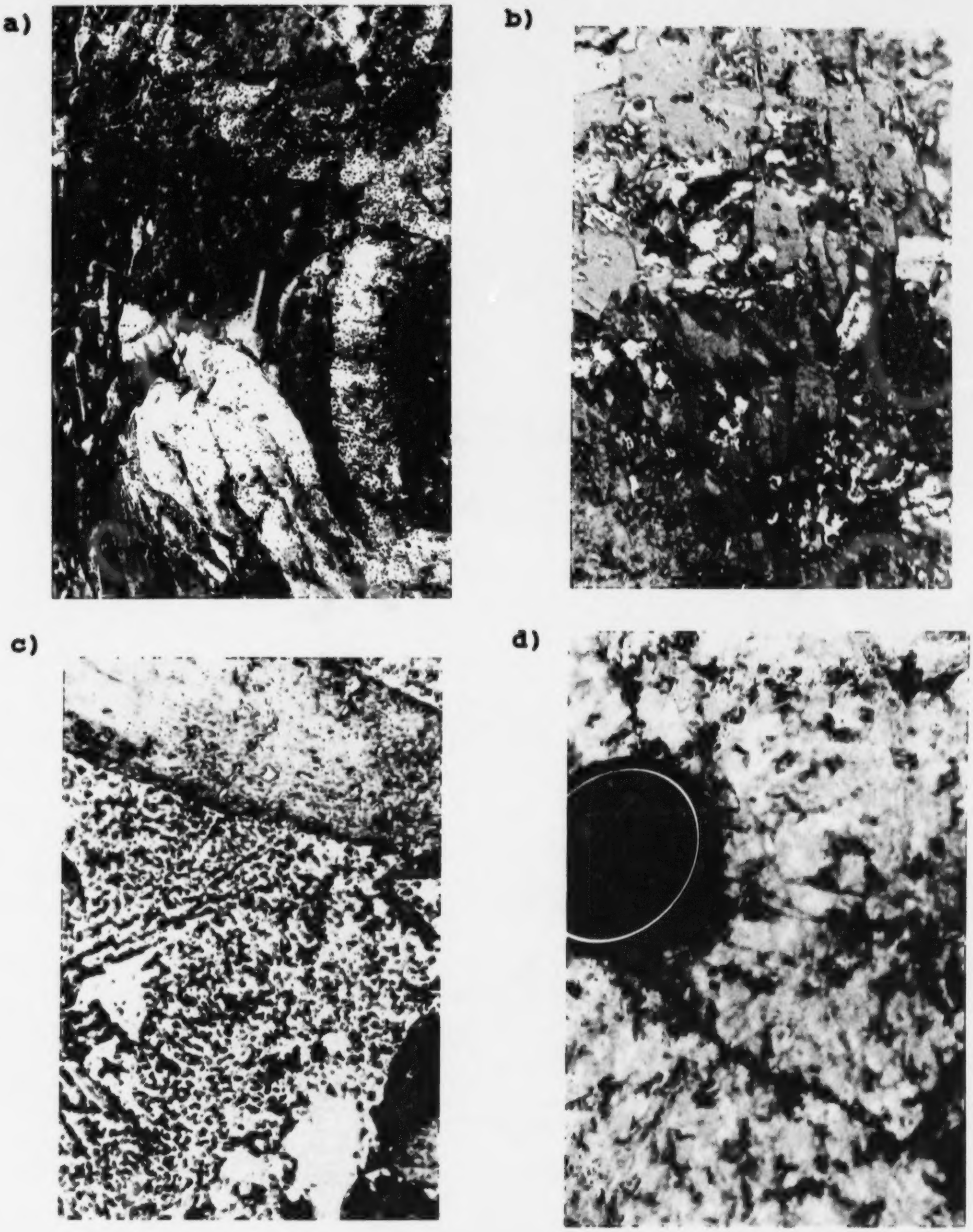

Figure 3.3 a) Granite engulfed by mafic material at north end of S-D intrusion b) Amphibolitized S-D rock, with biotite and stained plagioclase (SPA-88-11; ppl,0.9 cm wide). c) Quartz-plagioclase (stained) myrmekite in granophyric S-D sample SPA-88-14 (ppl,0.9 cm wide) d) Typical metagabbroic plag-amphibole Drury Twp. rock.

3.2.3 Tennyson Township Intrusion

All of the samples from this unit are extensively altered, recrystallized and replaced. The rocks are composed of approximately equal proportions of plagioclase and amphibole. Where albite twinning is preserved the plagioclase composition is sodic andesine. Plagioclase is invariably recrystallized, and is generally extensively saussuritized with fine-grained epidote. Where the plagioclase has been almost completely obliterated, coarse-grained epidote occurs. The amphibole is anhedral to subhedral, pale to olive green or blue-green pleochroic, commonly with darker blue-green rims. Simple twinning is common. Locally, brown pleochroic biotite may predate the latest (blue-green) amphibole. Late opaques and biotite are also present, often as fracture fillings.

3.2.4 May Township Intrusion

All of the samples obtained from this intrusion are also extensively altered and are comparable to those from Tennyson Township, except that the latter tends to be coarser-grained. Sample SPA-88-53 probably represents either metabasalt or meta-argillite, as its finer grain size distinguishes it from the metagabbro samples.

These samples are amphibole-plagioclase/epidote rocks, in which all of the original femic phases have been replaced by hydrous equivalents. Laths of plagioclase are preserved in one sample (SPA-88-16), but otherwise the feldspars are recrystallized and generally extensively epidotized, sericitized and albitized. Coarse-grained epidote and clinozoisite are common. Quartz is present in small quantities, commonly intergrown with plagioclase. Amphibole occurs as anhedral, often fibrous, dark green to olive green pleochroic grains. No evidence for pyroxene precursors has been preserved. Blue-green hornblende rims are absent, although darker green or brownish rims are common. Very pale green, grey-birefringent amphiboles consisting of aggregates of finer fibres are also observed.

Oxides are prominent in the May Twp. rocks, as coarse-grained opaque phases and alterations thereof. Late, coarse, anhedral opaques are common (up to 5 modal percent), and may contain inclusions of light-brown biotite grains, muscovite and amphibole. The opaques are commonly altered along rims and fractures or replaced entirely by an amorphous hydrous oxide. Six-sided, barrel shaped and skeletal pseudomorphs suggest leucoxene alteration from ilmenite. Medium-grained subhedral to anhedral titanite occurs as a late phase.

Sample SPA-88-53 comprises fine-grained foliated chlorite and coarse-grained titanite, and is texturally distinct from all other May Twp. samples obtained.

3.2.5 Drury Township Intrusion

The Drury Twp. samples are all altered to the extent that no original plagioclase has been preserved, and the amphibole is in relatively poor condition as well (Fig. 3.3d). Relict cumulate textures pseudomorphic after plagioclase laths and intercumulus (clino)pyroxene are distinct locally (*e.g.* SPA-88-56A).

Plagioclase has been recrystallized and entirely replaced by fine-grained epidote, clinozoisite and muscovite, constituting 60 to 75 modal percent of the rock. Plagioclase may be present as fine-grained aggregates. Pale green to colourless pleochroic amphibole occurs as coarse grains which may show simple twinning, but commonly occurs as coarse aggregates of fibrous grains. Amphibole is commonly rimmed by a weakly radially-oriented chlorite layer. Coarse-grained epidote and anhedral titanite occur, associated with alteration of plagioclase and amphibole, respectively. Apparent oxidized subhedral pseudomorphs after femic minerals occur, consisting of linear assemblages of opaques, (plus possibly rutile), and calcite, rimmed by fine-grained amorphous oxides. Amorphous oxides apparently pseudomorphing titanite also occur.

Late fractures may be filled with quartz, chlorite, hydrous iron oxides or nothing at all.

3.2.6 Falconbridge Township Intrusion

These samples consist of amphibole and plagioclase, or alterations thereof. Relict cumulate textures involving plagioclase and pseudomorphs of amphibole after clinopyroxene are well-preserved. Primary plagioclase is also preserved, at least as grain cores (see Fig. 3.4a).

Plagioclase is variably altered to fine-grained muscovite and epidote, but has largely been replaced by fine-grained anhedral plagioclase, leaving grain interiors which may show remnant albite twinning. Within the fine-grained feldspar, coarser-grained rosettes of plagioclase are common, usually adjacent to relict coarser grains. Amphibole is pale brownish-green and weakly pleochroic, and forms pseudomorphs after pre-existing clinopyroxene, preserving two-pyroxene exsolution lamellae and opaque exsolution textures. A thin rim of more pleochroic green amphibole surrounds the pseudomorphs.

Assemblages of dark- to olive-green amphibole, chlorite or biotite and opaque minerals may represent relict olivine. Calcite and coarse-grained epidote also occur. In more heavily altered rocks (*e.g.* SPA-88-08B) plagioclase has been completely replaced by fine- and coarse-grained epidote, clinozoisite and muscovite, and the amphiboles are polygranular aggregates.

Veins of coarse-grained quartz, characterized by linear grain boundaries and the absence of undulatory extinction cross-cut earlier textures.

3.2.7 Wanapitei Intrusion

Samples from the Wanapitei intrusion vary from massive to well-foliated and lineated, and from very weakly sericitized to coronitic. While the samples are gabbro-norites, in general, varying amounts of quartz, garnet or olivine are present, as well as hydrous minerals. Cumulate textures are not observed except in one sample (SPA-89-32; see Fig. 3.4b).

The majority of the samples are medium-grained equigranular plagioclase-two pyroxene rocks (Fig. 3.4c). Pale-green, weakly pleochroic augitic clinopyroxene and green to red pleochroic hypersthene comprise up to about 50 modal percent of the rock, but commonly the clinopyroxene is altered to green to greenish-brown, often poikiloblastic amphibole as discrete rims or complete replacement. The hornblende is subsequently replaced by biotite, whose composition corresponds to that of the co-existing amphibole. Dark green pleochroic biotite occurs in rocks with green hornblende, and reddish-brown biotite occurs with pale brown to greenish brown hornblende. In samples where biotite is prevalent (*e.g.* SPA-89-28), a strong foliation is evident (Fig. 3.4d). Plagioclase is of calcic andesine composition and may display albite and pericline twinning, although it is commonly untwinned. The feldspar is generally unaltered, although up to about 40% sericitization is observed (*e.g.* SPA-89-28), and minor epidotization.

Garnet is common, occurring as coarse, euhedral to anhedral poikiloblasts (*e.g.* SPA-89-30B and 89-30A, respectively). Inclusions of quartz, opaques and biotite occur within the garnets, often preserving growth zoning in garnet rims (*e.g.* SPA-89-30B). Opaques are commonly associated with garnet, and may display foliation-parallel elongation and poikiloblastic texture. Accessory apatite may also occur.

In sample SPA-88-32 olivine, clinopyroxene, orthopyroxene and plagioclase are preserved, displaying cumulate and coronitic textures. Cumulus olivine is separated from plagioclase by double coronas, consisting of an inner corona (adjacent to the olivine) of radial bronzitic orthopyroxene and an outer corona of radial pargasitic amphibole-pleonaste spinel symplectite. The olivine is commonly replaced by iddingsite and opaques, and may be separated from intercumulus augitic clinopyroxene by a thin rim of orthopyroxene. Pyroxene may also be altered to amphibole along boundaries with plagioclase. Plagioclase grains are clouded by fine-grained spinel.

3.2.8 St. Charles Anorthosite

The St. Charles samples are dominantly coarse-grained and anorthositic, consisting of 70 to 90 modal percent andesine to labradorite plagioclase plus altered femic minerals (mostly amphibole). Plagioclase is recrystallized but relatively unaltered, displaying good albite and pericline twinning, although it may be as much as 25% sericitized in altered samples. Laths are preserved occasionally (*e.g.* SPA-89-12A) and very coarse-grained plagioclase may be preserved (Figure 3.5a). Plagioclase can be altered to medium-grained epidote, usually in association with amphibole as well. In sample SPA-89-15 plagioclases show symplectitic intergrowths along grain boundaries, and contain coarser inclusions (exsolution?) which obscure the twinning locally.

Although intercumulus clinopyroxene may be preserved (*e.g.* SPA-89-18, 19), it is usually entirely replaced by pale-green to olive green to pale-brown pleochroic amphibole, which constitutes the dominant femic phase in these rocks. Amphibole does not display relict intercumulus textures, and is commonly altered itself along rims to chlorite, blue-green hornblende epidote and calcite. Late biotite, associated with opaques, hematization and titanite may pseudomorph amphibole (*e.g.* SPA-89-12B). These femic assemblages may be surrounded by "necklaces" of fine-grained equigranular pink garnet (*e.g.* SPA-89-18; Figure 3.5b). Titanite may also occur as rims around opaques (*e.g.* SPA-89-19), although both garnet and titanite may also occur as isolated grains within the groundmass. Trace anhedral interstitial quartz may also occur (*e.g.* SPA-89-12A).

3.2.9 Mercer Township Intrusion

These samples consist largely of well-preserved, recrystallized coarse-grained plagioclase, and are similar in texture and mineralogy to the St. Charles intrusion (Fig. 3.5d). The plagioclase may be moderately sericitized and/or epidotized, but albite and pericline twinning is well-preserved, indicating sodic andesine composition. Pale green to dark green amphibole comprises most of the remainder of the rock, variably altered to red-brown biotite, which is invariably strongly foliated. Assemblages of opaques plus serpentine and hydrous iron oxides appear to represent orthopyroxene breakdown. Accessory minerals include scattered medium-grained euhedral to subhedral garnet, apatite, epidote and opaques.

3.3 HURONIAN MAFIC VOLCANICS

Although textures and mineralogical proportions vary distinctly between different mafic volcanic formations (*i.e.* Salmay Lake, Elsie Mountain and Stobie), the samples obtained can be characterized as being altered, fine- to medium-grained plagioclase-amphibole rocks. Where the plagioclase has not been saussuritized and epidotized completely, relict albite twinning indicates calcic andesine composition. Feldspar is generally recrystallized.

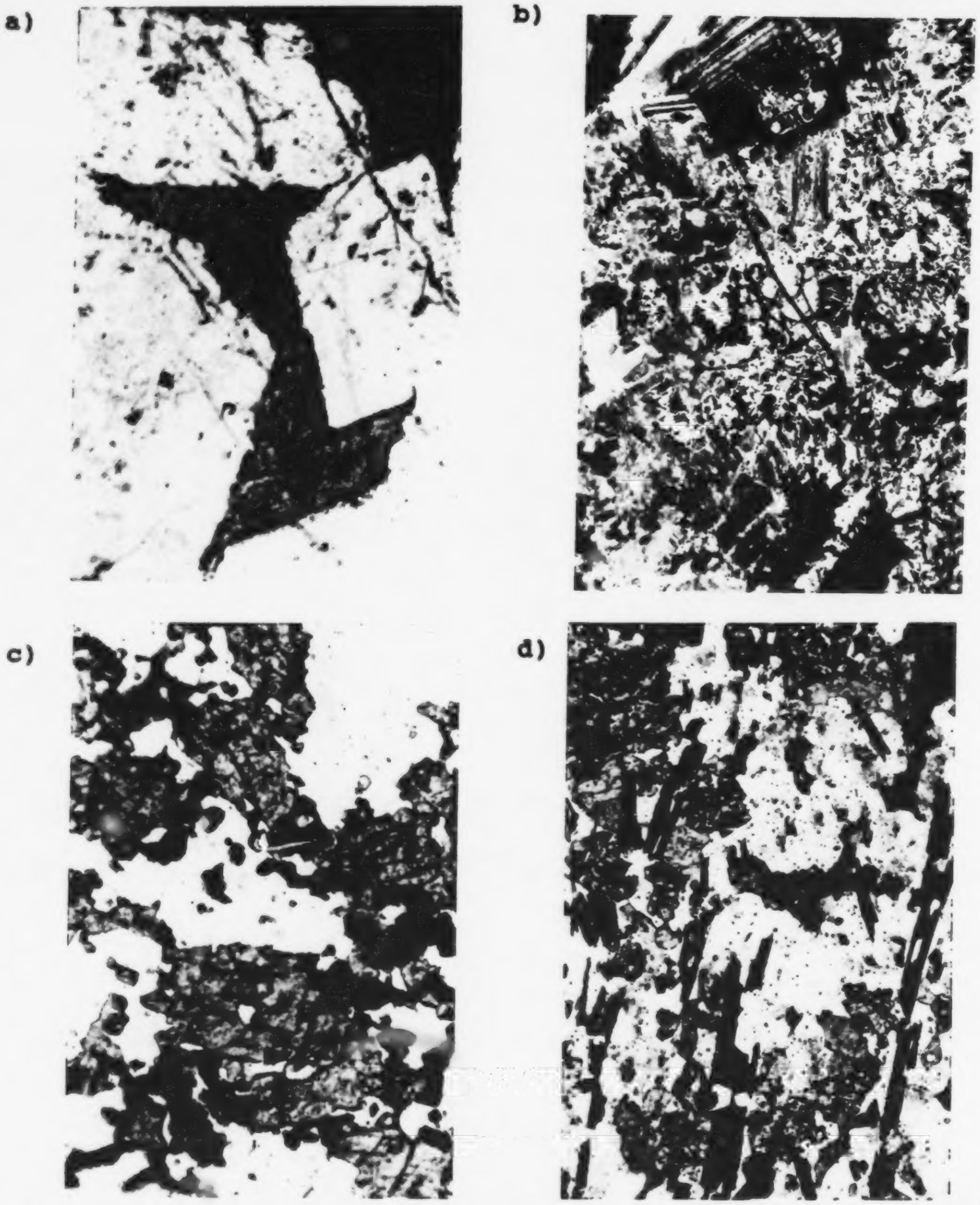

Figure 3.4 a) Relict intercumulus clinopyroxene in plag from Falconbridge intrusion (SPA-89-07A; ppl,2.2 cm wide) b) Coronitic olivine cumlate from Wanapitei (SPA-89-32; xpolar,2.2 cm wide) c) Two-pyroxene (plus amphibole and plag) texture more typical of Wanapitei rocks (SPA-89-33; ppl,0.9 cm wide) d) Biotitized equivalent, with amphibole, garnet (high relief) and plag, from SPA-89-28 (ppl, 2.2 cm wide).

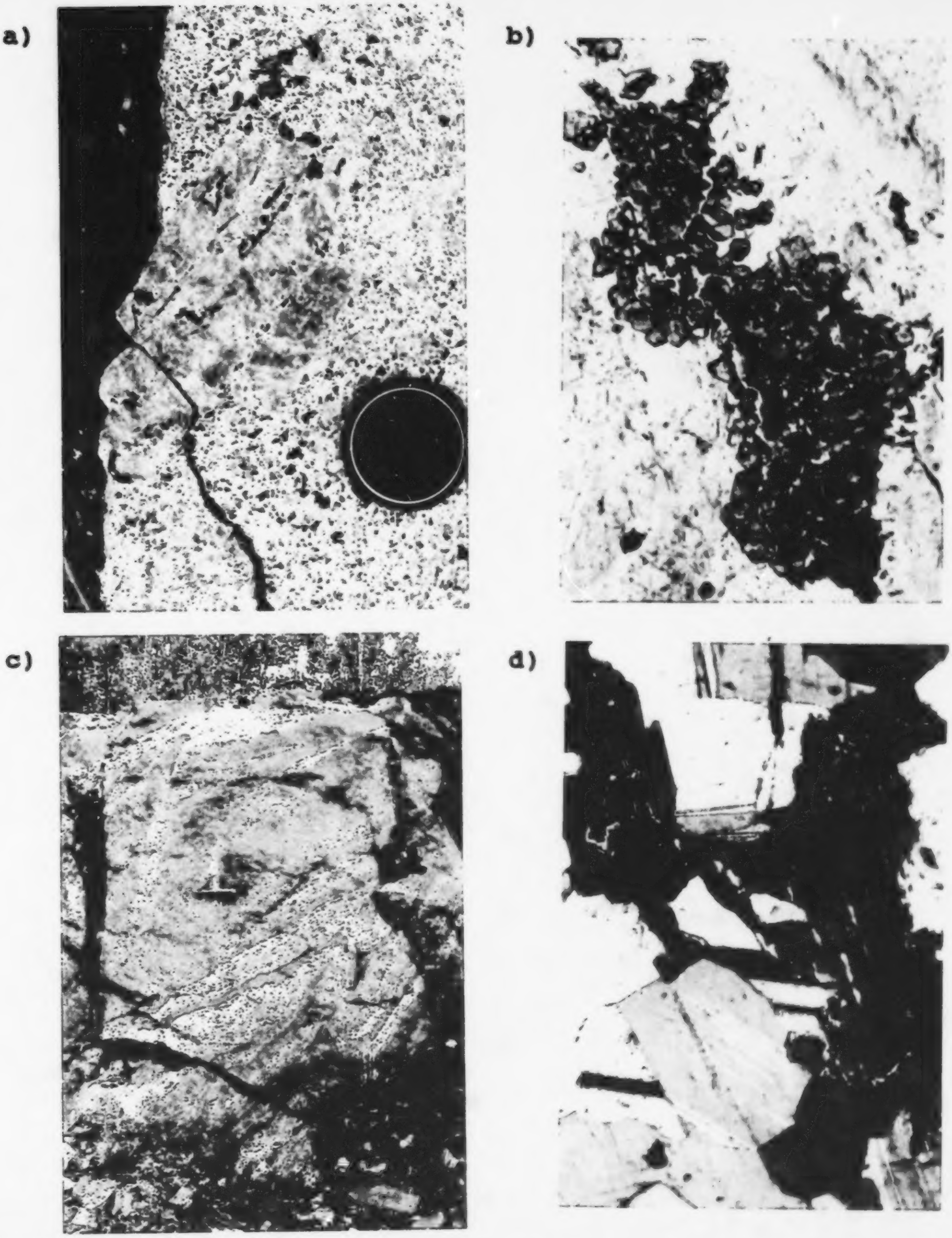

Figure 3.5 a) Plagioclase crystals from St. Charles anorthosite, near SPA-89-21. b) Amphibole with garnet necklace, in plagioclase from St. Charles (SPA-89-21; ppl,2.2 cm wide) c) Deformed Mercer anorthosite from north end of intrusion d) Typical recrystallized plag-amphibole texture from Mercer anorthosite (SPA-89-26; xpolar, 2.2 cm wide).

Amphibole is the main femic mineral, often showing simple twinning, and varying from anhedral pale green calcic amphibole (*e.g.* SPA-88-25) to euhedral darker green and blue-green amphibole (*e.g.* SPA-88-35). Orange-brown biotite may occur with titanite and limonite. Other accessory minerals include chlorite, calcite, epidote and locally, zircon (in SPA-88-28), identified by the presence of radioactive haloes in amphibole.

The samples are relatively massive, or very weakly foliated.

3.4 DISCUSSION AND SUMMARY

3.4.1 Superior Province Granitoids

The Algoman batholiths of the southernmost Abitibi belt are red, sodic, igneous-textured granitoids (*s.l.*). The samples are mildly to extensively sericitized, and show a secondary metamorphic assemblage which includes muscovite-chlorite-epidote-titanite, characteristic of middle to upper greenschist facies. The fabric varies from massive, with coarse-grained igneous textures to weakly-foliated, well-foliated and deformed, heavily altered rocks (such as SPA-88-18).

The portions of Levack Gneiss Complex that were sampled comprise tonalitic to quartz monzonitic gneiss which is strongly lineated and shows a peak metamorphic assemblage which includes orthopyroxene. The absence of prominent granular and perthitic textures suggests that the peak of metamorphism was in the lower granulite facies, perhaps hornblende-granulite, and uppermost amphibolite facies conditions are more widely represented. Overprinted onto the high-grade assemblage is a middle- to upper-greenschist assemblage of chlorite-muscovite-titanite-epidote-clinozoisite similar to that observed in the Algoman Granitoids. The upper amphibolite-granulite grades probably reflect *ca.* 2700 Ma old metamorphism early in the history of the complex, prior to intrusion of the Algoman batholiths, and the greenschist facies represents latest Archean or younger metamorphism.

3.4.2 Proterozoic Mafic Rocks

All of the gabbro-anorthositic bodies display, at least locally, pervasive metamorphism characterized by chlorite-epidote-clinozoisite-sericite assemblages, associated with progressive hydration and silicification of the original femic mineralogy. Petrologic distinctions can be made between the mafic intrusions located to the north of the Grenville Front Tectonic Zone (GFTZ) and those to the south of it.

All of the sampled intrusives lying north of the GFTZ (East Bull Lake, Shakespeare-Dunlop, Tennyson Twp., May Twp., Drury Twp. and Falconbridge Twp.) can be characterized as dominantly gabbroic to anorthositic cumulates, with noritic and troctolitic phases present locally, especially in the larger layered plutons (*e.g.* EBL and S-D). Plagioclase and olivine crystallized first and essentially simultaneously, as either mineral may enclose grains of the other, locally. Intercumulus clino- and orthopyroxene followed, dominated by the former, in general. Apatite and primary opaques are essentially absent, and in the sills there is no evidence for the presence of olivine either. None of the samples show evidence of a non-cumulate, liquid phase, although many are too extensively metamorphosed to distinguish between the two.

Primary olivine is only preserved in the East Bull Lake pluton and is characterized by reaction rims separating it from plagioclase. The replacement of olivine and plagioclase by (radially-oriented) talc and chlorite plus minor amphibole suggests a water-facilitated diffusion reaction whereby the conversion of olivine to talc (possibly with serpentine as an intermediate stage) adds water and silica and releases magnesium, coupled with the conversion of calcic plagioclase to chlorite and hornblende. This conversion requires open system behaviour for water, silica and particularly for calcium, as the breakdown of plagioclase produces calcium which is not taken up in any of the other phases except the relatively small volume of amphibole. The low-temperature, hydrous nature of the reaction phases and the open system requirements suggest that this reaction took place after emplacement and cooling, perhaps related to the pervasive greenschist-facies metamorphism. It is possible that calcium (and iron) produced by this reaction migrated away from the reaction zone and are related to subsequent formation of epidote in the plagioclase.

Progressive metamorphism corresponding to decreasing temperatures and/or increasing availability of water results in the replacement of pyroxenes by calcic amphiboles and subsequently by later amphiboles, biotite, epidote-group minerals and chlorite. Feldspars are progressively saussuritized and epidotized until no feldspar is preserved. The initial replacement of pyroxene (and olivine) by amphiboles and amphibolite-facies minerals probably represents an early, cooling replacement, based on the lack of deformation and the quality of the pseudomorphs. The peak of later metamorphism is middle- to upper greenschist ("epidote-amphibolite" facies).

The Wanapitei intrusion varies from unaltered to extensively saussuritized and epidotized, and preserves evidence for olivine-cumulates locally. The bulk of the Wanapitei, St. Charles and Mercer Twp. intrusions consist of relatively fresh, often coarse-grained plagioclase-two-pyroxene rocks with no cumulate textures. Alteration is largely limited to minor sericitization and progressive hydration of pyroxenes to amphibole and biotite, although all three intrusions contain gneissic phases.

The double coronas separating relict olivine and plagioclase in the Wanapitei intrusion are the result of constant-volume, essentially closed-system solid-state diffusion at relatively high temperatures (*e.g.* Prevec, 1988). These can occur during cooling from emplacement conditions (*e.g.* Prevec *et al.*, 1991) or from subsequent temperature and pressure elevation during metamorphism.

The three bodies within the Grenville Province differ from those to the north in that while a cumulate phase may be preserved in the former bodies, it does not characterize the entire intrusion. The proportion of orthopyroxene to clinopyroxene may be higher, and the effects and extent of pervasive low-grade metamorphism are much more limited. On the other hand, the St. Charles and Mercer Twp. intrusions show evidence (lineation and foliation) for higher total pressures and lower water pressures during metamorphism, possibly at or shortly after emplacement. Brittle deformation was not observed.

The basal Huronian basalts show the same peak greenschist-facies to lower-amphibolite facies metamorphic assemblage and metamorphic textures as the mafic intrusions north of the GFTZ.

3.4.3 Conclusions

The main implications of the petrologic evidence include the following points:

1) The St. Charles, Mercer Twp. and much of the Wanapitei intrusion have experienced higher grade, drier metamorphism. All of the mafic intrusions and extrusions lying north of the Grenville Front have been subjected to "late" upper-greenschist to lower-amphibolite facies metamorphism.

2) This metamorphism involves extensive hydration of all of the original mineralogy, and has potentially mobilized silica, calcium, and possibly the alkalis and other LILE.
3) The dominance of cumulate textures in many of the intrusions suggests that liquid compositions are not represented directly by the majority of the samples in this study, and that the liquid phase of these intrusions may have been separated from the remainder, possibly by post-emplacement erosion, tectonic displacement or by magmatic processes.

CHAPTER FOUR: GEOCHRONOLOGY

4.0 INTRODUCTION

This chapter presents geochronological data from U-Pb isotope systematics in zircons obtained from gabbroic, anorthositic and granitoid rocks. Other isotopic data such as Sm-Nd and Pb-Pb from whole-rocks is presented elsewhere (Chapter 6) in their capacity as geochemical tracers rather than as geochronological tools. Heavy mineral separates were extracted from samples from all units not previously dated (with the exception of the Tennyson Twp. intrusion), but unfortunately the samples from the Huronian mafic volcanics and from May Township did not yield sufficient sample for a reliable age. Baddeleyite was identified in thin section from the East Bull Lake intrusion, but was not present or preserved in the more highly metamorphosed intrusions further to the east. Geochronological data was obtained for the Mercer Twp., St. Charles, Wanapitei, Falconbridge and Drury Twp. intrusions, as well as for granitoids north of the EBL intrusion.

A summary of the U-Pb isotopic data is presented in Table 4.1 a) and b). Methodology is described in Appendix 1.

4.1 GABBRO-ANORTHOSITES

4.1.1 Mercer Anorthosite

Sample SPA-89-22 was obtained from one of the northern extensions of the intrusion (UTM zone 17, 556850E, 5113100N), and is a relatively unaltered, albeit recrystallized rock consisting largely of andesine, less than 20 modal percent amphibole, and accessory biotite, garnet and apatite.

Table 4.1. U-Pb analytical data for "conventional" analyses

Fraction, Size[a]	Wt. µg	U ppm	Pb* ppm	Pb[b] pg	$\frac{^{206}Pb}{^{238}U}$	$\frac{^{207}Pb}{^{235}U}$	$\frac{^{207}Pb}{^{206}Pb}$	$^{207}Pb/^{206}Pb$ Age (Ma)
Mercer Anorthosite, SPA-89-22								
AA,+105,NM1,cl	30	6.2	1	104	0.1932 ±1.7%	2.051 ±7.2%	0.07699 ±6.1%	1121 +226/-265
AB,+105,NM1,cl	62	3.7	1	176	0.1894 ±2.4%	1.903 ±10.7%	0.07289 ±9.2%	1010 +333/-425
BA,+105,NM1,fr	31	232	55	24	0.2078 ±.08%	2.323 ±.10%	0.08107 ±.04%	1223.2 ±1.6
BB,+105,NM1,cd	38	88	20	9	0.2073 ±.09%	2.315 ±.10%	0.08099 ±.04%	1221.2 ±1.7
Wanapitei Intrusion, SPA-89-31								
A,+105,NM1,cd,fr	57	288	94	28	0.2915 ±.08%	4.187 ±.10%	0.10418 ±.03%	1699.9 ±1.1
BA,+105,NM1,cl,fr	14	240	80	18	0.3038 ±.08%	4.430 ±.10%	0.10576 ±.04%	1727.6 ±1.5
BB,+105,NM1,cd,fr	38	311	107	38	0.3031 ±.08%	4.420 ±.10%	0.10579 ±.03%	1728.0 ±1.2
CA,+149,NM1,cl,s	13	279	96	10	0.3078 ±.08%	4.518 ±.10%	0.10648 ±.03%	1740.1 ±1.2
CC,+149,NM1,cd,s	16	1289	441	11	0.2961 ±.10%	4.330 ±.11%	0.10607 ±.03%	1732.9 ±1.2
Falconbridge Twp. Gabbro, SPA-89-08A								
A,+105,NM5,o,s	11	566	274	455	0.3800 ±.12%	7.283 ±.37%	0.13902 ±.30%	2215.1 ±10.4
BA,-105,NM5,cd,s	2	3693	2154	12	0.4472 ±.09%	9.811 ±.10%	0.15913 ±.03%	2446.4 ±1.0
BB,-105,NM5,o	9	772	419	29	0.4463 ±.09%	10.248 ±.10%	0.16654 ±.03%	2523.2 ±1.0
CA,-105,NM5,o	3	962	597	27	0.4608 ±.08%	11.167 ±.10%	0.17577 ±.04%	2613.4 ±1.2
CB,-105,NM5,cd,fr	5	134	72	10	0.4696 ±.10%	11.289 ±.11%	0.17435 ±.04%	2599.9 ±1.5

Errors are 1 std. error of mean in % except $^{207}Pb/^{206}Pb$ age errors which are 2 std. errors in Ma.

Pb* = Radiogenic Pb

[a] Numbers (i.e. +105, -149) indicate zircon size larger or smaller than given diameter, in microns

[b] Total common Pb in analysis in picograms

NMn = Non-magnetic at n degrees of tilt

cl = Clear grains; cd = Clouded grains; fr = Fractured grains; o = Opaque; s = Single grain analysis

Table 4.2. U-Pb analytical data for SHRIMP analyses

Spot I.D.	U ppm	Th ppm	Pb ppm	^{204}Pb ppb	$\frac{^{206}\text{Pb}}{^{238}\text{U}}$	$\frac{^{207}\text{Pb}}{^{235}\text{U}}$	^{207}Pb/^{206}Pb Age (Ma)
St. Charles anorthosite, SPA-89-14 (204-corrected)							
1-1	129	79	28	2	0.1992±40	2.207±80	1206+54/-56
2-1	94	83	22	2	0.2065±42	2.312±110	1226+78/-82
3-1	124	99	29	3	0.2051±41	2.330±77	1254+46/-48
4-1	113	57	25	4	0.2059±41	2.267±78	1193+50/-52
5-1	113	70	26	9	0.2059±41	2.156±104	1094+81/-85
6-1	217	145	49	7	0.2038±40	2.262±65	1209+36/-37
7-1	148	130	36	4	0.2099±40	2.356±73	1231+43/-41
8-1	163	148	39	9	0.2046±40	2.207±87	1152+62/-65
Drury Twp. intrusion, SPA-88-56A (204-corrected)							
9-1	176	412	88	1	0.3260±64	5.06±12	1842±19
10-1	142	248	65	4	0.3265±65	5.13±14	1862+28/-29
11-1	166	454	88	1	0.3262±64	5.12±12	1862±18
12-1	212	168	82	2	0.3338±65	5.20±12	1847±18
13-1	250	652	129	1	0.3209±62	5.08±11	1879±15
14-1	191	353	89	2	0.3273±64	5.17±11	1864±18
15-1	632	207	209	6	0.3226±62	5.02±10	1846+8/-9
Abitibi granitoid, SPA-88-17 (204-corrected)							
25-1	114	48	66	3	0.519±11	13.29±30	2705±12
26-1	160	73	81	0	0.507±10	12.88±28	2693±10
27-1	129	44	74	3	0.521±11	13.25±30	2694±12
Algoman granitoid, SPA-88-18 (208-corrected)							
1-1	100	31	51	15	0.4593±73	11.59±22	2680±15
2-1	115	40	61	30	0.4668±72	11.65±22	2662±14
3-1	169	88	94	41	0.4765±69	11.90±21	2663±14
4-1	139	48	77	26	0.4949±73	12.53±22	2685+12/-13
5-1	129	53	74	19	0.5069±77	12.68±23	2666±14
6-1	120	50	67	31	0.4861±76	12.14±23	2663±15

4.1.1.1 U-Pb results

Two distinct zircon morphologies were identified, consisting of extremely clear, subhedral grains with rounded tips (Fig. 4.1a) and coarser, often fragmented anhedral, darker and more fractured grains (fractions BA and BB; see Fig. 4.1b). Four zircon fractions were analysed after moderate abrasion. The clear fractions had extremely low U concentrations (≤6 ppm U) and produced very low-precision data, but the data from the "poorer-quality" fractions mutually overlap just below concordia and indicate an average $^{207}Pb/^{206}Pb$ age of 1222.2 ± 2.0 Ma (2σ), shown in Figure 4.2a).

4.1.1.2 Interpretation

The 1222 Ma age is interpreted to be an igneous crystallization age for the Mercer anorthosite. The observation that the two high precision analyses are slightly discordant allows for some potential flexibility in the age if an episodic lead-loss event is suggested. Using a Grenville-aged (*ca*. 1000 Ma, arbitrarily) lower intercept, an upper intercept of *ca*. 1240 Ma can be obtained.

4.1.2 St. Charles Anorthosite

Sample SPA-89-14 is a plagioclase-amphibole-bearing, weakly epidotized gabbroic-anorthosite, sampled from the northwestern end of the intrusion near the town of St. Charles (UTM zone 17, 544175E, 5134250N).

4.1.2.1 U-Pb results

Zircons were anhedral, equant to stubby prismatic clear, colourless grains, shown in Figure 4.1 c) and d). Zoning was observed in some grains, but internal structure and fracturing was generally absent. Zircon yield was very poor, such that a 15 to 20 kg sample yielded less than 0.1 mg of zircon.

SHRIMP U-Pb analyses from eight spots produced a cluster of points around concordia with an average $^{207}Pb/^{206}Pb$ age of 1206 ± 36 Ma (2σ) (Figure 4.2b). All of the analyses overlap this age and one another within two sigma imprecision limits.

4.1.2.2 Interpretation

This age of 1206 ± 36 Ma is interpreted as an igneous crystallization age for the St. Charles anorthosite. The zircons analysed show no physical or isotopic signs of inheritance and are morphologically typical of anorthositic zircon (*cf.* van Breemen *et al.*, 1986).

4.1.3 Wanapitei Intrusion

Sample SPA-89-31 is a plagioclase poikiloblastic hornblende rock from the hornblende norite zone of Rousell and Trevisiol (1988), from the south-central part of the complex (UTM zone 17, 515250E, 5144765N).

4.1.3.1 U-Pb results

Zircons were typically subhedral to anhedral, stubby prismatic grains with aspect ratios varying from 2:1 to 5:1. Grains were variably fractured grains, commonly containing fine-grained opaque inclusions (Figure 4.1 e). One single-grain fraction (CC) was euhedral. The zircons were strongly abraded and five fractions varying from as many as five grains (fraction A) to two of single grains were analysed (fractions CA, CB). A four-point regression through the resultant discordia, shown in Figure 4.3, produces an upper intercept age of 1747 +6/-5 Ma, with a Grenvillian (*ca.* 996 Ma) lower intercept.

4.1.3.2 Interpretation

The age of 1747 +6/-5 Ma is interpreted as the crystallization age of the norite. One single-grain fraction which falls below the discordia (fraction CC) has a $^{207}Pb/^{206}Pb$ age of about 1733 Ma. This is consistent with a 1747 Ma crystallization age but with less Grenville-aged lead-loss than the other four fractions.

4.1.4 Falconbridge Twp. Intrusion

Sample SPA-89-08A is a coarse-grained amphibole-plagioclase rock with cumulate texture pseudomorphs well-preserved, from the north end of the intrusion (UTM zone 17, 517730E, 5162135N).

4.1.4.1 U-Pb results

Zircons were without exception of extremely poor quality. Although euhedral grain shape was not uncommon, grains were red-brown and usually opaque or very weakly transluscent. Fraction BA, consisting of a single small grain, was relatively translucent and devoid of obvious internal structure such as the zoning observed in grains in fraction BB. After light abrasion on most fractions (except BA which was heavily abraded), five fractions were analysed. All fractions were highly discordant, with $^{207}Pb/^{206}Pb$ ages ranging from 2215 Ma to 2613 Ma (Figure 4.4a). A regression through three points, used as a reference line, indicates an Archean upper intercept and a Sudbury-aged (*ca.* 1850 Ma) lower intercept. Fraction BA lies above this reference discordia

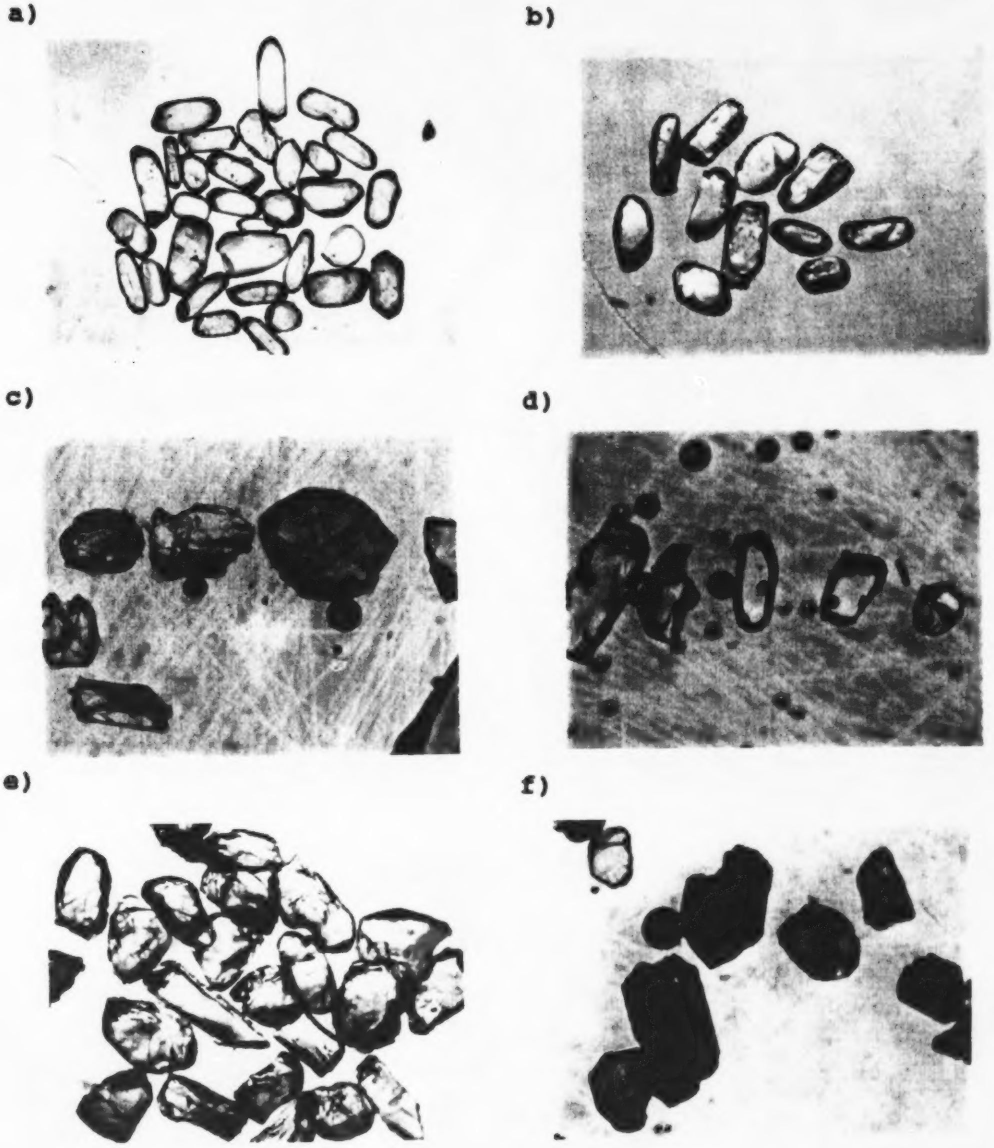

Figure 4.1. Zircon morphologies: ***a)*** *Low-U population from Mercer anorthosite (x50)* ***b)*** *High-U population (x100)* ***c)*** *Anhedral St. Charles anorthosite population (x100)* ***d)*** *St. Charles zircons, including possible low-U grains? (x100)* ***e)*** *Typical fractured, included Wanapitei zircons (x50)* ***f)*** *Drury Twp. zircon, including zoned, fractured and opaque grains (x100).*

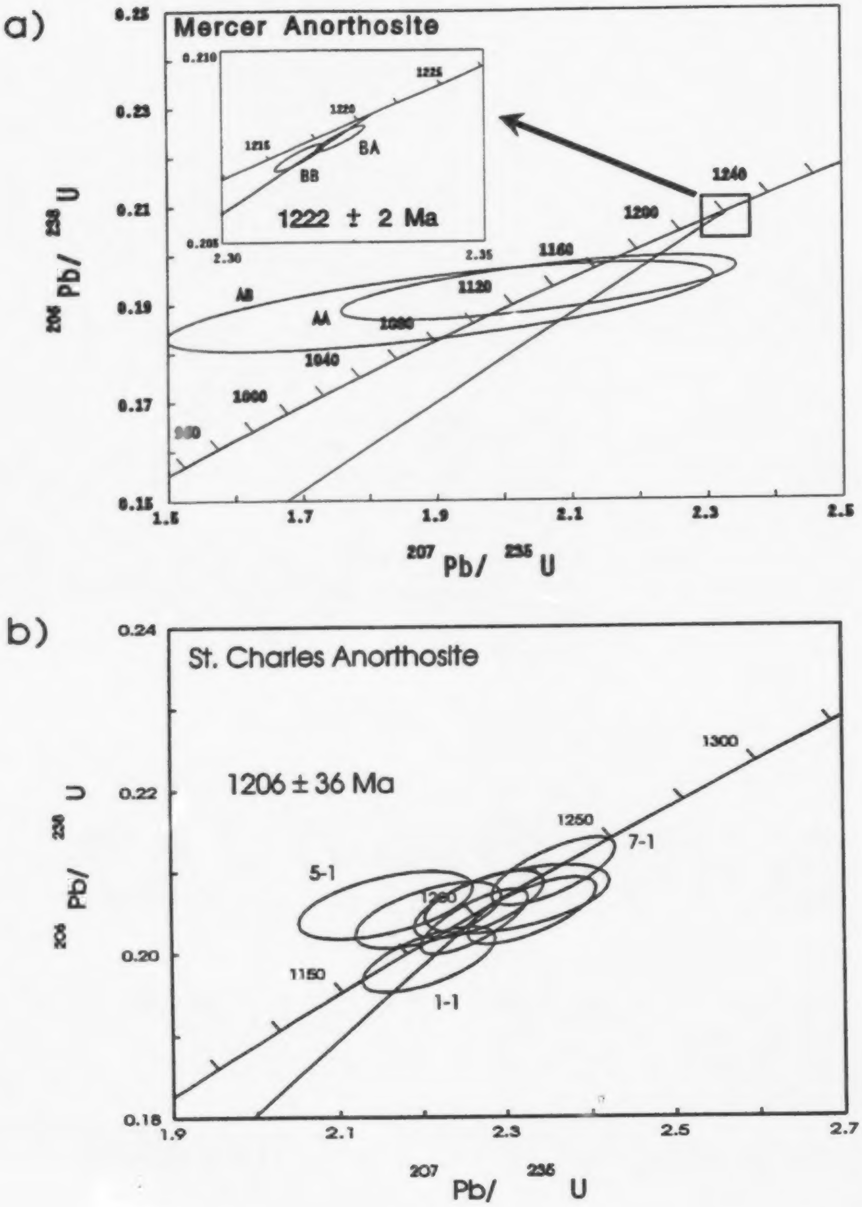

Figure 4.2 a) *Concordia diagram for Mercer anorthosite (inset shows the two near-concordant points* ***b)*** *Concordia diagram for SHRIMP data from St. Charles anorthosite (one-sigma errors).*

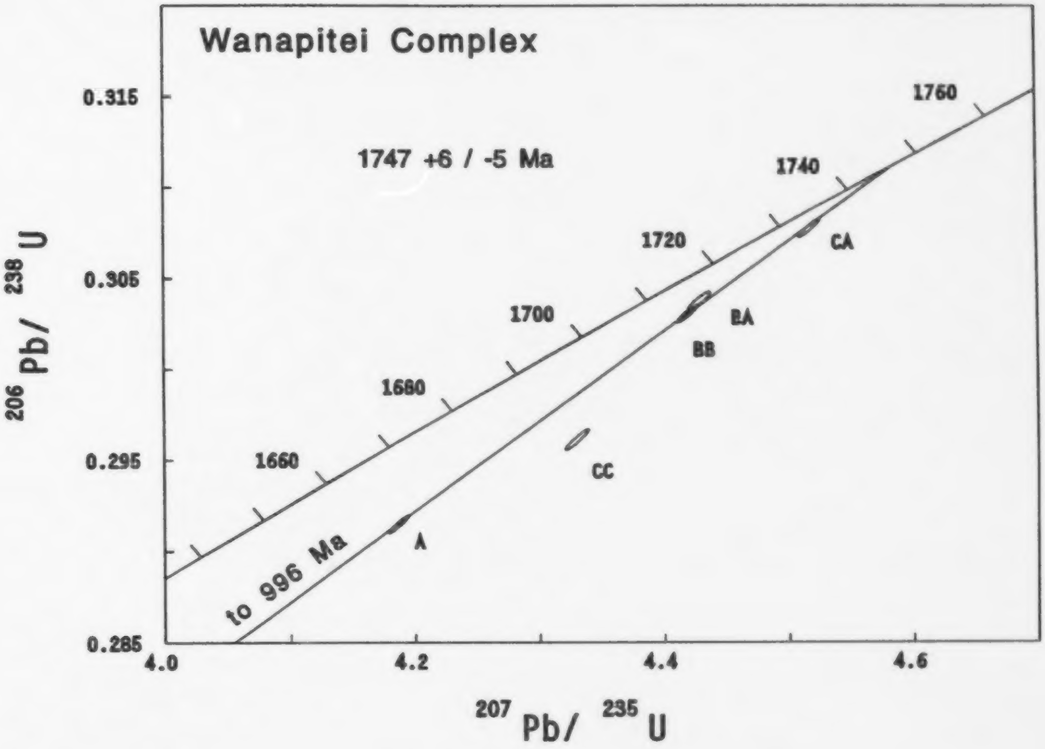

Figure 4.3. Concordia diagram for the Wanapitei intrusion.

and has a $^{207}Pb/^{206}Pb$ age of 2446 Ma. Fraction CA lies below the line, with a $^{207}Pb/^{206}Pb$ age of 2613 Ma.

4.1.4.2 Interpretation

A large amount of Archean, probably *ca.* 2700 Ma inheritance is indicated by the zircon data. The data for fraction CA is consistent with an Archean provenance which has undergone relatively recent lead-loss. The proximity of this intrusion to the Sudbury Structure such that it is actually in contact with the Sudbury Norite on the west side (Thomson, 1957), supports *ca.* 1850 Ma lead-loss related to the intrusion of the Sudbury Igneous Complex. However, the data for fraction BA precludes straightforward interpretation in terms of Archean inheritance in a Sudbury-aged intrusion, and suggests a *ca.* 2450 Ma component. A line from 1850 Ma through fraction BA produces an intercept at *ca.* 2550 Ma (indicated by dashed line in Figure 4.4a), which has no obvious geological relevance. Unfortunately, lack of exposure of contact relationships and the absence of up-to-date geological mapping preclude definitive interpretation of these zircon data based on field relationships for the Falconbridge Twp. intrusion. The available information suggests that a *ca.* 2450 Ma intrusion age is possible, with prominent Archean inheritance and episodic Pb-loss at 1850 Ma as a result of the emplacement of the Sudbury Igneous Complex.

4.1.5 Drury Twp. Intrusion

Sample SPA-88-56A is a chloritized, epidotized amphibole-plagioclase metagabbro from the north-central part of the intrusion (UTM zone 17, 464000E, 5141600N). Some relict igneous cumulate textures are preserved.

4.1.5.1 U-Pb results

Zircons obtained from the Drury Twp. sample were dark brown and relatively extensively fractured, although commonly subhedral with three or four crystal faces preserved (shown in Figure 4.1f). Grains were generally translucent, and while some zoning was observed, no obvious evidence for cores was noted.

SHRIMP U-Pb analyses of seven spots produced a cluster of points around concordia with an average $^{207}Pb/^{206}Pb$ age of 1855 ± 10 Ma (2σ), shown in Figure 4.4b). All analyses are within 2σ imprecision of one another and of the regression.

4.1.5.2 Interpretation

The morphological characteristics of the zircons and the absence of any isotopic evidence for inheritance suggests that the age of 1855 ± 10 Ma represents a crystallization age for the Drury Twp. intrusion. Although there is petrologic evidence for shock metamorphism of this intrusion during emplacement of the Sudbury Structure (Card, 1965), and there is extensive fracturing of the zircons, it seems unlikely that a shock metamorphic event would have completely reset the U-Pb zircon systematics without leaving some evidence of prehistory.

4.2 GRANITOIDS

4.2.1 Algoman Granitoid

Sample SPA-88-18 is a pink sodic biotite granite with a greenschist facies metamorphic overprint. This sample was obtained from about 6 km northwest of the EBL intrusion (UTM 17, 400955E, 5148875N).

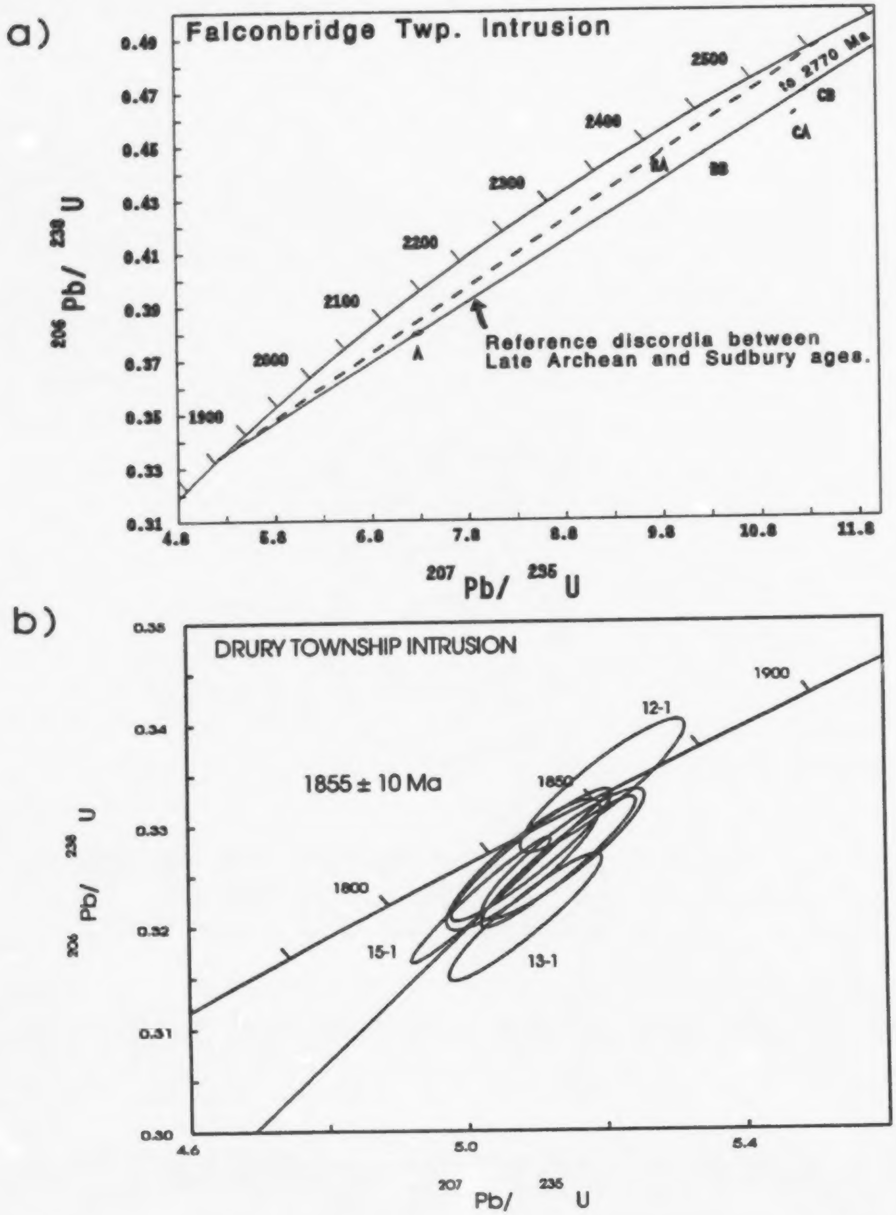

Figure 4.4 Concordia diagram for a) Falconbridge Twp. inherited zircons, and b) Drury Twp. "shocked" zircons.

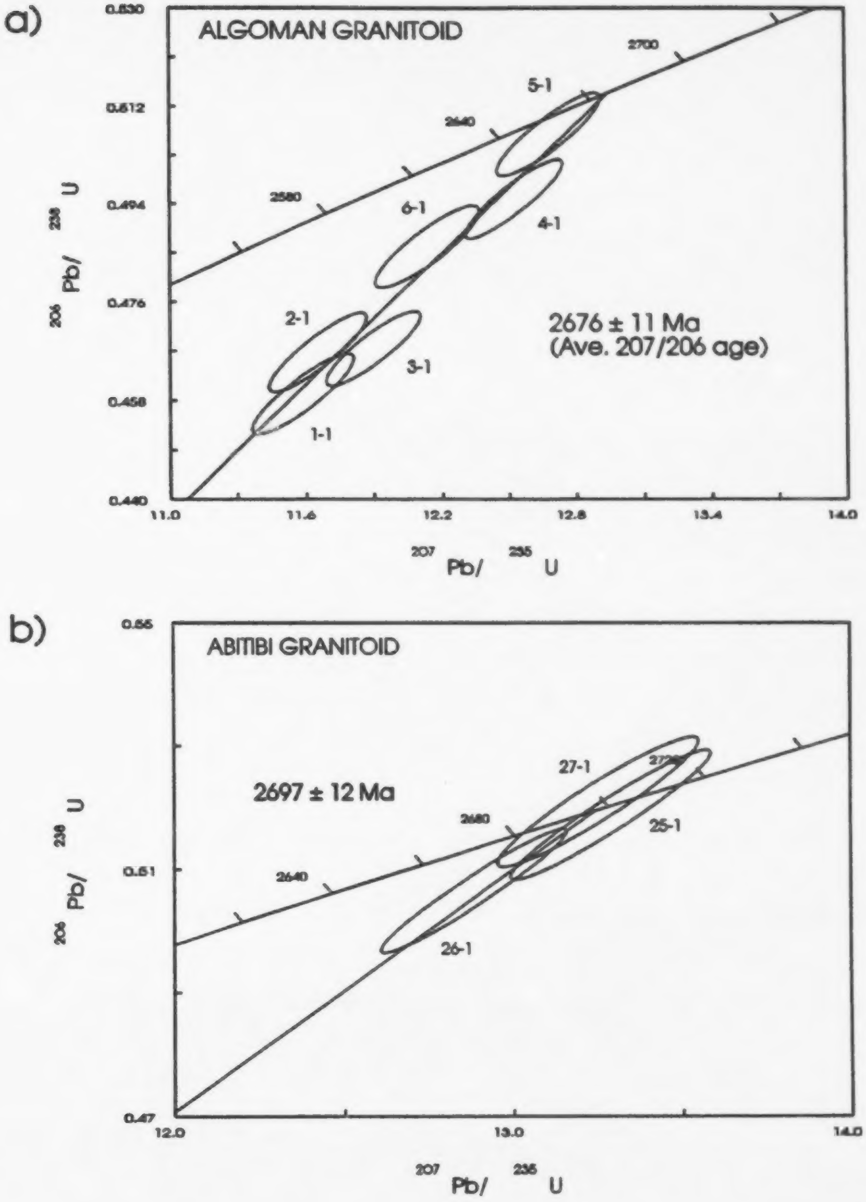

Figure 4.5. Abitibi Subprovince granitoids: a) Concordia diagram for Algoman granitoid b) Concordia diagram for deformed "Abitibi" granitoid.

4.2.1.1 U-Pb results

Zircons were pale pink, euhedral to subhedral clear grains, with minor inclusions of apatite and occasional length-normal fracturing. Grain dimensions varied from equant to weakly acicular (3:1 aspect ratios). SHRIMP analyses of six spots produced a discordant array which produced a Yorkfit regression of 2669 +31/-17 Ma (MSWD= 1.02) and an average $^{207}Pb/^{206}Pb$ age of 2676 ± 11 Ma (all errors as 2σ; Fig. 4.5a).

4.2.2 Abitibi Granitoid

Sample SPA-88-17 is a well-foliated tonalite located immediately to the north of the EBL intrusion (UTM zone 17, 407125E, 5145650N). Petrologic evidence suggests that this rock predates the Algoman granitoid intrusions.

4.2.2.1 U-Pb results

Sparse zircon yields resulted in the analysis of only three grains from this sample, which were euhedral, pale pink prismatic clear grains. Some evidence of internal structure including zoning, extensive fracturing, and possible cores was observed in grain fragments which were not analysed.

SHRIMP U-Pb analyses from three spots produced a cluster of points overlapping concordia, with an average $^{207}Pb/^{206}Pb$ age of 2697 ± 12 Ma (2σ), shown in Fig. 4.5b.

4.2.3 Interpretation

The *ca.* 2670 Ma age for the Algoman granite is interpreted as an igneous crystallization age, with the discordance attributable to non-episodic lead-loss over time. Using either regression and associated 2σ imprecision presented, the two granites are of equivalent age, within the error limits. However, the apparent older age for the Abitibi granite is consistent with the petrographic textural evidence.

4.3 DISCUSSION

4.3.1 Anorthosites

The age of 1222 ± 2 Ma for the Mercer Anorthosite is coincident with the relatively imprecise age of 1206 ± 36 Ma for the St. Charles Anorthosite, which lies about 20 km to the north of Mercer Twp. These two *ca*. 1220 Ma anorthosite ages are not coincident with any other mafic (or felsic) magmatism in the western Grenville Province. These ages slightly postdate *ca*. 1240 Ma intrusive ages for the Sudbury dyke swarm further to the north (Krogh *et al*., 1987), and the Mulock Granite (Lumbers *et al*., 1991). Possible (as yet undated) local correlatives to the southwest include the Eau Claire Anorthosite, the Rutter Granite and the Bigwood Nepheline Syenite (R.M. Easton, pers. comm. 1992).

The age of the Mercer Anorthosite combined with contemporaneous intrusion of the nearby St. Charles Anorthosite suggests minor magmatic activity at *ca*. 1220 Ma in the western Grenville. The fact that possibly correlative units nearby include another anorthosite and a nepheline syenite suggests that this magmatism was anorogenic. The presence of euhedral, very low-U zircons may indicate later metamorphic effects, possibly of Grenvillian age. If the presence of potentially Grenville-aged, low-uranium zircon in both anorthositic units is used to support a Grenville-aged lower intercept, a *ca*. 1240 Ma upper intercept is feasible for both intrusions.

4.3.2 Wanapitei Intrusion

The age of 1747 +6/-5 Ma for the Wanapitei intrusion correlates with the age of 1742.1 ± 1.4 Ma (van Breemen and Davidson, 1988) for the granitoid of the Killarney Complex some 60 km to the west. Both the Wanapitei and Killarney intrusive complexes are immediately adjacent to or cut by the Grenville Front Boundary Fault and/or mylonite (Davidson, 1986). These ages are comparable to those of *ca.* 1730 Ma granitoid orthogneiss from the northwestern Grenville Province (Krogh *et al.*, 1971;), *ca.* 1700 to 1750 Ma granite plutonism in the Southern Province (Davidson *et al.*, 1992), a *ca.* 1760 Ma granite-rhyolite terrane in Wisconsin, ca. 1700 to 1780 Ma orogenic material underlying southwestern and mid-continental North America (van Schmus and Bickford, 1981; van Schmus *et al.*, 1987) and with *ca.* 1750 to 1720 Ma arc activity in southeastern Laurentica-Baltica (*cf.* Gower *et al.*, 1991).

The major lithological difference between the Wanapitei intrusion and other possible correlatives is that the latter suites consist entirely of felsic material (intrusive and extrusive), with the exception of rocks of the Colorado Province which include tholeiite-dominated bimodal volcanics (van Schmus and Bickford, 1981). If the Wanapitei intrusion is related to orogenic activity, it represents the only identified manifestation of mafic magmatism associated with otherwise felsic plutonism and volcanism yet identified.

Age data for the Wanapitei Complex suggest an affinity, temporally and perhaps tectonically, with the Killarney Complex and the potentially related granite-rhyolite terranes to the southwest. Although the Wanapitei Complex is a relatively minor intrusion, it represents a departure from the felsic magmatism which characterizes the other contemporaneous suites, in that it is gabbro-noritic without an associated felsic component.

4.3.3 Metagabbroic Intrusions

The isotopic characteristics of zircons from the Falconbridge Twp. intrusion infer an Early Proterozoic emplacement age with significant late Archean component, possible sources of which include Abitibi granitoids and detrital grains from Huronian sediments, or higher-grade Levack gneiss-type material (representing potential lower crust in the Sudbury area). The observation that the inheritance clearly predates 2450 Ma material favours an Archean age (as opposed to a younger Creighton-Murray Granite age) for the granitoid which hosts the intrusion on its east flank, although the inheritance may reflect deeper-level contamination. Further analyses of single, relatively clear grains is required to establish the nature of the Early Proterozoic contributions (both at 2450 and 1850 Ma) to these systematics.

The *ca.* 1850 Ma "Sudbury-age" (*cf.* Krogh *et al.*, 1984) for the Drury Twp. intrusion is somewhat enigmatic, as petrologic and field evidence suggests an affinity between it and the other metagabbros along the northern boundary of the Southern Province. Evidence such as the presence throughout the Drury intrusion of shock metamorphic breccias related to the emplacement of the Sudbury Structure ("Sudbury breccias"; Card, 1965) requires that the emplacement of the Drury Twp. intrusion predates that of the Irruptive. The Drury Twp. body is also cut by Nipissing Diabase-type dykes, inferring an Early Proterozoic origin. The observation that the Falconbridge Twp. intrusion zircon population is almost exclusively composed of Archean inherited material, combined with its petrographic and lithological similarity to the Drury Twp. body suggests that an early Proterozoic intrusion age might be accommodated if relatively little zircon growth occurred at the time of intrusion, such that the population observed is a product of secondary, hydrothermally-facilitated zircon growth related to the emplacement of the Sudbury Structure.

4.3.4 Abitibi Subprovince Granitoids

The two 2670 to 2700 Ma ages for granitoids of the southernmost Superior Province agree with comparable age data from further north in the Abitibi and Wawa Subprovinces (*e.g.* Krogh and Turek, 1982; Corfu and Stott, 1986). The Algoman granite age of 2676 ± 11 Ma is also comparable to the age of 2667 +1.6/-1.4 Ma for the Parisien Lake Syenite (Krogh *et al.*, 1984), which is spatially associated with the EBL intrusion. The imprecision of the date for the Algoman granite minimizes the potential significance of the relatively young age.

4.4 SUMMARY

The implications of the U-Pb zircon geochronological evidence for this study are that the three bodies located to the south of the Grenville Front cannot be temporally associated with the Early Proterozoic mafic magmatic episode. The Mercer and St. Charles anorthosites (referred to collectively as "Burwash area anorthosites" by Simmons and Hanson, 1978) may represent relatively limited *ca.* 1220 Ma anorogenic activity in the western Grenville. The Wanapitei intrusion may be related to orogenic activity further to the west, albeit as a rare mafic expression thereof.

The Falconbridge and Drury Twp. intrusion ages remain somewhat speculative, although better constrained than before this study. Evidence for Sudbury-aged zircon growth exists in both intrusions, especially the latter. A *ca.* 2450 Ma intrusion age is only weakly indicated by isotopic evidence for the Falconbridge Twp. intrusion (and is absent for the Drury Twp. body), but field relationships strongly support an Early Proterozoic age of intrusion, especially for the latter.

The absence of datable minerals in the May Twp. and Huronian tholeiite samples examined leaves their ages poorly constrained between the ages of Algoman granite (a potential upper limit of around 2700 Ma) and Huronian rhyolite (with a 2440 Ma lower limit; Krogh *et al.*, 1984).

CHAPTER FIVE: GEOCHEMISTRY

5.0 INTRODUCTION

The major and trace element geochemistry of the units sampled will be used as signatures for classification and comparative purposes and as indicators of process. For the mafic intrusive rocks the geochemistry is investigated by separating the elemental abundance data into geochemical groups, namely, the large ion lithophile elements (LILE), including K, Na, Rb, and Ba, the more compatible elements including Sr and the siderophile elements, the (incompatible) high field strength elements (HFSE) including Nb, Zr and Y, and relatively immobile elements, such as the rare earth elements (REE). By investigating the geochemical coherence within each group, between each group and relating trace element and major element variations, the geochemical evolution and character of the gabbro-anorthosites can be delineated. Geochemical data are presented in Appendix 2, and the symbol legend for all plots is given in the List of Symbols at the front.

5.1 CLASSIFICATION

In spite of petrologic evidence for open system behaviour of the LILE, plotting total alkali (K_2O + Na_2O) against SiO_2 shows essentially all of the samples falling in the alkali-poor "basalt" field of Cox *et al.* (1979) and in the sub-alkaline field of Irvine and Baragar (1971), shown in Fig. 5.1 a) and b). This suggests that whereas the LILE may have been mobilized, exchange between the gabbros and relatively high-alkali rocks such as the host granitoids was not significant (in these samples). Evident from these two diagrams and from the ternary alkali-iron-magnesium (AFM) plot of Irvine and Baragar (1971) is that the units located to the south of the

Grenville Front Tectonic Zone show enrichment in alkalis relative to those units to the north of the GFTZ. The AFM plot (Fig. 5.2a) suggests that the majority of the units followed tholeiitic evolution trends, while the samples from Mercer Twp. and St. Charles show better aligned trends consistent with either more calc-alkaline magmas and/or enrichment with more alkalic, less femic material.

The addition of titanium to the diagrams allows, in general, for the discrimination of units north of the GFTZ from units to the south, and more specifically, of samples petrographically characterized as cumulates from the rest. A number of diagrams which plot Ti against other major and trace elements show a bulk separation of these two groups, including TiO_2 against FeO/MgO ratio (Myashiro, 1974), TiO_2 *vs.* MnO *vs.* P_2O_5 (Mullen, 1983), log Ti against log Cr (Pearce, 1975) and V against Ti (Shervais, 1982), shown in Figures 5.2 b), 5.3 and 5.4. All of these diagrams discriminate, to some extent, between samples from the Wanapitei, Mercer, St. Charles, and most notably, the May Twp. and the Huronian volcanic units (higher TiO_2) from the cumulates from EBL, S-D, Drury and Falconbridge Twps. (with lower TiO_2).

No intrinsic tectonic significance is attached to the particular fields into which these groups of samples fall since, in general, the units north of the GFTZ which comprise mostly cumulates also tend to be the least recrystallized, and comparisons of cumulates with possible liquid representatives which are also recrystallized would be suspect.

5.2 MAJOR ELEMENT GEOCHEMISTRY

The major element geochemistry of the metagabbros, presumably dependent on the major mineralogy, can be described using variation diagrams such as Harker diagrams in order to establish the geochemical coherence within units.

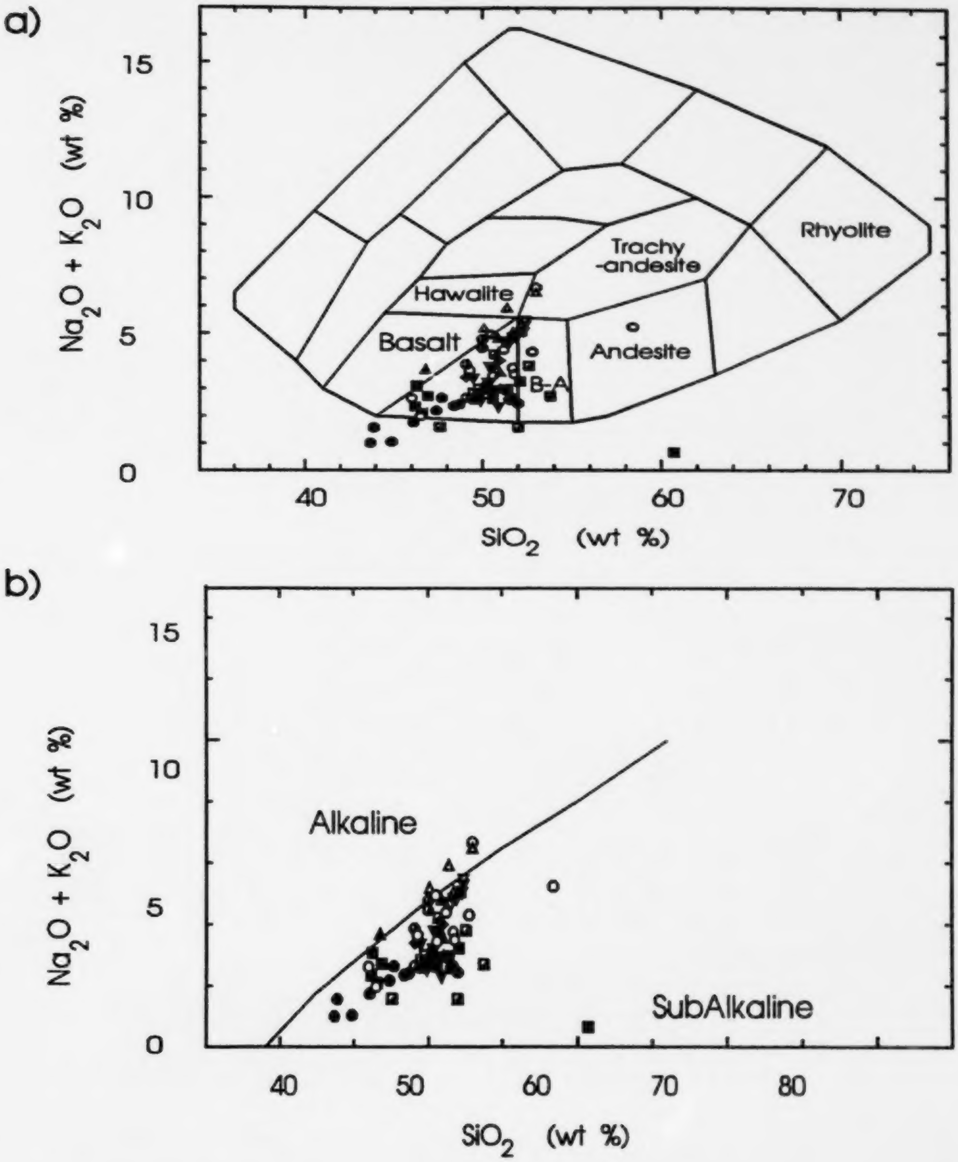

***Figure 5.1.** SiO_2 vs. total alkalis, using fields of **a)** Cox et al., 1979, (B-A = basaltic-andesite) and **b)** Irvine and Baragar (1971), for distinguishing alkaline from sub-alkaline mafic magmas. Symbols as shown in Table 5.1.*

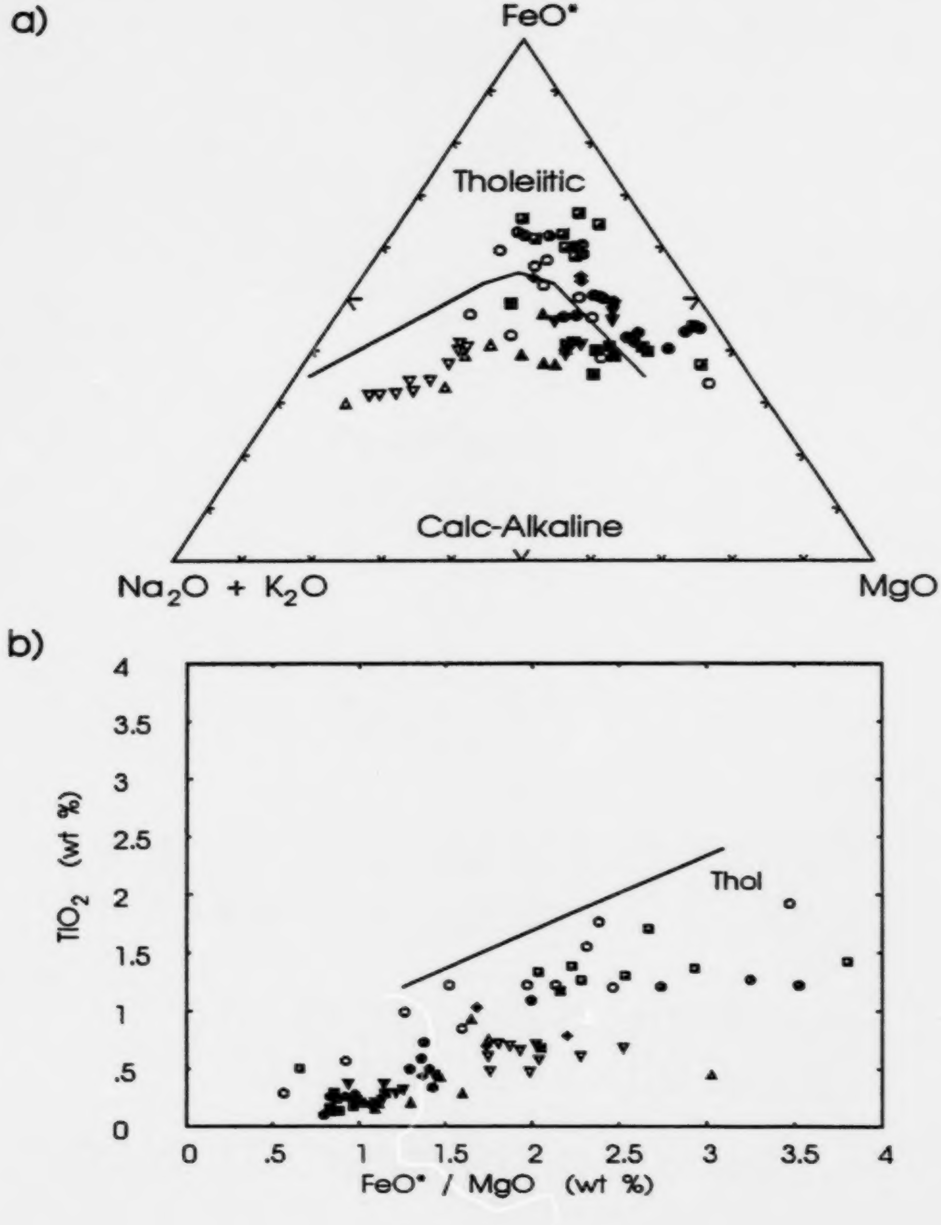

Figure 5.2 a) AFM diagram with tholeiitic and calc-alkaline "fields", from Irvine and Baragar (1971) b) FeO/MgO-TiO2 plot from Myashiro (1974), distinguishing the tholeiitic basalt field.*

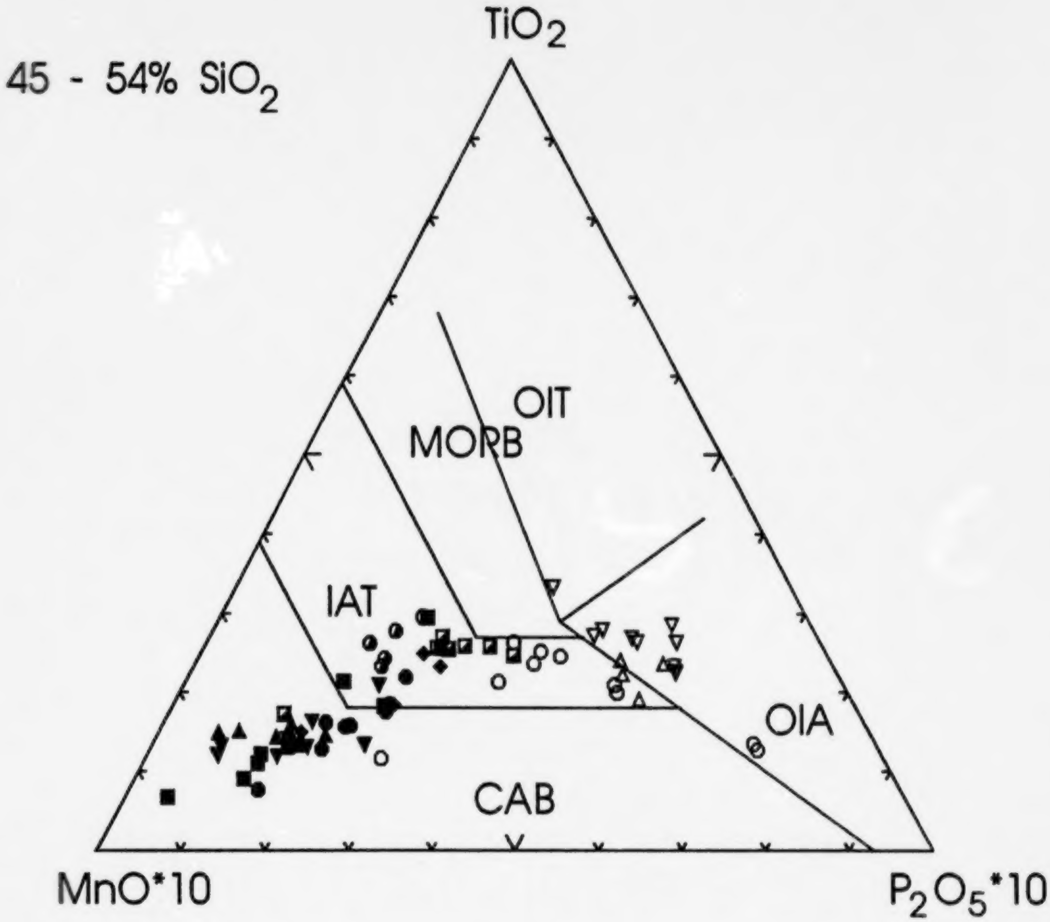

Figure 5.3. Ternary phosphorus-titanium-manganese variation diagram from Mullen (1983), where CAB= Calc-Alkaline Basalt, IAT= Island Arc Tholeiite, MORB= Mid-Oceanic Ridge Basalt, OIT= Ocean Island Tholeiite, and OIA= Ocean Island Andesite.

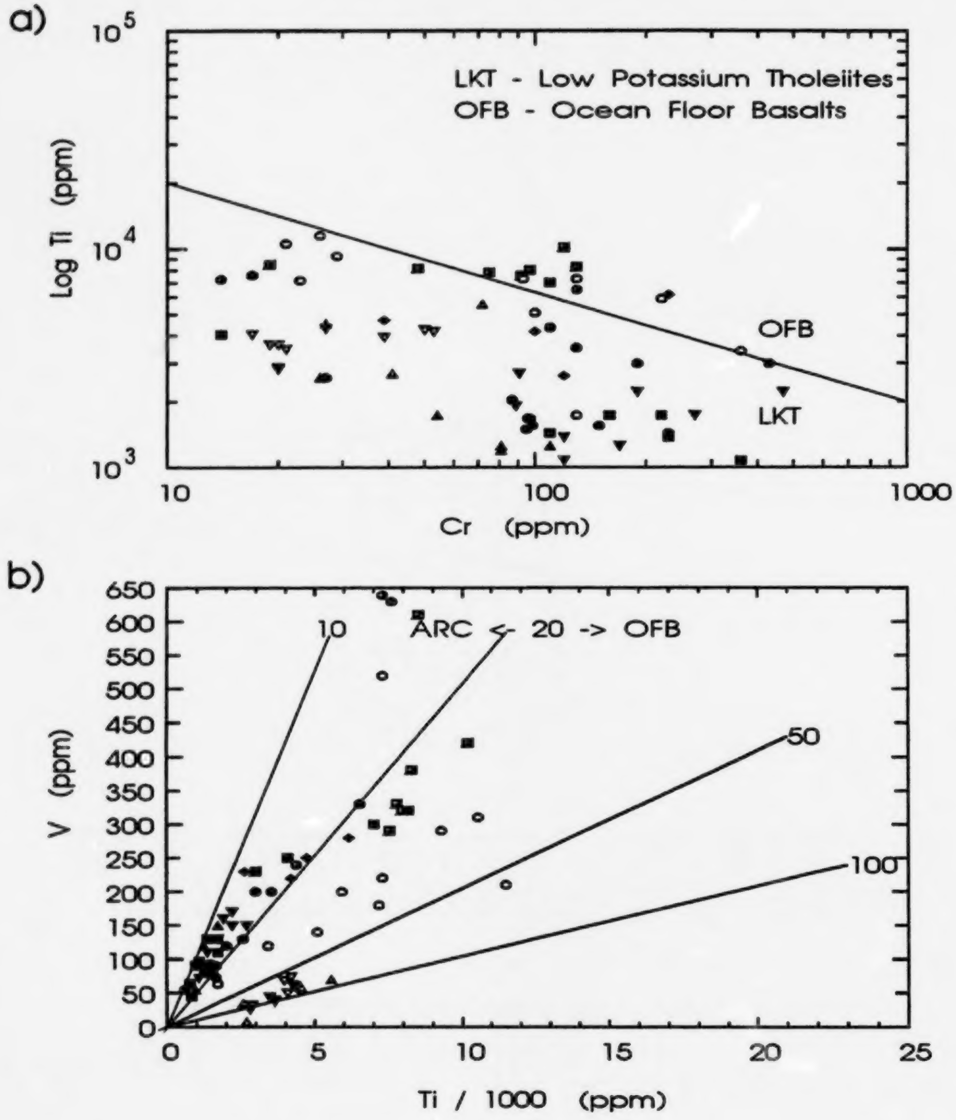

Figure 5.4. *Titanium-transition element variation.*
a) *Chromium-titanium variation, from Pearce (1975).*
b) *Titanium-vanadium variation, from Shervais (1982), where ARC= Island-arc type basalt, OFB= Ocean Floor Basalt.*

Alternatively, and particularly appropriately for metamorphosed gabbroic rocks which largely no longer reflect their original, probably anhydrous, mineralogy, normative mineralogy can be used to characterize major element geochemistry.

5.2.1 Normative Classification

Petrographic evidence suggests that these metagabbroic rocks originated as relatively dry rocks with anhydrous-mineral-bearing assemblages consisting essentially of ol-plag-cpx and/or opx, and that the abundant hydrous phases present such as amphiboles and biotite are secondary. Based on this premise, CIPW normative mineralogies were calculated (given in Appendix 2), to provide a basis for comparing units based on both their major element geochemistry and appropriate estimates of original mineralogy. Any normative calculation is constrained by the assumption of closed-system behaviour, which in this case has been violated to varying degrees. The consistency observed in the norms summarized below suggests that they retain sufficient validity for comparative purposes.

East Bull Lake Intrusion:

The EBL intrusion is relatively consistent in its normative mineralogies, given the range in observed modal compositions. EBL samples vary from weakly quartz normative (<2.5 wt%) to strongly olivine normative (20 to 30 wt.%), averaging about 10 wt.% ol-normative. All the norms are dominated by calcic plagioclase (bytownitic), and contain hypersthene and diopside in varying proportions (usually Hy > Di). Normative calcite is occasionally present in small amounts.

Shakespeare-Dunlop Intrusion:

The S-D intrusion has the same normative mineralogies as the EBL and in similar proportions, although with more variability. Pyroxene contents (Hy + Di) range from as high as 40 wt.% in sample SPA-88-11 to as low as 3 wt.% (in SPA-88-13). One sample (SPA-88-07) also shows andesine-type normative plagioclase.

Tennyson Township:

The three samples from Tennyson Twp. are distinct from the EBL and S-D norms in that they contain relatively sodic plagioclase (An ≈ Ab) and are weakly olivine-normative (< 5 wt.%).

Drury Township Intrusion:

The Drury Twp. samples also vary between weakly quartz-normative and olivine normative (≤ 10 wt.%), although one sample is nepheline normative (SPA-88-55). They are distinguished from the EBL and S-D norms by their relatively sodic plagioclase (< An_{60}), as well.

Falconbridge Township:

These samples are also weakly quartz- to olivine - normative, similar to the Drury Twp. samples, with comparable plagioclase compositions. Normative pyroxene averages 30 to 40 wt.% (as opposed to 10 to 20 wt.% from Drury Twp.), and commonly Di > Hy.

May Township:

These samples are typically olivine-normative, contain sodic plagioclase (Ab > An), and are calcite-normative. Both pyroxenes are present in sub-equal amounts, usually with Hy > Di. One sample (SPA-88-36) is quartz-normative and has calcic plagioclase.

Huronian Volcanics:

The volcanics are invariably quartz-normative, contain labradoritic normative-plagioclase, and have relatively high pyroxene contents compared to the intrusions described above.

Wanapitei Intrusion:

The Wanapitei samples vary from being weakly quartz-normative to olivine-normative, with two samples showing corundum in the norm (with quartz). Diopside may be absent, with total pyroxenes at about 25 wt.%, with Hy > Di. The plagioclase may be sodic or calcic, and orthoclase, typically 4 to 10 wt.% in the other intrusions, can be as high as 18 wt.%. Calcite is always present in the Wanapitei norms.

St. Charles Anorthosite:

The St. Charles anorthosite is distinctive in that its norm consists of 90 wt.% plagioclase, of sodic labradorite composition. Other normative minerals and proportions are comparable to the other units, albeit that they total 10 to 15 wt.% of the norm.

Mercer Anorthosite:

The Mercer Twp. norms are also plagioclase-dominated (70 to 80 wt.% andesine, where An only slightly exceeds Ab), and are olivine ± nepheline normative.

In summary, the normative mineralogies show the EBL and S-D intrusions to be comparable, with noritic to olivine-noritic norms, as distinct from the quartz-noritic volcanics. From Drury and Falconbridge Twps. through Tennyson to May Twp., the norms become less siliceous (occasionally nepheline-normative), with olivine replacing quartz and the feldspars becoming more alkalic. The Wanapitei norms are relatively variable but are comparable to the EBL and S-D type compositions. The St. Charles and Mercer Twp. norms are anorthositic.

5.2.2 Variation Diagrams

Variation diagrams for major elements against silica are shown in Fig. 5.5 and 5.6. Due to the extent of metamorphism and resultant primary mineral replacement, recognizable major element geochemical trends are apparent to varying degrees only in the larger, more pristine bodies, specifically the EBL pluton and to a lesser extent, the S-D intrusion. The absence of trends could also be the result of relatively limited compositional ranges in some units (notably the smaller dike-like intrusions).

Silica varies from about 44 wt.% (olivine cumulates from EBL) to about 54 wt.% in samples from the Grenville Province metagabbros. In general the three units from the Grenville Province have higher SiO_2 and lower $Mg^{\#}$ than the units to the north, so a bulk separation is observed regardless of the choice of ordinate. The cumulates from north of the GFTZ show less variation in the network modifying elements, although equal or greater variation in SiO_2 contents.

Based on broad geochemical distinctions and petrographic characteristics, the following associations of metagabbro units may be defined for convenience of further discussion:

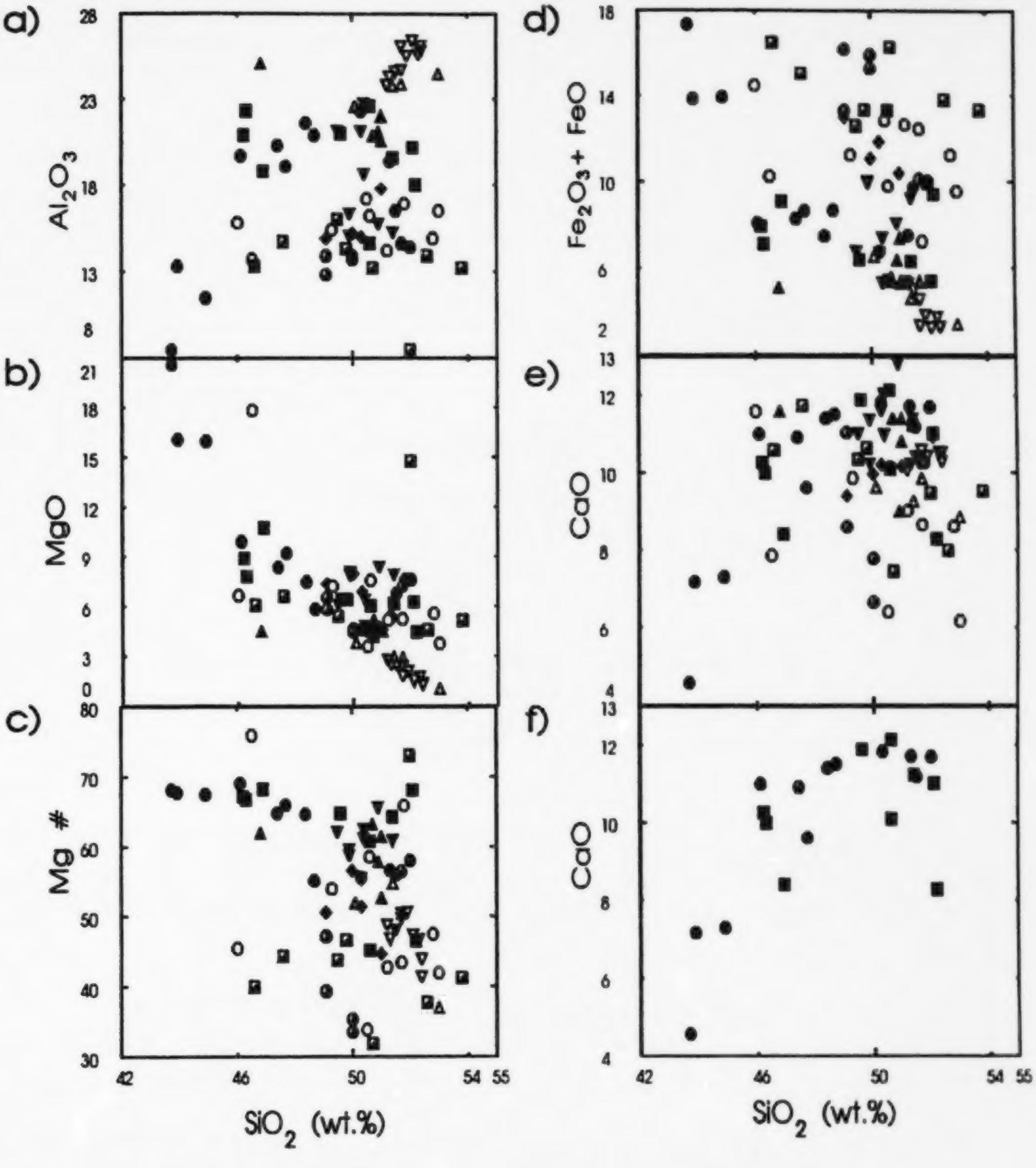

Figure 5.5. Variation of SiO_2 (wt.%) against a) Al_2O_3 b) MgO c) Mg# d) total Fe e) CaO and f) CaO for the EBL and S-D alone.

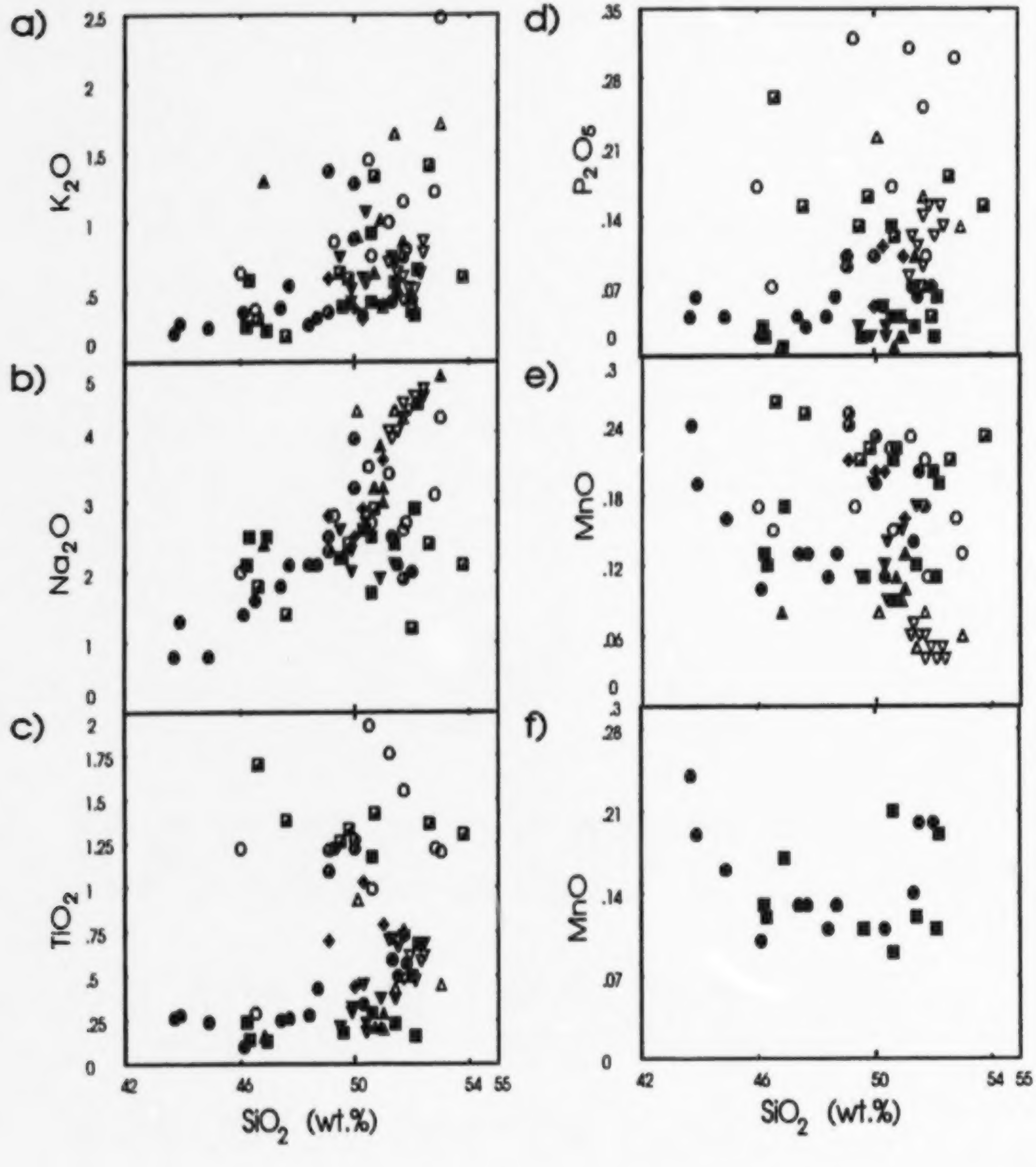

Figure 5.6. Variation of SiO_2 (wt.%) against a) K_2O b) Na_2O c) TiO_2 d) P_2O_5 e) MnO and f) MnO for the EBL and S-D alone.

Group 1 - Cumulate-textured metagabbros from the north side of the GFTZ, comprising the EBL, S-D, (Tennyson Twp.), Drury Twp. and Falconbridge Twp. bodies.

Group 2 - Non cumulate-textured mafic rocks from the north side of the GFTZ, comprising the basal Huronian mafic volcanics and samples from May Twp.

Group 3 - Recrystallized metagabbros (both cumulate and non-cumulate textured) from the south side of the GFTZ, comprising the Wanapitei, St. Charles and Mercer Twp. intrusions.

This grouping of units discriminates between the cumulate gabbros along the southern margin of the Superior Province and the volcanics. While there exists some geochemical coherence within Groups 1 and 2, Group 3 is defined most often by its exclusion from the other two groups and not for any coherence of its own.

Group 1: The EBL intrusion shows correlations of increasing SiO_2 with decreasing MgO (and $Mg^{\#}$), MnO, and total iron (FeO + Fe_2O_3), and increasing amounts of Na_2O, K_2O, and TiO_2. The S-D intrusion shows similar correlations with similar abundances but with more scatter, and the other, smaller units show very little discernable systematic variation.

Group 2: In general the Huronian volcanic samples and those from the May Twp. intrusion plot together and are often distinct from the cumulate samples and the units south of the GFTZ, especially evident in TiO_2-$Mg^{\#}$ space.

Group 3: The Wanapitei intrusion shows generally incoherent and relatively variable elemental abundances and tends to overlap with all of the Groups, except in TiO_2-SiO_2 space, where they overlap with Group 2 samples. The St. Charles intrusion samples have a limited range of elemental abundances, and are often overlapped by the Mercer Twp. samples, which show more variation. The St. Charles samples are distinguished from those of all the other units by relatively low abundances of total iron, MgO and MnO, and by high Na_2O, K_2O, and Al_2O_3.

The evidence from the discrimination diagrams in Chapter 5.1 and the observation that Group 1 is most clearly distinguished geochemically from Groups 2 and 3 in plots of SiO_2 or $Mg^{\#}$ against TiO_2 suggests that the most useful information is to be found in the distribution of trace elements, particularly the incompatible and HFS (high field strength) elements.

5.3 TRACE ELEMENT GEOCHEMISTRY

The trace element geochemistry will be investigated by examination of the LILE, the compatible metals and incompatible elements (HFSE and REE). Various two-element plots will be used to display geochemical associations, and normalized plots ("spidergrams") will be used to characterize and compare individual units.

5.3.1 Large Ion Lithophile Elements (LILE)

On the basis of petrological evidence previously presented, the distribution and abundances of the LILE must be treated with caution. On a plot of K *vs.* Rb (Fig. 5.7a) the EBL pluton shows a relatively linear trend with a K/Rb ratio around 75. The S-D intrusion has comparable ratios but more scatter, and all other units have much higher K/Rb ratios.

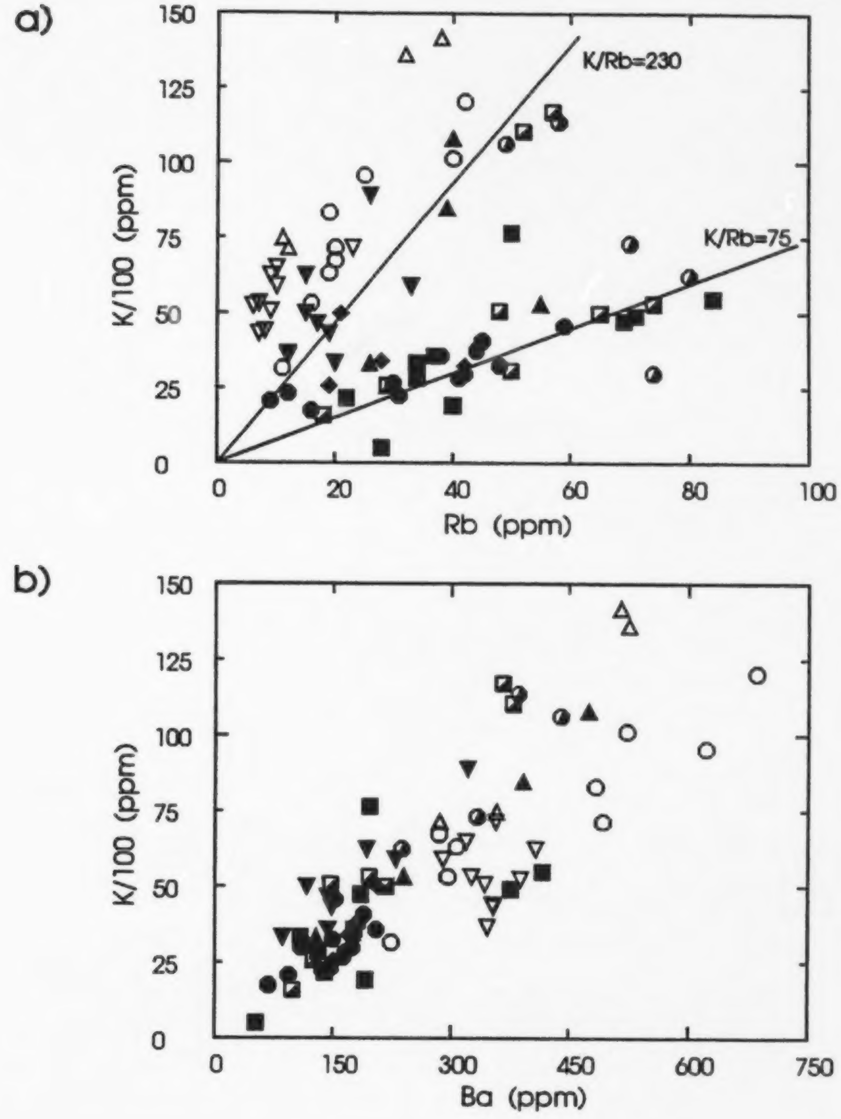

Figure 5.7. LILE variation. a) potassium-rubidium variation, with igneous trend (K/Rb=230) and K/Rb=75 reference lines. b) potassium-barium variation.

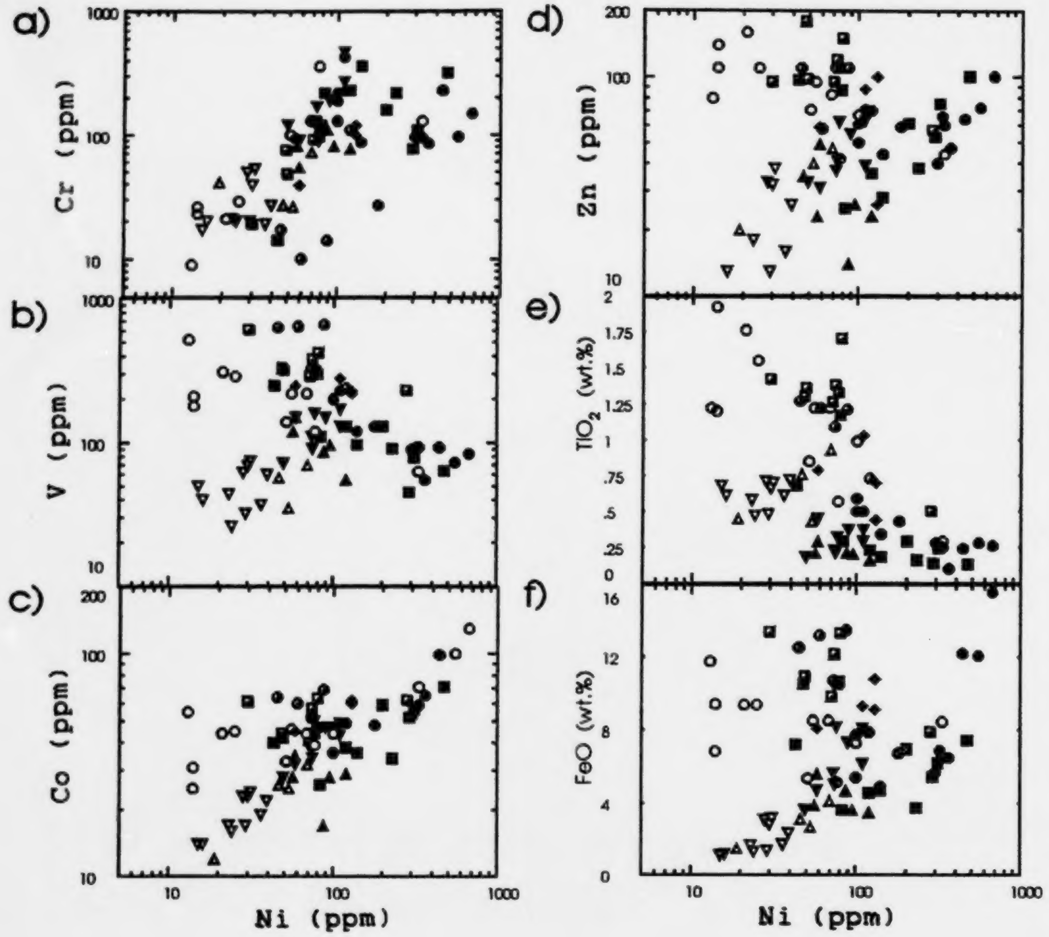

Figure 5.8. Variation of nickel (ppm) against a) chromium b) vanadium c) cobalt d) zinc e) titanium and f) FeO.

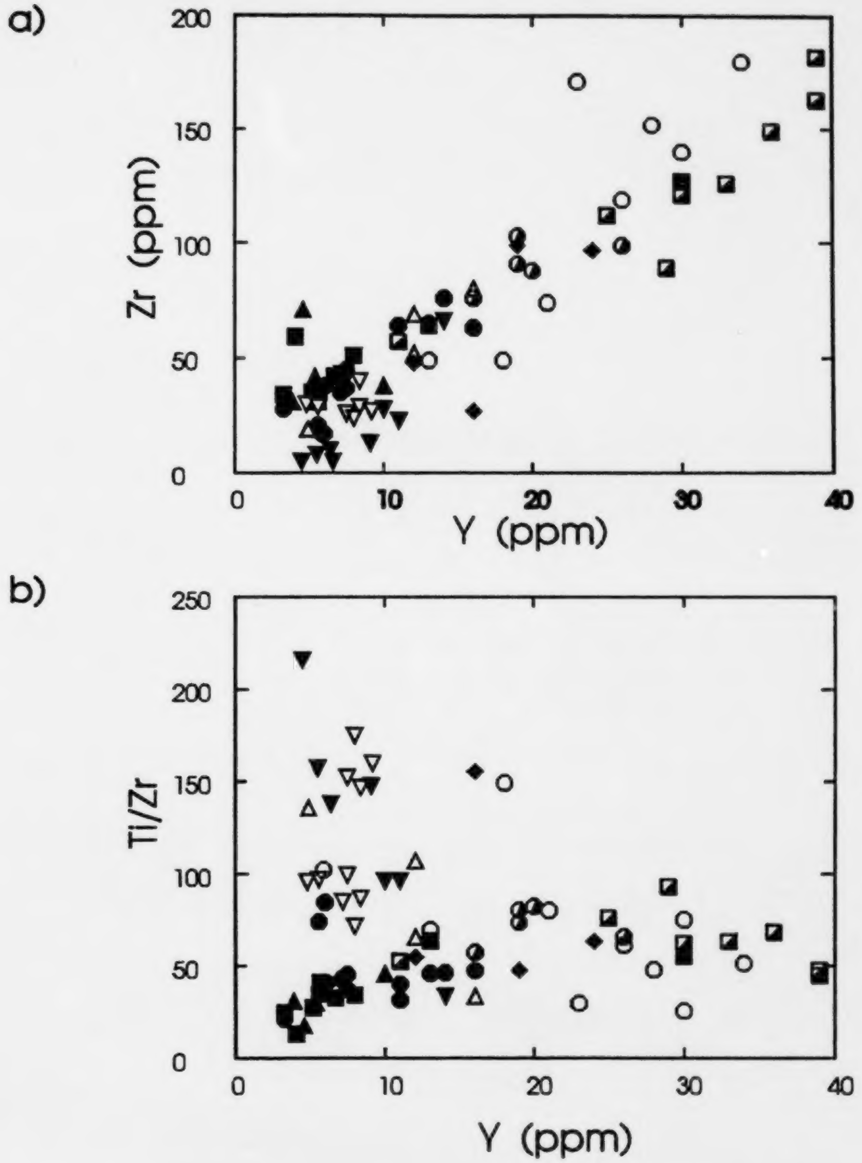

Figure 5.9. *Incompatible element variation **a)** Y-Zr variation, and **b)** Y-Ti/Zr.*

Rough linear trends shown by the St. Charles, Wanapitei and Falconbridge bodies are artifacts of K variation with essentially constant Rb content, and are unlikely to be products of magmatic differentiation processes, as these should not significantly fractionate K and Rb from one another. Plots involving Ba yield relatively scattered points, but are essentially comparable to the K-Rb distributions (Fig. 5.7b).

5.3.2 Compatible Elements

The compatible element data available are for siderophile elements such as Ni, Cr, V, Co and Zn (Fig. 5.8). Well-developed trends between these elements within units are absent as a rule, although a weak negative correlation between Ni and V is evident in the EBL samples. The May Twp. intrusion may be distinguished in compatible element plots by low Cr and Ni and high Co, Zn and V abundances, as well as high FeO contents, relative to the other Group 1 and 2 samples. The Huronian volcanics tend to lie between the May Twp. and the Group 1 samples. This distribution is particularly evident in the plots of Ni against Cr and V. A plot of Ni abundance against TiO_2 distinguishes Group 1 from Group 2 clearly, where the May Twp. intrusion samples plot between the volcanics and the cumulates. The implication of these plots is that the Group 2 samples represent more evolved material (liquids?) than the Group 1 cumulates, and further, that the May Twp. samples are less evolved than the volcanics.

5.3.3 Incompatible Elements

Incompatible elements (which are relatively insoluble in aqueous media) should most closely approximate their primary geochemical distributions. Binary incompatible element plots such as Zr and Ti/Zr ratio against Y show the same distribution pattern as the Ni-TiO_2 plot, in that the cumulates are distinguished from the May Twp. and mafic volcanic samples (Figure 5.9).

5.4 "SPIDERGRAMS" AND REE

The incompatible element distribution of each unit can best be characterized by plotting various elements on a line diagram, normalized to the reservoir of choice, producing a "spidergram". LILE, HFSE and REE data are normalized to a primitive mantle reservoir on the premise that the late Archean mantle would be more primitive than a modern MORB-type composition. Elements are plotted in a sequence (modified from Pearce, 1983) according to increasing degrees of incompatibility. Similarly, REE data are plotted normalized to chondritic abundances (Sun, 1982). These diagrams can be characterized in terms of three features; the abundance relative to the normalizing reservoir, the slope of the distribution pattern(s), and anomalous element abundances which result in positive or negative "spikes" in the profiles. This permits the relatively immobile components of the units to be compared with one another and, potentially, with the modelled source region.

5.4.1 Spidergrams

Spidergram and REE profiles are shown in Appendix 3. The following table (Table 5.1) summarizes the spidergram profiles, semi-quantitatively, where the abundance is represented by the range of abundances of the HREE elements, the slope of the profile by the chondrite-normalized La/Yb ratio, and irregularities in the profile by qualitative "spike" observation, given as positive or negative relative anomalies. Relatively poorly-pronounced anomalies are annotated as "weak".

Table 5.1. Spidergram Summary

Unit	**Abund.(HREE)**	**$(La/Yb)_N$**	**"Spikes"**
East Bull Lake	1x - 5x	3.3 - 5.7	-ve Ti, Zr (both weak)
Shakes.-Dunlop	0.9x - 2x	4.0 - 6.6	-ve Ti (weak)
Drury	1x - 3x	2.4 - 4.9	-ve Ti (weak)
Falconbridge	1x - 4x	2.3 - 5.1	-ve Zr, -ve Ti (weak)
May	4x - 7x	2.3 - 4.0	
Mafic volc.	3x - 10x	2.4 - 4.1	-ve Ti (weak)
Wanapitei	2x - 20x	3.7 - 16	-ve Zr, Nb +ve Y (weak)
St. Charles	1x - 2x	6.4 - 9.4	-ve Zr, (Rb), Nb (?)
Mercer	1x - 4x	5.8 - 10.7	-ve Zr, (Rb), Nb

The qualitative associations suggested by the binary geochemical diagrams are supported by the spidergram plots. The Group 1 units (EBL, S-D, Drury and Falconbridge Twp. intrusions) all show similar characteristics, albeit that the Falconbridge Twp. profiles display a significantly more pronounced negative spike for Zr. The May Twp. and Huronian mafic volcanic sample profiles have comparable abundances and slopes to one another, showing enriched abundances relative to Group 1 and generally flatter profiles. The Group 1 samples show only poorly pronounced negative Zr and Ti anomalies. The St. Charles and Mercer Twp. bodies are distinct from the other units and are mutually comparable. The St. Charles profile is annotated with a negative Nb spike. This reflects the analytical constraints on the Nb data, which were all below detection limit. Therefore, while a negative Nb spike probably exists, its magnitude is unknown. Rb is noted in parentheses because its geochemical mobility does not preclude secondary influence as well as the less mobile elements on the abscissa. The Wanapitei intrusion shows distinctive profiles in all traits.

5.4.2 REE Profiles

The chondrite-normalized REE profiles (Appendix 3) can be characterized by the same features as the spidergrams, albeit that the anomalies are, as a rule, restricted to spikes in the Eu relative abundances. The slopes are reflected in the $(La/Yb)_N$ ratio value ranges presented above. The Group 1 samples are all characterized by distinct negative Eu anomalies which diminish in size with increasing abundance, ultimately reflecting small negative Eu anomalies in the most REE-enriched sample profiles. The Group 2 samples display weakly negative to absent Eu spikes. The St. Charles and Mercer Twp. bodies show pronounced positive Eu spikes, especially the former unit, although the Mercer samples display the trend described above, with increasing REE enrichment. The Wanapitei intrusion displays the largest variation in abundances and slopes, and generally Eu anomalies are absent, although negative and positive spikes are present in the most REE-enriched and REE-depleted samples, respectively.

5.5 DISCUSSION AND SUMMARY

The previous sections of this chapter have examined the geochemical data, specifically the incompatible and relatively immobile trace element data in terms of data distribution and of pattern recognition and comparison, in the case of the normalized-element line diagrams. In this section the geological processes responsible for these trace element distributions are considered in terms of the two main processes affecting mafic igneous rock geochemistry. These are fractional crystallization and contamination/assimilation and/or mixing. A primary requirement in distinguishing these processes is the distinction between cumulates and possible liquid compositions. The effects of fractional crystallization and accumulation must therefore be accounted for first.

5.5.1 Effects of Fractional Crystallization

The petrographic evidence for all of the Group 1 samples suggests cumulate textures, where preservation permits. The May Twp. samples, which show no cumulate textures and the Huronian mafic volcanics, which are extrusive lavas (*e.g.* Jolly, 1987a) show some geochemical distinction from Groups 1 and Group 3, especially their incompatible HFSE abundances. The Wanapitei intrusion may contain both liquid and residual phases in varying amounts, based on petrographic evidence.

Given a) the apparent absence of any marginal chilled phases of the EBL and S-D intrusions which clearly represent liquid compositions (D. Peck, pers. comm., 1992); b) the observation that the May Twp. samples generally lie between the volcanic samples and the Group 1 cumulates on incompatible element plots and c) the relative enrichment of the May Twp. samples in spidergram plots; the May Twp. intrusion appears to represent material which is, in general, more evolved than the

Group 1 cumulates but less evolved than the Huronian basalts. Whether the May Twp. rocks are more representative of a "primary" magma (which is relatively primitive, representing a melt immediately following extraction from its source), or a "parental" magma (which has undergone evolution *via* fractional crystallization, using the terminology of Presnall, 1979), is difficult to distinguish based on the incompatible element variation diagrams. Investigation of the patterns displayed in the spidergrams and REE profiles provides more diagnostic semi-quantitative evidence for fractionation effects.

The main crystallizing minerals involved in basaltic-rock genesis are olivine, plagioclase (calcic), clinopyroxene, orthopyroxene and garnet (*e.g.* McKay, 1989). Excluding garnet, all of these minerals or their relicts and/or pseudomorphs are observed in the Group 1 cumulates, and are indicated in the CIPW normative mineralogies as well. Using available crystal-melt partition coefficients ($D_{x\text{-}l}$) appropriate for basaltic systems, the effects of fractional crystallization of these phases on the trace element composition of the melt can be calculated. The following sources were used to provide partition coefficient data: for all phases used, $D_{x\text{-}l}$ values for Y, Nb, Ti and Zr are from Pearce and Norry (1979). $D_{x\text{-}l}$ values for the REE and alkali elements are from Hanson (1977) for olivine, clino- and orthopyroxene, and for plagioclase, gabbroic-anorthosite values from Simmons and Hanson (1980) and Hanson (1980) are used. Calculated abundances of Cr for all minerals are based on $D_{x\text{-}l}$ values estimated from Henderson (1984).

Model 1: Bulk Fractional Crystallization

In order to provide a crude idealized approximation of the geochemical signature of a possible parental melt for the cumulates, a liquid composition was derived for each sample given the observed elemental abundances in the sample, the D_{x-l} values, and the normative abundances of olivine, plagioclase, clinopyroxene and orthopyroxene in each sample. This calculation therefore assumes perfect (no crystal-liquid interaction) and complete (100 % crystallized) fractional crystallization from a non-evolving parental melt, for any given sample. It also assumes that the elements in question reside entirely within the four mineral phases used. This assumption may be generally true, but accessory phases such as zircon, apatite, titanite, and iron oxides contain elements such as Zr, REE and Ti in abundance disproportionate to their modal and normative abundances. This may account for anomalous relative abundances in the resultant calculated liquids, especially for Zr.

The liquids generated by this calculation show a set of normalized profiles characterized by relatively consistent anomalies and abundances increasing from the Group 1 cumulates to the May Twp. samples to the volcanics. The spidergram profiles are characterized by pronounced positive anomalies for Nb and Zr (shown in Fig. 5.10a). HREE abundances for the cumulates range from between 10 and 100 times primitive mantle abundances. The REE profiles are characterized by pronounced Eu negative anomalies, with Eu/Eu^* on the order of 0.2. The profiles are relatively flat, as well. The consistency and variation in relative abundance of the Group 1 "parents" suggests that they may have been derived from a common primary melt which evolved during the crystallization of the cumulates.

Model 2: Fract. Cryst. of a May Twp.-type Primary Melt

The presence of a weak negative Eu-anomaly in the May Twp. REE profiles implies a composition which may have evolved by plagioclase crystallization. However, its elemental abundances relative to the cumulates and the volcanics suggest that as a unit, it may represent the closest composition available to a primary magma. Given this arbitrary starting point, fractional crystallization of a typical Group 1 cumulate mixture was calculated, using the NEWMELT module of the program NEWPET. This calculates an evolving melt composition assuming either fractional or equilibrium crystallization of minerals in fixed, predetermined proportions.

Based on normative mineral abundances, a cumulate consisting of 60 % plagioclase, 15 % each of clino- and orthopyroxene and 10 % olivine was crystallized in 5 weight percent increments from an average May Twp. composition. The spidergram profiles of the resultant liquids reflect the May Twp. profile slope and shape with progressive enrichment without significant deviation until about 50 % crystallization, at which point slight enrichment in Nb and Yb becomes apparent (Fig. 5.10 c). The Eu negative anomalies in the REE profiles increase in size, and are noticably more pronounced by 30 % crystallization. The $(La/Yb)_N$ ratio does not change appreciably, however.

The crystallized residue differs from the liquids in elemental abundances, profile shape, and in the degree to which it is enriched by progressive fractionation (Fig. 5.10b). The amount of variation observed in the parental melts derived by Model 1 could not be generated by fractional crystallization alone. The cumulate profiles are characterized by strong negative anomalies for Nb and Zr, weak negative anomalies for Ti and Yb, and pronounced positive Eu anomalies in the REE profiles, and typical HREE abundances of 0.5 to 1 times primitive mantle.

By comparison to profiles for crystallization of plagioclase and of clinopyroxene from a May Twp. primary melt, the Eu, Nb and Zr anomalies and most of the depletion in abundance relative to the primary magma can be attributed largely to plagioclase accumulation, and the weak Ti and Yb anomalies to clinopyroxene accumulation (see Figure 5.11).

5.5.2 Comparison with Observed Data

The slopes of the modelled residue and liquid profiles as reflected by chondrite-normalized La/Yb ratios (or Ce/Yb, in the absence of calculated La data) correspond to those observed in the Group 1 cumulates and the Huronian mafic volcanics, respectively. However, two obvious differences are apparent. Firstly, the europium negative-anomaly is significantly larger in the modelled residue than in the observed cumulates. Secondly, the relative abundances of the REE are low in the modelled residues, such that residues derived from melts which have been enriched by 80 or 90 % crystallization are comparable to the most REE-depleted samples from the cumulates.

Similarly, the spidergrams for the modelled residues are notable for the relatively large negative anomalies for Zr and Nb, and for their low incompatible element abundances relative to the profiles of the cumulates sampled.

Model 2A: Modified Model 2

These observations suggest that the effects of plagioclase fractionation are over-represented in this model. By increasing the quantity of pyroxene fractionation at the expense of plagioclase, the elemental abundances in the residue will be increased, and the size of the Zr and Nb anomalies decreased. A modified fractional crystallization model was calculated, using a crystallizing assemblage consisting of 30 % each of plagioclase, clinopyroxene and orthopyroxene, with the remaining 10 % as olivine (Fig. 5.11c).

While the profile patterns of these modelled residues are considerably closer to those observed in the cumulates, the abundances are still too low, and the size of the Zr and Eu anomalies in the spidergrams and REE-profiles respectively remain anomalously large (Fig. 5.12). Given that accumulation of the mineral zircon, the major Zr-sink, is ignored in these models, assuming an average composition of 60 wt.% ZrO_2 in zircon (based on Deer *et al.*, 1966), on the order of a gram of zircon in 20 kg of rock would be required to account for the calculated Zr anomaly. Weights of zircon extracted from the cumulates are on the order of a few milligrams (Krogh *et al.*, 1984; this study), so that even if mineral extraction techniques are resulting in zircon yields which are an order of magnitude too low (which seems unlikely), a significant amount of the Zr anomaly remains to be accounted for.

In summary, for the Group 1 cumulates, distributions of trace elements, particularly the relatively incompatible elements, can be accounted for in part by fractional crystallization of minerals which are observed to exist in the rocks, in not unrealistic proportions from a parent with a chemistry comparable to that of the May Twp. intrusion. However, without invoking anomalous proportions of crystallizing phases, or crystallizing minerals not observed in the rocks, such as amphibole or garnet, contributions from another source or sources are required to explain fully the trace element distributions.

5.5.3 Effects of "Contamination"

Apart from the residual component of fractional crystallization processes, other possible contributors to the geochemical signature of the cumulates include:

i) trapped (intercumulus) liquids;

Even slightly evolved liquids will be significantly enriched in incompatible elements relative to the cumulates which are derived from it, as shown in the previous models.

ii) upper crustal material;

Field evidence (*e.g.* Card and Palonen, 1976; Card, 1978; D. Peck, pers. comm., 1991) indicates that at least partial assimilation of the Superior Province Algoman granitoid rocks which host the Group 1 intrusions has occurred. The effects of this assimilation may be relatively localized, as the granitoid xenoliths occur in the marginal zones of the metagabbros (K. Card, pers. comm., 1991; D. Peck, pers. comm., 1992).

iii) lower crustal material;

The suggestion of tectonic emplacement of some of the metagabbros (*e.g.* Card and Palonen, 1976; Born and James, 1978; see chapter 2.2 also), and considerations such as that the primary melt would have been hotter when it began its ascent through the crust and may have pooled at the base of the crust prior to ascension favour contamination by a lower crustal component. More importantly, the lower crust would have been hotter initially, thereby making it much easier to assimilate. Possible lower crustal components observed locally include Late Archean gneissic rocks and granulites from the Levack Gneiss Complex in the Sudbury area and the Kapuskasing Uplift to the north.

For components ii) and iii) companion or alternate components in the form of first-melted constituents exist, since if the contamination does not occur by bulk assimilation of wall or roof country rock, the lowest-temperature melting fraction (as represented by granitoid phases) will be assimilated first.

iv) mantle material;

Mixing with an enriched mantle component may be an alternative to direct crustal contribution. The

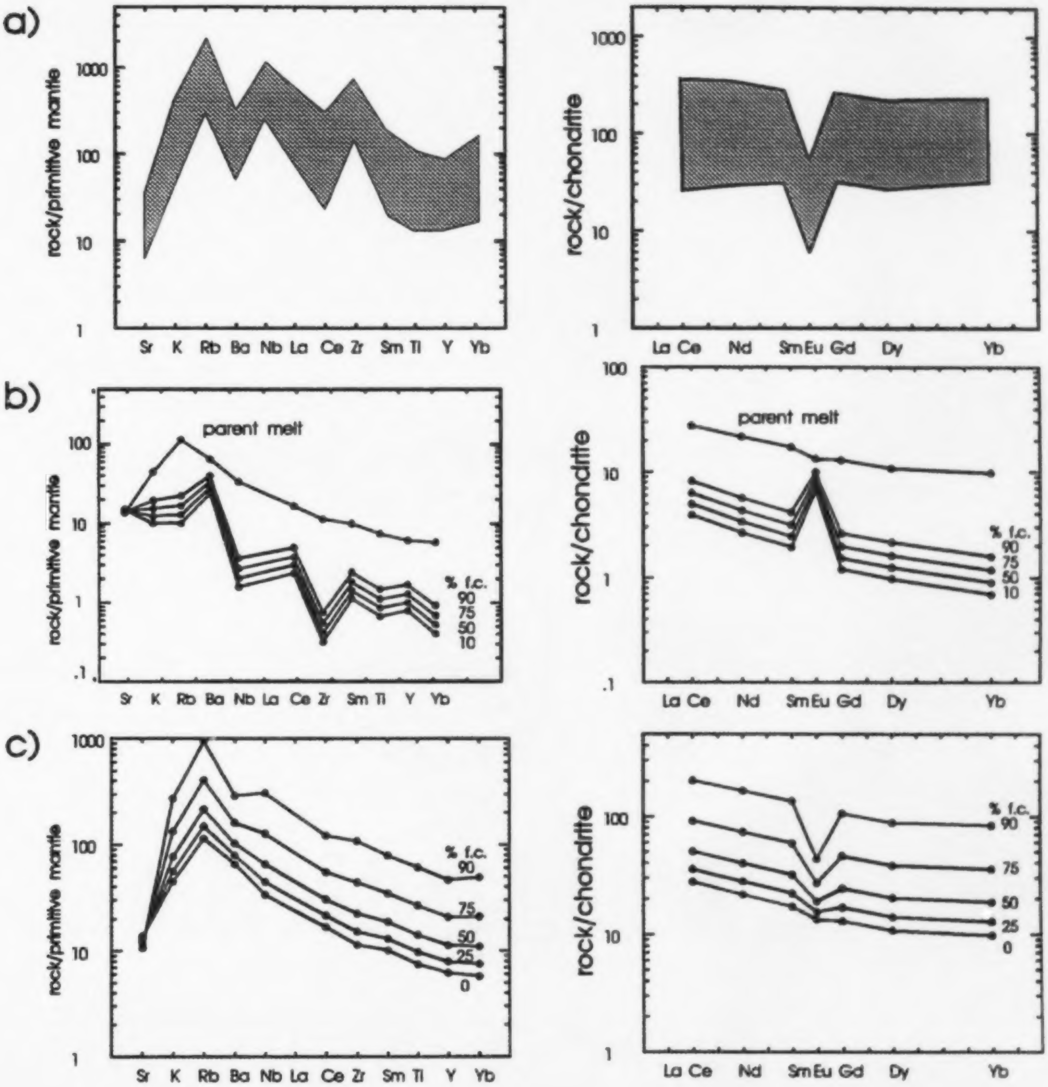

Figure 5.10. a) *Field of parent liquid compositions calculated by Model 1, for all samples* ***b)*** *Cumulates for varying degrees of fractional crystallization calculated by Model 2, and* ***c)*** *Liquid evolution calculated by Model 2. Spidergrams on the left, REE profiles on the right. See text for discussion.*

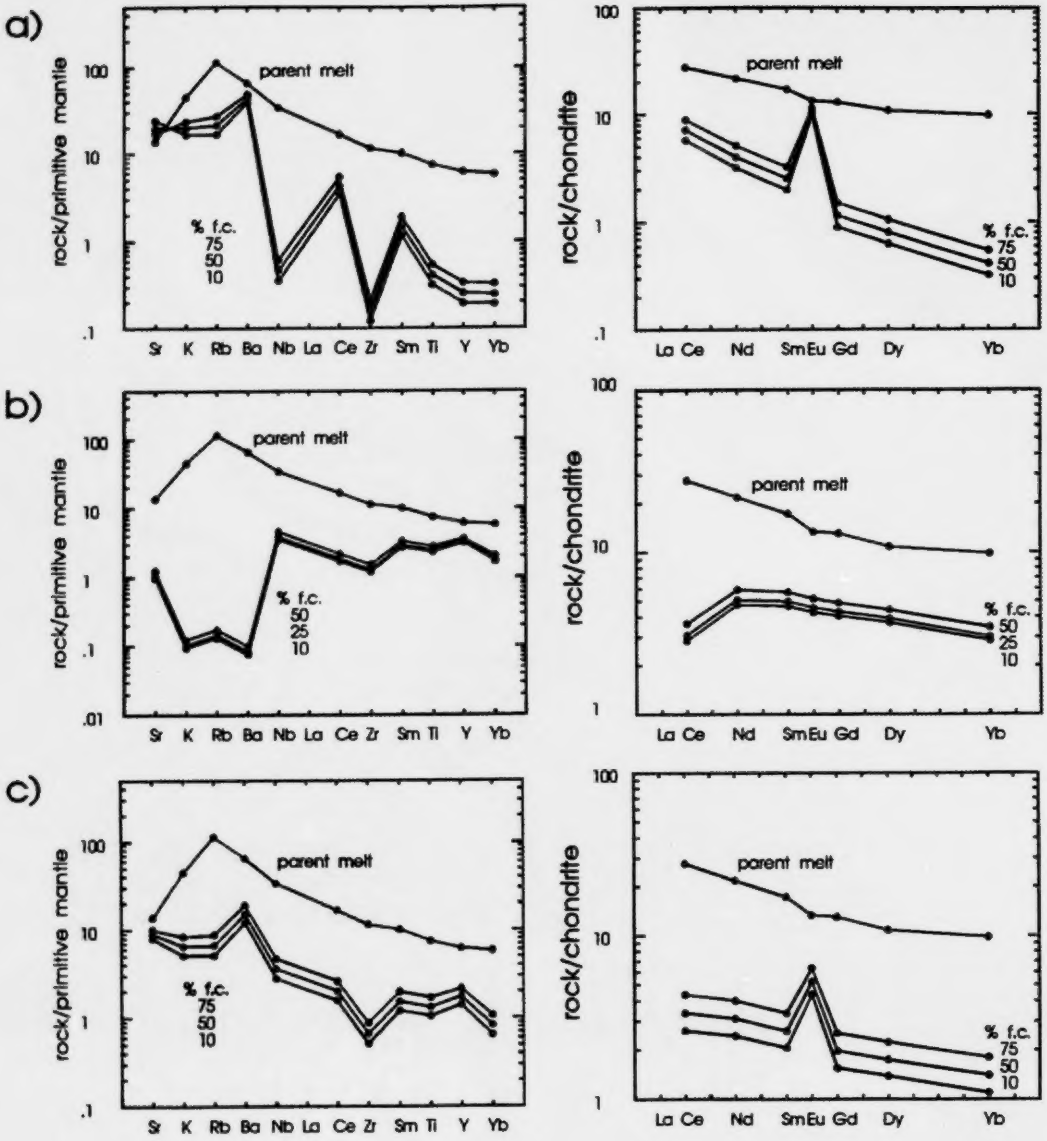

*Figure 5.11. **a)** Trace element variation attributable to plagioclase fractionation, **b)** clinopyroxene fractionation, and **c)** cumulates for varying degrees of fractional crystallization calculated by Model 2A. Spidergrams on the left, REE profiles on the right.*

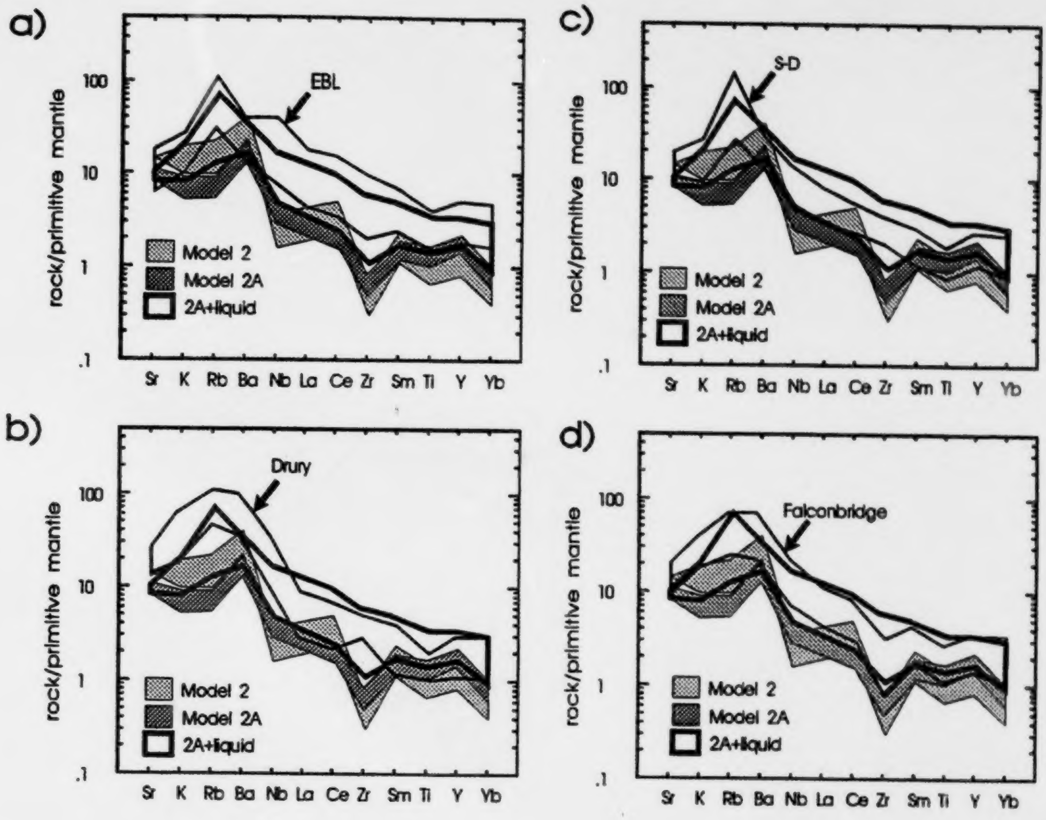

*Figure 5.12. Comparison of spidergrams of modelled cumulates from Model 2, 2A, and after addition of trapped liquid (see Chapter 5.5.3) with observed compositions, using **a)** East Bull Lake **b)** Drury **c)** Shakespeare-Dunlop and **d)** Falconbridge.*

geochemical effects of mantle mixing would be relatively subtle compared to those of crustal contamination.

As mentioned, it is difficult to estimate the relative proportions of trapped liquid, particularly where recrystallization and or secondary replacement has obliterated original grain boundaries and compositions. Evidence from the relatively unaltered EBL samples indicates plagioclase-olivine ortho- to mesocumulate textures. The amount of trapped liquid represented in a cumulate can vary from as low as 5 % (by volume) or less in adcumulates (Wager *et al.*, 1960) to over 50 % (Wager *et al.*, 1960; Simmons and Hanson, 1978). A model involving mixing of liquid and residue from 20 % fractional crystallization using Model 2A above was calculated. The 20 % figure was chosen arbitrarily, as this involves a liquid which is relatively modestly enriched from the May Twp. primary composition, and the element abundances of the modelled residues are relatively insensitive to the degree of fractional crystallization. With as little as 10 % liquid contribution, the spidergram profile and abundances are comparable to those observed in the Group 1 cumulates. They differ from the cumulates in the absence of the negative Ti anomaly and the slight enrichment of the HREE observed. The REE profiles at 10 to 20 % liquid in the mixture compare very well to those of the cumulates. Figure 5.12 shows the field for 0 to 25% trapped liquid added.

Small negative Ti-anomalies would be introduced into the spidergram profiles by introducing small amounts of upper crustal material as characterized by the Algoman granites or crustal melts as represented by Huronian rhyolitic material. While the Copper Cliff rhyolite postdates the gabbros, it is thought to be derived by melting of pre-existing crust (rather than by fractional crystallization of the basalts which preceded it; Jolly, 1987). The difficulty with mixing in

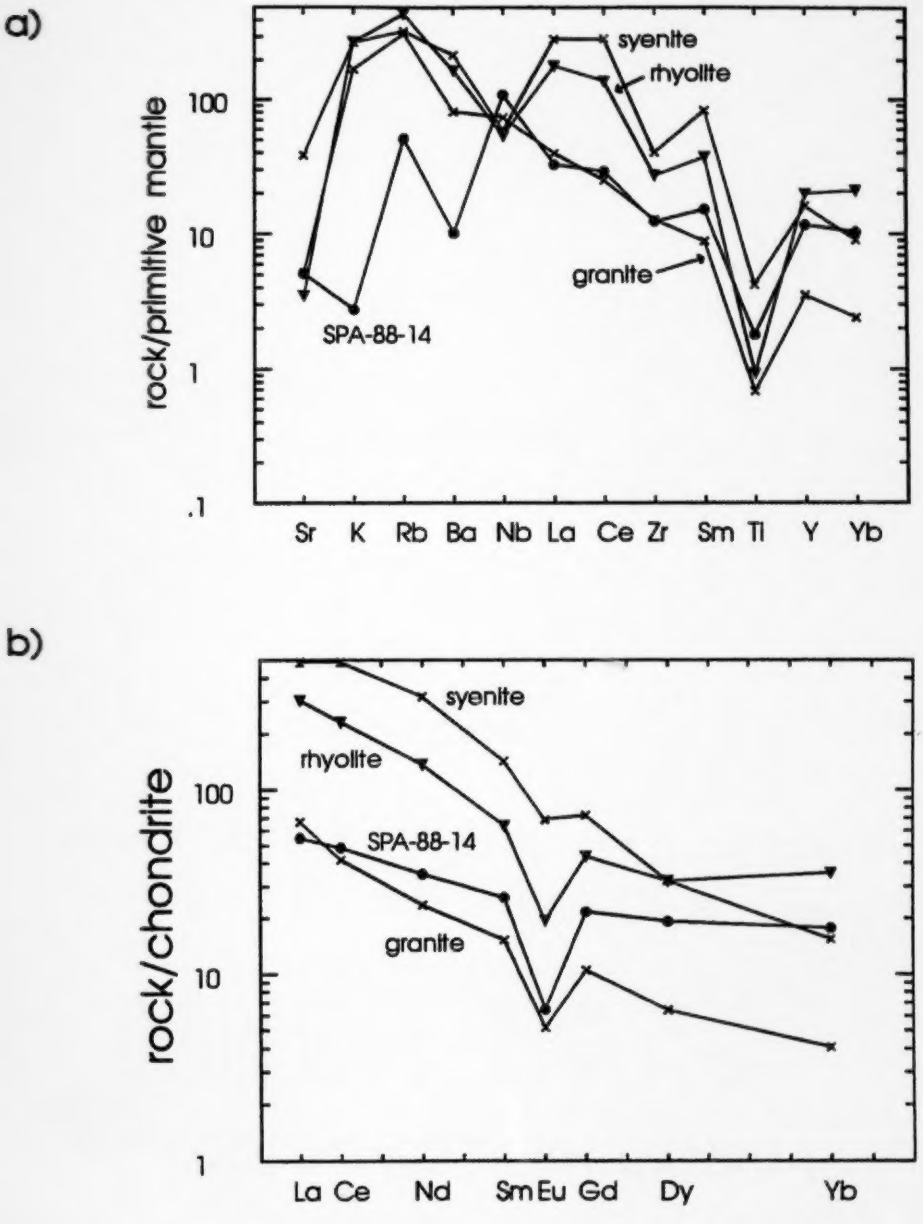

Figure 5.13. A comparison of trace element compositions of granophyric Shakespeare-Dunlop metagabbro SPA-88-14 with Algoman granite (SPA-88-15), Huronian Copper Cliff Rhyolite (SPA-88-30) and Parisien Lake Syenite (SPA-88-23).

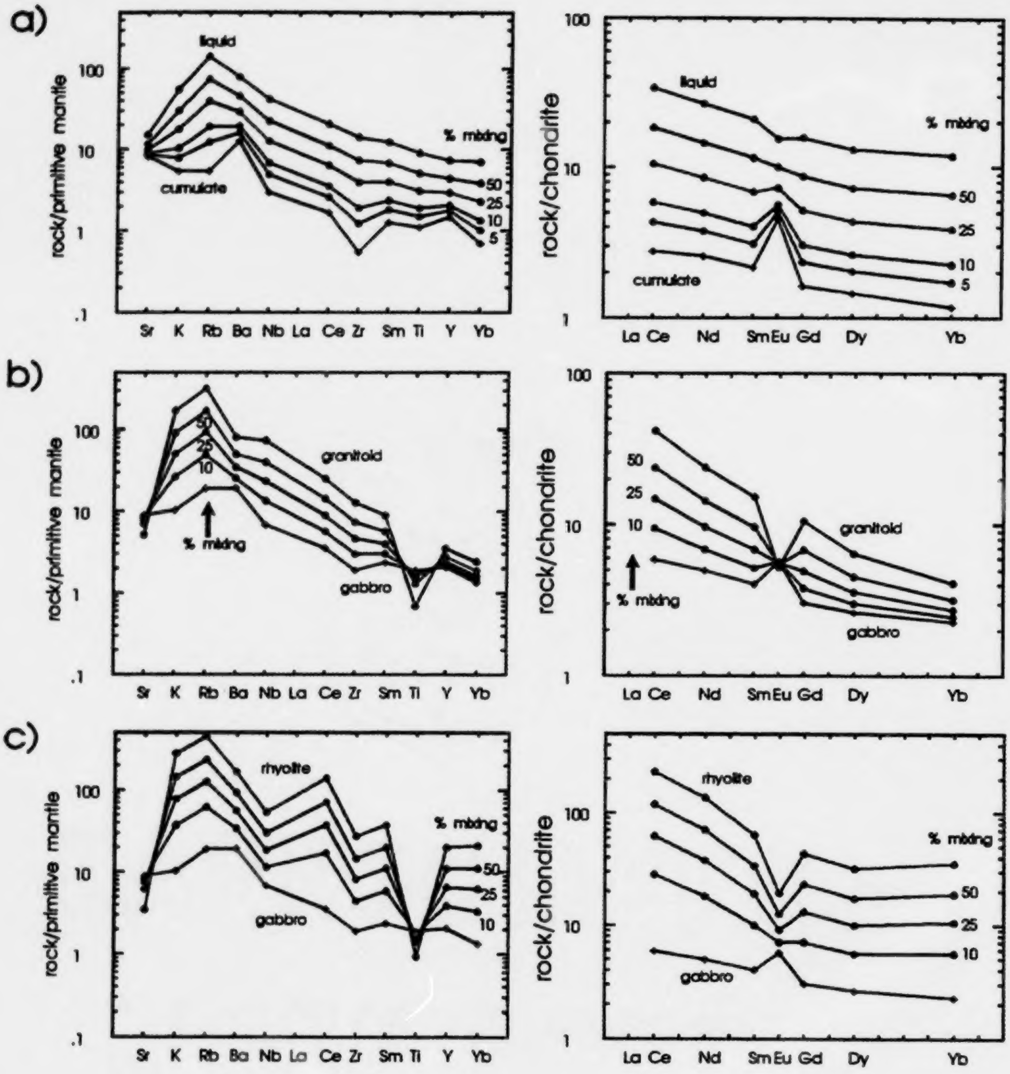

Figure 5.14. Bulk mixing of cumulate with enriched components: ***a)*** *Model 2A cumulate with evolved trapped liquid, and mixing of cumulate+10% liquid with* ***b)*** *Algoman granite (SPA-88-15) and* ***c)*** *Copper Cliff Rhyolite (SPA-88-30).*

Algoman Granites or any local crust is that production of the observed HREE enrichment requires large amounts of contamination which would then be reflected by very pronounced Ti anomalies. These Ti anomalies are not observed. Lower crustal material is unlikely to be involved in significant quantities as a bulk contaminant of the cumulates, as the very steep REE profile slopes and pronounced Nb anomalies generated by addition of this component are not observed (*i.e.* see Appendix 2). A comparison of the granophyric member of the S-D sample suite (SPA-88-14) with a "typical" Algoman Granite (SPA-88-15), the Copper Cliff Rhyolite (SPA-88-30) and a sample of the Parisien Lake Syenite (SPA-88-23), a late-Archean granitoid associated with the EBL intrusion, suggests that at least locally, upper crustal material has been introduced (Fig. 5.13, 5.14), based on the similarities of the profiles and abundances.

It is simpler to envisage a primary magma which is slightly enriched in HREE and depleted in Ti relative to the May Twp. average composition used for modelling, or alternatively provide the Ti anomaly by addition of small amounts (*i.e.* not more than 5 to 10 %) of Superior Province granitic crust.

CHAPTER SIX: ISOTOPE GEOCHEMISTRY

6.0 INTRODUCTION

A number of radiometric isotopic analyses were obtained for various gabbroic samples from the EBL, S-D, Drury, Falconbridge and Wanapitei intrusions. Whole-rock Rb-Sr, Sm-Nd and Pb-Pb isotope systematics were examined for potential application as geochemical tracers to complement available trace element geochemical data. Data are presented in Appendix 4.

6.1 Sm-Nd ISOTOPE GEOCHEMISTRY

Whole-rock Sm-Nd isotopic analyses were obtained for samples from the Early Proterozoic intrusions, particularly those whose geochronological constraints remain ambiguous following the results presented in chapter four. Samples were analysed from the EBL, S-D, Drury, Falconbridge and Wanapitei intrusions. A lack of variation in parent-daughter ratio, reflected in the $^{147}Sm/^{144}Nd$ ratio, is typical of the Sm-Nd system in mafic rocks (*e.g.* Prevec *et al.*, 1991). The whole-rock Sm-Nd system is also sensitive to contamination, such that whole-rock Sm-Nd geochronological information must be treated with great caution (*e.g.* Claoué-Long *et al.*, 1984; Cattell *et al.*, 1984; Chauvel *et al.*, 1985; Hegner *et al.* 1984). The effects of contamination are better displayed on plots of ϵ_{Nd} *vs.* time and ϵ_{Nd} *vs.* $f_{Sm/Nd}$ (the chondrite-normalized Sm/Nd ratio).

6.1.1 Results

6.1.1.1 Isochron diagram

Isotopic results for the above units plotted on an Sm-Nd isochron diagram show a general trend consistent with an Early Proterozoic age (Fig. 6.1a). However, individual units do not show linear correlations of geochronological significance, with the possible exception of the Drury Twp. samples. The four Drury Twp. samples give a regression age of 2100 ± 76 Ma, with an initial $^{143}Nd/^{144}Nd$ ratio of 0.50989 ± 0.00007 and a M.S.W.D. of 17.

6.1.1.2 ϵ_{Nd} diagrams

A plot of ϵ_{Nd} against time, showing the chondritic uniform reservoir (CHUR) and the depleted mantle (using the model of DePaolo, 1981) shows a fairly large scatter for all units, using ages based on zircon geochronology (Fig. 6.1b). These ages are particularly subjective for the Drury and Falconbridge Twp. intrusions.

The EBL intrusion has ϵ_{Nd} values ranging from depleted mantle values (of around +2.5 at 2480 Ma) to around -2.3 epsilon units. The Falconbridge Twp. intrusion also shows variation on the order of 5 epsilon units, varying from CHUR-type values to -5.4 at 2450 Ma. The S-D intrusion shows a dramatic variation from +7.1 to -8.7 epsilon units. Unfortunately these extreme values are represented by single samples, while the remaining two samples lie within error of about $\epsilon_{Nd}= -1.5$.

The Drury Twp. intrusion values have a range of about 2.5 epsilon units at either 1850 or 2450 Ma. At 2450 Ma the values range from slightly in excess of the depleted mantle value to about +1.5. Lastly, the Wanapitei intrusion values vary from -2.1 to -5.3 at about 1750 Ma. Some of the Wanapitei samples are distinguished by relatively low Sm/Nd ratios, reflected in the steepness of the slope of their evolution lines on an ϵ_{Nd}-time diagram, or more effectively on a plot of $f_{Sm/Nd}$ *vs.* ϵ_{Nd}.

Plotting Sm-Nd isotopic data in $f_{Sm/Nd}$ *vs.* ϵ_{Nd} space, as demonstrated by Shirey and Hanson (1986), displays in essence a time-corrected, magnified isochron diagram. Normalization to chondritic values provides more accessible CHUR reference compositions and causes the diagram to be more sensitive to small variations.

Plotting the available data at *ca.* 2500 Ma shows an overall trend from values of about $f_{Sm/Nd}$=-0.45 and ϵ_{Nd}=+4 (with one exception at +7) towards values of $f_{Sm/Nd}$=-0.20 and ϵ_{Nd}=-5 (with one exception at -8). Trends within individual units are generally similar, but not well-defined.

6.1.2 Discussion

In general the scatter observed in sample distribution on the isochron diagram is too high and the number of samples too few to provide useful age information. Although the Drury Twp. samples provide a linear array, given the high M.S.W.D., application of more realistic errors places the age within reach of both an 1850 and a 2450 Ma age. It does, however, suggest that for the Drury Twp. intrusion the Sm-Nd system has remained largely closed since the Early Proterozoic. Data for most of the other units are consistent with this broad conclusion as well, with the notable exception of the S-D intrusion samples. These (four) samples lie along a trend of slightly negative slope. The implications of this are better examined using the ϵ_{Nd} diagram.

The S-D samples are distinguished on the Time-ϵ_{Nd} diagram by their extremely large variation, from around ϵ_{Nd}=+7 to -8.

Although any conclusions based on this variation must be treated with extreme caution as the sample base is minimal, this would appear to require an extraordinarily depleted mantle at 2.5 Ga and a very old (*ca*. 3.5 Ga) crust. Samples for all of the other units (and two of the S-D samples) lie between typical Abitibi depleted mantle values (*cf*. Shirey and Hanson, 1986) and average Superior Province crustal values (from Stern *et al*., 1992), as shown in Fig. 6.2a). This indicates that the Sm-Nd isotopic composition of all but the two extreme S-D samples are consistent with mixing of depleted mantle with variable amounts of average Superior Province crust. For some of the more LREE-enriched Falconbridge Twp. samples, this requires a very large volume percent of relatively young (*i.e. ca*. 2700 Ma) crustal contaminant, or a smaller volume of older crust, such as *ca*. 3.5 to 3.6 Ga material. The strongly-enriched S-D sample (SPA-88-10) appears to require contamination by a large amount of old crust to generate its ϵ_{Nd} value of -8.7 ± 0.4.

The plot of $f_{Sm/Nd}$ *vs*. ϵ_{Nd} is broadly consistent with these conclusions, but demands further discrimination of the mixing end members. This diagram is complicated by the fact that the samples represent cumulates, for the most part, so that observed trends represent a combination of the variations reflected in the parent liquids plus the variation due to differential mineral accumulation. Mixing between materials of equivalent temperatures (such as two mafic magmas) is displayed as a straight line on this diagram. Mixing of a mafic magma and cold (sialic) crust necessarily involves a cumulate phase as well due to heat-conservation considerations (Taylor, 1980), becoming a three end-member, assimilation-fractional-crystallization (AFC) process. The effect of this additional end member on this plot will be reflected in variation of the $f_{Sm/Nd}$ value, controlled by clinopyroxene fractionation. Liquids will move towards lower (more

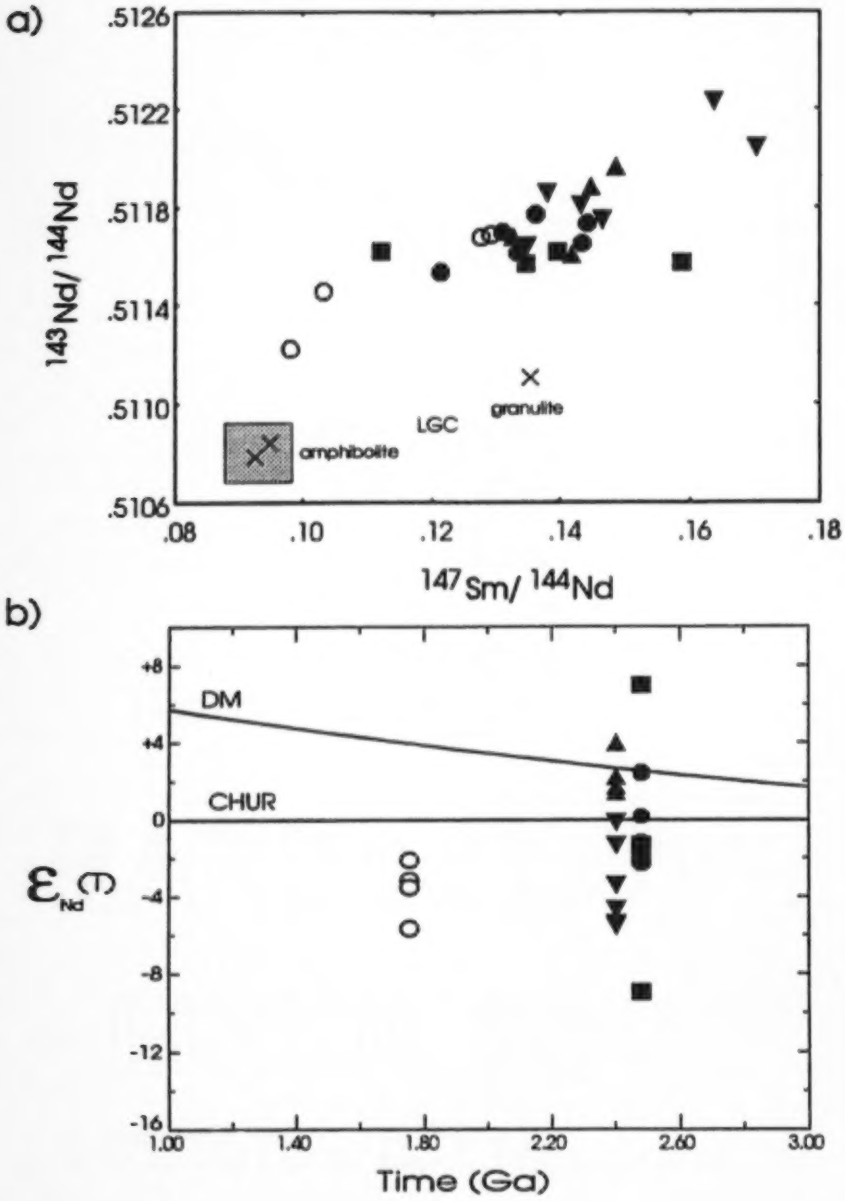

***Figure 6.1 a)** Sm-Nd isochron diagram for gabbro-anorthosites and three Levack Gneiss Complex samples. **b)** ϵ_{Nd}-Time diagram, with depleted mantle (DM) and chondritic uniform reservoir reference lines.*

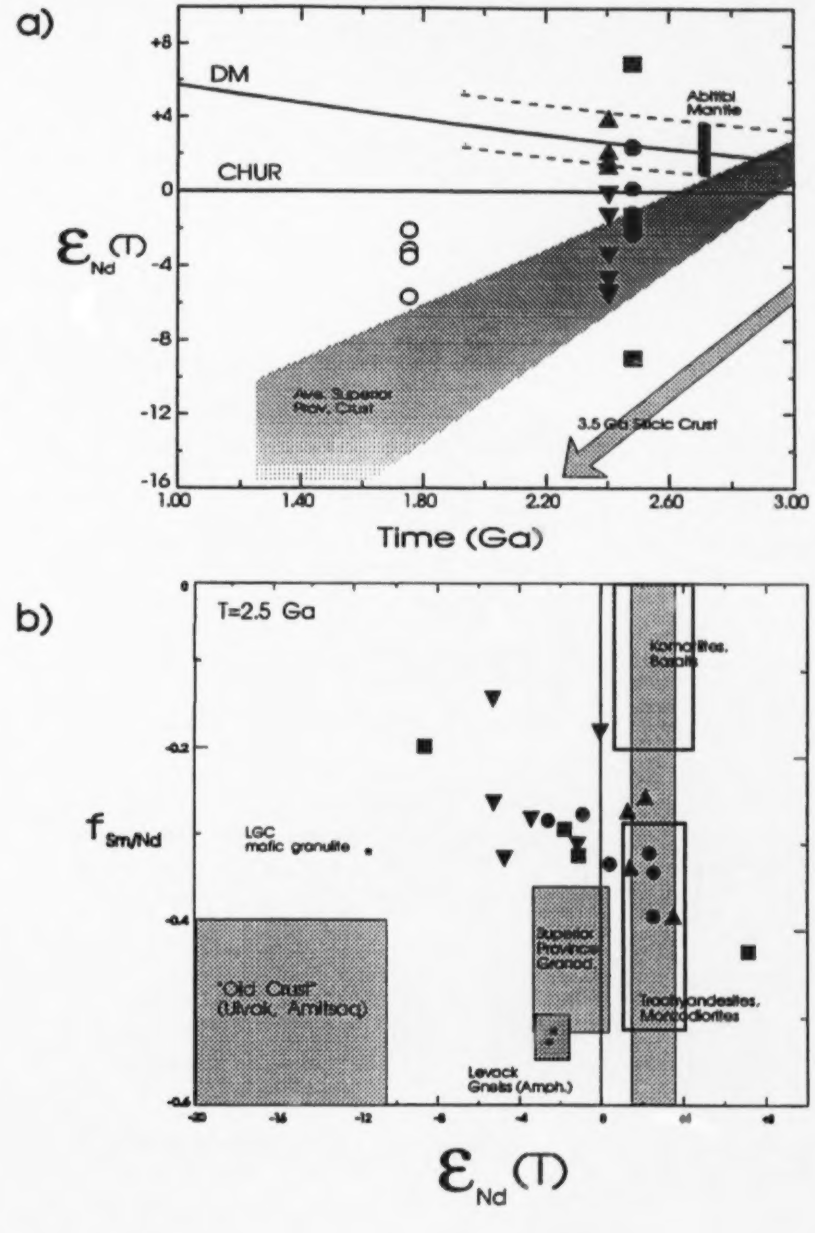

Figure 6.2 a) ϵ_{Nd}-time diagram showing evolution paths of mantle and possible contaminant crustal reservoirs. b) ϵ_{Nd}-$f_{Sm/Nd}$ diagram, showing comparable mantle and crustal reservoirs (see text for references and discussion).

negative) $f_{Sm/Nd}$ values and cumulates towards higher values for a given time and ϵ_{Nd} value.

Although there is an apparent trend from negative $f_{Sm/Nd}$ and high positive ϵ_{Nd} towards less negative $f_{Sm/Nd}$ and negative ϵ_{Nd} values, the distribution of values can be accounted for by varying contributions from three possible end members; "depleted" mantle, juvenile crust (*i.e. ca.* 2700 Ma) and old crust (*ca.* 3.5 Ga?; see Fig. 6.2b).

The depleted mantle at 2500 Ma has an ϵ_{Nd} value of around +2.5. The mantle can be represented by a field of constant ϵ_{Nd} (at a given time) and variable $f_{Sm/Nd}$ values. Data of Shirey and Hanson (1986) indicate that Superior Province greenstone belt juvenile material plots between $f_{Sm/Nd}$ values of about +0.3 to -0.6, ranging progressively from komatiitic through basaltic to trachyandesitic and monzodioritic in composition. Late Archean (*ca.* 2700 Ma) crust, based on data from Levack gneiss (this study), granitoids from the Rainy Lake area (Shirey and Hanson, 1986), average Minto Subprovince crust (Stern *et al.*, 1992) and tonalite and syenite from the southern Abitibi Subprovince (Prevec and Peck, unpublished material) has ϵ_{Nd} values between 0 and -3, and $f_{Sm/Nd}$ ranging from about -0.4 to -0.6 at 2500 Ma. Old crust as typefied by *ca.* 3.5 to 3.6 Ga Uivak gneiss from Labrador and Amitsoq gneiss from west Greenland (calculated from Collerson *et al.*, 1986) and sub-Minto Subprovince tonalite (Stern *et al.*, 1992) have ϵ_{Nd}(2500 Ma) values between about -10 and -25 and $f_{Sm/Nd}$ values between -0.4 and -0.7.

The Drury Twp. and EBL samples are consistent with basaltic to intermediate-composition mantle-derived material combined with variable contributions from late Archean (*i.e.* Superior Province) sialic crust. The S-D and Falconbridge Twp. samples, however, require contributions from material with significantly more negative ϵ_{Nd} values than 2700 Ma crust can provide. Explanations for this distribution include:

1. Mixing between basaltic to intermediate-composition mantle-derived material and a hypothetical reservoir in the upper left of this diagram (*i.e.* ϵ_{Nd}= -10 and $f_{Sm/Nd}$= -0.1). Although this reservoir could conceivably be generated by weakly-LREE-enriched material derived from the mantle at 3.5 Ga (as material of at least this approximate age would be required to allow time for evolution of the ϵ_{Nd} values), there is no evidence for the existence of such a reservoir.

2. Mixing between basaltic mantle-derived material and a combination of young (*ca.* 2700 Ma) and old (*ca.* 3500 Ma) crust. This would generate the range of ϵ_{Nd} values observed in the S-D and Falconbridge Twp. samples. Quantification is dependent on the choice of depleted mantle (particularly with regards to $f_{Sm/Nd}$ composition) and old crust (both $f_{Sm/Nd}$ and ϵ_{Nd}) which remains so poorly constrained as to be arbitrary. Calculations to follow are based on a mantle end-member with ϵ_{Nd}= +2.5, 14 ppm total Nd (based on typical May Twp. values) and $f_{Sm/Nd}$= -0.15 to -0.2 and old crust with ϵ_{Nd}=-15, 40 ppm Nd (based on Minnesota River Valley-type gneiss, from McCulloch and Wasserburg, 1980) and $f_{Sm/Nd}$= -0.5. Young crust can be modelled using Superior Province granitoids with ϵ_{Nd}= -2.5, 10 to 15 ppm Nd (from this study and Shirey and Hanson, 1986) and $f_{Sm/Nd}$= -0.45. Young tonalitic material such as the Levack gneisses would have a similar ϵ_{Nd} value, but with about 30 ppm Nd and $f_{Sm/Nd}$= -0.5.

Mixing of a mantle-derived melt with old crust with the above parameters requires the involvement of relatively large amounts of sialic crust; In order to generate ϵ_{Nd} values of +8, in excess of 30

% crust is required. About 20 % is required to generate ϵ_{Nd} values of +5 comparable to the most negative Falconbridge Twp. sample values. For ϵ_{Nd} values in the -1 to -3 range, between 8 and 15 % old crust is required, or alternatively very large volumes of younger crust (well in excess of 50 %). Clearly, introducing volumes of sialic crust much in excess of about 20 to 25 % will have a significant effect on the bulk rock geochemistry. This will be examined in the final discussion in the following chapter.

3. Scatter in the "y"-direction is not readily attributable to mixing with old crust. Even after addition of 10 % old crust, on the order of 30 or 40 % addition of young crust is required to explain the variation in $f_{Sm/Nd}$ values observed. The variation of $f_{Sm/Nd}$ values with relatively constant ϵ_{Nd} values for the Drury Twp. and some of the EBL samples does not require involvement by 2700 Ma material, and can be generated either by mixing between two mantle-derived components (of variable LREE enrichment) or by fractional-crystallization and/or accumulation of minerals, particularly of clinopyroxene (where $f_{Sm/Nd}$cpx > $f_{Sm/Nd}$WR) and plagioclase ($f_{Sm/Nd}$plag < $f_{Sm/Nd}$WR). The effects of mineral accumulation on $f_{Sm/Nd}$ will be examined with the addition of constraints provided by other geochemical criteria in the following chapter.

The Wanapitei intrusion samples indicate contamination of a mantle-derived magma by late Archean (*ca.* 2700 Ma) silicic crust (Fig. 6.3).

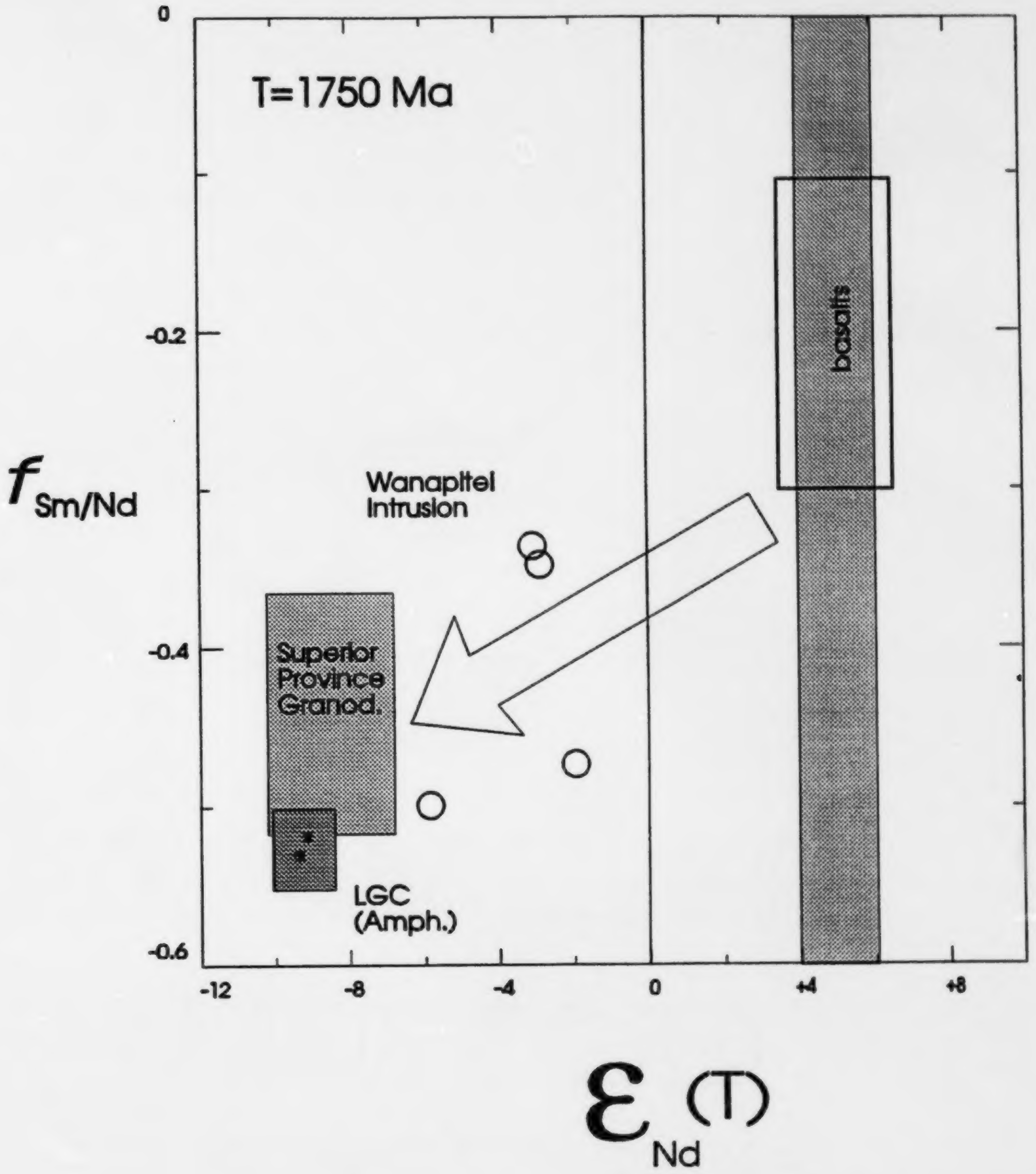

Figure 6.3. ϵ_{Nd}-$f_{Sm/Nd}$ *diagram showing probable origin of Wanapitei intrusion isotopic compositions. LGC=Levack Gneiss Complex.*

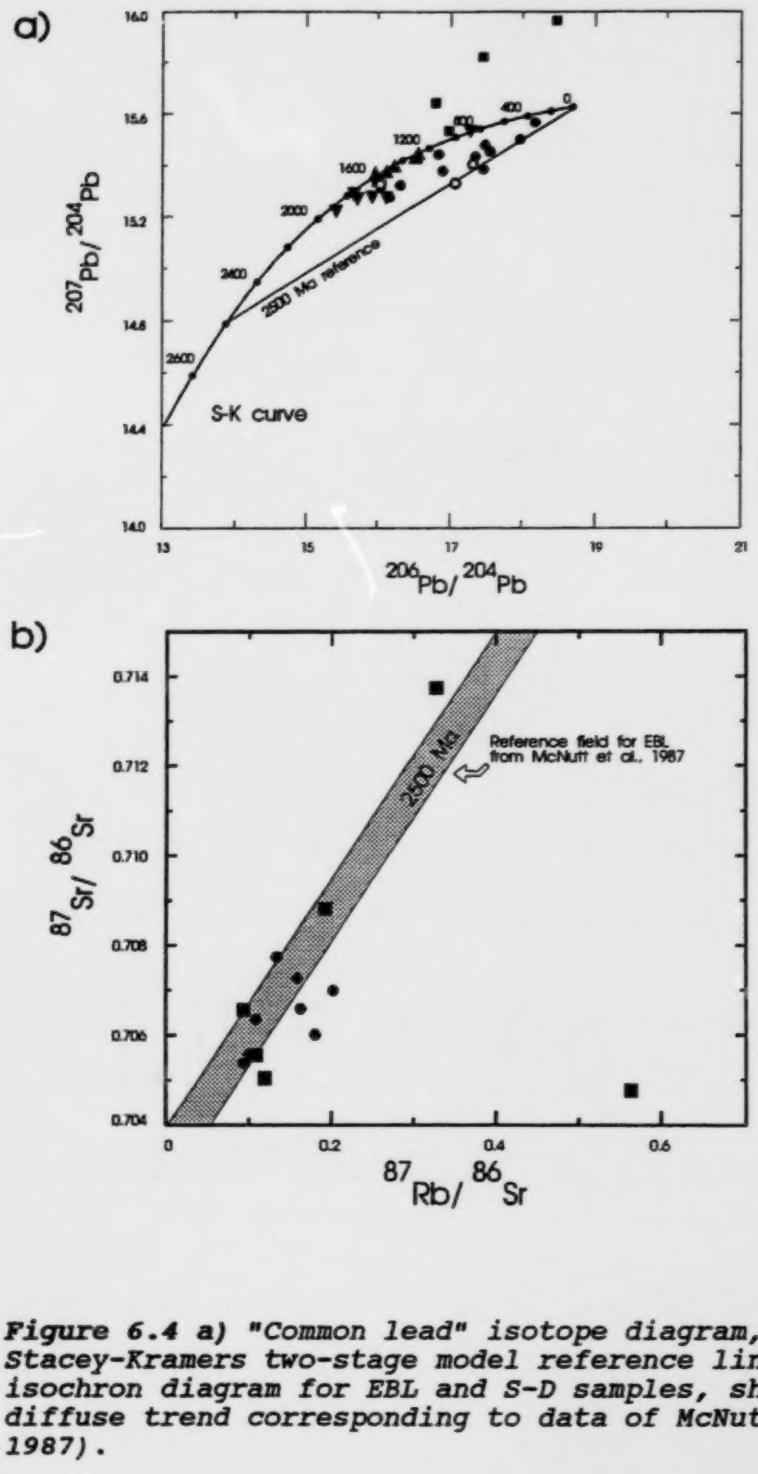

Figure 6.4 *a) "Common lead" isotope diagram, with Stacey-Kramers two-stage model reference line b) Rb-Sr isochron diagram for EBL and S-D samples, showing diffuse trend corresponding to data of McNutt et al., 1987).*

6.2 Pb-Pb ISOTOPE GEOCHEMISTRY

Whole-rock lead isotopic data were obtained for samples from the EBL, S-D, Drury Twp., Falconbridge Twp. and Wanapitei intrusions. The intent was to investigate the possibility of obtaining meaningful geochronological data or tracer data capable of distinguishing otherwise similar units from one another. Evidence from Archean mafic rocks (*e.g.* Roddick, 1984) suggests that in cases where the Sm-Nd (and Rb-Sr) systems have been rendered geochronologically meaningless by crustal contamination, the lead isotope system remains geochronologically valid. As a consequence of the large difference between crustal and mantle abundances of lead (about an order of magnitude), the lead isotopic system is more sensitive to crustal contamination than the Sm-Nd system. As a result, syn-emplacement contamination may cause sufficient enrichment and homogenization of the Pb-isotope system to produce elevated initial isotopic compositions yet with meaningful age relationships. Ages can be derived from the slope of a best-fit line on a $^{206}Pb/^{204}Pb$ *vs.* $^{207}Pb/^{204}Pb$ diagram, representing an average $^{207}Pb/^{206}Pb$ age, or alternatively from modelled ages of extraction from a reservoir such as that for the Stacey-Kramers two-stage mantle-evolution curve (Stacey and Kramers, 1975), or alternative evolved reservoirs (Zartman and Doe, 1981).

The most prominent difficulty in applying lead as a tracer in these rocks is the difficulty in determining accurate initial lead compositions. Uranium determinations would be suspect due to the extensive alteration of the rocks. Similarly, lead isotopic analyses of low-U phases such as feldspar would also be potentially suspect, particularly in strongly altered rocks such as the S-D intrusion samples.

6.2.1 Results

Common-lead isotopic data plotted on a $^{206}Pb/^{204}Pb$ *vs.* $^{207}Pb/^{204}Pb$ diagram (Fig. 6.4a) shows groups of roughly linear scattered data. With the exception of most of the S-D samples, all of the data plot beneath the Stacey-Kramers growth curve. The EBL samples can be constrained between reference geochrons of about 2500 and 1600 Ma. A best-fit regression line through the EBL data indicates a slope age of about 1865 Ma. The Falconbridge and Drury Twp. data plot in separate clusters below the Stacey-Kramers curve. The Drury Twp. samples plot along the bulk-earth curve between about 1600 and 1300 Ma, and a best-fit line through the data indicates a slope age of 2120 Ma. The Falconbridge samples plot as a cluster consistent with a *ca.* 1850 Ma model age, plus one sample plotting at about 900 Ma on the Stacey-Kramers curve (sample SPA-89-09), and have a slope age of about 2475 Ma.

Consistent with the Sr and Nd isotopic data, the S-D samples have Pb isotopic compositions which are very distinct from those of the other units. Most of the S-D samples plot above the S-K curve, displaying a roughly linear trend towards extraordinarily radiogenic compositions. A best-fit line through these data (excluding sample SPA-88-14) indicates a slope-age of around 2445 Ma, consistent with the crystallization age of the intrusion. Inclusion of SPA-88-14 in the regression produces an age of around 1855 Ma.

Of the three samples of the middle-Proterozoic Wanapitei intrusion, one plots near the Stacey-Kramers curve consistent with a *ca.* 1750 Ma age, and the other two lie near the 2500 Ma reference line.

6.2.2 Discussion

The lead-isotopic data are geochronologically imprecise due to the amount of scatter relative to the variation in isotopic ratios. Imprecisions on data regressions are all on the order of 300 Ma. However, observation of the slope and model ages may provide some basis for comparison of the units. The distributions of common lead compositions within a given unit are affected by their evolution through time as a result of radioactive decay and potentially by mixing and/or contamination as well as by open system behaviour due to metamorphism.

The slope ages for these intrusions tend to cluster around two ages of geological significance, at *ca*. 2450 and *ca*. 1850 Ma, with the exception of the Drury Twp. intrusion whose slope age lies in between the two. This may reflect varying degrees of resetting of originally Early Proterozoic ages by subsequent metamorphism induced by the intrusion of the Sudbury Structure at 1850 Ma. The observation that inclusion of the strongly radiogenic sample SPA-88-14 into the S-D regression produces a slope age of *ca*. 1850 Ma, controlled by that sample, suggests that Sudbury-aged metamorphism has affected that intrusion, at least locally, as well as the EBL intrusion (based on its slope age). This suggests activation at 1850 Ma of the major east-west fault systems that traverse those units.

Values of μ calculated for the S-D intrusion are exceptionally high, ranging from values comparable to bulk earth (μ=9.735; Stacey and Kramers, 1975) up to nearly 12. Values of μ for all other units are comparable to or lower than bulk earth. One S-D sample (SPA-88-14) has a measured isotopic composition more radiogenic than those measured for Algoman granitoids.

It is difficult to explain why the Falconbridge and Drury Twp. intrusions, which are more proximal to and presumably more strongly affected by the emplacement of the Sudbury Structure, do not reflect this more prominently in their lead isotope systematics. Possibly enhanced fluid access and mobility due to faulting has resulted in more lead mobility in the EBL and S-D intrusions than in the two smaller sills. While the slope ages of the Falconbridge and Drury Twp. intrusions are too imprecise to distinguish the two from one another, the Drury Twp. samples are more radiogenic than the Falconbridge samples. Based on the position of these samples relative to the Stacey-Kramers curve, the Drury Twp. samples are consistent with wholesale resetting of the lead isotope system in the mid-Proterozoic, conceivably at 1850 Ma. The Falconbridge Twp. samples are not consistent with this interpretation based on both slope and model age considerations.

The Wanapitei intrusion lead data are consistent with a *ca.* 1750 Ma emplacement age and contamination with late Archean material.

Additional constraints on contamination may be obtained by examining lead isotopic data in conjunction with other elemental abundances in the following chapter.

6.3 Rb-Sr ISOTOPE GEOCHEMISTRY

Isotopic analyses of Rb and Sr were conducted on whole-rock samples from the largest, least-altered bodies in order to determine whether any useful geochronological or tracer information would be likely to have been retained in these metamorphosed gabbroic rocks. Even in cases where a closed system has been maintained, the low abundance of the parent element and the resultant lack of variation in Rb/Sr ratios limits the potential usefulness of this system in gabbroic and anorthositic rocks.

6.3.1 Results

Rb-Sr data were obtained for a small number of samples from the EBL and S-D intrusions. Samples from the S-D intrusion are very widely scattered and show large variations in both $^{87}Rb/^{86}Sr$ and $^{87}Sr/^{86}Sr$ (Fig. 6.4b). While the EBL samples are more isotopically homogeneous than the S-D samples, the EBL samples have $^{87}Sr/^{86}Sr$ ratios varying from 0.705 to 0.708. ϵ_{Sr} values at 2480 Ma vary from +25 to -25, with one S-D sample at -240 (sample SPA-88-10).

6.3.2 Discussion

The Rb-Sr data obtained for these two units is geochronologically meaningless due to the large amount of scatter. The EBL data can be broadly characterized by a band representing an age of 2500 Ma from initial compositions ranging from 0.704 to 0.703. This is consistent with the results of McNutt *et al.* (1987) who investigated Rb-Sr systematics in hydrothermally-altered rocks from the EBL intrusion. The S-D samples fall within this age envelope, but show some additional enrichment in Rb abundance. Of the two S-D samples with Rb concentrations greater than 20 ppm (SPA-88-07, -10), the latter sample has a low $^{87}Sr/^{86}Sr$ ratio of 0.7049 while the the former has a ratio of 0.7138. While single samples provide insufficient information on which to infer trends, these data may indicate contamination of the gabbro with more than one end member (*i.e.* one with high $^{87}Sr/^{86}Sr$ and $^{87}Rb/^{86}Sr$, and the other with low $^{87}Sr/^{86}Sr$ and high $^{87}Rb/^{86}Sr$). Alternatively, Rb enrichment at around the time of intrusion (to account for the more radiogenic end member) and a recent Rb enrichment could also explain the observed distribution. The latter alternative is consistent with the conclusions of Kamineni *et al.* (1987) from the EBL intrusion, such that geochemical remobilization has occurred (at least locally) throughout the history of the intrusion, with progressively lower grade episodes with time.

Model age data consisting of calculated extraction ages from the "Uniform Reservoir" are extremely scattered (ranging from in excess of 4.0 Ga to as low as 50 Ma). There is also no correlation between T_{UR} model ages and (measured) $^{87}Sr/^{86}Sr$ ratio, indicating that even the most isotopically primitive samples have undergone some open system behaviour of Rb and/or Sr.

6.4 DISCUSSION

Relatively little additional information can be obtained from examining combinations of isotopic data from different decay schemes in this case. The small amount of Rb-Sr data clearly shows evidence of post-emplacement open system behaviour and as initial lead compositions are not available, data from these systems are therefore largely incompatible with (age corrected) Sm-Nd data. There are no obvious correlations shown within individual units in plots combining ϵSr, ϵNd and measured lead isotopic ratios which can be used to qualify or quantify sources of contamination. However, some broad conclusions indicated by examination of the individual systems can be presented.

All isotopic data are consistent with derivation of the EBL, S-D, Drury and Falconbridge Twp. intrusions from a LREE-depleted mantle in the Early Proterozoic. While Sm-Nd data indicate relatively modest amounts of contamination of the EBL and Drury Twp. magmas by juvenile LREE-enriched material at the time of emplacement, large contributions from older crust are required to explain Sm-Nd compositions for the S-D and Falconbridge Twp. intrusions. The source and proportion of contaminants must be constrained by examination of complementary geochemical data in the following chapter. Lead isotopic data for the S-D intrusion are consistent with addition of strongly radiogenic material at the time of emplacement, with values of μ approaching 12. However, Rb-Sr and Sm-Nd data for sample SPA-88-10 indicate relatively recent addition of LREE and Rb.

It is perhaps worth noting that the Drury Twp. intrusion has slope ages of *ca.* 2100 Ma using both the Sm-Nd and the ^{207}Pb-^{206}Pb systems. The large imprecision on these ages and the systems involved means that this may be coincidental and neither a *ca.* 2450 Ma or an 1850 Ma intrusion age can be ruled out on this basis. However, this may suggest an affinity with 2120 Ma Nipissing Diabase, which represents the only prominent local magmatism near that age.

CHAPTER SEVEN: SUMMARY AND CONCLUSIONS

7.0 INTRODUCTION

The intent of this chapter is to reconcile the conclusions based on petrographic, geochronological, geochemical and isotopic evidence, and to attempt to place them in a regional geological context. While a genetic relationship between the units to the north of the Grenville Front is inferred based on geochemical and petrological evidence, the geochronological and isotopic evidence is not definitive. Isotopic data from these units provides evidence concerning the nature and extent of crustal contamination of mantle-derived magmas in the early Proterozoic and the nature of the upper mantle. The former three lines of evidence allow the three units located to the south of the Grenville Front to be distinguished from those to the north of it.

7.1 LATE-PROTEROZOIC ANORTHOSITES

The two small sill-like intrusions from the Burwash area near St. Charles and in Mercer Twp. appear to represent a limited anorogenic episode of mafic magmatism and anorthosite formation. The petrography and geochemistry of both units is dominated by the effects of plagioclase accumulation. Simmons and Hanson (1978) suggest a plagioclase-rich, mantle-derived, REE-rich parent magma, from which plagioclase-accumulation and various amounts of trapped coexisting liquid (5 to 10% for the St. Charles; 30 to 50% for the Mercer) have produced the observed geochemistry. This is, in part, consistent with the more extensive database from this study, which shows an inverse correlation of Eu/Eu^* with total REE content and infers relatively high REE abundances in the associated liquid and therefore the parent magma. However, a comparison of the observed REE patterns for the anorthosites with the pattern modelled for plagioclase-only fractionation from a May Twp.-type parent indicates that while a May Twp.-type parent is too REE-depleted to account for the REE contents of the anorthosites, the slope of the REE profiles ($(Ce/Yb)_N$ ratios of <10 for the anorthosites *versus* ratios of about 16 for the calculated plag. cumulate) appears to favour a less-LREE-enriched parent for the anorthosites. Since plagioclase preferentially incorporates LREE over HREE (as shown by distribution coefficients in Simmons and Hanson (1978), for example), the parent liquid for rocks consisting of 90% plagioclase must necessarily have a lower LREE/HREE ratio than the cumulate. A broad inverse correlation between total REE and $(La/Yb)_N$ ratio favours mixing of plagioclase cumulate with a liquid which is REE-enriched and has a flatter REE profile slope. This may suggest a basaltic-type parent liquid rather than an anorthositic one.

The geochronological evidence distinguishes the two anorthosites from other local magmatism. U-Pb zircon ages of 1222 ± 2 Ma and 1206 ± 36 Ma for the Mercer and St. Charles anorthosites respectively are the youngest ages for any of the units in this study and indicate that these intrusions are not related to the Early Proterozoic mafic magmatism to the north. There is, however, sufficient uncertainty in the ages such that if Grenville-aged lower intercepts are used to anchor the zircon discordia these units could be correlated with *ca*. 1240 Ma mafic and felsic magmatism to the north within the Grenville Province (the Sudbury dykes and Mulock Granite, respectively). Simmons and Hanson (1978) suggest melt-derivation at 50 to 60 km depth from an orogenically-thickened crust, possibly due to continent-continent collision.

7.2 MID-PROTEROZOIC MAFIC INTRUSION

The Wanapitei intrusion also represents a relatively limited mafic magmatic event distinct from Early Proterozoic rifting. A U-Pb zircon intrusion age of 1747 +6/-5 Ma indicates that the Wanapitei Intrusion is not temporally related to the Early Proterozoic River Valley gabbro-anorthosite to the northeast. The absence of an anorthositic phase associated with the otherwise gabbronoritic or troctolitic material also distinguishes the Wanapitei from the other intrusions in this study. Most of the Wanapitei Complex reflects high grade, relatively anhydrous metamorphism which may be related to northwest-directed thrusting (*e.g.* Davidson, 1986) related to the formation of the Grenville Front Tectonic Zone. This is supported by the Grenville-aged (*ca.* 996 Ma) lower intercept of the zircon discordia. The coronitic textures separating primary olivine and plagioclase in some samples are probably related to this Grenville-aged heating, as delicate textures such as this are not likely to have been generated during post-emplacement cooling (for example) and then survived a subsequent intense metamorphism.

Geochemical evidence such as strongly elevated (*i.e.* incompatible-element enriched) spidergram and REE profiles and the similarity of these profiles with those of Early Proterozoic granitoids (shown in Fig. 5.13a and Appendix 3) indicates a large contribution from crustal material to the Wanapitei mafic magma. Nd isotopic data is consistent with a large contribution from late Archean (*i.e. ca.* 2700 Ma) sialic crust.

The correlation between the Wanapitei gabbro-norite and other *ca.* 1750 Ma orogenic material to the west, including the Killarney Complex, remains unclear. This correlation requires that the tectonic processes responsible for granitic plutonism and volcanism elsewhere at this time would be manifested solely as a mafic intrusion in this area (alone).

7.3 EARLY-PROTEROZOIC MAFIC INTRUSIONS

The East Bull Lake, Shakespeare-Dunlop, Tennyson, May, Drury and Falconbridge Twp. intrusions appear to be consanguinous and probably contemporaneous, based on trace element geochemical, isotopic and geochronological evidence. However, this conclusion is complicated by ambiguous geochronological data for the bodies proximal to the Sudbury Irruptive.

7.3.1 Gabbro-Anorthosite Sills

Four small, sill-like intrusions were sampled in this study. These can be divided into two pairs based on petrographic evidence. The intrusions in Drury and Falconbridge Twps. both display relict gabbroic textures dominated by cumulate plagioclase and intercumulus clinopyroxene which have been extensively amphibolitized and saussuritized. These units have mutually comparable trace element abundances and distributions, except for a pronounced relative depletion of Zr in the Falconbridge Twp. samples which is absent in the other Early Proterozoic cumulates. The intrusions further to the west in May and Tennyson Twps. are both characterized by finer-grained, recrystallized gabbroic compositions. Clearly-defined cumulate textures are absent from these intrusions.

7.3.1.1 Drury and Falconbridge Twp.

Both the Drury and Falconbridge Twp. intrusions are bounded on one side by the gabbro-noritic outer member of the Sudbury Irruptive. The presence of Sudbury breccias within the Drury Twp. intrusion and metamorphic-related features proximal to the Falconbridge unit (*e.g.* Grant and Bite, 1984), as well as extensive faulting and fracturing suggests the possibility of profound secondary geochemical effects as a consequence of the formation of the Sudbury Irruptive. The apparent total resetting of the Drury Twp. zircons to *ca*. 1850 Ma may be attributed to Irruptive-related metamorphic heating and shock effects. Some lead-loss was likely induced by the Sudbury event, as indicated by the modelled lower intercept of the reference line on the concordia diagram for the Falconbridge samples. Similarly, common lead compositions for both intrusions are consistent with total resetting of the lead systematics at 1850 Ma and with variable resetting during Grenville-aged reheating.

The apparent absence of primary (non-xenocrystic) zircon in the Falconbridge Twp. sample examined and the Zr depletion are not readily attributable to metamorphism. A comparison of the Falconbridge profiles with those of the other Early Proterozoic cumulates shows that the Zr negative-anomaly is more pronounced in the former and also that the most enriched alkali element is Ba in the former and Rb in the spidergrams of all the other intrusions (with the notable exceptions of the mid-Proterozoic anorthosites). This is also consistent with the trace element distributions in the modelled cumulates. This indicates that the Falconbridge Twp. intrusion can be modelled from the same source composition as the intrusions to the west, but displays a composition with a significantly smaller (trapped) gabbroic liquid contribution.

Sm-Nd isotopic evidence also distinguishes these two intrusions from one another, as the Falconbridge Twp. intrusion requires a moderate contribution (<20 weight %) from older crust to explain its isotopic composition. The Drury Twp. intrusion, like the EBL intrusion, has an isotopic composition consistent with mixing of a basaltic-type mantle with variable amounts of Late Archean ("juvenile") continental crust.

7.3.1.2 May and Tennyson Twp.

Although these two units are relatively poorly defined in a field context, they are both narrow, elongate gabbroic intrusions without well-defined cumulate textures, in general. These units are geochemically similar to one another, displaying relatively flat normalized trace element profiles and small negative Eu anomalies, although the May Twp. intrusion is characterized by flatter patterns and higher abundances. This evidence suggests that these intrusions represent gabbros with relatively large proportions of liquid to cumulate. Trace element modelling indicates that a May Twp. type parent can provide a relatively good approximation of the starting composition of the parent magma for the other Early Proterozoic cumulates. The similarity of the May Twp. geochemistry to that observed in the basal Huronian mafic volcanics supports this hypothesis. Unfortunately, accessory minerals suitable for high precision U-Pb geochronology such as zircon or baddeleyite were not identified in samples from the May Twp. intrusion.

7.3.2 Gabbro-Anorthosite Plutons

The two larger gabbro-anorthositic plutons investigated in this study, the Shakespeare-Dunlop and East Bull Lake intrusions, show comparable geochemical and petrographic characteristics. The samples from the EBL pluton preserve some primary mineralogy as well as cumulate textures and low-temperature olivine-plagioclase reaction rims, while the S-D samples are dominated by secondary hydrous minerals. Both units show similar trace element abundances and normalized profiles, although some of the S-D samples show extreme contamination by local upper crust. The range of geochemical abundances and distributions in these rocks can be accounted for by modelling fractional crystallization of a mixture of plagioclase plus two pyroxenes in roughly equal volumes plus minor olivine from a May Twp. or Huronian basalt-type parent magma. The actual amount of fractionation required is not critical, as the variation in trace element abundances is relatively insensitive to fractionation percent. On the order of 20 to 30 wt.% fractional crystallization would suffice, in addition to which 10 to 20 % trapped parent liquid would account for the range in abundances and patterns observed.

7.4 CONSTRAINTS ON CRUST-MANTLE MIXING

The effects on the geochemistry of the cumulates from crustal contamination are relatively subtle, in general. Although field and trace element evidence indicates that large quantities of Algoman granitoid have been locally incorporated by the mafic intrusion (*re.* the S-D intrusion in particular), the effects of contamination of the parent magma prior to fractional crystallization are relatively poorly constrained. Large volumes of bulk contamination (*i.e.* on the order of 25 to 30 %) of a May Twp.-type parent magma by either an Algoman granitoid or a Minnesota River Valley-type sialic rock would not be dramatically reflected in the composition of subsequent cumulates, as shown in Figure 7.1. On the other hand, comparable amounts of contamination late in the crystallization process, modelled as two end-member mixing, has a profound effect on geochemical abundances. It is likely that the process which was active during the formation of these intrusions was a combination of the two, favouring the former, described as combined assimilation-fractional-crystallization (AFC). Large-scale assimilation of "cold" sialic material by hot mafic magma requires sympathetic fractional crystallization as a consequence of energy considerations (Taylor, 1980), at least after the melt has cooled past the liquidus. It is logical that a mantle-derived magma will be contaminated by lower (older?) crust prior to its contamination by upper crust, assuming that the former takes place at all.

7.4.1 Constraints on Ancient Crustal Contributions

Evidence for lower, older crustal contamination of the gabbro-anorthosite intrusions is provided by Sm-Nd isotopic data from the S-D and Falconbridge Twp. samples, summarized in Fig. 7.2. Some samples from these units have ϵ_{Nd} values which cannot be accounted for by mixing mantle material with *ca*. 2700 Ma crust. Also, a number of the EBL samples have ϵ_{Nd} values which require very large (on the order of 50%) juvenile crustal contamination, which might be better explained by a combination of smaller amounts of both juvenile and ancient crust. However, if the majority of the contamination occurred prior to or simultaneously with the crystallization of early cumulates, even these large proportions of assimilation can be reconciled with the trace element abundances. Hence, between about 10 and 30 wt% assimilation of ancient sialic crust is indicated based on samples from S-D and Falconbridge Twp., keeping in mind, however, that apart from a single S-D sample, the maximum contamination required is about 20 %. The nature of the ancient crustal component is poorly constrained, except that an ϵ_{Nd}(2500 Ma) of at least -8 is required. The observation that the one mafic granulite sample of the Levack Gneiss Complex gives an ϵ_{Nd}=-8.6 and an $f_{Sm/Nd}$=-0.31 indicates involvement of an ancient component with a more radiogenic ϵ_{Nd}(2500), perhaps more like -20, and/or a relatively flat REE profile ($f_{Sm/Nd}$ closer to -0.4 than -0.6). A contaminant with these characteristics would require a somewhat smaller contribution than an average Amitsoq composition.

The potential variation in $f_{Sm/Nd}$ generated by fractional crystallization varies from approximately +0.20 (relative to the parent liquid) for crystallization of clinopyroxene alone

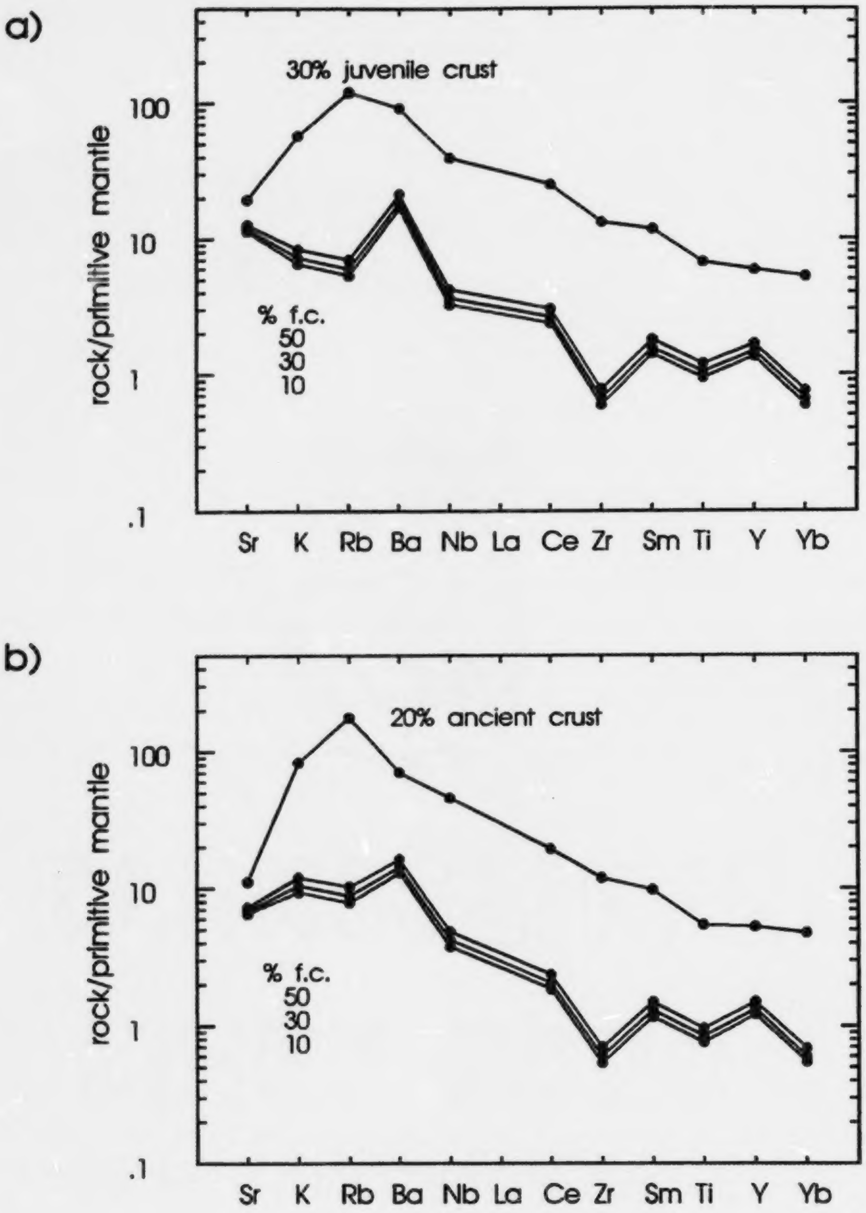

Figure 7.1. Effects on the geochemistry of the resultant cumulate of contaminating their gabbroic source magma with large volumes of a) young (ca. 2.7 Ga) and b) old (ca. 3.6 Ga) sialic crust.

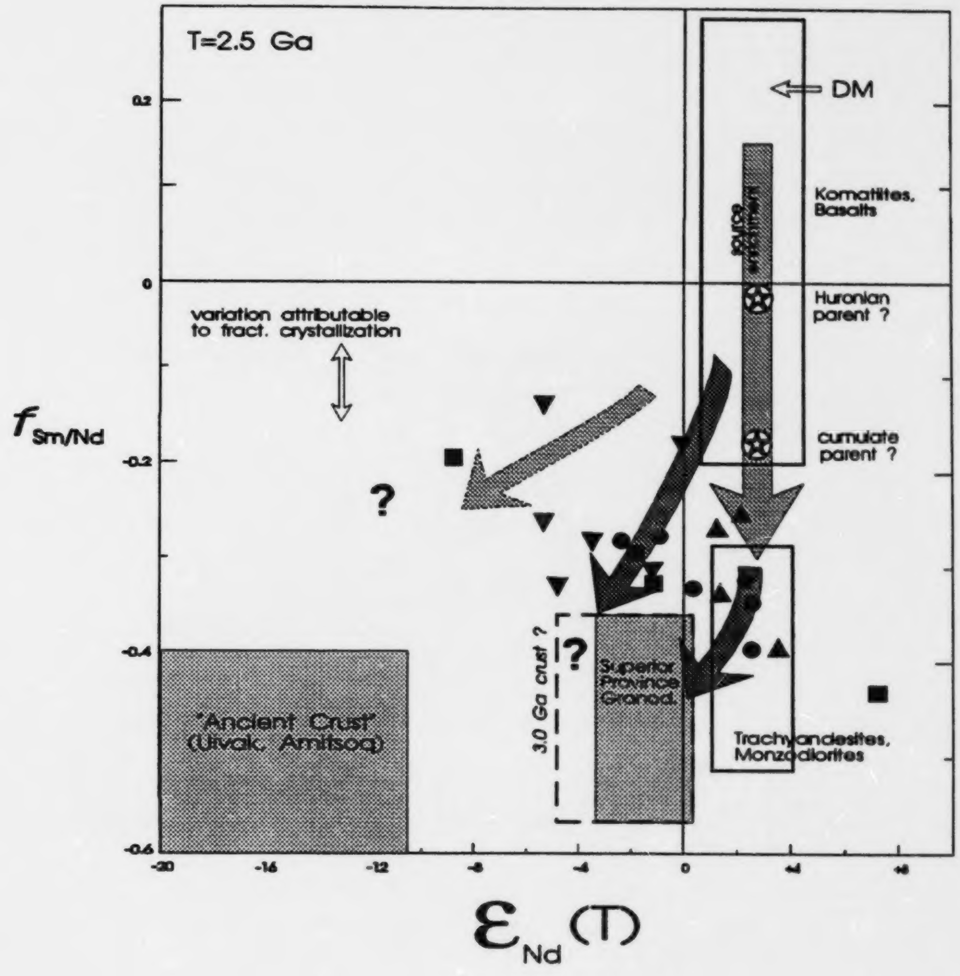

Figure 7.2. ϵ_{Nd}-$f_{Sm\text{-}Nd}$ plot, showing mantle and crustal reservoirs and possible evolutionary path of the cumulate parent liquid.

to about -0.16 for plagioclase alone. For the generally plagioclase-dominated cumulates observed the dominant effect of fractional crystallization will be to lower the $f_{Sm/Nd}$ value from that of the parent liquid by probably not more than 0.1. Cumulates with comparable amounts of plagioclase and pyroxene would have $f_{Sm/Nd}$ values elevated by on the order of 0.04. Calculated normative compositions suggest that while some of the cumulates may have had comparable volumes of plagioclase and pyroxene, no pyroxenitic compositions are represented which might cause large elevations (i.e. +0.1 or greater) of the $f_{Sm/Nd}$ value relative to the parent. This suggests, therefore, that the plotted values for the cumulates in ϵ_{Nd}-$f_{Sm/Nd}$ space are comparable to those of their parent liquid(s) or have $f_{Sm/Nd}$ values which are probably low by 0 to 0.1 $f_{Sm/Nd}$ units. This then favours the involvement of a relatively LREE-depleted ancient component (compared to "average" Amitsoq or MRV tonalitic rocks, or solely juvenile crust), particularly in the case of the two high $f_{Sm/Nd}$ samples which plot towards the upper left of the ϵ_{Nd}-$f_{Sm/Nd}$ diagram (SPA-88-10 and -89-09 in Figure 7.2).

Lower crustal contamination could occur during initial penetration of the crust by the relatively hot mafic magma when the conduit through the crust is most susceptible. Alternatively, pooling of the mafic magma at the base of the crust prior to ascension could promote exchange. This latter model would suggest that melting of the mantle took place prior to the event which generated the rifting and allowed the magma to ascend into the lithospheric crust.

7.4.2 Constraints on Mantle-Derived End Member

The composition of the mantle end-member is equally problematic. If a LREE-depleted mantle is considered to be the original source of the mafic magma(s), $f_{Sm/Nd}$ values of

+0.15 to 0.2 would correspond to ϵ_{Nd} values of around +2.5. The difficulty in generating the observed data by mixing this depleted mantle with the proposed crustal end-members at *ca*. 2500 Ma is that an unrealistically large proportion of crustal component would be required. Also. one would expect to see a greater observed range of $f_{Sm/Nd}$ values, and to see the data plot towards more negative ϵ_{Nd} values (*i.e.* in line with a straight line joining the depleted mantle and the crust). While the lowest-ϵ_{Nd} samples might support direct mixing between a more LREE-depleted mantle and an ancient crust, the large number of samples with ϵ_{Nd}(2500) values of +2 to +3 with $f_{Sm/Nd}$ between -0.3 and -0.4 suggests that an alternative enrichment process is required.

Based on trace element modelling, Jolly (1987b) calculated a Huronian mantle source composition. He determined that 10 to 20% partial melting of a mantle peridotite would produce liquids comparable to early and late Huronian tholeiitic basalts, respectively. His calculated Huronian parent shows significant enrichment in incompatible element abundances relative to Archean mantle, particularly in the LILE. This enrichment is reflected by a $f_{Sm/Nd}$ value of around -0.03. Jolly suggests a subduction-related mechanism for this enrichment, correlating it with late-Abitibi-aged Kenoran Orogeny activity. A *ca*. 2700 Ma enrichment of depleted mantle up to approximately chondritic Sm/Nd ratios would still retain a relatively depleted isotopic signature, as a near-chondritic Sm/Nd ratio will not evolve relative to a chondritic reference. Isotopic data suggest that the melting event that generated the parent magma to the cumulates occurred at *ca*. 2500 Ma rather than *ca*. 2700 Ma. This is based on the observation of samples with depleted-mantle-type ϵ_{Nd} values and LREE-enriched $f_{Sm/Nd}$. There is probably sufficient flexibility in the precise ϵ_{Nd} limits of the depleted mantle and in the timing constraints that a late-

Kenoran enrichment cannot be ruled out. For instance, *ca.* 2650 Ma contamination of a magma with ϵ_{Nd}=+3 or +4 would not produce sufficiently evolved mixtures to be distinguishable outside reasonable errors from the observed data. This would require that an apparently variably enriched partial melt resided somewhere in the upper mantle or basal lithosphere beneath the Abitibi Subprovince for at least 150 Ma without homogenizing, cooling significantly (*i.e.* crystallizing), or ascending, until induced to do so by crustal extension at *ca.* 2500 Ma.

The absence of geological activity between the end of Abitibi greenstone belt formation at *ca.* 2650 Ma and the initiation of Huronian-related rifting at *ca.* 2500 to 2450 Ma begs the question of a melting mechanism. A hotspot-type mechanism might be invoked to provide an anorogenic heat source shortly prior to 2500 Ma, and would also be consistent with the subsequent extensional regime manifested in the *ca.* 2450 Ma Hearst-Matachewan dyke swarm, as well as perhaps large scale doming, extension and aulacogen development as suggested by Fahrig (1987) as a model for Huronian rift formation.

7.5 EVOLUTIONARY SUMMARY AND TECTONIC IMPLICATIONS

In summary, the best coherent model, albeit not necessarily a unique solution given the geochemical and isotopic resolution presented, is as follows:

1) The Archean depleted mantle beneath the Abitibi was enriched in incompatible elements via hydrous metsomatism as a consequence of active subduction during the formation of Abitibi greenstone belts (Jolly, 1987b) at *ca.* 2700 Ma.

2) Subsequent small amounts (10 to 20%) of partial melting of mantle peridotite generated basaltic magmas, at or immediately prior to 2500 Ma. East-west rifting of

the cratonic margin of the Superior Province and associated extension induced the extrusion of low-K tholeiitic lavas (and related crustal melting), the emplacement of mafic dykes (Matachewan) radiating north from the rift zone, and the intrusion of gabbro-anorthositic cumulates and/or sills into the cratonic margin between 2485 and 2500 Ma.

3) Simultaneous and subsequent subsidence encouraged the deposition of the sediments of the Huronian Supergroup among and on top of the volcanics.

4) The volcanic-sedimentary pile was then intruded by mafic dykes (Nipissing) at *ca*. 2220 Ma.

5) The area was subsequently overprinted by Sudbury-aged (*ca*. 1850 Ma) and Grenvillian (*ca*. 1000 Ma) reheating.

Trace element modelling indicates that the cumulate gabbro-anorthosite intrusions at East Bull Lake, Shakespeare-Dunlop, Tennyson, Drury and Falconbridge could have been produced by fractional crystallization of plagioclase and pyroxene from a parent composition comparable to that observed in May Twp. intrusion or primitive Huronian basalt samples. The melting by which the parent magma was derived probably only slightly predated intrusion of the magma, and may therefore reflect an anorogenic, post-Kenoran event such as plume-related heating. The distribution of Sm-Nd isotopic data suggest that the formation of basaltic liquid(s) was simulataneous with or followed immediately by contamination with LREE-enriched sialic material. This produced a further LREE-enrichment reflected by $f_{Sm/Nd}$ values potentially ranging from -0.35 to -0.15. It is impossible to account for the observed range of cumulate REE compositions (as reflected by $f_{Sm/Nd}$ and ϵ_{Nd}) from a single parent composition. The extent and source of the crustal contamination varied from extensive assimilation of juvenile (*ca*. 2700 Ma) crust in the EBL and Drury Twp. intrusions to an additional contribution from ancient (ca. 3500 Ma) crust evident in some S-D and Falconbridge Twp. samples.

Quantifications of the extent of crustal contamination from different compositions have been undertaken previously, but based largely on relatively poorly-constrained bulk end-member compositions. If early melting, incompatible-element enriched sialic compositions (such as granitic plutons) are envisioned as crustal end-members rather than tonalites, and given potential uncertainties in ϵ_{Nd} of up to ± 1 epsilon unit (2σ), the requirements on ancient crustal involvement may be significantly decreased. Given these limitations, the influence of ancient crust is still required, albeit by a potentially very sparse data set. The only practical local source of ancient crust is represented in northern Michigan and Wisconsin and southern Minnesota, typified by the Minnesota River Valley tonalitic gneiss (*cf.* Sims *et al.*, 1981). There is some evidence for slightly older (*ca.* 3.0 to 3.1 Ga) sialic lower crust underlying the Superior Province margins (*e.g.* Beakhouse, 1985; Gariépy and Allégre, 1985), and a small amount of xenocrystic zircon evidence suggesting the existence of a ca. 3.5 Ga component underlying the Minto Subprovince (Stern *et al.*, 1991; Stern *et al.*, in prep., 1992).

Models for the formation of the granite-greenstone belt terranes of the Abitibi may involve the presence of older sialic material, although it is generally not actively involved in the generation of these terranes (*e.g.* Blackburn *et al.*, 1985; Dimroth *et al.*, 1983; Jackson and Fyon, 1992, and references therein). These authors favour island-arc models involving generally (although not necessarily) north-dipping subduction. Dimroth *et al.* (1983) suggest that subduction was terminated by collision with older sialic material, which may have been the Minnesota River Valley gneiss (Jackson and Fyon, 1992). Sims *et al.* (1981) suggest that the surface manifestation of the boundary or join between the Late Archean granite-greenstone terrain and the older gneissic one is represented by the Murray Fault zone, which traverses the study area from west to east. While this major fault system may not have been an active magma conduit during the extension leading to rifting and subsidence of the Huronian basin, it does suggest that the potential influence of older sialic crust may extend sufficiently far north to contribute to the intrusions in this study and perhaps to the Levack Gneiss Complex as well.

Finally, the regional association of a rifted Archean cratonic margin which has been intruded by Early Proterozoic gabbro-anorthosites may be tentatively correlated with an apparently similar assemblage in north central Finland (Laajoki, 1986). The paucity of high-resolution geochronological and REE isotopic data from that area precludes a detailed comparison at this point. However, available information suggests an environment which includes Early Proterozoic (basal) metavolcanics, quartzites, and other low to medium-grade metasediments (the Karelian Formations) overlying late Archean greenstones. Layered mafic intrusions with an age of 2440 Ma intrude the granitoids at the cratonic margin adjacent to the Karelian Formations.

REFERENCES

Ashwal, L.D. and Wooden, J.L.

1989: River Valley Pluton, Ontario: A late-Archean/early-Proterozoic anorthositic intrusion in the Grenville Province; Geochim. et Cosmochim. Acta, vol. 53, no. 3, p. 633-641.

Beakhouse, G.P.

1985: The relationship of supracrustal sequences to a basement complex in the western English River Subprovince; Evolution of Archean supracrustal sequences, edited by L.D. Ayres, P.C. Thurston, K.D. Card and W. Weber. Geological Association of Canada Special Paper 28, p. 169-178.

Blackburn, C.E., Bond, W.D., Breaks, F.W., Davis, D.W., Edwards, G.R., Poulsen, K.H., Trowell, N.F. and Wood, J.

1985: Evolution of Archean volcanic-sediment sequences of the western Wabigoon Subprovince and its margins: a review; in Evolution of Archean supracrustal sequences, edited by L.D. Ayres, P.C. Thurston, K.D. Card and W. Weber. Geological Association of Canada Special Paper 28, p. 89-123.

Born, P.

1979: Geology of the East Bull Lake layered complex, District of Algoma, Ontario; M.Sc. thesis, Laurentian University, Sudbury Ontario, 108 pp. plus appendices.

Born, P. and James, R.S.

1978: Geology of the East Bull Lake layered gabbro anorthosite intrusion, District of Algoma, Ontario;

Geological Survey of Canada Current Research, Part A, Paper 78-1A, p. 91-95.

Cambray, F.W.

1978: Plate tectonics as a model for the environment of deposition and deformation of the early Proterozoic (Precambrian X) of northern Michigan; in Geological Society of America Abstracts with Programs, v. 7, no. 7, p. 376.

Cape, D.F.

1973: A petrologic and geochemical study of a gabbro, anorthositic gabbro intrusionand neighbouring volcanics, northwest corner of May Township; Unpublished B.Sc. thesis, University of Windsor, 58 p.

Card, K.D.

1965: Geology of Hyman and Drury Townships, District of Sudbury; Ontario Department of Mines, Geological Report No. 34, 36 p.

Card, K.D.

1968: Geology of the Denison-Waters area; Ontario Department of Mines, Geological Report No. 60, 63 p.

Card, K.D.

1978: Geology of the Sudbury-Manitoulin area, Districts of Sudbury and Manitoulin; Ontario Geological Survey, Report 166, 238 p.

Card, K.D.

1988 (in prep.): Proterozoic geology of the north shore of Lake Huron: Huronian Fold Belt and the Sudbury Structure; DNAG: Geology of the Canadian Shield, 37 p. plus figures.

Card, K.D. and Innes, D.G.

1981: Geology of the Benny area, District of Sudbury; Ontario Geological Survey, Report 206, 117 p.

Card, K.D., Innes, D.G. and Debicki, R.L.

1977: Stratigraphy, sedimentology and petrology of the Huronian Supergroup in the Sudbury-Espanola area; Ontario Division of Mines, Geoscience Study 16, 99 p.

Card, K.D. and Palonen, P.A.

1976: Geology of the Dunlop-Shakespeare area, District of Sudbury; Ontario Division of Mines, Geoscience Report 139, 52 p.

Carmichael, I.S., Turner, F.J. and Verhoogen, J.

1974: Igneous Petrology; McGraw-Hill, Inc., 724 pp.

Cattell, A., Krogh, T.E. and Arndt, N.T.

1984: Conflicting Sm-Nd whole-rock and U-Pb zircon ages for Archean lavas from Newton Township, Abitibi Belt, Ontario; Earth and Planetary Science Letters, v. 70, p. 280-290.

Chauvel, C., Dupré, B. and Jenner, G.A.

1985: The Sm-Nd age of Kambalda volcanics is 500 Ma too old!; Earth and Planetary Science Letters, v. 74, p. 315-324.

Claoué-Long, J.C., Thirlwall, M.F. and Nesbitt, R.W.
1984: Revised Sm-Nd systematics of Kambalda greenstones, Western Australia; Nature, v. 307, p. 697-701.

Collerson, K.D., McCulloch, M.T., Bridgwater, D., McGregor, V.R. and Nutman, A.P.
1986: Strontium and neodymium isotopic variations in Early Archean gneisses affected by Middle to Late Archean high-grade metamorphic processes: West Greenland and Labrador; in Early Crustal Genesis: The World's Oldest Rocks, LPI Technical Report Number 86-04, p. 30-36.

Collins, W.H.
1936: Sudbury Series; Geological Society of America Bulletin, Vol. 47, p. 1680-1681.

Corfu, F. and Andrews, A.J.
1986: A U-Pb age for mineralized Nipissing diabase, Gowganda, Ontario; Canadian Journal of Earth Sciences, v. 23, no. 1, p. 107-109.

Corfu, F. and Stott, G.M.
1986: U-Pb ages for late magmatism and regional deformation in the Shebandowan Belt, Superior Province, Canada; Canadian Journal of Earth Sciences, Volume 23, No. 8, p. 1075-1082.

Corfu, F. and Wallace, H.
1986: U-Pb zircon ages for magmatism in the Red Lake greenstone belt, northwestern Ontario; Canadian Journal of Earth Sciences, Volume 23, No. 1, p. 27-42.

Corfu, F. and Wood, J.

1986: U-Pb zircon ages in supracrustal and plutonic rocks; North Spirit Lake area, northwestern Ontario; Canadian Journal of Earth Sciences, Volume 23, No. 7, p. 967-977.

Cox, K.G., Bell, J.D. and Pankhurst, R.J.

1979: The Interpretation of Igneous Rocks; George Allen and Unwin, London.

Cumming, B.

1985: Petrography, geochemistry, and petrogenesis of Huronian volcanic rocks of the Elliot Lake region, Ontario; M.Sc. Thesis, Brock University, St. Catherines, Ontario.

Davidson, A.

1986: Grenville Front relationships near Killarney, Ontario; in The Grenville Province, (ed.) J.M. Moore, A. Davidson and A.J. Baer; Geological Association of Canada Special Paper 31, p. 107-117.

Davidson, A., van Breemen, O. and Sullivan, R.W.

1992: Circa 1.75 Ma ages for plutonic rocks from the Southern Province and adjacent Grenville Province: what is the expression of the Penokean orogeny? in Radiogenic Age and Isotopic Studies: Report 6, Geological Survey of Canada, Paper 92-2, p. 107-118.

Deer, W.A., Howie, R.A. and Zussman, J.

1966: *An Introduction to the Rock-Forming Minerals*, Longman Group Limited, London, 528 pp; crystallography, mineralogy.

DePaolo, D.J.

1988: Neodymium Isotope Geochemistry; Springer-Verlag, 187 pp.

Dickin, A.P., McNutt, R.H. and Clifford, P.M.

1990: A neodymium isotope study of plutons near the Grenville Front in Ontario, Canada; Chemical Geology, 83, p. 315-324.

Dimroth, E., Imreh, L., Goulet, N. and Rocheleau, M.

1983: Evolution of the south-central segment of the Archean Abitibi Belt, Quebec. Part III: Plutonic and metamorphic evolution and geotectonic model; Canadian Journal of Earth Sciences, vol. 20, p. 1374-1388.

Easton, R.M.

1986: Geochronology of the Grenville Province; Part I: Compilation of data; Part II: Synthesis and interpretation; The Grenville Province, Special Paper 31, p. 127-174.

Fahrig, W.F.

1987: The tectonic setting of continental mafic dyke swarms: failed arms and early pasive margins; in Mafic Dyke Swarms, Geological Association of Canada Special Paper 34, p. 331-348.

Fairbairn, H.W., Hurley, P.M. and Pinson, W.H.

1960: Mineral and rock ages at Sudbury-Blind River, Ontario; Geological Association of Canada Proceedings, Vol. 12, p. 41-66.

Gariépy, C. and Allégre, C.J.

1985: The lead isotope geochemistry and geochronology of late-kinematic intrusives from the Abitibi greenstone belt, and the implications for late Archean crustal evolution; Geochimica et Cosmochimica Acta, v. 49, p. 2371-2383.

Gates, T.M. and Hurley, P.M.

1973: Evaluation of Rb-Sr dating methods applied to the Matachewan, Abitibi, Mackenzie, and Sudbury dike swarms in Canada; Canadian Journal of Earth Science, 10, p. 900-919.

Goldich, S.S. and Hedge, C.E.

1974: 3,800 - Myr granitic gneiss in southwestern Minnesota; Nature, 252, no. 5483, p. 467-468.

Gower, C.F., Ryan, A.B. and Rivers, T.

1991: Mid-Proterozoic Laurentica-Baltica: an overview of its geological evolution and a summary of the contributions made by this volume; in Mid-Proterozoic Laurentica-Baltica, (ed.) Gower, C.F., Rivers, T. and Ryan, A.B.; Geological Association of Canada, Special Paper 38, p. 1-20.

Grant, R.W. and Bite, A.

1984: Sudbury quartz diorite offset dikes; In The Geology and Ore Deposits of the Sudbury Structure (eds. E.G. Pye, A.J. Naldrett and P.E. Giblin), Ontario Geological Survey Special Volume 1, p. 275-300.

Hanson, G.N.

1977: Geochemical evolution of the suboceanic mantle; Journal of the Geological Society of London, vol. 134, p. 235-253.

Hanson, G.N.

1980: Rare earth elements in petrogenetic studies of igneous systems; Annual Review of Earth and Planetary Sciences, 8, p. 371-406.

Heaman, L.M.

1989: U-Pb dating of mafic dyke swarms: what are the options?; in International Association of Volcanology and Chemistry of the Earth's Interior, Congress Abstracts; New Mexico Bureau of Mines and Mineral Resources Bulletin, v. 131, p. 125.

Hegner, E., Kröner, A. and Hofmann, A.W.

1984: Age and isotope geochemistry of the Archaean Pongola and Asushwana suites in Swaziland, southern Africa: a case for crustal contamination of mantle-derived magma; Earth and Planetary Science Letters, v. 70, p. 267-279.

Henderson, P.

1984: General geochemical properties and abundances of the rare earth elements; in *Rare Earth Element Geochemistry*, P. Henderson, ed., Elsevier, Amsterdam, Netherlands, p. 1-32.

Irvine, T.N. and Baragar, W.R.A.

1971: A guide to the chemical classification of the common volcanic rocks; Canadian Journal of Earth Sciences, 8, p. 523-548.

Jackson, S.L. and Fyon, J.A.

1992: The western Abitibi Subprovince in Ontario; in Geology of Ontario. Ontario Geological Survey Special Volume 4, Part 1, p. 405-482.

James, R.S. and Harris, B.J.

1977: Geology of the Shakespeare-Dunlop layered gabbro-anorthosite intrusion, Ontario; Report of Activities, Part A, Geological Survey of Canada, Paper 77-1A.

James, R.S., Born, P. and Bigauskas, J.

1983: Geology of the East Bull Lake layered complex, District of Algoma, Ontario; Current Research, Part B, Geological Survey of Canada, Paper 83-1B, p. 1-11.

Jolly, W.T.

1987 a: Geology and geochemistry of Huronian rhyolites and low-Ti continental tholeiites from the Thessalon region, central Ontario; Canadian Journal of Earth Sciences, Vol. 24, No. 7, p. 1360-1385.

Jolly, W.T.

1987 b: Lithophile elements in Huronian low-Ti continental tholeiites from Canada, and evolution of the Precambrian mantle; Earth and Planetary Science Letters, 85, p. 401-415.

Jolly, W.T., Dickin, A.P. and Wu, T.-W.

1992: Geochemical stratigraphy of the Huronian continental volcanics at Thessalon, Ontario: contributions of two-stage crustal fusion; Contributions to Mineralogy and Petrology, 110, p. 411-428.

Kamineni, D.C.

1986: A petrochemical study of calcic amphiboles from the East Bull Lake anorthosite-gabbro layered complex, District of Algoma, Ontario; Contributions to Mineralogy and Petrology, .

Kamineni, D.C., McCrank, G.F. and Stone, D.

1987: Multiple alteration events in the East Bull Lake anorthosite-gabbro layered complex, NE Ontario, Canada: evidence from fracture mineralogy and ^{40}Ar-^{39}Ar dating; Applied Geochemistry, Vol. 2, p. 73-80.

Kamineni, D.C., McCrank, G.F., Stone, D., Ejeckam, R.B., Flindall, R. and Sikorsky, R.

1984: Geology of the central plateau of the East Bull Lake pluton, northeastern Ontario; Current Research, Part B, Geological Survey of Canada, Paper 84-1B, p. 75-83.

Kamineni, D.C., McCrank, G.F., Stone, D., Ejeckam, R.B. and Sikorsky, R.

1985: A preliminary report of alteration and fracture-filling mineralogy in the East Bull Lake pluton, District of Algoma, Ontario; Current Research, Part B, Geological Survey of Canada, Paper 85-1B, p. 81-88.

Kerrich, R., Kamineni, D.C., Borre, D., Baldwin, D.K., McLarty, E. and Thivierge, R.H.

1987: Cyclic deformation and chemical transport in the Folson Lake fault zone, East Bull Lake anorthosite-gabbro complex: evidence for seismic pumping?; Applied Geochemistry, Vol. 2, p. 103-126.

Knight, C.J.

1967: Rb-Sr ages of volcanic rocks of the north shore of Lake Huron, Ontario, Canada; Ph.D. Thesis, University of Toronto, Toronto, Ontario.

Krogh, T.E., Davis, G.L. and Frarey, M.J.

1971: Isotopic ages along the Grenville Front in the Bell Lake area, southwest of Sudbury, Ontario; Carnegie Institute of Washington Yearbook, v. 69, p. 337-339.

Krogh, T.E., Davis, D.W. and Corfu, F.

1984: Precise U-Pb zircon and baddeleyite ages for the Sudbury area; In The Geology and Ore Deposits of the Sudbury Structure (eds. E.G. Pye, A.J. Naldrett and P.E. Giblin), Ontario Geological Survey Special Volume 1, p. 431-446.

Krogh, T.E. and Turek, A.

1982: Precise U-Pb zircon ages from the Gamitagama greenstone belt, southern Superior Province; Canadian Journal of Earth Science, 19, p. 859-867.

Kurtz, R.D. and Niblett, E.R.

1984: A magnetotelluric survey over the East Bull Lake gabbro-anorthosite complex; Atomic Energy of Canada Limited, Technical Record TR-236, 27 pp.

Laajoki, K.

1986: The Precambrian supracrustal rocks of Finland and their tectono-exogenic evolution; Precambrian Research, 33, p. 67-85.

Larue, D.K. and Sloss, L.L.

1980: Early Proterozoic sedimentary basins of the Lake Superior region: Summary; Geological Society of America Bulletin, Part 1, v. 91, p. 450-452.

Lowdon, J.A.

1960: Age determinations by the Geological Survey of Canada; Report 1 - Isotopic ages; Geological Survey of Canada, Department of Mines and Technical Surveys Canada, Paper 60-17.

Lowdon, J.A.

1961: Age determinations by the Geological Survey of Canada; Report 2 - Isotopic ages; Geological Survey of Canada, Department of Mines and Technical Surveys Canada, Paper 61-17.

Lowdon, J.A.

1962: Age determinations by the Geological Survey of Canada; Report 3 - Isotopic ages; Geological Survey of Canada, Department of Mines and Technical Surveys Canada, Paper 62-17.

Lowdon, J.A.

1963: Age determinations by the Geological Survey of Canada; Report 4 - Isotopic ages; Geological Survey of Canada, Department of Mines and Technical Surveys Canada, Paper 63-17.

Lumbers, S.B.

1975: Geology of the Burwash area, Districts of Nipissing, Parry Sound, and Sudbury; Ontario Division of Mines, Geoscience Report 116, 158 pp.

Lumbers, S.B.

1984: ; In The Geology and Ore Deposits of the Sudbury Structure (eds. E.G. Pye, A.J. Naldrett and P.E. Giblin), Ontario Geological Survey Special Volume 1, p. .

Lumbers, S.B., Way, W.-T., Heaman, L.M., Vertolli, V.M. and MacRae, N.D.

1991: Petrology and age of the A-type Mulock granite batholith, northern Grenville Province, Ontario; Precambrian Research, v. 53, p. 199-231.

McCrank, G.F.D., Misiura, J.D. and Brown, P.A.

1981: Plutonic rocks in Ontario; Atomic Energy of Canada, TR-114, 47 p.

McCrank, G.F.D., Stone, D., Kamineni, D.C., Zayachkivsky, B. and Vincent, G.

1983: Regional geology of the East Bull Lake area, Ontario; In Current Research, Part A, Geological Survey of Canada, Paper 83-1A, p. 457-464.

McCulloch, M.T. and Wasserburg, G.J.

1980: Early Archean Sm-Nd model ages from a tonalitic gneiss, northern Michigan; in Selected Studies of Archean Gneisses and Lower Proterozoic Rocks, Southern Canadian Shield; (ed.) Morey, G.B. and Hanson, G.N., Geological Society of America Special Paper 182, p. 135-138.

McKay, G.A.

1989: Partitioning of rare earth elements between major silicate minerals and basaltic melts; in Geochemistry and Mineralogy of Rare Earth Elements, B.R. Lipin and G.A. McKay, eds., Reviews in Mineralogy, vol. 21, p. 45-77.

McNutt, R.H., Gascoyne, M. and Kamineni, D.C.

1987: $^{87}Sr/^{86}Sr$ values in groundwaters of the East Bull Lake pluton, Superior Province, Ontario, Canada; Applied Geochemistry, Vol. 2, p. 93-101.

Moore, E.S. and Armstrong, H.S.

1945: Geology of the East Bull Lake area; Ontario Department of Mines, Fify-second annual report, Vol. LII, Part VI, 17 p.

Mullen, E.D.

1983: $MnO/TiO_2/P_2O_5$: a minor element discriminant for basaltic rocks of oceanic environments and its implications for petrogenesis; Earth and Planetary Science Letters, vol. 62, p. 53-62.

Myashiro, A.

1974: Volcanic rock series in island arcs and active continental margins; American Journal of Science, vol. 274, p. 321-355.

Pearce, J.A.

1975: Basalt geochemistry used to investigate past tectonic environments on Cyprus; Tectonophysics, vol. 25, p. 44-67.

Pearce, J.A.

1983: Role of the sub-continental lithosphere in magma genesis at active continental margins; in Continental Basalts and Mantle Xenoliths; (ed.)

Hawkesworth, C.J. and Norry, M.J.; Shiva Publishing Limited, p. 230-272.

Pearce, J.A. Norry, M.J.

1979: Petrogenetic implications of Ti, Zr, Y, and Nb variations in volcanic rocks; Contrib. to Mineral. and Petrol., vol. 69, p. 33-47.

Peck, D.C., Chubb, P.T. and James, R.S.

1991: Magmatic platinum group elements and copper + nickel sulphide mineralization along the base of the East Bull Lake gabbro-anorthosite intrusion; in Ontario Geological Survey Misc. Paper 157, p. 64-72.

Presnall, D.C.

1979: Fractional crystallization and partial fusion; in *The Evolution of the Igneous Rocks: Fiftieth Anniversary Perspectives*, H.S. Yoder, ed., Princeton University Press, p. 59-75.

Prevec, S.A.

1988: The petrology, geochronology and geochemistry of the White Bear Arm Complex and associated units, Grenville Province, eastern Labrador; M.Sc. Thesis, McMaster University, Hamilton, Ontario, 155 p. plus appendices.

Prevec, S.A.

1992: U-Pb age constraints on Early Proterozoic mafic magmatism from the southern Superior and western Grenville provinces, Ontario; in Radiogenic Age and Isotopic Studies, Report 6, Geological Survey of Canada Paper 92-2, p. 97-106.

Prevec, S.A., McNutt, R.H. and Dickin, A.P.

1991: Sr and Nd isotopic and petrological evidence for the age and origin of the White Bear Arm Complex and associated units from the Grenville Province in eastern Labrador; In Mid-Proterozoic Laurentica-Baltica, Geological Association of Canada Special Paper 38, p. 65-78.

Robertson, J.A.

1976: Geology of the Massey area, Districts of Algoma, Manitoulin , and Sudbury; Ontario Division of Mines, Geoscience Report 136, 130 pp.

Robertson, J.A.

1977: Geology of the Cutler area, District of Algoma; Ontario Division of Mines, Geoscience Report 147, 73 pp.

Roddick, J.C.

1984: Emplacement and metamorphism of Archaean mafic volcanics at Kambalda, Western Australia - geochemical and isotopic constraints; Geochimica et Cosmochimica Acta, 48, p. 1305-1318.

Rousell, D.H.

1978: Geology of the anorthositic sill at St. Charles, Ontario; In Current Research, Part A, Geological Survey of Canada, Paper 78-1A, p. 163-168.

Rousell, D.H.

1981: Fabric and origin of gneissic layers in anorthositic rocks of the St. Charles sill, Ontario; Canadian Journal of Earth Sciences, Vol. 18, p. 1681-1693.

Rousell, D.H. and Trevisiol, D.D.

1988: Geology of the mineralized zone of the Wanapitei Complex, Grenville Front, Ontario; Mineralium Deposita, v. 23, p. 138-149.

Sawiuk, M.J.

1978: Geochemistry of the Thessalon volcanics; Honours Thesis, University of Western Ontario, London, Ontario.

Shervais, J.W.

1982: Ti-V plots and the petrogenesis of modern and ophiolitic lavas; Earth and Planetary Science Letters, vol. 59, p. 101-118.

Shirey, S.B. and Hanson, G.N.

1986: Mantle heterogeneity and crustal recycling in Archean graniote-greenstone belts: Evidence from Nd isotopes and trace elementxs in the Rainy Lake area, Superior Province, Ontario, Canada; Geochimica et Cosmochimica Acta, v. 50, p. 2631-2651.

Simmons, E.C. and Hanson, G.N.

1978: Geochemistry and origin of massif-type anorthosites; Contributions to Mineralogy and Petrology, 66, p. 119-135.

Simmons, E.C. and Hanson, G.N.

1980: Geochemistry of the Shawmere Anorthosite Complex, Kapuskasing Structural Zone, Ontario; Precambrian Research, 11, p. 43-71.

Sims, P.K.

1976: Precambrian tectonics and mineral deposits, Lake Superior region; Economic Geology, v. 71, p. 1092-1127.

Sims, P.K., Card, K.D. and Lumbers, S.B.

1981: Evolution of early Proterozoic basins of the Great Lakes region; in Proterozoic Basins of Canada, F.H.A. Campbell, editor; Geological Survey of Canada, Paper 81-10, p. 379-397.

Stacey, J.S. and Kramers, J.D.

1975: Approximation of terrestrial lead isotope evolution by a two-stage model; Earth and Planetary Science Letters, v. 26, p. 207-221.

Stern, R.A., Percival, J.A. and Mortensen, J.K.

1992: Geochemical evolution of the Minto block: a 2.7 Ga continental magmatic arc built on the Superior proto-craton; Submitted to Precambrian Research.

Stern, R.A., Percival, J.A., Card, K.D. and Mortensen, J.K.

1991: Geochemistry and geochronology of the Minto Subprovince, Quebec; in Geological Association of Canada/Mineralogical Association of Canada Program with Abstracts, vol. 16, p. A118.

Stockwell, C.H.

1969: Structural provinces, orogenies, and time-classifications of rocks of the Canadian Shield; Age determinations by the Geological Survey of Canada; Report 2, Isotopic Ages: Geological Survey of Canada Paper 61-17, p. 108-118.

Stockwell, C.H., McGlynn, J.C., Emslie, R.F., Sanford, B.V., Norris, A.W., Donaldson, J.A., Fahrig, W.F. and Currie, K.L.

1970: Geology of the Canadian Shield; Geology and economic minerals of Canada, Part A, Chapter IV, p. 108-119.

Sun, S.S.

1982: Chemical composition and origin of the Earth's primitive mantle; Geochim. Cosmochim. Acta, vol. 46, p. 179-192.

Taylor, H.P., Jr.

1980: The effects of assimilation of country rocks by magmas on $^{18}O/^{16}O$ and $^{87}Sr/^{86}Sr$ systematics in igneous rocks; Earth and Planetary Science Letters, 47, p. 243-254.

Thomson, J.E.

1957: Geology of Falconbridge Township; Ontario Department of Mines, Sixty-sixth annual report, Vol. LXVI, Part 6, 36 pp.

van Breemen, O., Davidson, A., Loveridge, W.D. Sullivan, R.W.

1986: U-Pb zircon geochronology of Grenville tectonites, granulites and igneous precursors, Parry Sound, Ontario; in Geological Association of Canada Special Paper 31, (J.M. Moore, A. Davidson and A.J. Baer, eds.), p. 191-207.

van Schmus, R.

1965: The geochronology of the Blind River-Bruce Mines area, Ontario, Canada; Journal of Geology, Vol. 73, p. 755-780.

van Schmus, R. and Bickford, M.E.

1981: Proterozoic chronology and evolution of the midcontinent region, North America; in Precambrian Plate Tectonics; (ed.) Kröner, A.; Elsevier, Amsterdam, p. 261-296.

van Schmus, R., Bickford, M.E. and Zietz, I.

1987: Early and Middle Proterozoic provinces in the central United States; in Proterozoic Lithospheric Evolution, (ed.) Kröner, A.; Geodynamics Series Volume 17, p. 43-68.

Wager, L.R., Brown, G.M. and Wadsworth, W.J.

1960: Types of igneous cumulates; Journal of Petrology, vol. 1, part 1, p. 73-85.

Zartman, R.E. and Doe, B.R.

1981: Plumbotectonics-the model; Tectonophysics, v. 75, p. 135-162.

Zolnai, A.I., Price, R.A. and Helmstaedt, H.

1984: Regional cross section of the Southern Province adjacent to Lake Huron, Ontario:implications for the tectonic significance of the Murray Fault Zone; Canadian Journal of Earth Sciences, v. 21, no. 4, p. 447-456.

APPENDIX 1. RESEARCH METHODS

Contents:

1.1 Sampling Logistics

1.2.1 Crushing

1.2.2 Mineral separation

1.2.3 Wet chemistry

1.3 Analyses

1.3.1 Isotopic compositions

1.3.2 Elemental abundances

1.3.3 Petrography

1.2 Sample Locations

1.1 Sampling Logistics

Rock samples were obtained over approximately six weeks during the summers of 1988 and 1989. All of the units were accessible by secondary roads, or short traverses of two to three kilometres. The East Bull Lake and Shakespeare-Dunlop intrusions were accessed by an Atomic Energy of Canada road and a logging road, respectively. Some of the access roads to the St. Charles and Mercer Twp. intrusions were impassable to conventional vehicles due to wet weather in June, 1989. Samples varied in size from about ten kilograms to forty or fifty kilograms, depending on whether or not heavy (trace) mineral geochronology was intended. Minimum sample size was based on obtaining effective geochemical (and isotopic) sample homogeneity, based on grain size of the rock. Samples were removed from the outcrop using sledgehammers.

Support was obtained from the Geological Survey of Canada through the resident geologist, in the form of rock pails for sample transport. Weathered rinds were removed from samples in the field, where possible, and samples were transported from Sudbury to Edmonton by train in forty-five gallon drums and by van in rock pails.

1.2 Sample Preparation

1.2.1 Crushing

Weathered surfaces remaining on the samples were removed at the University of Alberta by hammer and by rock saw in some cases, where care was taken to minimize contamination of the samples, especially with lead, by using saw blades with the lead-based paint stripped off and using a water-based instead of an oil-based lubricant. Slabs for thin sectioning were removed from hand specimens using a water-cooled rock saw. The sample was broken into fist-sized pieces by hand (sledgehammer) and subsequently crushed into thumbnail-sized chips in the "chipmunk crusher" and then into fine gravel using a Braun pulverizer equipped with steel plates. All crushing equipment was thoroughly cleaned using hard and soft-bristled brushes, running water and compressed air. In order to "pre-contaminate" the crusher, a small amount of the sample was run through the pulverizing plates after the "intensive" cleaning, after which the plates were again cleaned with brushes and compressed air. After pulverizing, the sample was repeatedly quartered until a representative sample of about 500 grams for whole-rock analysis was obtained. The remainder was stored in sealed plastic bags or bottles. The whole-rock split was then ground to -300 mesh in an agate mortar and pestle, which was cleaned between samples by thoroughly washing all parts with water. "Clean" quartz of grain size comparable to that of the sample was then run for two minutes, followed by precontamination with an aliquot of the sample. The apparatus was disassembled and cleaned with a soft-bristled brush between the latter steps. The fine-grained sample powder was then stored in plastic vials.

1.2.2 Mineral Separation

In order to extract heavy minerals for isotopic analysis, pulverized sample powders were run on the Wilfley Table or had the finest fraction removed by repeatedly washing and pouring off the suspended material, in the case of relatively small samples. The heavy mineral fraction from the Wilfley Table (or the bulk sample) was then purefied by alternately settling it in high density (heavy) liquids and separating fractions of differing paramagnetic character on the Frantz Isodynamic Magnetic Separator. The heavy liquids used were tetrabromoethane (ρ=2.96 g/cm^{3}) and methylene iodide (ρ=3.30 g/cm^{3}). The pyrexware for heavy liquid separation was cleaned thoroughly between samples using acetone, soap, hot water, and soft-bristled brushes. Pyrex stopcocks were lubricated with silicon grease. Acetone was used to remove the heavy liquids from the sample powders after separation. The fraction which sank in methylene iodide and was non-magnetic at a slope of 10 degrees and a tilt of between 5 and 1 degree was examined for zircons.

Zircon preparation was completed in Dr. Baadsgaard's laboratory at the University of Alberta for samples SPA-88-17, SPA-88-18, SPA-88-54 and SPA-89-14. The heavy, least-magnetic fractions of samples SPA-89-08A, SPA-89-22 and SPA-89-31 were processed at the geochronology lab of the Geological Survey of Canada in Ottawa. Preparation at the Univ. of Alta. consisted of hand-picking preferred grains in acetone or occasionally ethanol. Preparation at the G.S.C. consisted of sieving of the sample followed by zircon selection in ethanol. Selected zircon populations were then abraded with pyrite and repicked. Chemical procedures followed methods referenced in Prevec (1992).

1.2.3 Wet Chemistry

In preparation for isotopic analyses, elemental separation and purefication was undertaken using various chemical procedures. Sample dissolution involved addition of about 10 ml of HF (42%) and 0.5 to 1 ml of HNO_3 (16 N) to 0.25 to 1.0 g of sample in Savillex beakers, heating on a hotplate for 24 to 36 hours, evaporation to near-dryness and repeated addition of a few mls of HNO_3 to remove insoluble fluorides. After evaporation to dryness, procedures varied depending on which element was being purefied and whether of not the sample had been spiked. For elemental concentrations, samples were spiked as powders immediately prior to dissolution. Splitting sample solutions as nitrates led to fractionation of elements into the solid residue producing variations both in absolute concentrations and in ratios thereof. Ion-exchange chemistry was undertaken in quartz columns containing Dowex Bio-Rad AG50W, 200-400 mesh hydrogen-form cation exchange resin and 200 mesh chloride-form anion exchange resin. Sm and Nd were purified using cation exchange resin and MLA. Unspiked Nd was also separated from the REE on columns containing very fine-grained (-300 mesh) teflon powder coated with 2,2 diethyl-hexyl-orthophosphoric acid activator (HEDP).

Elemental separates were prepared for isotopic analysis by loading sample chlorides onto Re filaments on glass beads. Sr, Nd and Sm were loaded in dilute acid solutions onto the side filaments of double-filament beads. Pb was loaded in dilute phosphoric acid and mixed on the filament with silica gel.

1.3 Analyses

1.3.1 Isotopic Compositions

Isotopic analyses for Nd and Sr were carried out at the Univ. of Alta. on the VG354 five-collector solid-source mass spectrometer, equipped with a Daly collector. Magnetic field switching and data analysis were controlled by a Hewlett-Packard 9816A computer. Isotopic analyses for Pb, Sr and spiked Nd and Sm were carried out at the Univ. of Alta. on a VG Micromass 30 single-collector machine, with data collection and processing controlled by an HP as well. Data were compared with replicate analyses of standards, using La Jolla Nd and Nd oxide (Univ. of Alberta) for Nd, NBS 981 for Pb, and NBS 987 for Sr. Standard values for NBS 981 and 987 were consistent and within error of the accepted values, so no correction was required. Mean values for La Jolla Nd and Nd oxide obtained during analyses of samples for this study were consistent with those obtained on the VG 354 during the same period by other users (approximately 0.511820 and 0.511035, respectively). The sample Nd isotopic ratios were corrected to a ^{143}Nd/^{144}Nd ratio of 0.511860 for La Jolla, based on data summarized in Shirey and Hanson (1986). Due to the variety of different chemical and analytical procedures used over the course of this study, it is difficult to report a well-characterized blank for all analyses. In order to minimize the effects of background abundances, large sample volumes were invariably used, ranging from 300-400 mg to as much as 1.0 g, in extreme cases. Blanks determined for Sm and Nd were on the order of 150 pg. For further information on procedural constraints, see M.J.M. Duke unpublished Ph.D. thesis, 1992. Imprecisions used for epsilon calculations and regressions were based on standard reproducibility or individual run imprecision, whichever was poorer. The two-sigma imprecision on the La Jolla mean was 0.000014 (n=29), on NBS 987 2σ was 0.000024 (n=11), and on NBS 981 2σ was about 0.007 on 207/204 and 206/204 ratios (n=9).

U-Pb zircon isotopic analyses for the samples prepared at the Univ. of Alta. were carried out at the RSES of the Australian National University, Canberra, Australia, on the Sensitive High-Resolution Ion-Microprobe ("SHRIMP"). Ages were derived from spot analyses on individual grains. U-Pb zircon isotopic analyses for the samples prepared at the G.S.C. in Ottawa were analysed there on a Finnigan MAT 261 nine-collector solid-source mass spectrometer, equipped with a secondary ion amplifier.

1.3.2 Elemental Abundances

Major and trace element abundances were determined at the G.S.C. in two batches during the winters of 1988 and 1989 by XRF analysis. REE abundances were measured by Inductively Coupled Plasma Spectroscopy (ICP) after preconcentration of the REE on cation-exchange columns. Some of the 1989 REE analyses show unusual Sm and Nd abundances, suggesting an uncorrected interference causing elevated Nd and depressed Sm concentrations. This has been determined to be an analytical artifact rather than a geological one, and corrected for accordingly. Rb and Sr concentrations were also determined in winter 1991 at McMaster University in Hamilton by XRF using a molybdenum tube-Compton peak procedure.

1.3.3 Petrography

Thin sections for SPA-88-prefix samples were prepared from appropriately sized rock slabs at the Univ. of Alta. Most of the thin sections for SPA-89-prefix samples were prepared by GEOMINEX, in Waterloo, Ontario. Thin sections were etched and stained for potassium and calcium using sodium cobaltinitrite and a combination of $BaCl_2$ and rhodizonate solutions respectively, at the Univ. of Alberta.

1.2 Sample I.D.s and Locations

Number	Unit	Description (Field designation)	Location (NTS) N	E	Map	Date Sampled
SPA-88-01	Birch L. Bath.	Algoman granite	5137400	430000	41-I/5	11/06/88
SPA-88-02	Dyke	gabbro, cuts 01	5137400	430000	"	"
SPA-88-03	S-D Pluton	msv metagabb.	5137300	432100	"	"
SPA-88-04	S-D Pluton	Msv metagabb.	5137450	432400	"	"
SPA-88-05	S-D Pluton	msv metagabb.	5137450	432500	"	"
SPA-88-06	B.L. Bath.	granite	5129755	427300	"	"
SPA-88-07	S-D Pluton	granophyre?	5133350	431850	"	"
SPA-88-08A	S-D Pluton	gran. enclave	5133350	431850	"	"
SPA-88-08B	S-D Pluton	sheared A?	5133350	431850	"	"
SPA-88-09	S-D Pluton	msv. metagabb.	5135950	426955	"	12/06/88
SPA-88-10	S-D Pluton	msv. metagabb.	5135950	426900	"	"
SPA-88-11	S-D Pluton	msv. metagabb.	5136000	426950	"	"
SPA-88-12	S-D Pluton	msv. metagabb.	5133400	425425	"	13/06/88
SPA-88-13	S-D Pluton	msv. metagabb.	5133400	425425	"	"
SPA-88-14	S-D Pluton	msv. metagabb.	5133355	415455	"	"
SPA-88-15A	BLB Algoman	granite	5123255	413450	41-J/8	"
SPA-88-15B	BLB	mafic granite	5123255	413450	"	"
SPA-88-16	May Twp.	metagabbro	5121600	415100	41-J/1	"
SPA-88-17	pre-Algoman	fol. granite	5148875	400955	41-J/8	14/06/88
SPA-88-18	Proteroz. gr.	granite	5145650	407125	"	"
SPA-88-19	EBL	metagabb.-an.	5143200	409675	"	"
SPA-88-20	EBL	metagabb.-an.	5143050	409600	"	"
SPA-88-21	EBL	metagabb.-an.	5142995	409625	"	"
SPA-88-22	EBL	metagabb.-an.	5142900	409675	"	"
SPA-88-23	Parisien L.	porph. sy.	5140225	408000	"	"
SPA-88-24	Tennyson Twp.	metagabbro	5133000	408125	"	"
SPA-88-25	Salmay L.	metavolc.	5131150	441400	41-I/5	15/06/88
SPA-88-26	Stobie Fm.	metavolc.	5140700	485600	41-I/6	16/06/88
SPA-88-27A	Elsie Mt. Fm.	metavolc.	5144000	485600	"	"
SPA-88-27B	Elsie Mt. Fm.	metavolc.	5144000	485600	"	"
SPA-88-28	Elsie Mt. Fm.	metavolc.	5143000	488625	"	"
SPA-88-29	Elsie Mt. Fm.	metavolc.	5150900	495000	41-I/11	"
SPA-88-30	Copper Cliff	rhyolite	5146300	493875	41-I/6	"
SPA-88-31	Drury Twp.	metagabbro	5141150	464100	"	"
SPA-88-32	Drury Twp.	metagabbro	5141150	464200	"	"
SPA-88-33	Copper Cliff	rhyolite	5139000	474125	"	17/06/88

		Description	Location (NTS)			Date
Number	Unit	(Field designation)	N	E	Map	Sampled
SPA-88-34	Elsie Mt. Fm.	metavolc.	5141750	473825	"	"
SPA-88-35	Salmay L.	metavolc.	5121800	416100	41-J/1	19/06/88
SPA-88-36	May Twp.	metagabbro	5121900	416100	"	"
SPA-88-37	May Twp.	metagabbro	5122005	416100	"	"
SPA-88-38	May Twp.	metagabbro	5122040	416100	"	"
SPA-88-39	Tennyson Twp.	metagabbro	5133150	408225	41-J/8	21/06/88
SPA-88-40	Tennyson Twp.	metagabbro	5133300	408225	"	"
SPA-88-41	Dinny L. Algoman	granite	5154010	411375	41-J/9	"
SPA-88-42	EBL	trans. phase	5141875	408975	41-J/8	"
SPA-88-43	EBL	gabb. (EBL-2)	5142400	407000	"	"
SPA-88-44	EBL	metagabbro	5142800	407600	"	"
SPA-88-45	EBL	metagabbro	5142500	407600	"	"
SPA-88-46	EBL	metagabbro	5140650	408100	"	"
SPA-88-47A	EBL	EBL-3 fract.	5141150	406375	"	23/06/88
SPA-88-47B	EBL	EBL-3 fract.	5141150	406375	"	"
SPA-88-47C	EBL	EBL-3 fract.	5141150	406375	"	"
SPA-88-47D	EBL	EBL-3 fract.	5141150	406375	"	"
SPA-88-48	EBL	EBL-1	5142300	406350	"	"
SPA-88-49	EBL	EBL-4	5142100	406800	"	"
SPA-88-50	EBL	metagabbro	5142460	406910	"	"
SPA-88-51A	May Twp.	meta-argillite	5120900	412125	41-J/1	"
SPA-88-51B	May Twp.	metagabbro	5120900	412125	"	"
SPA-88-51C	May Twp.	meta-argillite	5120900	412125	"	"
SPA-88-52	May Twp.	metagabbro	5121050	410900	"	"
SPA-88-53	May Twp.	metagabbro	5121000	410675	"	"
SPA-88-54	Drury Twp.	metagabbro	5142100	464200	41-I/6	24/06/88
SPA-88-55	Drury Twp.	metagabbro	5141950	464175	"	"
SPA-88-56A	Drury Twp.	metagabbro	5141600	464000	"	"
SPA-88-56B	Dyke	gabbro, cuts A	5141600	464000	"	"
SPA-89-01	Levack Gneiss	fels migmatite	5163000	466475	41-I/11	28/05/89
SPA-89-02	"	granulite	5163450	465750	"	"
SPA-89-03	"	granulite	5162063	463963	"	"
SPA-89-04	"	mafic gneiss	5161050	462125	"	"
SPA-89-05	Tennyson Twp.	metagabbro	5133025	408125	41-J/8	29/05/89
SPA-89-06	EBL	metagabbro	5142463	409325	"	"
SPA-89-07A	Falconbridge	metagabbro	5162275	517700	41-I/10	30/05/89
SPA-89-07B	"	"	5162275	517700	"	"
SPA-89-07C	"	"	5162250	517650	"	"

Number	Unit	Description (Field designation)	Location (NTS) N	E	Map	Date Sampled
SPA-89-08A	"	"	5162135	517730	"	"
SPA-89-08B	"	"	5162150	517750	"	"
SPA-89-09	"	"	5161925	519025	"	"
SPA-89-10	"	"	5161875	518950	"	"
SPA-89-11	"	"	5161825	518850	"	"
SPA-89-12A	St. Charles	"	5134250	544300	41-I/8	"
SPA-89-12B	"	"	5134250	544300	"	"
SPA-89-13	"	"	5134250	544225	"	"
SPA-89-14	"	"	5134250	544175	"	"
SPA-89-15	"	"	5133500	545300	"	"
SPA-89-16	"	"	5133400	545300	"	"
SPA-89-17A	Parisien L.	f.g. syenite	5140200	408000	41-J/8	29/05/89
SPA-89-17B	BLB?	2-mica granite	5123125	412150	"	"
SPA-89-18	St. Charles	metagabbro	5131600	549900	41-I/8	01/06/89
SPA-89-19	"	"	5131575	549850	"	"
SPA-89-20A	"	gabbroic gnss	5131575	549850	"	"
SPA-89-20B	"	felsic gneiss	5131575	549850	"	"
SPA-89-21	"	metagabbro	5131575	549850	"	"
SPA-89-22	Mercer Twp.	diorite gneiss	5113100	556850	41-I/1	"
SPA-89-23	Grenville	granitic gnss	5113100	556950	"	"
SPA-89-24	Mercer Twp.	ga. alt zone	5113100	556850	"	"
SPA-89-25	"	gabbroic gnss	5112650	555925	41-I/1	02/06/89
SPA-89-26	"	"	5113030	556625	"	"
SPA-89-27	"	"	5114250	558785	"	"
SPA-89-28	Wanapitei	"	5146900	516680	41-I/7	03/06/89
SPA-89-29	"	"	5146625	516700	"	"
SPA-89-30A	"	"	5146500	516750	"	"
SPA-89-30B	"	ga seds?	5146500	516750	"	"
SPA-89-31	"	metagabbro	5144765	515250	"	"
SPA-89-32	"	"	5144925	515230	"	"
SPA-89-33	"	gabbroic gnss	5145050	514875	"	"
SPA-89-34	"	metagabbro	5145900	514925	"	04/06/89
SPA-89-35	"	"	5145800	515050	"	"
SPA-89-36	"	"	5145850	514750	"	"
SPA-89-37	"	"	5145825	514650	"	"
SPA-89-38	"	"	5145800	514525	"	"
SPA-89-39	Post-Algom?	granite	5145165	515150	"	"

Appendix 2. Geochemical Data

Contents:

2.1 Major and trace element data
2.2 Standards and replicate data
2.3 CIPW normative mineralogy

See Appendix 1 for details on analytical procedures.
In 2.1 data tables, **n.d.**="not detected"
Blank spaces are left for elements not analysed for.

In 2.2, GSC B-1 is a GSC Benchmark standard from the Univ. of Alberta labs, and the other numbered standards are GSC in-house standards used to monitor the analyses.

In 2.3 normative mineral abbreviations are as follows:
Q=quartz
C=corundum
Z=zircon
Or=orthoclase
Ab=albite
An=anorthite
Plag=plagioclase
An#=An content
Ne=nepheline
Di=diopside
Hy=hypersthene
Ol=olivine
Mt=magnetite
Cm=chrome
Hm=hematite
Il=ilmenite
Ru=rutile
Ap=apatite
Cc=calcite

where plagioclase was calculated based on An+Ab, and the An content of the normative plagioclase calculated based on An/(An+Ab).

Appendix 2. Geochemical Data

Contents:

2.1 Major and trace element data
2.2 Standards and replicate data
2.3 CIPW normative mineralogy

See Appendix 1 for details on analytical procedures.
In 2.1 data tables, **n.d.**="not detected"
Blank spaces are left for elements not analysed for.

In 2.2, GSC B-1 is a GSC Benchmark standard from the Univ. of Alberta labs, and the other numbered standards are GSC in-house standards used to monitor the analyses.

In 2.3 normative mineral abbreviations are as follows:

Q=quartz
C=corundum
Z=zircon
Or=orthoclase
Ab=albite
An=anorthite
Plag=plagioclase
An#=An content
Ne=nepheline
Di=diopside
Hy=hypersthene
Ol=olivine
Mt=magnetite
Cm=chrome
Hm=hematite
Il=ilmenite
Ru=rutile
Ap=apatite
Cc=calcite

where plagioclase was calculated based on An+Ab, and the An content of the normative plagioclase calculated based on An/(An+Ab).

2.1 Major and Trace element Data

Unit	Sample no.	SiO_2	TiO_2	Al_2O_3	Cr_2O_3	Fe_2O_3T	Fe_2O_3	FeO
EBL	EBL-1-182	43.9	0.28	13.3	n.d.	15.2		
EBL	EBL-4-133	44.9	0.24	11.5	n.d.	15.3		
EBL	EBL-4-140	43.7	0.26	8.5	n.d.	19.1		
EBL	SPA-88-19	48.7	0.43	20.9	0.0	9.4	1.6	7.0
EBL	SPA-88-20	50.3	0.34	22.3	0.0	7.3	1.3	5.4
EBL	SPA-88-21	48.4	0.28	21.6	0.0	8.1	1.4	6.0
EBL	SPA-88-22	47.4	0.25	20.3	0.0	9.0	1.4	6.8
EBL	SPA-88-42	66.8	0.15	17.5	0.0	2.5	1.3	1.1
EBL	SPA-88-43	51.3	0.59	19.4	0.0	8.1	1.8	5.7
EBL	SPA-88-45	47.7	0.26	19.1	0.0	9.4	1.6	7.0
EBL	SPA-88-46	46.1	0.10	19.7	0.0	8.8	1.6	6.5
EBL	SPA-88-48	51.5	0.50	16.5	0.0	10.6	1.5	8.2
EBL	SPA-88-49	52.0	0.50	14.4	0.1	10.9	2.3	7.8
SKPR-DUNLOP	SPA-88-03	52.1	0.16	20.2	0.0	5.8	0.9	4.4
SKPR-DUNLOP	SPA-88-04	51.4	0.23	19.6	0.0	6.8	1.6	4.7
SKPR-DUNLOP	SPA-88-05	46.2	0.24	20.9	0.0	8.6	1.4	6.4
SKPR-DUNLOP	SPA-88-07	52.2	0.68	18.0	0.0	10.2	2.5	6.9
SKPR-DUNLOP	SPA-88-09	49.6	0.18	21.0	0.1	6.9	1.3	5.1
SKPR-DUNLOP	SPA-88-10	50.6	0.29	22.6	0.0	5.8	1.4	4.0
SKPR-DUNLOP	SPA-88-11	50.6	1.17	14.6	0.0	14.5	3.7	9.7
SKPR-DUNLOP	SPA-88-12	46.9	0.13	18.8	0.1	9.9	1.8	7.3
SKPR-DUNLOP	SPA-88-13	46.3	0.14	22.3	0.0	7.7	1.7	5.4
SKPR-DUNLOP	SPA-88-14	60.7	0.29	8.1	0.0	9.5	2.4	6.4
DRURY TWP	SPA-88-31	51.0	0.20	22.0	0.0	5.7	1.6	3.7
DRURY TWP	SPA-88-32	51.0	0.29	20.6	0.0	8.0	2.1	5.3
DRURY TWP	SPA-88-54	50.9	0.21	21.1	0.0	6.9	2.4	4.0
DRURY TWP	SPA-88-55	46.8	0.16	25.1	0.0	5.5	1.6	3.5
DRURY TWP	SPA-88-56A	50.7	0.21	20.9	0.0	6.0	1.8	3.8
FALCONBRIDGE	SPA-89-07A	50.4	0.18	22.7		5.7		
FALCONBRIDGE	SPA-89-07B	51.4	0.37	15.2		10.0		
FALCONBRIDGE	SPA-89-07C	49.5	0.21	21.1		7.3		
FALCONBRIDGE	SPA-89-08A	50.3	0.45	21.1		7.2		
FALCONBRIDGE	SPA-89-08B	50.9	0.37	15.7		8.7		
FALCONBRIDGE	SPA-89-09	49.9	0.29	16.3		10.8		
FALCONBRIDGE	SPA-89-10	49.9	0.32	15.0		10.9		
FALCONBRIDGE	SPA-89-11	50.4	0.23	18.6		8.0		
TENNYSON	SPA-89-05	49.1	0.70	14.9		14.2		
TENNYSON	SPA-88-24	50.3	1.03	15.0	0.0	12.9	2.6	9.3
TENNYSON	SPA-88-39	51.0	0.79	17.8	0.0	11.3	2.8	7.7
TENNYSON	SPA-88-40	50.0	0.44	15.2	0.0	12.1	2.0	9.1
TENNYSON	SPA-89-05	49.1	0.70	14.9	n.d.	14.2		
MAY TWP	SPA-88-36	51.7	0.73	14.6	0.0	11.0	2.5	7.7

Unit	Sample no.	SiO_2	TiO_2	Al_2O_3	Cr_2O_3	Fe_2O_3T	Fe_2O_3	FeO
MAY TWP	SPA-88-37	50.0	1.27	13.7	0.0	16.7	5.4	10.2
MAY TWP	SPA-88-38	49.1	1.21	12.8	0.0	17.7	6.1	10.4
MAY TWP	SPA-88-52	50.0	1.22	13.9	0.0	17.4	6.1	10.2
MAY TWP.	SPA-88-16	49.1	1.09	13.9	0.0	14.5	4.0	9.4
VOLC (CC)	SPA-88-30	78.6	0.15	11.5	0.0	1.2	0.3	0.8
VOLC (ELSIE)	SPA-88-27A	49.5	1.26	16.0	0.0	13.7	2.6	10.0
VOLC (ELSIE)	SPA-88-27B	49.8	1.33	14.3	0.0	14.5	2.9	10.4
VOLC (ELSIE)	SPA-88-28	53.8	1.30	13.2	0.0	14.5	3.1	10.2
VOLC (ELSIE)	SPA-88-29	47.6	1.38	14.7	0.0	16.4	3.0	12.0
VOLC (ELSIE)	SPA-88-34	46.6	1.70	13.3	0.0	18.0	3.8	12.8
VOLC (SALMAY)	SPA-88-25	52.0	0.50	8.5	0.3	10.8	1.9	8.0
VOLC (SALMAY)	SPA-88-35	50.7	1.42	13.2	0.0	17.8	6.0	10.6
VOLC (STOBIE)	SPA-88-26	52.6	1.36	13.9	0.0	15.0	2.9	10.9
ST. CHARLES	SPA-89-12B	51.3	0.71	24.3		5.6		
ST. CHARLES	SPA-89-13	51.2	0.70	23.8		5.7		
ST. CHARLES	SPA-89-14	51.5	0.66	24.6		5.3		
ST. CHARLES	SPA-89-15	51.7	0.48	26.1		3.5		
ST. CHARLES	SPA-89-16	52.1	0.47	26.4		3.4		
ST. CHARLES	SPA-89-18	51.9	0.61	25.5		4.0		
ST. CHARLES	SPA-89-19	52.3	0.58	25.6		3.9		
ST. CHARLES	SPA-89-20A	52.4	0.68	25.8		3.4		
ST. CHARLES	SPA-89-20B	52.4	0.61	26.1		3.4		
ST. CHARLES	SPA-89-21	51.7	0.72	24.7		4.8		
MERCER	SPA-89-22	50.1	0.93	22.6		7.0		
MERCER	SPA-89-25	51.4	0.43	23.8		4.9		
MERCER	SPA-89-26	51.7	0.76	23.9		5.7		
MERCER	SPA-89-27	53.0	0.45	24.5		3.6		
WANAPITEI	SPA-89-28	58.4	0.85	15.4		8.3		
WANAPITEI	SPA-89-29	51.7	1.55	14.6		13.5		
WANAPITEI	SPA-89-30A	51.2	1.76	14.2		13.7		
WANAPITEI	SPA-89-31	51.8	0.57	16.9		7.8		
WANAPITEI	SPA-89-32	46.5	0.29	13.7		11.2		
WANAPITEI	SPA-89-33	52.8	1.22	14.9		12.2		
WANAPITEI	SPA-89-34	53.0	1.20	16.5		10.3		
WANAPITEI	SPA-89-35	46.0	1.22	15.8		15.8		
WANAPITEI	SPA-89-36	50.5	1.92	17.2		13.9		
WANAPITEI	SPA-89-37	50.6	0.99	16.2		10.6		
WANAPITEI	SPA-89-38	49.3	1.22	15.4		12.2		
GRANITE	SPA-89-39	77.0	0.15	12.1		1.1		
GRANITE	SPA-88-17	73.5	0.16	14.3	0.0	1.5	0.5	0.9
GRANITE	SPA-88-18	68.4	0.36	14.9	0.0	2.5	0.8	1.5
GRANITE (BLB)	SPA-88-01	75.5	0.08	13.5	0.0	0.6	0.4	0.2
GRANITE (BLB)	SPA-88-06	77.4	0.05	13.2	0.0	0.7	0.0	0.6

Unit	Sample no.	SiO_2	TiO_2	Al_2O_3	Cr_2O_3	Fe_2O_3T	Fe_2O_3	FeO
GRANITE (BLB)	SPA-88-15	74.5	0.11	14.2	0.0	1.2	0.4	0.7
GRANITE (DL)	SPA-88-41	74.8	0.18	14.2	0.0	1.4	0.5	0.8
PAR.L. SY	SPA-88-23	59.5	0.68	16.5	0.0	5.2	2.9	2.1
GNEISS	SPA-89-23	72.1	0.30	12.9		3.5		
LEVACK	SPA-89-03	66.3	0.51	16.7		3.1		
LEVACK	SPA-89-04	62.6	0.50	15.6		4.2		
LEVACK	SPA-89-01	70.0	0.32	15.5		2.4		
LEVACK	SPA-89-02	59.3	0.75	17.0		5.9		
LEVACK	SPA-89-02B	60.6	0.78	17.4		5.6		

						VOLATILES		
Unit	Sample No.	MnO	MgO	CaO	Na_2O	K_2O	H_2OT	CO_2T
EBL	EBL-1-182	0.19	16.09	7.17	1.3	0.28	3.3	0.1
EBL	EBL-4-133	0.16	15.98	7.29	0.8	0.25	4.6	0.0
EBL	EBL-4-140	0.24	20.60	4.57	0.8	0.21	3.3	0.1
EBL	SPA-88-19	0.13	5.82	11.52	2.1	0.32	2.1	0.0
EBL	SPA-88-20	0.11	4.61	11.84	2.6	0.34	1.5	0.0
EBL	SPA-88-21	0.11	7.47	11.41	2.1	0.27	1.1	0.0
EBL	SPA-88-22	0.13	8.35	10.92	1.8	0.39	2.9	0.0
EBL	SPA-88-42	0.04	1.44	5.00	4.7	0.67	1.1	0.1
EBL	SPA-88-43	0.14	5.35	11.72	2.5	0.43	1.5	0.0
EBL	SPA-88-45	0.13	9.18	9.62	2.1	0.55	3.4	0.1
EBL	SPA-88-46	0.10	9.90	11.00	1.4	0.36	3.8	0.0
EBL	SPA-88-48	0.20	6.80	11.20	2.1	0.49	1.7	0.0
EBL	SPA-88-49	0.20	7.60	11.70	2.0	0.45	1.6	0.0
SKPR-DUNLOP	SPA-88-03	0.11	6.24	11.02	2.9	0.34	1.7	0.0
SKPR-DUNLOP	SPA-88-04	0.12	6.17	11.24	2.4	0.57	2.1	0.0
SKPR-DUNLOP	SPA-88-05	0.13	8.87	10.26	2.1	0.26	3.3	0.0
SKPR-DUNLOP	SPA-88-07	0.19	4.47	8.27	4.4	0.66	1.6	0.1
SKPR-DUNLOP	SPA-88-09	0.11	6.40	11.89	2.2	0.40	1.9	0.0
SKPR-DUNLOP	SPA-88-10	0.09	4.54	12.14	2.5	0.43	1.6	0.0
SKPR-DUNLOP	SPA-88-11	0.21	6.03	10.10	1.7	0.92	1.8	0.0
SKPR-DUNLOP	SPA-88-12	0.17	10.71	8.40	2.5	0.23	3.6	0.0
SKPR-DUNLOP	SPA-88-13	0.12	7.79	9.99	2.5	0.59	3.2	0.0
SKPR-DUNLOP	SPA-88-14	0.17	9.97	9.59	0.6	0.06	2.1	0.0
DRURY TWP	SPA-88-31	0.10	4.60	11.40	3.0		2.1	0.0
DRURY TWP	SPA-88-32	0.13	4.50	10.83	3.2	0.40	2.1	0.1
DRURY TWP	SPA-88-54	0.09	4.79	9.01	3.8	1.02	2.7	0.1
DRURY TWP	SPA-88-55	0.08	4.52	11.60	2.4	1.30	2.9	0.0
DRURY TWP	SPA-88-56A	0.11	5.21	11.41	3.2	0.64	2.4	0.0
FALCONBRIDGE	SPA-89-07A	0.09	4.79	12.02	2.6	0.56	1.1	0.0
FALCONBRIDGE	SPA-89-07B	0.17	7.86	11.39	2.1	0.71	1.6	0.1
FALCONBRIDGE	SPA-89-07C	0.11	6.02	11.00	2.6	0.75	2.3	0.1
FALCONBRIDGE	SPA-89-08A	0.12	4.52	11.59	2.6	0.60	1.8	0.0
FALCONBRIDGE	SPA-89-08B	0.15	8.33	12.80	1.9	0.40	1.7	0.0
FALCONBRIDGE	SPA-89-09	0.19	8.01	10.22	2.3	0.43	2.6	0.0
FALCONBRIDGE	SPA-89-10	0.19	7.82	11.35	2.0	0.52	2.5	0.0
FALCONBRIDGE	SPA-89-11	0.14	6.34	10.98	2.7	1.07	2.3	0.0
TENNYSON	SPA-89-05	0.21	7.34	9.40	2.8	0.60	1.9	0.0
TENNYSON	SPA-88-24	0.20	6.90	10.21	2.9	0.31	1.5	0.0
TENNYSON	SPA-88-39	0.16	4.61	10.17	3.6	0.41	1.3	0.0
TENNYSON	SPA-88-40	0.20	7.97	9.97	2.5	0.39	2.0	0.0
TENNYSON	SPA-89-05	0.21	7.34	9.40	2.8	0.60	1.9	0.0
MAY TWP	SPA-88-36	0.17	7.20	10.27	1.9	0.75	2.6	0.1
MAY TWP	SPA-88-37	0.23	4.62	7.77	3.2	1.28	2.3	0.2

Unit	Sample No.	MnO	MgO	CaO	Na_2O	K_2O	H_2OT	CO_2T
MAY TWP	SPA-88-38	0.25	5.81	8.59	2.5	1.37	2.4	0.1
MAY TWP	SPA-88-52	0.19	4.44	6.64	3.9	0.88	2.4	0.1
MAY TWP.	SPA-88-16	0.24	6.53	11.04	2.3	0.36	2.4	0.0
VOLC (CC)	SPA-88-30	0.02	0.14	0.20	2.3	6.03	0.3	0.0
VOLC (ELSIE)	SPA-88-27A	0.21	5.39	10.34	2.2	0.64	1.8	0.1
VOLC (ELSIE)	SPA-88-27B	0.22	6.40	10.64	2.4	0.60	1.4	0.0
VOLC (ELSIE)	SPA-88-28	0.23	5.14	9.53	2.1	0.61	1.4	0.0
VOLC (ELSIE)	SPA-88-29	0.25	6.60	11.74	1.4	0.19	1.5	0.0
VOLC (ELSIE)	SPA-88-34	0.26	6.06	10.59	1.8	0.31	1.9	0.6
VOLC (SALMAY)	SPA-88-25	0.20	14.77	9.48	1.2	0.37	3.2	0.0
VOLC (SALMAY)	SPA-88-35	0.22	4.21	7.44	2.9	1.33	2.3	0.3
VOLC (STOBIE)	SPA-88-26	0.21	4.60	7.97	2.4	1.41	1.8	0.2
ST. CHARLES	SPA-89-12B	0.07	2.49	10.21	3.9	0.75	0.7	0.0
ST. CHARLES	SPA-89-13	0.06	2.74	10.06	4.0	0.71	1.0	0.1
ST. CHARLES	SPA-89-14	0.06	2.47	10.40	4.0	0.64	0.7	0.1
ST. CHARLES	SPA-89-15	0.04	1.79	10.58	4.4	0.44	0.6	0.1
ST. CHARLES	SPA-89-16	0.04	1.54	10.91	4.5	0.52	0.6	0.0
ST. CHARLES	SPA-89-18	0.05	2.06	10.42	4.3	0.53	0.6	0.0
ST. CHARLES	SPA-89-19	0.05	1.72	10.52	4.4	0.63	0.5	0.0
ST. CHARLES	SPA-89-20A	0.04	1.21	10.51	4.6	0.86	0.8	0.0
ST. CHARLES	SPA-89-20B	0.04	1.34	10.28	4.5	0.78	0.7	0.0
ST. CHARLES	SPA-89-21	0.06	2.39	10.42	4.2	0.61	0.5	0.1
MERCER	SPA-89-22	0.08	3.82	9.63	4.3	0.90	1.0	0.0
MERCER	SPA-89-25	0.05	3.00	9.27	4.3	1.64	1.3	0.0
MERCER	SPA-89-26	0.08	2.93	9.85	4.2	0.86	0.8	0.0
MERCER	SPA-89-27	0.06	1.07	8.86	4.8	1.71	0.8	0.0
WANAPITEI	SPA-89-28	0.11	4.68	4.71	2.2	3.04	1.6	0.2
WANAPITEI	SPA-89-29	0.21	5.24	8.65	2.6	1.15	1.4	0.2
WANAPITEI	SPA-89-30A	0.23	5.17	9.02	3.4	1.00	1.2	0.3
WANAPITEI	SPA-89-31	0.11	7.60	10.27	2.7	0.81	1.3	0.0
WANAPITEI	SPA-89-32	0.15	17.84	7.85	1.6	0.38	0.9	0.4
WANAPITEI	SPA-89-33	0.16	5.57	8.61	3.1	1.22	0.6	0.1
WANAPITEI	SPA-89-34	0.13	3.76	6.16	4.2	2.48	1.4	0.1
WANAPITEI	SPA-89-35	0.17	6.65	11.59	2.0	0.64	0.8	0.1
WANAPITEI	SPA-89-36	0.22	3.60	6.39	3.5	1.45	0.9	0.1
WANAPITEI	SPA-89-37	0.15	7.56	10.14	2.7	0.76	0.8	0.1
WANAPITEI	SPA-89-38	0.17	7.22	9.86	2.8	0.86	1.0	0.1
GRANITE	SPA-89-39	0.01	0.28	0.48	2.7	5.72	0.5	0.2
GRANITE	SPA-88-17	0.04	0.65	1.48	4.5	2.93	0.7	0.1
GRANITE	SPA-88-18	0.03	1.26	1.33	3.6	6.04	1.1	0.2
GRANITE (BLB)	SPA-88-01	0.01	0.21	0.56	3.9	5.32	0.3	0.0
GRANITE (BLB)	SPA-88-06	0.01	0.22	0.31	5.0	3.31	0.3	0.0
GRANITE (BLB)	SPA-88-15	0.03	0.34	1.04	4.6	3.70	0.4	0.0

Unit	Sample No.	MnO	MgO	CaO	Na_2O	K_2O	H_2OT	CO_2T
GRANITE (DL)	SPA-88-41	0.01	0.68	0.28	6.8	1.16	0.5	0.0
PAR.L. SY	SPA-88-23	0.10	1.90	3.20	5.0	5.92	0.6	0.6
GNEISS	SPA-89-23	0.03	0.23	0.89	2.9	5.57	0.3	0.0
LEVACK	SPA-89-03	0.03	1.41	4.02	5.2	0.93	1.3	0.0
LEVACK	SPA-89-04	0.05	4.18	5.27	4.5	1.21	1.5	0.0
LEVACK	SPA-89-01	0.03	0.89	3.14	5.0	1.36	0.7	0.1
LEVACK	SPA-89-02	0.07	3.28	5.40	4.8	1.58	0.9	0.0
LEVACK	SPA-89-02B	0.07	3.01	5.43	4.9	1.37	0.9	0.0

				TRACE ELEMENTS				
Unit	Sample No.	P_2O_5	S	Ba	Be	Co	Cr	Cu
EBL	EBL-1-182	0.06	0.01	148	0.4	100	97	55
EBL	EBL-4-133	0.04	0.06	94	0.4	99	230	68
EBL	EBL-4-140	0.04	0.02	68	0.4	130	150	58
EBL	SPA-88-19	0.06	0.02	164	0.5	48	27	72
EBL	SPA-88-20	0.05	0.01	166	0.5	36	87	81
EBL	SPA-88-21	0.04	0.00	137	0.4	53	96	51
EBL	SPA-88-22	0.04	0.00	150	0.4	59	95	45
EBL	SPA-88-42	0.04	0.01	397	1.3	9	22	30
EBL	SPA-88-43	0.07	0.00	206	0.6	36	130	89
EBL	SPA-88-45	0.03	0.00	153	0.3	58	99	67
EBL	SPA-88-46	0.02	0.00	110	0.2	65	85	41
EBL	SPA-88-48	0.06	0.01	190	0.5	47	190	79
EBL	SPA-88-49	0.07	0.00	182	0.6	49	430	69
SKPR-DUNLOP	SPA-88-03	0.02	0.02	132	0.5	34	220	290
SKPR-DUNLOP	SPA-88-04	0.03	0.00	186	0.4	38	230	20
SKPR-DUNLOP	SPA-88-05	0.03	0.00	140	0.3	56	110	29
SKPR-DUNLOP	SPA-88-07	0.06	0.00	417	0.5	40	14	86
SKPR-DUNLOP	SPA-88-09	0.02	0.00	109	0.3	36	360	26
SKPR-DUNLOP	SPA-88-10	0.04	0.00	178	0.4	26	220	51
SKPR-DUNLOP	SPA-88-11	0.13	0.02	198	0.9	47	110	110
SKPR-DUNLOP	SPA-88-12	0.01	0.00	192	0.6	71	320	56
SKPR-DUNLOP	SPA-88-13	0.02	0.00	376	0.4	52	77	31
SKPR-DUNLOP	SPA-88-14	0.02	0.04	52	0.9	59	160	280
DRURY TWP	SPA-88-31	0.02	0.01	214	0.4	28	81	94
DRURY TWP	SPA-88-32	0.04	0.00	129	0.6	35	54	62
DRURY TWP	SPA-88-54	0.02	0.00	392	0.4	17	110	32
DRURY TWP	SPA-88-55	0.01	0.00	475	0.3	29	77	14
DRURY TWP	SPA-88-56A	0.01	0.00	241	0.3	28	81	18
FALCONBRIDGE	SPA-89-07A	0.0	0.0	144.0	0.4	28.0	120.0	27.0
FALCONBRIDGE	SPA-89-07B	0.1	0.0	231.0	0.5	47.0	190.0	93.0
FALCONBRIDGE	SPA-89-07C	0.0	0.0	194.0	0.4	34.0	170.0	100.0
FALCONBRIDGE	SPA-89-08A	0.1	0.0	117.0	0.5	32.0	91.0	59.0
FALCONBRIDGE	SPA-89-08B	0.0	0.0	86.0	0.4	43.0	470.0	40.0
FALCONBRIDGE	SPA-89-09	0.0	0.0	144.0	0.4	49.0	270.0	150.0
FALCONBRIDGE	SPA-89-10	0.0	0.0	149.0	0.4	50.0	89.0	140.0
FALCONBRIDGE	SPA-89-11	0.0	0.0	321.0	0.4	37.0	120.0	46.0
TENNYSON	SPA-89-05	0.1	0.0	208.0	0.8	62.0	100.0	84.0
TENNYSON	SPA-88-24	0.11	0.07	151	0.7	49	230	100
TENNYSON	SPA-88-39	0.10	0.01	170	0.8	45	39	120
TENNYSON	SPA-88-40	0.05	0.00	177	0.5	60	120	42
TENNYSON	SPA-89-05	0.10	0.01	208	0.8	62	100	84
MAY TWP	SPA-88-36	0.07	0.03	239	0.7	49	110	100
MAY TWP	SPA-88-37	0.10	0.05	440	0.9	64	17	360

						TRACE ELEMENTS		
Unit	Sample No.	P_2O_5	S	Ba	Be	Co	Cr	Cu
MAY TWP	SPA-88-38	0.09	0.02	386	0.9	69	14	190
MAY TWP	SPA-88-52	0.10	0.08	333	0.9	60	10	690
MAY TWP.	SPA-88-16	0.10	0.15	175	0.8	52	130	190
VOLC (CC)	SPA-88-30	0.02	0.00	848	4.5	2	4	20
VOLC (ELSIE)	SPA-88-27A	0.13	0.04	197	0.8	41	92	140
VOLC (ELSIE)	SPA-88-27B	0.16	0.04	218	1.2	44	97	160
VOLC (ELSIE)	SPA-88-28	0.15	0.02	148	1.2	44	75	130
VOLC (ELSIE)	SPA-88-29	0.15	0.01	99	0.9	57	130	150
VOLC (ELSIE)	SPA-88-34	0.26	0.17	126	1.3	63	120	250
VOLC (SALMAY)	SPA-88-25	0.04	0.02	111	0.5	62	1300	69
VOLC (SALMAY)	SPA-88-35	0.12	0.06	379	1.0	61	19	310
VOLC (STOBIE)	SPA-88-26	0.18	0.06	366	1.5	42	48	120
ST. CHARLES	SPA-89-12B	0.1	0.0	408.0	0.6	23.0	50.0	10.0
ST. CHARLES	SPA-89-13	0.1	0.0	290.0	0.7	24.0	53.0	9.0
ST. CHARLES	SPA-89-14	0.1	0.0	326.0	0.6	23.0	39.0	13.0
ST. CHARLES	SPA-89-15	0.1	0.0	346.0	0.5	17.0	20.0	13.0
ST. CHARLES	SPA-89-16	0.1	0.0	354.0	0.5	16.0	20.0	13.0
ST. CHARLES	SPA-89-18	0.2	0.0	353.0	0.6	19.0	19.0	12.0
ST. CHARLES	SPA-89-19	0.2	0.0	389.0	0.6	17.0	21.0	11.0
ST. CHARLES	SPA-89-20A	0.1	0.0	357.0	0.6	14.0	17.0	16.0
ST. CHARLES	SPA-89-20B	0.1	0.0	319.0	0.6	14.0	20.0	6.0
ST. CHARLES	SPA-89-21	0.1	0.0	343.0	0.6	22.0	27.0	16.0
MERCER	SPA-89-22	0.2	0.1	358.0	0.9	32.0	72.0	23.0
MERCER	SPA-89-25	0.1	0.0	525.0	0.8	25.0	26.0	5.0
MERCER	SPA-89-26	0.2	0.0	286.0	0.8	26.0	27.0	18.0
MERCER	SPA-89-27	0.1	0.0	515.0	1.4	12.0	41.0	4.0
WANAPITEI	SPA-89-28	0.2	0.7	1143.0	2.2	33.0	100.0	95.0
WANAPITEI	SPA-89-29	0.3	0.1	622.0	1.6	45.0	29.0	43.0
WANAPITEI	SPA-89-30A	0.3	0.1	484.0	1.5	44.0	21.0	30.0
WANAPITEI	SPA-89-31	0.1	0.2	285.0	0.9	39.0	360.0	64.0
WANAPITEI	SPA-89-32	0.1	0.1	225.0	0.5	71.0	130.0	34.0
WANAPITEI	SPA-89-33	0.3	0.2	523.0	1.5	46.0	93.0	52.0
WANAPITEI	SPA-89-34	0.6	0.2	1487.0	1.7	31.0	23.0	34.0
WANAPITEI	SPA-89-35	0.2	0.3	296.0	0.9	55.0	9.0	35.0
WANAPITEI	SPA-89-36	1.1	0.0	685.0	2.0	25.0	26.0	14.0
WANAPITEI	SPA-89-37	0.2	0.1	307.0	0.9	44.0	220.0	59.0
WANAPITEI	SPA-89-38	0.3	0.1	493.0	1.2	44.0	130.0	56.0
GRANITE	SPA-89-39	0.0	0.0	190.0	2.0	4.0	6.0	2.0
GRANITE	SPA-88-17	0.04	0.00	668	1.6	5	9	18
GRANITE	SPA-88-18	0.19	0.02	1700	3.9	8	14	1
GRANITE (BLB)	SPA-88-01	0.01	0.00	553	2.3	3	5	3
GRANITE (BLB)	SPA-88-06	0.01	0.00	139	4.2	2	5	6

				TRACE ELEMENTS				
Unit	Sample No.	P_2O_5	S	Ba	Be	Co	Cr	Cu
GRANITE (BLB)	SPA-88-15	0.02	0.00	414	2.1	0	5	0
GRANITE (DL)	SPA-88-41	0.06	0.00	266	2.1	2	7	0
PAR.L. SY	SPA-88-23	0.39	0.15	1117	7.6	17	22	94
GNEISS	SPA-89-23	0.1	0.0	1018.0	2.7	6.0	9.0	3.0
LEVACK	SPA-89-03	0.1	0.0	392.0	1.2	12.0	21.0	13.0
LEVACK	SPA-89-04	0.2	0.0	371.0	1.4	12.0	150.0	1.0
LEVACK	SPA-89-01	0.1	0.0	513.0	0.8	9.0	13.0	6.0
LEVACK	SPA-89-02	0.3	0.1	1147.0	1.2	20.0	72.0	28.0
LEVACK	SPA-89-02B	0.3	0.1	964.0	1.2	20.0	49.0	21.0

Unit	Sample No.	La	Nb	Ni	Rb	Sr	V	Y
EBL	EBL-1-182	5	9	550	12	171	73	5
EBL	EBL-4-133	2	11	440	9	125	93	4
EBL	EBL-4-140	3	6	670	16	114	84	4
EBL	SPA-88-19	8	16	180	30	266	130	21
EBL	SPA-88-20	9	19	140	41	315	120	25
EBL	SPA-88-21	7	1	300	31	300	90	25
EBL	SPA-88-22	6	4	330	48	247	93	13
EBL	SPA-88-42	12	22	19	64	595	30	15
EBL	SPA-88-43	11	22	100	38	299	200	35
EBL	SPA-88-45	2	5	320	59	257	92	6
EBL	SPA-88-46	0	0	360	42	267	55	11
EBL	SPA-88-48	5	14	100	45	214	200	29
EBL	SPA-88-49	6	23	110	44	229	230	32
SKPR-DUNLOP	SPA-88-03	3	19	230	34	343	91	6
SKPR-DUNLOP	SPA-88-04	3	0	120	69	290	130	15
SKPR-DUNLOP	SPA-88-05	1	0	310	22	257	79	3
SKPR-DUNLOP	SPA-88-07	9	7	43	84	244	250	27
SKPR-DUNLOP	SPA-88-09	2	0	140	34	312	97	18
SKPR-DUNLOP	SPA-88-10	4	5	83	37	360	110	4
SKPR-DUNLOP	SPA-88-11	13	15	79	50	217	300	58
SKPR-DUNLOP	SPA-88-12	0	15	470	40	213	64	5
SKPR-DUNLOP	SPA-88-13	0	0	290	71	322	45	12
SKPR-DUNLOP	SPA-88-14	16	61	200	28	91	130	37
DRURY TWP	SPA-88-31	3	15	95	58	355	96	7
DRURY TWP	SPA-88-32	8	0	58	26	295	150	31
DRURY TWP	SPA-88-54	1	32	87	39	416	86	10
DRURY TWP	SPA-88-55	1	0	120	40	346	55	5
DRURY TWP	SPA-88-56A	0	6	56	55	288	120	16
FALCONBRIDGE	SPA-89-07A	1.0	10.0	49.0	17.0	300.0	72.0	3.0
FALCONBRIDGE	SPA-89-07B	5.0	9.0	89.0	33.0	190.0	150.0	12.0
FALCONBRIDGE	SPA-89-07C	1.0	6.0	74.0	15.0	311.0	91.0	4.0
FALCONBRIDGE	SPA-89-08A	5.0	4.0	58.0	15.0	355.0	150.0	8.0
FALCONBRIDGE	SPA-89-08B	4.0	17.0	110.0	20.0	196.0	170.0	9.0
FALCONBRIDGE	SPA-89-09	1.0	7.0	110.0	12.0	222.0	130.0	5.0
FALCONBRIDGE	SPA-89-10	1.0	11.0	76.0	19.0	248.0	160.0	7.0
FALCONBRIDGE	SPA-89-11	2.0	7.0	73.0	26.0	306.0	110.0	5.0
TENNYSON	SPA-89-05	9.0	7.0	130.0	21.0	227.0	220.0	16.0
TENNYSON	SPA-88-24	14	10	110	19	199	280	54
TENNYSON	SPA-88-39	10	16	58	28	299	250	47
TENNYSON	SPA-88-40	6	3	130	42	184	230	27
TENNYSON	SPA-89-05	9	7	130	21	227	220	16
MAY TWP	SPA-88-36	8	10	120	80	215	240	43
MAY TWP	SPA-88-37	13	16	45	49	303	630	45
MAY TWP	SPA-88-38	12	24	87	58	293	660	47

Unit	Sample No.	La	Nb	Ni	Rb	Sr	V	Y
MAY TWP	SPA-88-52	11	18	60	70	188	640	41
MAY TWP.	SPA-88-16	12	16	73	74	195	330	65
VOLC (CC)	SPA-88-30	110	30	4	247	62	1	69
VOLC (ELSIE)	SPA-88-27A	13	23	71	74	155	290	64
VOLC (ELSIE)	SPA-88-27B	14	16	77	65	160	320	65
VOLC (ELSIE)	SPA-88-28	22	19	48	48	116	330	77
VOLC (ELSIE)	SPA-88-29	11	23	74	18	129	380	56
VOLC (ELSIE)	SPA-88-34	16	21	80	29	160	420	70
VOLC (SALMAY)	SPA-88-25	11	14	280	50	90	230	24
VOLC (SALMAY)	SPA-88-35	15	6	30	52	212	610	56
VOLC (STOBIE)	SPA-88-26	26	20	49	57	158	320	77
ST. CHARLES	SPA-89-12B	7.0	0.0	28.0	9.0	874.0	62.0	7.0
ST. CHARLES	SPA-89-13	6.0	0.0	31.0	10.0	853.0	74.0	6.0
ST. CHARLES	SPA-89-14	6.0	0.0	30.0	7.0	872.0	69.0	6.0
ST. CHARLES	SPA-89-15	6.0	0.0	29.0	12.0	875.0	32.0	4.0
ST. CHARLES	SPA-89-16	6.0	0.0	24.0	7.0	889.0	26.0	4.0
ST. CHARLES	SPA-89-18	7.0	0.0	36.0	8.0	837.0	37.0	6.0
ST. CHARLES	SPA-89-19	7.0	0.0	23.0	6.0	867.0	44.0	7.0
ST. CHARLES	SPA-89-20A	6.0	0.0	15.0	23.0	823.0	50.0	6.0
ST. CHARLES	SPA-89-20B	7.0	0.0	16.0	10.0	863.0	40.0	6.0
ST. CHARLES	SPA-89-21	7.0	0.0	39.0	9.0	917.0	60.0	8.0
MERCER	SPA-89-22	10.0	3.0	69.0	11.0	722.0	70.0	11.0
MERCER	SPA-89-25	5.0	0.0	53.0	32.0	765.0	35.0	4.0
MERCER	SPA-89-26	10.0	3.0	46.0	12.0	758.0	57.0	11.0
MERCER	SPA-89-27	17.0	7.0	19.0	38.0	816.0	8.0	15.0
WANAPITEI	SPA-89-28	37.0	10.0	51.0	110.0	382.0	140.0	20.0
WANAPITEI	SPA-89-29	20.0	16.0	25.0	25.0	326.0	290.0	30.0
WANAPITEI	SPA-89-30A	22.0	19.0	21.0	19.0	406.0	310.0	26.0
WANAPITEI	SPA-89-31	9.0	2.0	77.0	20.0	508.0	120.0	11.0
WANAPITEI	SPA-89-32	5.0	6.0	330.0	11.0	380.0	63.0	4.0
WANAPITEI	SPA-89-33	28.0	10.0	55.0	40.0	458.0	220.0	24.0
WANAPITEI	SPA-89-34	62.0	0.0	14.0	56.0	917.0	180.0	25.0
WANAPITEI	SPA-89-35	12.0	5.0	13.0	16.0	619.0	520.0	15.0
WANAPITEI	SPA-89-36	82.0	28.0	14.0	42.0	584.0	210.0	63.0
WANAPITEI	SPA-89-37	14.0	7.0	100.0	19.0	388.0	200.0	18.0
WANAPITEI	SPA-89-38	19.0	8.0	68.0	20.0	436.0	220.0	22.0
GRANITE	SPA-89-39	43.0	20.0	5.0	240.0	43.0	7.0	22.0
GRANITE	SPA-88-17	14	25	3	96	193	12	38
GRANITE	SPA-88-18	110	54	7	279	386	34	58
GRANITE (BLB)	SPA-88-01	10	51	1	114	143	2	31
GRANITE (BLB)	SPA-88-06	4	63	1	163	55	0	74
GRANITE (BLB)	SPA-88-15	19	41	0	176	92	2	48
GRANITE (DL)	SPA-88-41	48	36	0	57	101	12	25

Unit	Sample No.	La	Nb	Ni	Rb	Sr	V	Y
PAR.L. SY	SPA-88-23	220	33	12	184	682	68	51
GNEISS	SPA-89-23	69.0	29.0	0.0	132.0	95.0	7.0	47.0
LEVACK	SPA-89-03	18.0	0.0	19.0	21.0	835.0	49.0	2.0
LEVACK	SPA-89-04	30.0	0.0	70.0	35.0	881.0	84.0	12.0
LEVACK	SPA-89-01	10.0	6.0	7.0	15.0	656.0	35.0	1.0
LEVACK	SPA-89-02	40.0	0.0	36.0	20.0	923.0	96.0	9.0
LEVACK	SPA-89-02B	35.0	0.0	36.0	21.0	911.0	91.0	8.0

					RARE EARTH ELEMENTS			
Unit	Sample No.	Yb	Zn	Zr	La REE	Ce REE	Nd REE	Sm REE
EBL	EBL-1-182	0.4	72	37	6.0	12.0	8.0	1.5
EBL	EBL-4-133	0.3	64	17	4.3	8.2	6.5	1.1
EBL	EBL-4-140	0.2	100	21	4.6	8.9	6.4	1.1
EBL	SPA-88-19	0.9	59	64	7.2	15.0	8.1	1.7
EBL	SPA-88-20	0.9	44	64	7.3	15.0	8.5	1.7
EBL	SPA-88-21	0.6	40	45	5.5	11.0	5.9	1.2
EBL	SPA-88-22	0.5	60	35	5.7	12.0	6.0	1.1
EBL	SPA-88-42	0.8	28	120	13.0	24.0	8.8	1.5
EBL	SPA-88-43	1.5	50	76	9.1	20.0	16.0	2.0
EBL	SPA-88-45	0.4	66	38	3.6	8.1	8.9	0.8
EBL	SPA-88-46	0.1	47	28	2.3	4.8	5.4	0.3
EBL	SPA-88-48	1.1	61	65	7.1	15.0	10.0	1.8
EBL	SPA-88-49	1.4	71	63	8.4	18.0	12.0	2.2
SKPR-DUNLOP	SPA-88-03	0.4	38	35	4.9	8.8	5.1	0.8
SKPR-DUNLOP	SPA-88-04	0.5	36	42	5.4	11.0	5.7	1.1
SKPR-DUNLOP	SPA-88-05	0.3	75	35	4.5	9.1	4.4	0.9
SKPR-DUNLOP	SPA-88-07	1.2	97	64	8.3	18.0	10.0	2.0
SKPR-DUNLOP	SPA-88-09	0.3	28	31	3.6	7.1	3.7	0.7
SKPR-DUNLOP	SPA-88-10	0.6	25	51	5.1	11.0	5.5	1.2
SKPR-DUNLOP	SPA-88-11	2.6	87	127	13.0	29.0	17.0	3.8
SKPR-DUNLOP	SPA-88-12	0.1	100	59	2.6	4.8	2.2	0.5
SKPR-DUNLOP	SPA-88-13	0.1	53	34	2.7	5.4	2.4	0.5
SKPR-DUNLOP	SPA-88-14	3.4	61	104	18.0	42.0	22.0	5.3
DRURY TWP	SPA-88-31	0.6	26	32	3.2	6.3	3.5	0.7
DRURY TWP	SPA-88-32	1.1	49	38	6.1	12.0	6.3	1.3
DRURY TWP	SPA-88-54	0.3	14	42	4.4	8.5	4.9	0.7
DRURY TWP	SPA-88-55	0.3	23	31	2.4	4.8	4.7	0.4
DRURY TWP	SPA-88-56A	0.3	23	71	1.8	3.7	4.0	0.4
FALCONBRIDGE	SPA-89-07A	0.3	33.0	5.0	3.0	5.5	4.4	0.6
FALCONBRIDGE	SPA-89-07B	1.2	55.0	66.0	6.8	14.0	8.9	1.8
FALCONBRIDGE	SPA-89-07C	0.4	41.0	8.0	3.1	5.9	3.2	0.8
FALCONBRIDGE	SPA-89-08A	0.8	31.0	28.0	6.8	13.0	7.4	1.6
FALCONBRIDGE	SPA-89-08B	0.9	39.0	23.0	6.6	10.0	5.4	1.5
FALCONBRIDGE	SPA-89-09	0.4	63.0	5.0	3.2	5.5	1.8	0.8
FALCONBRIDGE	SPA-89-10	0.7	62.0	13.0	3.4	6.7	4.8	1.2
FALCONBRIDGE	SPA-89-11	0.5	37.0	10.0	3.4	6.6	1.9	0.9
TENNYSON	SPA-89-05	1.5	100.0	72.0	11.0	22.0	14.0	2.6
TENNYSON	SPA-88-24	2.4	88	97	8.5	20.0	14.0	3.1
TENNYSON	SPA-88-39	1.9	59	99	12.0	24.0	14.0	2.7
TENNYSON	SPA-88-40	1.3	100	48	5.7	12.0	7.2	1.6
TENNYSON	SPA-89-05	0.8	26	27	11.0	22.0	14.0	2.6
MAY TWP	SPA-88-36	1.4	70	76	9.5	20.0	12.0	2.5
MAY TWP	SPA-88-37	2.1	110	103	12.0	25.0	14.0	2.9

Unit	Sample No.	Eu REE	Gd REE	Dy REE	Yb REE	Y REE
EBL	EBL-1-182	0.5	1.2	1.3	0.7	7.5
EBL	EBL-4-133	0.4	0.9	1.1	0.6	6.0
EBL	EBL-4-140	0.4	0.8	0.9	0.6	5.6
EBL	SPA-88-19	0.6	1.9	1.9	1.1	11.0
EBL	SPA-88-20	0.6	1.9	1.9	1.1	11.0
EBL	SPA-88-21	0.5	1.4	1.4	0.7	7.5
EBL	SPA-88-22	0.5	1.3	1.3	0.7	7.1
EBL	SPA-88-42	0.9	1.4	1.2	0.9	6.7
EBL	SPA-88-43	0.8	3.1	2.7	1.5	14.0
EBL	SPA-88-45	0.5	1.7	1.3	0.6	6.1
EBL	SPA-88-46	0.3	0.9	0.6	0.4	3.3
EBL	SPA-88-48	0.7	2.4	2.3	1.4	13.0
EBL	SPA-88-49	0.8	2.8	2.8	1.7	16.0
SKPR-DUNLOP	SPA-88-03	0.5	1.2	0.9	0.5	5.2
SKPR-DUNLOP	SPA-88-04	0.5	1.3	1.2	0.7	6.7
SKPR-DUNLOP	SPA-88-05	0.4	1.1	1.1	0.6	5.7
SKPR-DUNLOP	SPA-88-07	0.7	2.3	2.4	1.4	13.0
SKPR-DUNLOP	SPA-88-09	0.5	1.0	1.0	0.6	5.6
SKPR-DUNLOP	SPA-88-10	0.6	1.5	1.5	0.8	8.0
SKPR-DUNLOP	SPA-88-11	1.3	4.7	5.1	3.0	30.0
SKPR-DUNLOP	SPA-88-12	0.3	0.7	0.7	0.4	4.1
SKPR-DUNLOP	SPA-88-13	0.4	0.7	0.6	0.3	3.3
SKPR-DUNLOP	SPA-88-14	0.5	6.0	6.6	3.9	40.0
DRURY TWP	SPA-88-31	0.4	0.9	1.0	0.6	5.6
DRURY TWP	SPA-88-32	0.7	1.6	1.8	1.1	10.0
DRURY TWP	SPA-88-54	0.4	1.1	0.9	0.6	5.4
DRURY TWP	SPA-88-55	0.3	0.8	0.7	0.4	3.9
DRURY TWP	SPA-88-56A	0.4	0.9	0.8	0.5	4.6
FALCONBRIDGE	SPA-89-07A	0.4	0.7	0.8	0.4	4.5
FALCONBRIDGE	SPA-89-07B	0.6	2.2	2.4	1.5	14.0
FALCONBRIDGE	SPA-89-07C	0.4	0.9	1.0	0.6	5.5
FALCONBRIDGE	SPA-89-08A	0.6	1.7	1.8	1.0	10.0
FALCONBRIDGE	SPA-89-08B	0.5	1.7	1.9	1.2	11.0
FALCONBRIDGE	SPA-89-09	0.5	0.9	1.2	0.7	6.6
FALCONBRIDGE	SPA-89-10	0.5	1.4	1.6	1.0	9.1
FALCONBRIDGE	SPA-89-11	0.5	1.0	1.1	0.7	6.4
TENNYSON	SPA-89-05	0.9	3.1	3.1	1.3	16.0
TENNYSON	SPA-88-24	1.1	4.0	4.2	2.4	24.0
TENNYSON	SPA-88-39	1.0	3.5	3.4	2.0	19.0
TENNYSON	SPA-88-40	0.6	2.1	2.3	1.3	12.0
TENNYSON	SPA-89-05	0.9	3.1	3.1	1.3	16.0
MAY TWP	SPA-88-36	0.8	3.2	3.1	1.6	16.0
MAY TWP	SPA-88-37	1.0	3.5	3.5	2.0	19.0
MAY TWP	SPA-88-38	0.9	3.5	3.5	2.0	20.0

Unit	Sample No.	Eu REE	Gd REE	Dy REE	Yb REE	Y REE
MAY TWP	SPA-88-52	1.1	3.4	3.4	2.0	19.0
MAY TWP.	SPA-88-16	1.1	3.9	4.4	2.6	26.0
VOLC (CC)	SPA-88-30	1.5	12.0	11.0	7.8	68.0
VOLC (ELSIE)	SPA-88-27A	1.3	4.9	5.3	3.0	30.0
VOLC (ELSIE)	SPA-88-27B	1.4	5.1	5.6	3.3	33.0
VOLC (ELSIE)	SPA-88-28	1.5	6.1	6.7	3.9	39.0
VOLC (ELSIE)	SPA-88-29	1.3	4.6	5.1	3.1	29.0
VOLC (ELSIE)	SPA-88-34	1.7	6.4	6.4	3.6	36.0
VOLC (SALMAY)	SPA-88-25	0.5	2.0	2.1	1.1	11.0
VOLC (SALMAY)	SPA-88-35	1.3	4.3	4.4	2.5	25.0
VOLC (STOBIE)	SPA-88-26	1.6	6.4	6.7	3.9	39.0
ST. CHARLES	SPA-89-12B	1.3	1.9	1.6	0.7	8.4
ST. CHARLES	SPA-89-13	1.2	1.7	1.5	0.7	8.0
ST. CHARLES	SPA-89-14	1.2	1.6	1.5	0.7	7.5
ST. CHARLES	SPA-89-15	0.9	1.0	0.9	0.4	4.8
ST. CHARLES	SPA-89-16	1.0	1.2	1.1	0.5	5.6
ST. CHARLES	SPA-89-18	1.2	1.7	1.6	0.7	8.0
ST. CHARLES	SPA-89-19	1.1	1.8	1.6	0.7	8.4
ST. CHARLES	SPA-89-20A	1.1	1.5	1.4	0.6	7.5
ST. CHARLES	SPA-89-20B	1.1	1.5	1.3	0.6	7.2
ST. CHARLES	SPA-89-21	1.2	1.8	1.7	0.8	9.2
MERCER	SPA-89-22	1.2	2.4	2.2	1.1	12.0
MERCER	SPA-89-25	0.8	1.0	0.9	0.4	4.9
MERCER	SPA-89-26	1.2	2.3	2.1	1.1	12.0
MERCER	SPA-89-27	1.4	3.2	2.9	1.6	16.0
WANAPITEI	SPA-89-28	1.4	4.9	4.1	2.1	23.0
WANAPITEI	SPA-89-29	2.0	6.3	6.2	3.3	34.0
WANAPITEI	SPA-89-30A	1.9	5.6	5.4	2.9	30.0
WANAPITEI	SPA-89-31	0.9	2.4	2.3	1.3	13.0
WANAPITEI	SPA-89-32	0.6	1.2	1.1	0.6	5.9
WANAPITEI	SPA-89-33	1.8	5.5	5.0	2.7	28.0
WANAPITEI	SPA-89-34	3.0	8.5	5.6	2.3	30.0
WANAPITEI	SPA-89-35	1.3	3.6	3.2	1.7	18.0
WANAPITEI	SPA-89-36	3.6	17.0	13.0	4.8	74.0
WANAPITEI	SPA-89-37	1.2	3.6	3.5	2.0	21.0
WANAPITEI	SPA-89-38	1.7	4.9	4.5	2.4	26.0
GRANITE	SPA-89-39	0.4	4.4	4.1	2.4	25.0
GRANITE	SPA-88-17	0.6	1.9	1.6	0.7	9.0
GRANITE	SPA-88-18	2.1	6.3	3.8	1.6	20.0
GRANITE (BLB)	SPA-88-01	0.3	1.7	1.5	0.7	6.9
GRANITE (BLB)	SPA-88-06	0.2	2.0	3.2	2.0	18.0
GRANITE (BLB)	SPA-88-15	0.4	2.9	2.2	0.9	12.0
GRANITE (DL)	SPA-88-41	0.7	2.2	1.4	0.8	7.3

Unit	Sample No.	Eu REE	Gd REE	Dy REE	Yb REE	Y REE
PAR.L. SY	SPA-88-23	5.3	20.0	11.0	3.4	55.0
GNEISS	SPA-89-23	1.5	9.2	8.6	5.2	52.0
LEVACK	SPA-89-03	1.0	1.2	0.6	0.3	3.2
LEVACK	SPA-89-04	1.7	4.5	2.7	1.0	13.0
LEVACK	SPA-89-01	0.7	0.8	0.4	0.1	2.0
LEVACK	SPA-89-02	2.0	4.2	2.3	0.8	11.0
LEVACK	SPA-89-02B	1.9	3.8	2.1	0.7	10.0

2.2 Standards and Replicate Data

STANDARDS			MAJOR ELEMENTS				
Sample no.	SiO_2	TiO_2	Al_2O_3	Cr_2O_3	Fe_2O_3T	Fe_2O_3	FeO
MRG-1	39.1	3.73	8.5	0.1	17.9	8.9	8.1
GSC B-1	49.5	2.52	15.5	0.0	14.5	4.4	9.1
177-88-56	52.1	0.16	20.2	0.0	5.9	1.2	4.2
177-88-57	47.2	0.26	20.2	0.0	8.9	1.6	6.6
177-88-58	74.9	0.18	14.1	0.0	1.4	0.5	0.8
163-89-45	50.3	0.31	15.2		10.9		
163-89-46	46.2	0.34	13.5		10.9		
REPLICATES							
SPA-88-15	74.5	0.11	14.2	0.0	1.2	0.4	0.7
SPA-88-15	75.2	0.11	14.3	0.0	1.2	0.1	1.0
Average	74.9	0.11	14.3	0.0	1.2	0.3	0.9
2 Std. Dev.	0.7	0.00	0.1	0.0	0.0	0.3	0.3
SPA-88-24	49.9	1.04	15.1	0.0	12.8	2.4	9.4
SPA-88-24	50.3	1.03	15.0	0.0	12.9	2.6	9.3
SPA-88-24	49.8	1.04	14.9	0.0	12.8	2.4	9.3
Average	50.1	1.04	15.0	0.0	12.9	2.5	9.3
2 Std. Dev.	0.5	0.00	0.1	0.0	0.1	0.2	0.0

						VOLATILES	
Sample No.	MnO	MgO	CaO	Na_2O	K_2O	H_2OT	CO_2T
MRG-1	0.2	13.3	14.8	0.6	0.15	0.9	1.1
GSC B-1	0.2	4.0	9.2	2.8	0.73	1.6	0.3
177-88-56	0.1	6.3	11.0	2.9	0.35	1.6	0.0
177-88-57	0.1	8.3	10.9	1.8	0.38	2.9	0.0
177-88-58	0.0	0.7	0.3	6.7	1.13	0.5	0.0
163-89-45	0.19	7.89	11.36	2.0	0.51	2.5	0.1
163-89-46	0.14	17.85	7.79	1.6	0.38	0.9	0.2

REPLICATES							
SPA-88-15	0.0	0.3	1.0	4.6	3.70	0.4	0.0
SPA-88-15	0.0	0.4	1.1	4.5	3.74	0.4	0.0
Average	0.0	0.4	1.0	4.6	3.7	0.4	0.0
2 Std. Dev.	0.0	0.0	0.0	0.1	0.0	0.0	0.0
SPA-88-24	0.2	7.0	10.2	2.9	0.31	1.6	0.0
SPA-88-24	0.2	6.9	10.2	2.9	0.31	1.5	0.0
SPA-88-24	0.2	6.9	10.2	2.9	0.31	1.5	0.0
Average	0.2	6.9	10.2	2.9	0.3	1.5	0.0
2 Std. Dev.	0.0	0.0	0.0	0.0	0.0	0.0	0.0

			TRACE ELEMENTS				
Sample No.	P_2O_5	S	Ba	Be	Co	Cr	Cu
MRG-1	0.1	0.06	138	0.8	88.0	430.0	140.0
GSC B-1	0.3	0.02	221	1.3	39.0	92.0	380.0
177-88-56	0.0	0.02	152	0.5	35.0	200.0	290.0
177-88-57	0.0	0.00	165	0.3	60.0	92.0	46.0
177-88-58	0.1	0.00	290	2.2	1.0	7.0	0.0
163-89-45	0.0	0.0	210.0	0.5	49.0	86.0	130.0
163-89-46	0.1	0.1	174.0	0.5	64.0	120.0	32.0
REPLICATES							
SPA-88-15	0.0	0.00	414	2.1	0.0	5.0	0.0
SPA-88-15	0.0	0.00	410	2.2	2.0	6.0	1.0
Average	0.0	0.0	412.0	2.2	1.0	5.5	0.5
2 Std. Dev.	0.0	0.0	4.0	0.1	2.0	1.0	1.0
SPA-88-24	0.1	0.07	165	0.7	45.0	240.0	98.0
SPA-88-24	0.1	0.07	151	0.7	49.0	230.0	100.0
SPA-88-24	0.1	0.07	119	0.7	49.0	250.0	110.0
Average	0.1	0.1	135.0	0.7	49.0	240.0	105.0
2 Std. Dev.	0.0	0.0	32.0	0.0	0.0	20.0	10.0

Sample No.	La	Nb	Ni	Rb	Sr	V	Y
MRG-1	16.0	43.0	190.0	16.0	278.0	550.0	39.0
GSC B-1	19.0	30.0	49.0	53.0	270.0	350.0	40.0
177-88-56	2.0	7.0	230.0	39.0	335.0	91.0	15.0
177-88-57	3.0	1.0	340.0	53.0	251.0	95.0	13.0
177-88-58	48.0	37.0	2.0	57.0	102.0	11.0	27.0
163-89-45	3.0	7.0	73.0	15.0	248.0	160.0	7.0
163-89-46	5.0	0.0	320.0	12.0	381.0	61.0	4.0
REPLICATES							
SPA-88-15	19.0	41.0	0.0	176.0	92.0	2.0	48.0
SPA-88-15	21.0	49.0	0.0	181.0	89.0	3.0	49.0
Average	20.0	45.0	0.0	178.5	90.5	2.5	48.5
2 Std. Dev.	2.0	8.0	0.0	5.0	3.0	1.0	1.0
SPA-88-24	9.0	17.0	100.0	23.0	194.0	280.0	58.0
SPA-88-24	14.0	10.0	110.0	19.0	199.0	280.0	54.0
SPA-88-24	10.0	15.0	110.0	25.0	195.0	290.0	57.0
Average	12.0	12.5	110.0	22.0	197.0	285.0	55.5
2 Std. Dev.	4.0	5.0	0.0	6.0	4.0	10.0	3.0

				RARE EARTH ELEMENTS			
Sample No.	Yb	Zn	Zr	La REE	Ce REE	Nd REE	Sm REE
MRG-1	1.3	190.0	125	10.0	28.0	21.0	4.5
GSC B-1	4.2	120.0	231	16.0	40.0	29.0	7.0
177-88-56	0.4	42.0	35	4.0	7.6	3.9	0.7
177-88-57	0.5	61.0	44	5.9	12.0	5.4	1.0
177-88-58	0.6	0.0	172	48.0	86.0	29.0	3.6
163-89-45	0.7	58.0	11.0	3.0	6.3	5.7	1.1
163-89-46	0.3	36.0	14.0	6.6	13.0	8.5	1.5
REPLICATES							
SPA-88-15	0.5	18.0	107	22.0	36.0	15.0	3.1
SPA-88-15	0.6	19.0	111	22.0	37.0	14.0	3.1
Average	0.6	18.5	109.0	22.0	36.5	14.5	3.1
2 Std. Dev.	0.1	1.0	4.0	0.0	1.0	1.0	0.0

				RARE EARTH ELEMENTS			
Sample No.	Yb	Zn	Zr	La REE	Ce REE	Nd REE	Sm REE
SPA-88-24	2.3	83.0	98	9.3	20.0	14.0	3.1
SPA-88-24	2.4	88.0	97	8.5	20.0	14.0	3.1
SPA-88-24	2.5	87.0	99	8.0	19.0	12.0	3.0
Average	2.5	87.5	98.0	8.3	19.5	13.0	3.1
2 Std. Dev.	0.1	1.0	2.0	0.5	1.0	2.0	0.1

Sample No.	Eu REE	Gd REE	Dy REE	Yb REE	Y REE
MRG-1	1.5	4.6	3.3	0.9	14.0
GSC B-1	2.5	8.7	8.4	4.2	45.0
177-88-56	0.4	0.9	0.9	0.5	4.7
177-88-57	0.5	1.2	1.2	0.7	6.6
177-88-58	0.7	2.2	1.3	0.8	7.4
163-89-45	0.5	1.0	0.9	n.d.	n.d.
163-89-46	0.6	1.0	0.7	n.d.	n.d.
REPLICATES					
SPA-88-15	0.4	2.9	2.2	0.9	12.0
SPA-88-15	0.4	2.9	2.1	0.9	12.0
Average	0.4	2.9	2.2	0.9	12.0
2 Std. Dev.	0.0	0.0	0.1	0.0	0.0
SPA-88-24	1.1	4.1	4.4	2.5	25.0
SPA-88-24	1.1	4.0	4.2	2.4	24.0
SPA-88-24	1.1	4.0	4.3	2.4	23.0
Average	1.1	4.0	4.3	2.4	23.5
2 Std. Dev.	0.0	0.0	0.1	0.0	1.0

Sample	Q	C	Z	Or	Ab	An	Plag	An #
SPA-88-01	30.87	0.27	0.02	31.49	33.00	2.92	35.92	8
SPA-88-06	34.63	0.83	0.01	19.63	42.30	1.53	43.83	3
SPA-88-15	30.81	0.73	0.02	21.94	38.92	5.18	44.10	12
SPA-88-17	32.24	1.29	0.02	17.35	38.07	6.70	44.77	15
SPA-88-18	20.42	0.75	0.05	35.81	30.46	4.65	35.11	13
SPA-88-23	0.59	0.00	0.07	35.06	42.30	5.10	47.40	11
SPA-88-41	29.31	1.36	0.03	6.88	57.53	1.10	58.63	2
EBL-4-133	0.00	0.00	0.00	1.48	6.77	27.06	33.83	80
EBL-4-140	0.00	0.00	0.00	1.25	6.77	18.99	25.76	74
EBL-1-182	0.00	0.00	0.01	1.66	11.00	29.65	40.65	73
SPA-88-19	0.00	0.00	0.01	1.90	17.77	46.68	64.45	72
SPA-88-20	0.67	0.00	0.01	2.03	22.00	48.20	70.20	69
SPA-88-21	0.00	0.00	0.01	1.61	17.77	48.74	66.51	73
SPA-88-22	0.00	0.00	0.01	2.32	15.23	46.18	61.41	75
SPA-88-42	24.29	0.18	0.02	3.98	39.77	24.24	64.01	38
SPA-88-43	2.48	0.00	0.02	2.56	21.15	40.46	61.61	66
SPA-88-45	0.00	0.00	0.01	3.27	17.77	41.08	58.85	70
SPA-88-46	0.00	0.00	0.01	2.14	11.85	46.42	58.27	80
SPA-88-48	2.43	0.00	0.01	2.91	17.77	34.16	51.93	66
SPA-88-49	2.85	0.00	0.01	2.68	16.92	29.00	45.92	63
SPA-88-31	2.09	0.00	0.01	0.02	25.38	46.59	71.97	65
SPA-88-32	0.02	0.00	0.01	2.37	27.07	40.69	67.76	60
SPA-88-54	0.00	0.00	0.01	6.04	32.15	37.55	69.70	54
SPA-88-55	0.00	0.00	0.01	7.70	17.83	53.92	71.75	75
SPA-88-56A	0.00	0.00	0.01	3.80	27.07	40.79	67.86	60
SPA-88-16	0.00	0.00	0.02	2.16	19.46	26.54	46.00	58
SPA-88-36	4.58	0.00	0.02	4.46	16.08	29.10	45.18	64
SPA-88-37	0.00	0.00	0.02	7.58	27.07	19.26	46.33	42
SPA-88-38	0.00	0.00	0.02	8.12	21.15	19.67	40.82	48
SPA-88-52	0.00	0.00	0.02	5.23	33.00	17.83	50.83	35
SPA-88-03	1.46	0.00	0.01	2.02	24.54	41.12	65.66	63
SPA-88-04	2.06	0.00	0.01	3.40	20.31	41.04	61.35	67
SPA-88-05	0.00	0.00	0.01	1.55	17.77	46.86	64.63	73
SPA-88-07	0.00	0.00	0.01	3.93	37.23	27.44	64.67	42
SPA-88-09	0.00	0.00	0.01	2.38	18.61	46.26	64.87	71
SPA-88-10	1.83	0.00	0.01	2.56	21.15	49.20	70.35	70
SPA-88-11	3.95	0.00	0.03	5.46	14.38	29.50	43.88	67
SPA-88-12	0.00	0.00	0.01	1.37	21.15	39.42	60.57	65
SPA-88-13	0.00	0.00	0.01	3.51	21.15	47.92	69.07	69
SPA-88-14	22.63	0.00	0.02	0.37	5.08	19.23	24.31	79
SPA-88-24	0.00	0.00	0.02	1.84	24.54	27.01	51.55	52
SPA-88-39	0.00	0.00	0.02	2.43	30.46	31.22	61.68	51
SPA-88-40	0.00	0.00	0.01	2.32	21.15	29.11	50.26	58
SPA-89-05	0.00	0.00	0.01	3.55	23.69	26.33	50.02	53

Sample	Q	C	Z	Or	Ab	An	Plag	An #
SPA-88-25	2.23	0.00	0.01	2.21	10.15	16.71	26.86	62
SPA-88-26	6.14	0.00	0.04	8.36	20.31	23.01	43.32	53
SPA-88-27A	2.10	0.00	0.02	3.81	18.61	31.90	50.51	63
SPA-88-27B	0.16	0.00	0.03	3.57	20.31	26.48	46.79	57
SPA-88-28	9.23	0.00	0.03	3.62	17.77	24.79	42.56	58
SPA-88-29	1.04	0.00	0.02	1.13	11.85	33.27	45.12	74
SPA-88-30	41.41	0.79	0.05	35.73	19.46	1.11	20.57	5
SPA-88-34	0.94	0.00	0.03	1.84	15.23	27.30	42.53	64
SPA-88-35	1.68	0.00	0.02	7.88	24.54	19.09	43.63	44
SPA-89-07A	0.28	0.00	0.00	3.32	22.00	48.64	70.64	69
SPA-89-07B	1.00	0.00	0.01	4.21	17.77	29.96	47.73	63
SPA-89-07C	0.00	0.00	0.00	4.44	22.00	43.72	65.72	67
SPA-89-08A	1.24	0.00	0.01	3.55	22.00	44.16	66.16	67
SPA-89-08B	0.79	0.00	0.00	2.37	16.08	33.14	49.22	67
SPA-89-09	0.00	0.00	0.00	2.55	19.46	32.90	52.36	63
SPA-89-10	0.00	0.00	0.00	3.08	16.92	30.43	47.35	64
SPA-89-11	0.00	0.00	0.00	6.33	22.84	35.50	58.34	61
SPA-89-39	38.50	1.10	0.03	33.90	22.84	0.98	23.82	4
SPA-89-23	31.24	0.51	0.09	32.97	24.54	4.40	28.94	15
SPA-89-01	28.09	0.48	0.03	8.04	42.30	14.61	56.91	26
SPA-89-02	9.22	0.00	0.05	9.35	40.61	20.27	60.88	33
SPA-89-02B	11.13	0.00	0.05	8.11	41.46	21.53	62.99	34
SPA-89-03	22.01	0.04	0.03	5.50	44.00	19.44	63.44	31
SPA-89-04	15.52	0.00	0.03	7.17	38.07	18.85	56.92	33
SPA-89-22	0.00	0.00	0.01	5.32	32.98	39.77	72.75	55
SPA-89-25	0.00	0.00	0.00	9.71	32.11	40.87	72.98	56
SPA-89-26	0.00	0.00	0.01	5.09	35.54	43.88	79.42	55
SPA-89-27	0.00	0.00	0.02	10.12	38.83	40.33	79.16	51
SPA-89-12B	0.00	0.00	0.01	4.44	33.00	46.66	79.66	59
SPA-89-13	0.00	0.00	0.00	4.20	33.84	44.95	78.79	57
SPA-89-14	0.00	0.00	0.01	3.79	33.84	47.35	81.19	58
SPA-89-15	0.00	0.00	0.01	2.61	37.23	50.24	87.47	57
SPA-89-16	0.00	0.00	0.01	3.08	37.96	50.38	88.34	57
SPA-89-18	0.02	0.00	0.01	3.14	36.38	48.79	85.17	57
SPA-89-19	0.00	0.00	0.01	3.73	37.23	48.32	85.55	56
SPA-89-20A	0.00	0.00	0.01	5.09	38.09	47.28	85.37	55
SPA-89-20B	0.00	0.00	0.01	4.61	38.07	48.79	86.86	56
SPA-89-21	0.00	0.00	0.01	3.61	35.54	46.82	82.36	57
SPA-89-28	14.71	0.69	0.03	18.01	18.61	21.37	39.98	53
SPA-89-29	4.57	0.00	0.04	6.81	22.00	24.81	46.81	53
SPA-89-30A	1.07	0.00	0.03	5.92	28.77	20.56	49.33	42
SPA-89-31	0.73	0.00	0.01	4.80	22.84	31.63	54.47	58
SPA-89-32	0.00	0.00	0.00	2.25	13.54	29.11	42.65	68
SPA-89-33	2.73	0.00	0.03	7.23	26.23	23.17	49.40	47

Sample	Q	C	Z	Or	Ab	An	Plag	An #
SPA-89-34	0.00	0.00	0.06	14.68	35.54	18.93	54.47	35
SPA-89-35	0.00	0.00	0.01	3.79	16.92	32.28	49.20	66
SPA-89-36	3.40	1.00	0.04	8.59	29.61	24.27	53.88	45
SPA-89-37	0.00	0.00	0.01	4.50	22.84	29.87	52.71	57
SPA-89-38	0.00	0.00	0.02	5.09	23.69	26.95	50.64	53

Sample	Ne	Di	Hy	Ol	Mt	Cm	Hm	Il
SPA-88-01	0.00	0.00	0.52	0.00	0.00	0.00	0.60	0.02
SPA-88-06	0.00	0.00	0.55	0.00	0.00	0.00	0.70	0.02
SPA-88-15	0.00	0.00	0.85	0.00	0.00	0.00	1.20	0.06
SPA-88-17	0.00	0.00	1.62	0.00	0.00	0.00	1.70	0.09
SPA-88-18	0.00	0.00	3.14	0.00	0.91	0.00	1.23	0.68
SPA-88-23	0.00	4.00	5.07	0.00	3.16	0.00	0.00	1.29
SPA-88-41	0.00	0.00	1.69	0.00	0.00	0.00	1.40	0.02
EBL-4-133	0.00	7.23	29.25	20.32	2.52	0.05	0.00	0.46
EBL-4-140	0.00	2.31	27.45	36.37	2.55	0.03	0.00	0.49
EBL-1-182	0.00	4.06	15.03	31.77	2.58	0.02	0.00	0.53
SPA-88-19	0.00	8.37	18.90	1.33	2.80	0.01	0.00	0.82
SPA-88-20	0.00	8.46	14.53	0.00	2.67	0.02	0.00	0.65
SPA-88-21	0.00	6.27	14.55	7.10	2.58	0.02	0.00	0.53
SPA-88-22	0.00	6.38	15.75	8.98	2.54	0.02	0.00	0.47
SPA-88-42	0.00	0.00	3.59	0.00	2.17	0.00	0.16	0.28
SPA-88-43	0.00	14.13	13.96	0.00	3.03	0.03	0.00	1.12
SPA-88-45	0.00	4.82	15.73	11.48	2.55	0.02	0.00	0.49
SPA-88-46	0.00	6.57	14.67	12.64	2.32	0.02	0.00	0.19
SPA-88-48	0.00	17.31	20.57	0.00	2.90	0.04	0.00	0.95
SPA-88-49	0.00	23.46	20.05	0.00	2.90	0.09	0.00	0.95
SPA-88-31	0.00	8.10	12.63	0.00	2.46	0.02	0.00	0.38
SPA-88-32	0.00	10.09	14.82	0.00	2.60	0.01	0.00	0.55
SPA-88-54	0.00	5.41	5.01	8.20	2.48	0.02	0.00	0.40
SPA-88-55	1.34	3.08	0.00	10.59	2.41	0.02	0.00	0.30
SPA-88-56A	0.00	12.84	6.15	4.46	2.48	0.02	0.00	0.40
SPA-88-16	0.00	22.91	20.25	0.64	3.75	0.03	0.00	2.07
SPA-88-36	0.00	17.07	21.38	0.00	3.23	0.02	0.00	1.39
SPA-88-37	0.00	14.82	18.37	3.55	4.02	0.00	0.00	2.41
SPA-88-38	0.00	18.39	17.86	6.26	3.93	0.00	0.00	2.30
SPA-88-52	0.00	11.81	14.86	7.93	3.94	0.00	0.00	2.32
SPA-88-03	0.00	10.90	15.76	0.00	2.41	0.05	0.00	0.30
SPA-88-04	0.00	11.85	16.45	0.00	2.51	0.05	0.00	0.44
SPA-88-05	0.00	3.21	9.44	15.11	2.52	0.02	0.00	0.46
SPA-88-07	0.00	10.56	8.78	5.77	3.16	0.00	0.00	1.29
SPA-88-09	0.00	10.29	17.20	0.66	2.44	0.08	0.00	0.34
SPA-88-10	0.00	8.83	11.88	0.00	2.60	0.05	0.00	0.55
SPA-88-11	0.00	16.49	22.65	0.00	3.87	0.02	0.00	2.22
SPA-88-12	0.00	1.88	10.38	20.18	2.36	0.07	0.00	0.25
SPA-88-13	0.00	1.40	1.62	18.67	2.38	0.02	0.00	0.27
SPA-88-14	0.00	22.82	24.95	0.00	2.60	0.03	0.00	0.55
SPA-88-24	0.00	18.93	18.11	2.56	3.67	0.05	0.00	1.96
SPA-88-39	0.00	15.53	10.52	3.88	3.32	0.01	0.00	1.50
SPA-88-40	0.00	16.51	20.62	4.38	2.81	0.03	0.00	0.84
SPA-89-05	0.00	16.35	12.59	10.95	3.19	0.02	0.00	1.33

Sample	Ne	Di	Hy	Ol	Mt	Cm	Hm	Il
SPA-88-25	0.00	24.15	37.57	0.00	2.90	0.28	0.00	0.95
SPA-88-26	0.00	11.93	21.34	0.00	4.15	0.01	0.00	2.58
SPA-88-27A	0.00	14.95	20.13	0.00	4.00	0.02	0.00	2.39
SPA-88-27B	0.00	20.97	20.75	0.00	4.10	0.02	0.00	2.53
SPA-88-28	0.00	17.97	19.16	0.00	4.06	0.02	0.00	2.47
SPA-88-29	0.00	19.98	24.67	0.00	4.18	0.03	0.00	2.62
SPA-88-30	0.00	0.00	0.35	0.00	0.00	0.00	1.20	0.04
SPA-88-34	0.00	16.56	26.32	0.00	4.64	0.03	0.00	3.23
SPA-88-35	0.00	12.96	24.18	0.00	4.23	0.00	0.00	2.70
SPA-89-07A	0.00	8.88	12.77	0.00	2.44	0.03	0.00	0.34
SPA-89-07B	0.00	20.82	21.04	0.00	2.71	0.04	0.00	0.70
SPA-89-07C	0.00	8.26	11.24	5.39	2.48	0.04	0.00	0.40
SPA-89-08A	0.00	10.72	12.60	0.00	2.83	0.02	0.00	0.85
SPA-89-08B	0.00	24.39	18.36	0.00	2.71	0.10	0.00	0.70
SPA-89-09	0.00	14.53	21.84	3.13	2.60	0.06	0.00	0.55
SPA-89-10	0.00	21.16	21.78	0.51	2.64	0.02	0.00	0.61
SPA-89-11	0.00	15.42	8.74	6.09	2.51	0.03	0.00	0.44
SPA-89-39	0.00	0.00	0.70	0.00	0.00	0.00	1.10	0.02
SPA-89-23	0.00	0.00	1.46	0.00	2.61	0.00	0.00	0.57
SPA-89-01	0.00	0.00	2.22	0.00	0.86	0.00	1.23	0.61
SPA-89-02	0.00	4.08	9.29	0.00	3.26	0.02	0.00	1.42
SPA-89-02B	0.00	3.14	8.45	0.00	3.31	0.01	0.00	1.48
SPA-89-03	0.00	0.00	3.51	0.00	1.79	0.00	0.78	0.97
SPA-89-04	0.00	4.91	9.36	0.00	2.90	0.03	0.00	0.95
SPA-89-22	1.84	5.60	0.00	7.94	3.52	0.02	0.00	1.77
SPA-89-25	2.31	3.93	0.00	5.97	2.80	0.01	0.00	0.82
SPA-89-26	0.00	3.46	3.02	3.85	3.28	0.01	0.00	1.44
SPA-89-27	0.97	2.55	0.00	1.39	2.83	0.01	0.00	0.85
SPA-89-12B	0.00	2.94	7.06	0.34	3.20	0.01	0.00	1.35
SPA-89-13	0.00	3.38	6.31	1.31	3.19	0.01	0.00	1.33
SPA-89-14	0.00	2.66	6.78	0.38	3.13	0.01	0.00	1.25
SPA-89-15	0.00	1.13	3.05	0.73	2.87	0.00	0.00	0.91
SPA-89-16	0.06	2.65	0.00	1.86	2.86	0.00	0.00	0.89
SPA-89-18	0.00	1.84	4.75	0.00	3.06	0.00	0.00	1.16
SPA-89-19	0.00	2.61	3.40	0.06	3.02	0.00	0.00	1.10
SPA-89-20A	0.45	3.44	0.00	1.00	1.71	0.00	1.00	1.29
SPA-89-20B	0.00	1.38	2.06	0.44	2.11	0.00	0.65	1.16
SPA-89-21	0.00	3.00	5.00	0.64	3.22	0.01	0.00	1.37
SPA-89-28	0.00	0.00	18.35	0.00	3.41	0.02	0.00	1.61
SPA-89-29	0.00	12.81	19.31	0.00	4.42	0.01	0.00	2.94
SPA-89-30A	0.00	16.97	16.59	0.00	4.73	0.00	0.00	3.34
SPA-89-31	0.00	15.21	18.63	0.00	3.00	0.08	0.00	1.08
SPA-89-32	0.00	5.65	15.67	28.72	2.60	0.03	0.00	0.55
SPA-89-33	0.00	14.21	18.60	0.00	3.94	0.02	0.00	2.32

Sample	Ne	Di	Hy	Ol	Mt	Cm	Hm	Il
SPA-89-34	0.00	6.22	14.04	0.64	3.91	0.00	0.00	2.28
SPA-89-35	0.00	19.73	4.95	14.39	3.94	0.00	0.00	2.32
SPA-89-36	0.00	0.00	20.70	0.00	4.96	0.01	0.00	3.65
SPA-89-37	0.00	15.35	18.41	2.16	3.61	0.05	0.00	1.88
SPA-89-38	0.00	15.95	13.68	6.01	3.94	0.03	0.00	2.32

Sample	Ru	Ap	Cc	Total
SPA-88-01	0.07	0.02	0.00	99.79
SPA-88-06	0.04	0.02	0.00	100.26
SPA-88-15	0.08	0.05	0.00	99.83
SPA-88-17	0.11	0.10	0.23	99.53
SPA-88-18	0.00	0.47	0.48	99.06
SPA-88-23	0.00	0.94	1.39	98.98
SPA-88-41	0.17	0.15	0.00	99.64
EBL-4-133	0.00	0.09	0.00	95.23
EBL-4-140	0.00	0.09	0.23	96.53
EBL-1-182	0.00	0.14	0.23	96.67
SPA-88-19	0.00	0.14	0.00	98.73
SPA-88-20	0.00	0.12	0.00	99.35
SPA-88-21	0.00	0.09	0.00	99.27
SPA-88-22	0.00	0.09	0.00	97.98
SPA-88-42	0.00	0.10	0.23	99.00
SPA-88-43	0.00	0.17	0.00	99.11
SPA-88-45	0.00	0.07	0.23	97.53
SPA-88-46	0.00	0.05	0.00	96.88
SPA-88-48	0.00	0.14	0.00	99.20
SPA-88-49	0.00	0.17	0.00	99.08
SPA-88-31	0.00	0.05	0.00	97.72
SPA-88-32	0.00	0.09	0.23	98.55
SPA-88-54	0.00	0.05	0.23	97.55
SPA-88-55	0.00	0.02	0.00	97.22
SPA-88-56A	0.00	0.02	0.00	98.06
SPA-88-16	0.00	0.24	0.00	98.07
SPA-88-36	0.00	0.17	0.23	97.72
SPA-88-37	0.00	0.24	0.46	97.80
SPA-88-38	0.00	0.21	0.23	98.14
SPA-88-52	0.00	0.24	0.23	97.40
SPA-88-03	0.00	0.05	0.00	98.61
SPA-88-04	0.00	0.07	0.00	98.18
SPA-88-05	0.00	0.07	0.00	97.02
SPA-88-07	0.00	0.14	0.23	98.54
SPA-88-09	0.00	0.05	0.00	98.31
SPA-88-10	0.00	0.09	0.00	98.75
SPA-88-11	0.00	0.31	0.00	98.88
SPA-88-12	0.00	0.02	0.00	97.10
SPA-88-13	0.00	0.05	0.00	96.99
SPA-88-14	0.00	0.05	0.00	98.32
SPA-88-24	0.00	0.26	0.00	98.94
SPA-88-39	0.00	0.24	0.00	99.13
SPA-88-40	0.00	0.12	0.00	97.90
SPA-89-05	0.00	0.24	0.00	98.25

Sample	Ru	Ap	Cc	Total
SPA-88-25	0.00	0.09	0.00	97.25
SPA-88-26	0.00	0.43	0.46	98.73
SPA-88-27A	0.00	0.31	0.23	98.47
SPA-88-27B	0.00	0.38	0.00	99.29
SPA-88-28	0.00	0.36	0.00	99.48
SPA-88-29	0.00	0.36	0.00	99.14
SPA-88-30	0.13	0.05	0.00	100.32
SPA-88-34	0.00	0.62	1.37	98.10
SPA-88-35	0.00	0.29	0.68	98.26
SPA-89-07A	0.00	0.05	0.00	98.74
SPA-89-07B	0.00	0.17	0.23	98.67
SPA-89-07C	0.00	0.07	0.23	98.26
SPA-89-08A	0.00	0.12	0.00	98.09
SPA-89-08B	0.00	0.09	0.00	98.73
SPA-89-09	0.00	0.05	0.00	97.66
SPA-89-10	0.00	0.05	0.00	97.19
SPA-89-11	0.00	0.07	0.00	97.97
SPA-89-39	0.14	0.07	0.46	99.85
SPA-89-23	0.00	0.12	0.00	98.50
SPA-89-01	0.00	0.26	0.23	98.96
SPA-89-02	0.00	0.77	0.00	98.34
SPA-89-02B	0.00	0.77	0.00	99.43
SPA-89-03	0.00	0.33	0.00	98.41
SPA-89-04	0.00	0.55	0.00	98.33
SPA-89-22	0.00	0.52	0.00	99.29
SPA-89-25	0.00	0.24	0.00	98.77
SPA-89-26	0.00	0.38	0.00	99.95
SPA-89-27	0.00	0.31	0.00	98.20
SPA-89-12B	0.00	0.29	0.00	99.28
SPA-89-13	0.00	0.19	0.23	98.96
SPA-89-14	0.00	0.26	0.23	99.69
SPA-89-15	0.00	0.21	0.23	99.23
SPA-89-16	0.00	0.29	0.00	100.02
SPA-89-18	0.00	0.36	0.00	99.49
SPA-89-19	0.00	0.36	0.00	99.84
SPA-89-20A	0.00	0.31	0.00	99.67
SPA-89-20B	0.00	0.31	0.00	99.61
SPA-89-21	0.00	0.33	0.23	99.75
SPA-89-28	0.00	0.43	0.46	97.72
SPA-89-29	0.00	0.59	0.46	98.76
SPA-89-30A	0.00	0.74	0.68	99.39
SPA-89-31	0.00	0.24	0.00	98.26
SPA-89-32	0.00	0.17	0.91	99.18
SPA-89-33	0.00	0.71	0.23	99.41

Sample	Ru	Ap	Cc	Total
SPA-89-34	0.00	1.54	0.23	98.07
SPA-89-35	0.00	0.40	0.23	98.96
SPA-89-36	0.00	2.62	0.23	99.07
SPA-89-37	0.00	0.40	0.23	99.31
SPA-89-38	0.00	0.76	0.23	98.67

Appendix 3. Spidergrams and REE profiles

Spidergrams and REE profiles were created using the program NEWPET, with normalizing values as discussed in the text (Chapter 5.4). Abundances of Nd and Sm have been adjusted to compensate for analytical interferences as mentioned in Appendix 1. The correction consisted of generating a linear profile between normalized Ce and Gd. While this limits somewhat the significance of LREE *vs*. HREE slope comparisons, it presents a more useful reference diagram.

Plots are presented for the following units, shown as the spidergram (upper diagram) and REE profile (lower diagram):

East Bull Lake
Shakespeare-Dunlop
Drury Twp.
Falconbridge Twp.
Tennyson Twp.
May Twp.
Huronian volcanics
Wanapitei
St. Charles
Mercer Twp.

For Nb analyses below detection limits, dashed lines are drawn to indicate the negative anomaly, as it is not quantifiable based on available data.

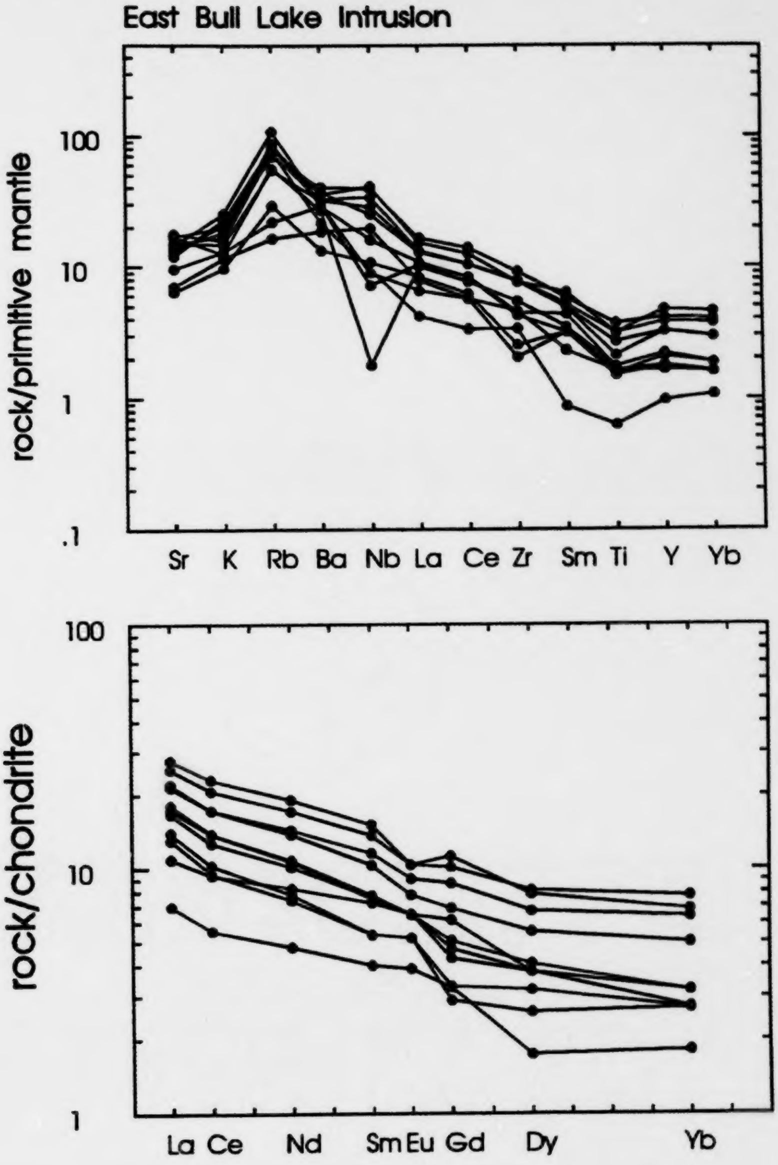
East Bull Lake Intrusion

Shakespeare-Dunlop Intrusion

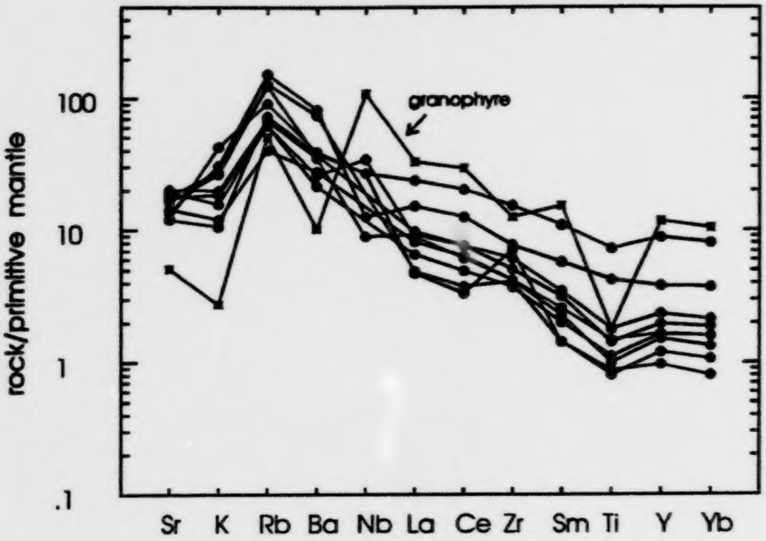

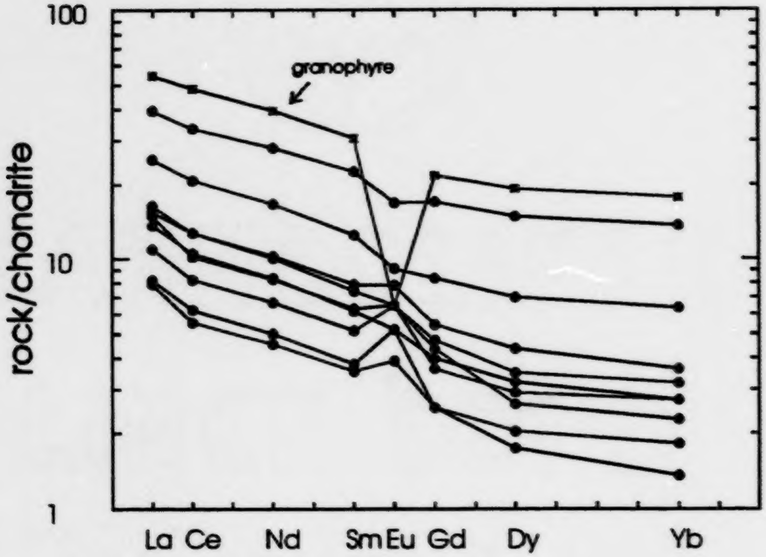

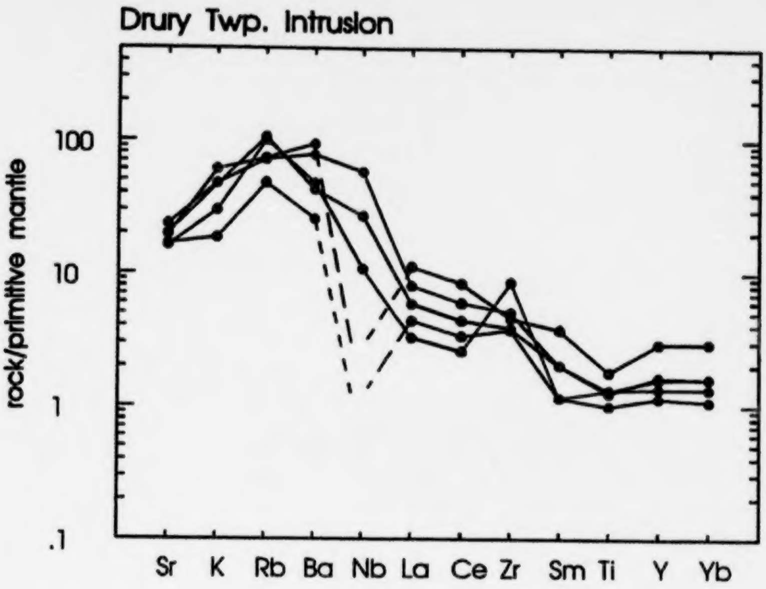
Drury Twp. Intrusion
rock/primitive mantle
100
10
1
.1
Sr
K
Rb
Ba
Nb
La
Ce
Zr
Sm
Ti
Y
Yb

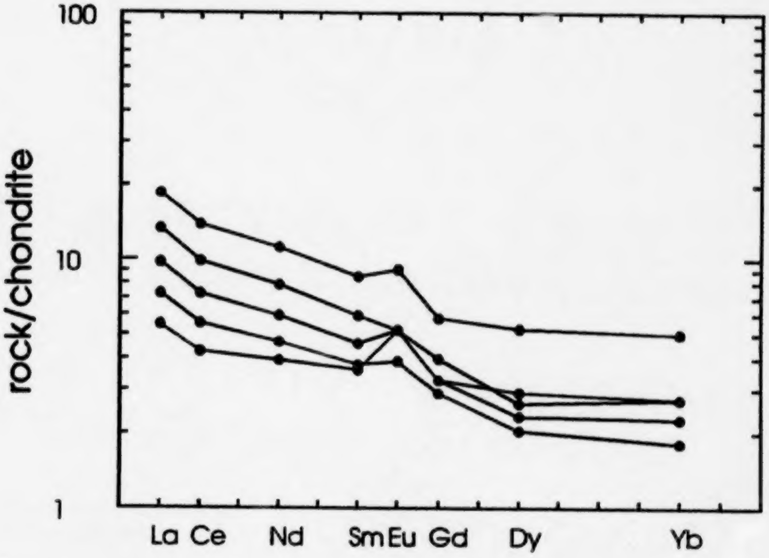
rock/chondrite
100
10
1
La
Ce
Nd
Sm
Eu
Gd
Dy
Yb

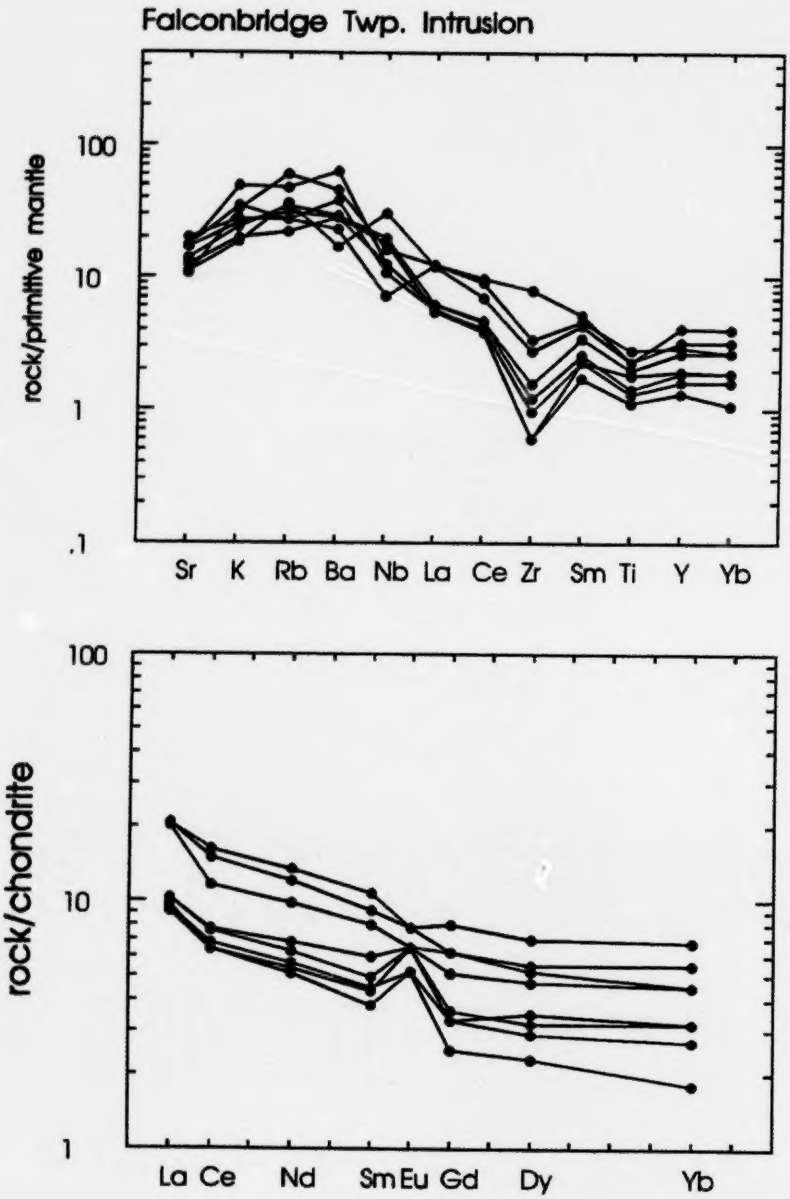
Falconbridge Twp. Intrusion
rock/primitive mantle
100
10
1
.1
Sr
K
Rb
Ba
Nb
La
Ce
Zr
Sm
Ti
Y
Yb
rock/chondrite
100
10
1
La
Ce
Nd
Sm
Eu
Gd
Dy
Yb

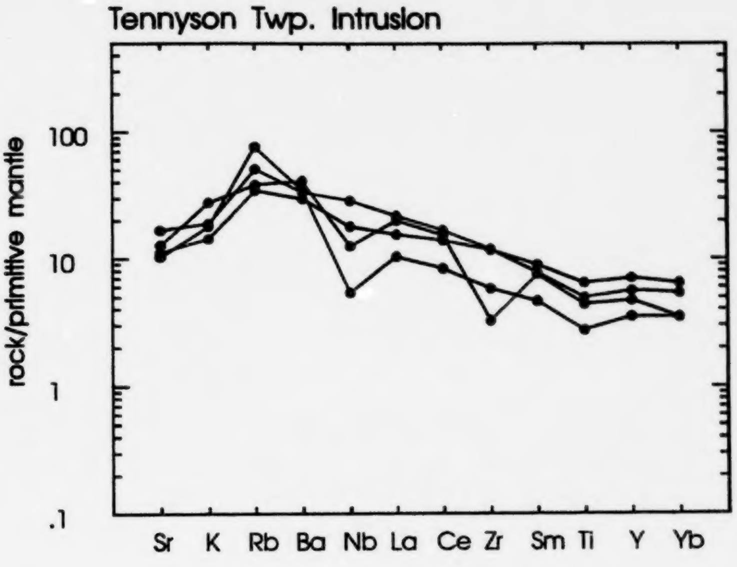
Tennyson Twp. Intrusion

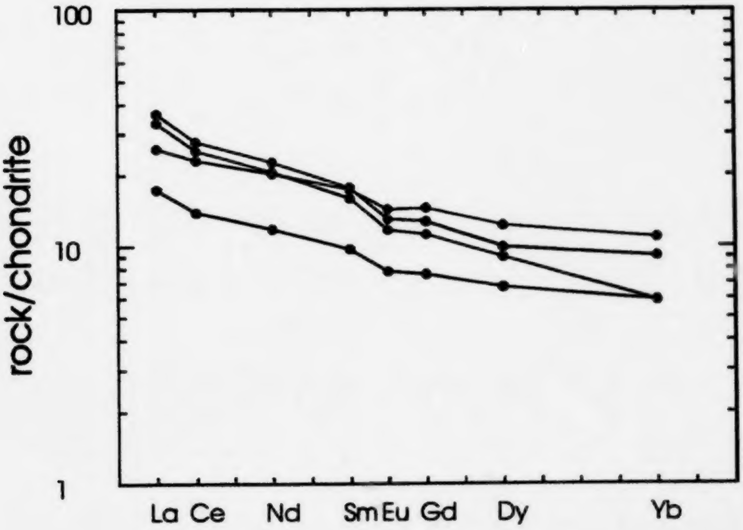

May Twp. Intrusion

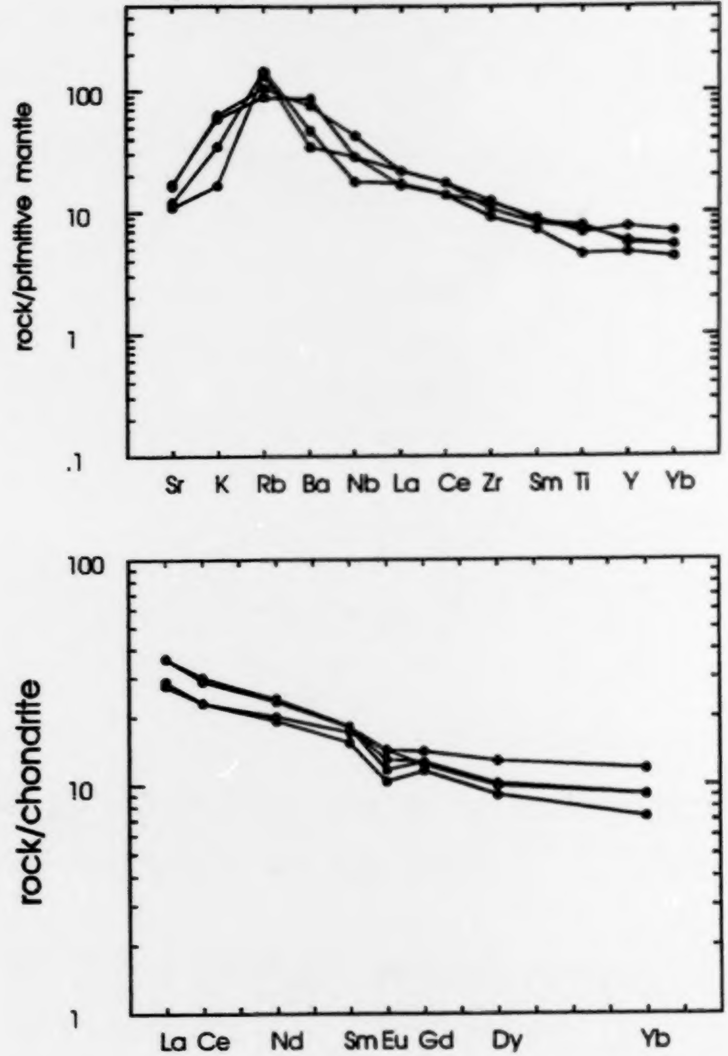

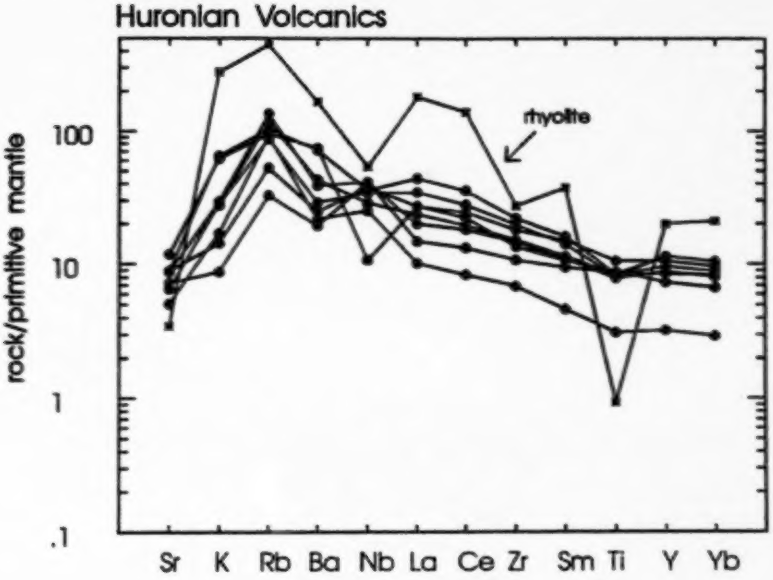
Huronian Volcanics
rock/primitive mantle
.1
1
10
100
rhyolite
Sr
K
Rb
Ba
Nb
La
Ce
Zr
Sm
Ti
Y
Yb

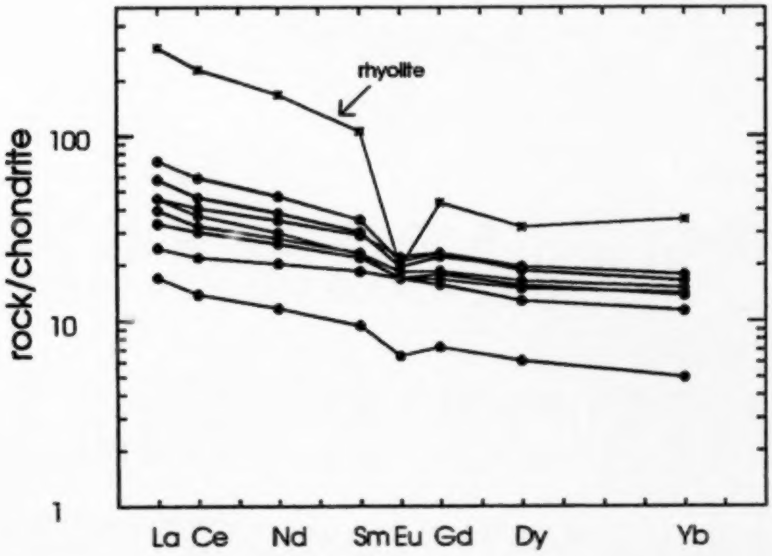
rock/chondrite
1
10
100
rhyolite
La
Ce
Nd
Sm
Eu
Gd
Dy
Yb

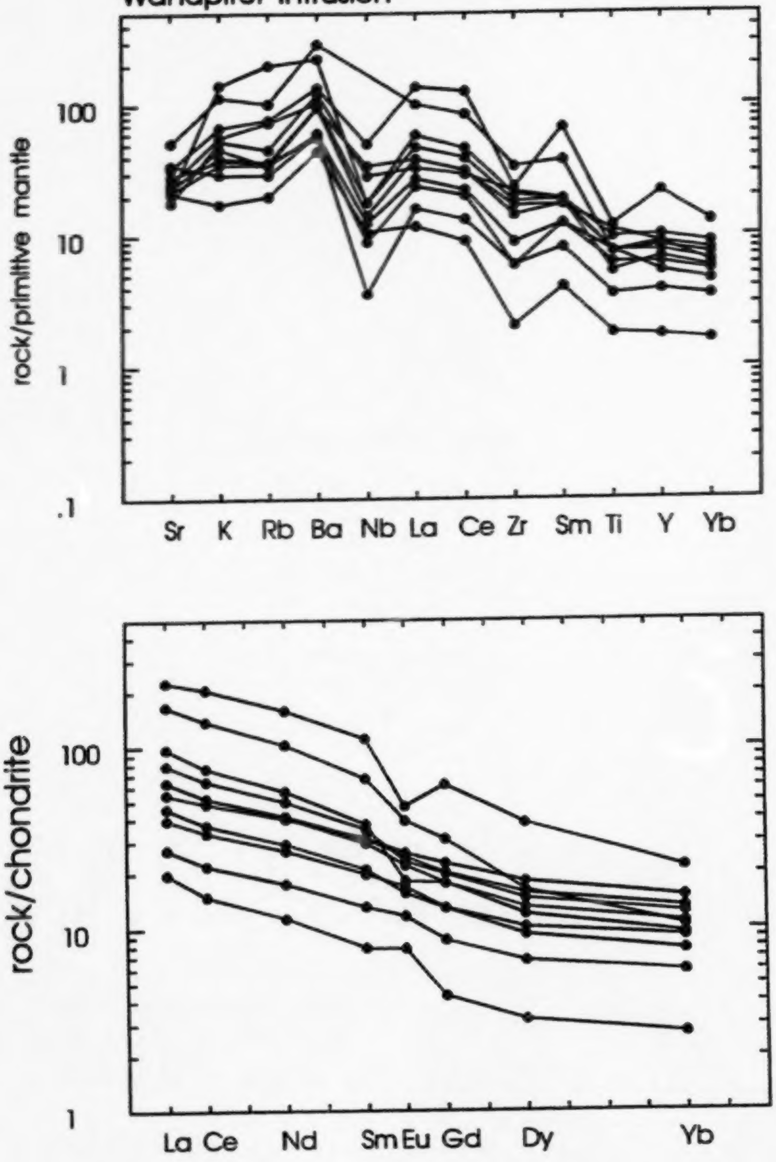

Wanapitei Intrusion

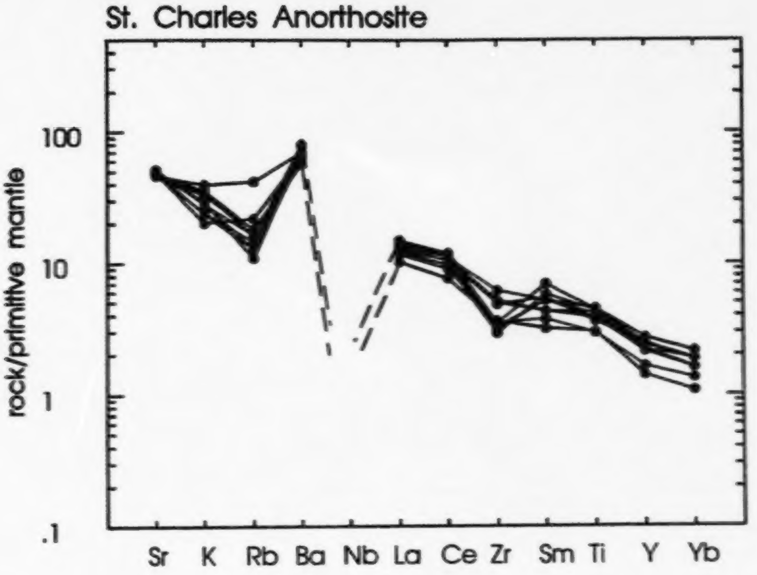
St. Charles Anorthosite

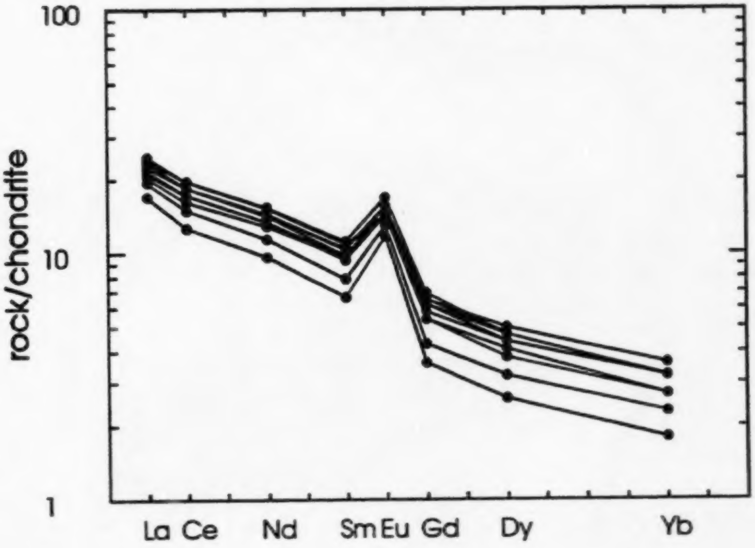

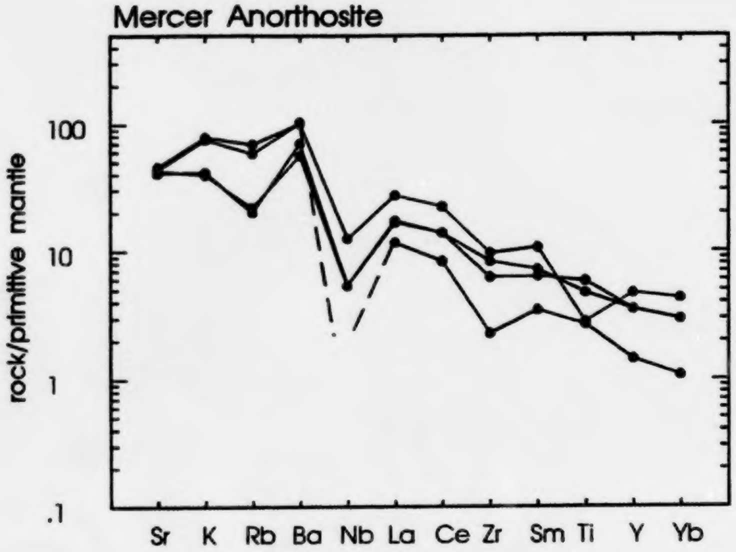
Mercer Anorthosite
rock/primitive mantle
100
10
1
.1
Sr
K
Rb
Ba
Nb
La
Ce
Zr
Sm
Ti
Y
Yb

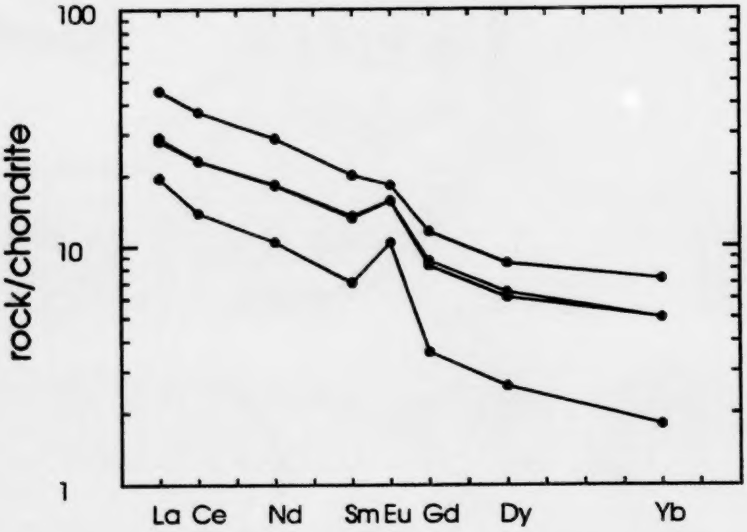
rock/chondrite
100
10
1
La
Ce
Nd
Sm
Eu
Gd
Dy
Yb

Appendix 4. Isotopic data

Contents:

4.1 Sm-Nd data
4.2 Pb-Pb data
4.3 Rb-Sr data

See Appendix 1 for information on analyses, blanks and standard

$$\epsilon_{\mathrm{Nd}} = \left(\frac{(^{143}\mathrm{Nd}/^{144}\mathrm{Nd})_s - (^{143}\mathrm{Nd}/^{144}\mathrm{Nd})_{\mathrm{CHUR}}}{(^{143}\mathrm{Nd}/^{144}\mathrm{Nd})_{\mathrm{CHUR}}} \right) * 10^4$$

at a given time, and

$$f_{\mathrm{Sm/Nd}} = \left(\frac{(^{147}\mathrm{Sm}/^{144}\mathrm{Nd})_s - (^{147}\mathrm{Sm}/^{144}\mathrm{Nd})_{\mathrm{CHUR}}}{(^{147}\mathrm{Sm}/^{144}\mathrm{Nd})_{\mathrm{CHUR}}} \right) * 10^4$$

where subscript s = sample,
and CHUR = chondritic uniform reservoir values
(see DePaolo, 1988, for chondritic and depleted mantle (DM) reference values).
$\epsilon(T)$ is calculated for intrusion ages as discussed in the text; T_{CHUR}, T_{DM1} and T_{DM2} are model ages calculated based on derivation from a chondritic reservoir, a progressively depleting mantle, and a linearly depleted mantle, respectively.

Lead model ages and values for μ (^{238}U/^{204}Pb) were calculated using the program ISOPLOT. "SE6/4" = Standard Error of ^{206}Pb/^{204}Pb, etc.

4.1 Sm-Nd Isotopic Data

Location	Sample	Nd	Sm	$^{147}Sm/^{144}Nd$	$^{143}Nd/^{144}Nd$	2σ	/mil
Drury	SPA-88-31	3.424	0.821	0.1449	0.511882	0.000010	0.010
Drury	SPA-88-54	4.411	0.889	0.1219	0.511605	0.000011	0.011
Drury	SPA-88-55	2.973	0.653	0.1327	0.511677	0.000010	0.010
Drury	SPA-88-56A	2.475	0.609	0.1487	0.511965	0.000021	0.021
EBL	EBL-1-182	6.589	1.454	0.1334	0.511614	0.000015	0.015
EBL	EBL-4-133	4.578	0.993	0.1311	0.511697	0.000009	0.009
EBL	EBL-4-140	4.266	0.857	0.1214	0.511534	0.000008	0.008
EBL	SPA-88-43	9.718	2.308	0.1435	0.511652	0.000006	0.006
EBL	SPA-88-45	5.304	1.196	0.1362	0.511771	0.000009	0.009
EBL	SPA-88-49	9.771	2.334	0.1443	0.511734	0.000007	0.007
Falcon	SPA-89-07A	2.327	0.531	0.1380	0.511860	0.000032	0.032
Falcon	SPA-89-07B	7.698	1.826	0.1433	0.511809	0.000010	0.010
Falcon	SPA-89-08A	6.278	1.401	0.1348	0.511642	0.000008	0.008
Falcon	SPA-89-09	3.556	1.002	0.1704	0.512044	0.000019	0.019
Falcon	SPA-89-10	2.722	0.738	0.1638	0.512231	0.000018	0.018
Falcon	SPA-89-11	3.091	0.750	0.1466	0.511749	0.000038	0.038
Levack	SPA-89-01	6.288	0.987	0.0949	0.510843	0.000007	0.007
Levack	SPA-89-03	10.819	1.655	0.0925	0.510789	0.000007	0.007
Levack	SPA-89-04	34.520	7.732	0.1354	0.511106	0.000009	0.009
S-D	SPA-88-03	3.957	0.882	0.1347	0.511568	0.000008	0.008
S-D	SPA-88-05	5.373	1.413	0.1588	0.511573	0.000007	0.007
S-D	SPA-88-07	9.218	2.130	0.1396	0.511617	0.000005	0.005
S-D	SPA-88-10	6.355	1.182	0.1123	0.511619	0.000006	0.006
Wanap	SPA-89-34	72.287	11.740	0.0981	0.511224	0.000008	0.008
Wanap	SPA-89-35	18.091	3.825	0.1278	0.511678	0.000011	0.011
Wanap	SPA-89-36	121.132	20.704	0.1033	0.511456	0.000008	0.008
Wanap	SPA-89-37	16.441	3.518	0.1293	0.511688	0.000033	0.033

Location	Sample	$f_{Sm/Nd}$	ε(T)	2sigma	ε(0)	T_{CHUR}	T_{DM1}	T_{DM2}
Drury	SPA-88-31	-0.4159	4.70	0.34	-14.75	1407	1790	1953
Drury	SPA-88-54	-0.3803	-2.40	0.37	-20.15	2097	2399	2556
Drury	SPA-88-55	-0.3254	-3.57	0.36	-18.75	2279	2591	2760
Drury	SPA-88-56A	-0.2440	-1.74	0.60	-13.13	2129	2549	2768
EBL	EBL-1-182	-0.3218	0.22	0.52	-19.97	2454	2741	2902
EBL	EBL-4-133	-0.3335	2.58	0.39	-18.36	2178	2500	2671
EBL	EBL-4-140	-0.3828	2.50	0.36	-21.54	2226	2508	2658
EBL	SPA-88-43	-0.2705	-2.28	0.35	-19.23	2808	3076	3234
EBL	SPA-88-45	-0.3076	2.40	0.40	-16.91	2176	2519	2701
EBL	SPA-88-49	-0.2664	-0.93	0.37	-17.63	2615	2919	3094
Falcon	SPA-89-07A	-0.2984	-1.24	0.81	-15.18	2013	2394	2588
Falcon	SPA-89-07B	-0.2715	-3.51	0.37	-16.17	2356	2700	2891
Falcon	SPA-89-08A	-0.3147	-4.75	0.32	-19.43	2441	2735	2900
Falcon	SPA-89-09	-0.1337	-5.37	0.59	-11.59	3415	3699	3867
Falcon	SPA-89-10	-0.1673	-0.13	0.56	-7.94	1880	2502	2798
Falcon	SPA-89-11	-0.2547	-5.47	0.94	-17.34	2689	2990	3166
Levack	SPA-89-01	-0.5175	0.51	0.31	-35.02	2673	2849	2944
Levack	SPA-89-03	-0.5297	0.29	0.30	-36.07	2690	2861	2953
Levack	SPA-89-04	-0.3116	-8.55	0.42	-29.88	3774	3899	3946
S-D	SPA-88-03	-0.3152	-1.10	0.38	-20.87	2616	2883	3037
S-D	SPA-88-05	-0.1927	-8.74	0.40	-20.77	4237	4337	4339
S-D	SPA-88-07	-0.2903	-1.71	0.32	-19.92	2710	2979	3136
S-D	SPA-88-10	-0.4291	7.09	0.30	-19.88	1835	2145	2295
Wanap	SPA-89-34	-0.5013	-5.52	0.27	-27.58	2177	2410	2530
Wanap	SPA-89-35	-0.3503	-3.31	0.36	-18.73	2116	2435	2602
Wanap	SPA-89-36	-0.4748	-2.14	0.28	-23.06	1923	2197	2331
Wanap	SPA-89-37	-0.3427	-3.45	0.81	-18.53	2140	2461	2630

4.2 Pb-Pb Isotopic Data

Unit	Sample	^{206}Pb/^{204}Pb	^{207}Pb/^{204}Pb	^{208}Pb/^{204}Pb	6/4SE	7/4SE
DRURY	SPA-88-31	16.5510	15.4384	37.7014	0.0021	0.0021
DRURY	SPA-88-32	16.2356	15.3871	37.0033	0.0013	0.0015
DRURY	SPA-88-54	16.5265	15.4289	36.7725	0.0039	0.0027
DRURY	SPA-88-55	15.9612	15.3643	36.4940	0.0025	0.0027
DRURY	SPA-88-56A	16.1204	15.3676	36.3478	0.0023	0.0025
EBL	EBL-1-182	18.1513	15.5620	38.6886	0.0031	0.0027
EBL	EBL-4-133	17.4807	15.4754	37.5743	0.0050	0.0027
EBL	EBL-4-140	17.4559	15.3885	37.6819	0.0012	0.0006
EBL	SPA-88-19	16.1642	15.2741	36.2414	0.0034	0.0055
EBL	SPA-88-20	16.9031	15.3770	36.5350	0.0036	0.0041
EBL	SPA-88-21	17.3541	15.4350	37.9562	0.0015	0.0019
EBL	SPA-88-22	16.0361	15.3095	35.7630	0.0011	0.0011
EBL	SPA-88-42	17.9566	15.5023	36.9274	0.0012	0.0008
EBL	SPA-88-45	16.8239	15.4396	36.7895	0.0023	0.0023
EBL	SPA-88-46	16.3112	15.3222	36.5762	0.0034	0.0025
EBL	SPA-88-48	17.5310	15.4510	37.7980	0.0120	0.0140
FALC	SPA-89-07A	15.3949	15.2196	35.5154	0.0017	0.0026
FALC	SPA-89-07B	16.1353	15.2773	36.5317	0.0034	0.0072
FALC	SPA-89-08A	15.9206	15.2753	36.2213	0.0035	0.0034
FALC	SPA-89-09	17.2778	15.5359	37.1994	0.0034	0.0040
FALC	SPA-89-10	15.6541	15.2925	35.4085	0.0028	0.0048
FALC	SPA-89-11	15.7111	15.2676	35.6696	0.0017	0.0026
LEVACK	SPA-89-01	14.1931	14.7833	33.7103	0.0091	0.0096
LEVACK	SPA-89-03	14.3220	14.8570	34.3530	0.0190	0.0350
MAY	SPA-88-29	19.2986	15.7570	36.7784	0.0038	0.0059
SD	SPA-88-03	20.8526	16.2495	37.1424	0.0212	0.0154
SD	SPA-88-04	19.6122	15.9999	37.2370	0.0082	0.0112
SD	SPA-88-05	16.8019	15.6381	35.8637	0.0038	0.0044
SD	SPA-88-07	15.9936	15.3315	35.7432	0.0115	0.0136
SD	SPA-88-09	16.0589	15.3240	35.4902	0.0391	0.0363
SD	SPA-88-10	17.0002	15.5340	36.6828	0.0010	0.0010
SD	SPA-88-11	22.1617	16.2747	42.0143	0.0010	0.0010
SD	SPA-88-12	18.4611	15.9615	35.9998	0.0010	0.0010
SD	SPA-88-13	17.4459	15.8174	35.1913	0.0010	0.0010
SD	SPA-88-14	47.6690	19.0279	48.3518	0.0050	0.0050
WANAP	SPA-89-32	16.0162	15.3195	35.7333	0.0067	0.0040
WANAP	SPA-89-35	17.0348	15.3279	37.2371	0.0036	0.0017
WANAP	SPA-89-36	17.2962	15.4010	37.7977	0.0014	0.0020

Unit	Sample	8/4SE	μ	Model Age (Ma)
DRURY	SPA-88-31	0.0076	9.68	1270
DRURY	SPA-88-32	0.0045	9.64	1429
DRURY	SPA-88-54	0.0080	9.65	1273
DRURY	SPA-88-55	0.0102	9.78	1609
DRURY	SPA-88-56A	0.0066	9.64	1488
EBL	EBL-1-182	0.0059	9.57	279
EBL	EBL-4-133	0.0117	9.38	619
EBL	EBL-4-140	0.0058	8.99	460
EBL	SPA-88-19	0.0095	9.10	1288
EBL	SPA-88-20	0.0105	9.15	882
EBL	SPA-88-21	0.0089	9.24	638
EBL	SPA-88-22	0.0039	9.36	1457
EBL	SPA-88-42	0.0042	9.36	304
EBL	SPA-88-45	0.0063	9.51	1061
EBL	SPA-88-46	0.0054	9.20	1256
EBL	SPA-88-48	0.0260	9.25	531
FALC	SPA-89-07A	0.0087	9.54	1841
FALC	SPA-89-07B	0.0083	9.09	1319
FALC	SPA-89-08A	0.0096	9.26	1493
FALC	SPA-89-09	0.0077	9.76	889
FALC	SPA-89-10	0.0124	9.68	1742
FALC	SPA-89-11	0.0077	9.44	1653
LEVACK	SPA-89-01	0.0207	8.43	2236
LEVACK	SPA-89-03	0.0400	8.77	2232
MAY	SPA-88-29	0.0183	10.17	-167
SD	SPA-88-03	0.0433	11.98	-230
SD	SPA-88-04	0.0225	11.15	104
SD	SPA-88-05	0.0094	10.63	1406
SD	SPA-88-07	0.0262	4.76	761
SD	SPA-88-09	0.0819	9.43	1463
SD	SPA-88-10	0.0010	9.90	1093
SD	SPA-88-11	0.0010	11.93	-1031
SD	SPA-88-12	0.0010	11.33	788
SD	SPA-88-13	0.0010	11.15	1232
SD	SPA-88-14	0.0050		
WANAP	SPA-89-32	0.0156	9.44	1490
WANAP	SPA-89-35	0.0334	8.85	676
WANAP	SPA-89-36	0.0059	9.10	615

4.3 Rb-Sr Isotopic Data

Location	Sample	Rb	Sr	$^{87}Rb/^{86}Sr$	$^{87}Sr/^{86}Sr$	2σ	/mil	$\epsilon(T)$	2σ
DRURY	SPA-88-56A	17	269	0.1819	0.70696	0.000016	0.012	-2.08	0.93
EBL	SPA-88-19	9	260	0.0997	0.70556	0.000023	0.017	7.09	0.85
EBL	SPA-88-20	11	296	0.1070	0.70634	0.000053	0.038	14.48	1.31
EBL	SPA-88-21	9	283	0.0916	0.70542	0.000014	0.010	9.23	0.67
EBL	SPA-88-22	13	232	0.1613	0.70657	0.000021	0.015	-9.99	1.13
EBL	SPA-88-43	13	280	0.1337	0.70778	0.000029	0.021	21.36	1.11
EBL	SPA-88-46	14	254	0.1587	0.70726	0.000025	0.018	1.18	1.17
EBL	SPA-88-48	15	215	0.2008	0.70697	0.000009	0.007	-24.47	1.17
EBL	SPA-88-49	14	225	0.1791	0.70605	0.000028	0.020	-26.50	1.31
FALC	SPA-89-07A	16	270	0.1706	0.70581	0.000014	0.010		
S-D	SPA-88-03	10	312	0.0923	0.70661	0.000026	0.019	25.84	0.85
S-D	SPA-88-04	19	281	0.1947	0.70884	0.000018	0.013	5.31	1.26
S-D	SPA-88-05	9	243	0.1066	0.70557	0.000011	0.008	3.71	0.71
S-D	SPA-88-07	27	241	0.3225	0.71381	0.000025	0.018	10.85	2.01
S-D	SPA-88-09	12	291	0.1187	0.70506	0.000028	0.020	-9.75	1.01
S-D	SPA-88-10	41	209	0.5647	0.70485	0.000038	0.027	-240.63	3.43
VOLC	SPA-88-29	5	131	0.1099	0.71093	0.000031	0.022		
WANAP	SPA-89-36	41	556	0.2123	0.70858	0.000045	0.032		